University of Agronomic Sciences
and Veterinary Medicine of Bucharest
Faculty of Veterinary Medicine

SCIENTIFIC WORKS

SERIES C. VETERINARY MEDICINE

VOL. LXX (2)

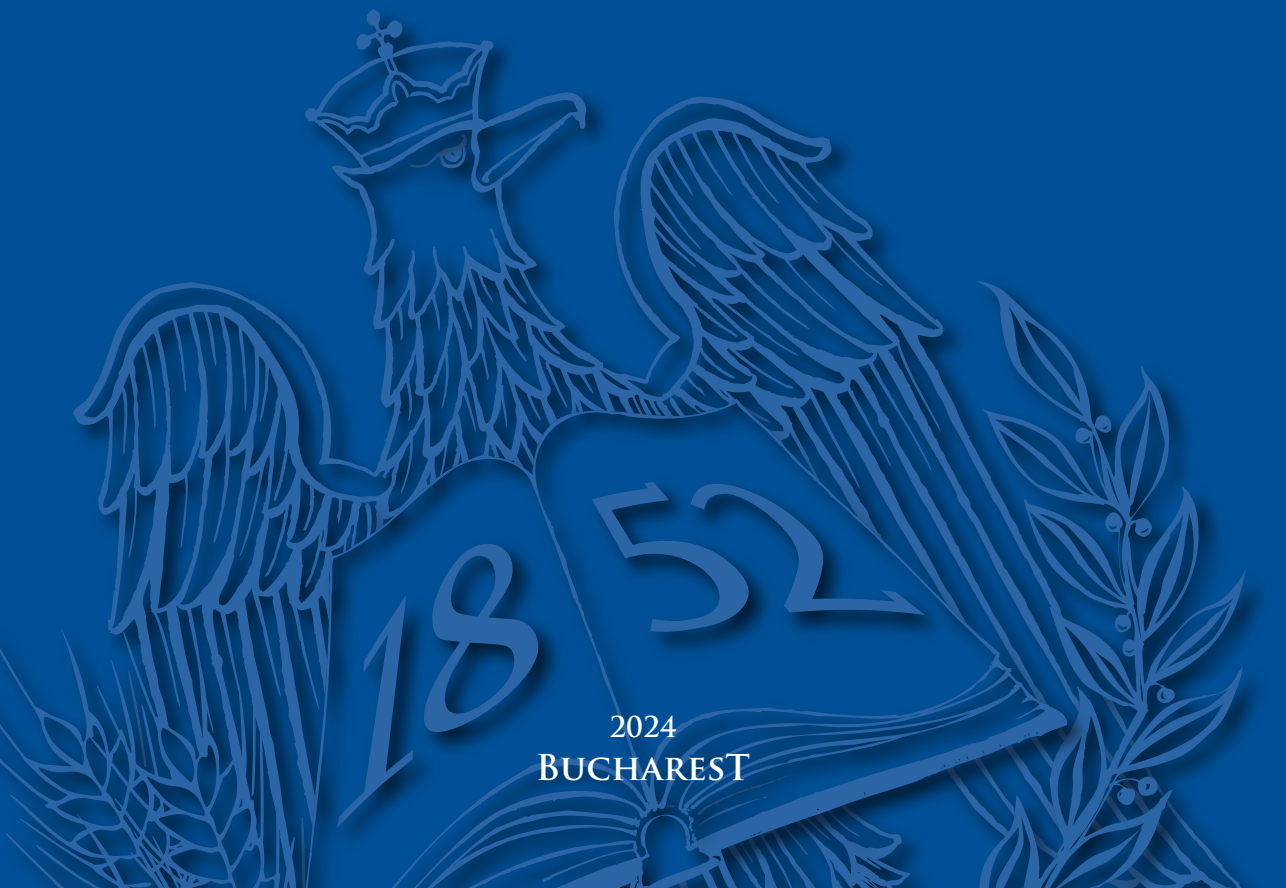

2024
BUCHAREST

SCIENTIFIC WORKS
SERIES C. VETERINARY MEDICINE
VOLUME LXX (2), 2024

University of Agronomic Sciences
and Veterinary Medicine of Bucharest
Faculty of Veterinary Medicine

SCIENTIFIC WORKS
SERIES C.
VETERINARY MEDICINE

Volume LXX (2)

2024
BUCHAREST

PUBLISHERS:

University of Agronomic Sciences and Veterinary Medicine of Bucharest, Romania - Faculty of Veterinary Medicine
Address: 105 Splaiul Independentei, District 5, Zip code 050097, Bucharest, Romania
Phone: + 40 213 182 564, Fax: +40 213 182 888
E-mail: veterinarymedicinejournal@usamv.ro, Webpage: http://veterinarymedicinejournal.usamv.ro

CERES Publishing House
Address: 29 Oastei Street, District l, Bucharest, Romania
Phone: + 40 21 317 90 23, E-mail: edituraceres@yahoo.com, Webpage: www.editura-ceres.ro

To be cited: Scientific Works. Series C. Veterinary Medicine, Vol. LXX (2), 2024

ISSN 2065-1295, ISSN 2343-9394 (CD-ROM), ISSN 2067-3663 (Online), ISSN-L 2065-1295

International Database Indexing:
Index Copernicus; CABI; Google Scholar; Scipio; OCLC; PNB (Polish Scholarly Bibliography);
Cite Factor; Research Bible; Universal Impact Factor

SCIENTIFIC COMMITTEE

1. Larry ADAMS - Purdue University College of Veterinary Medicine, Indiana, USA
2. Sarah BAILLIE - Bristol Veterinary School, University of Bristol, UK
3. Stelian BĂRĂITĂREANU - Faculty of Veterinary Medicine, USAMV of Bucharest, Romania
4. Cinzia BENAZZI - Veterinary Medical Sciences, University of Bologna, Italy
5. Laurentiu BENGA -Veterinary Laboratory of the Central Unit for Animal Research and Welfare Affairs, University Hospital, Heinrich Heine University Dusseldorf, Germany
6. Cornel CĂTOI - Faculty of Veterinary Medicine, USAMV of Cluj-Napoca, Romania
7. Emilia CIOBOTARU-PÎRVU - Faculty of Veterinary Medicine, USAMV of Bucharest, Romania
8. Iuliana CODREANU - Faculty of Veterinary Medicine, USAMV of Bucharest, Romania
9. Mario CODREANU - Faculty of Veterinary Medicine, USAMV of Bucharest, Romania
10. Cristin COMAN - National Institute for Medical-Military Research and Development "Cantacuzino", Romania
11. Doina DANEŞ - Faculty of Veterinary Medicine, USAMV of Bucharest, Romania
12. Nicodim FIŢ - Faculty of Veterinary Medicine, USAMV of Cluj-Napoca, Romania
13. Claudio GENCHI - Dep. of Veterinary Sciences and Public Health, University of Milan, Italy
14. Viorel HERMAN - Faculty of Veterinary Medicine, ULS from Timisoara, Romania
15. Anja KIPAR - Institute of Veterinary Pathology, Vetsuisse Faculty Zurich, University of Zurich, Switzerland
16. Mihai MAREŞ - Faculty of Veterinary Medicine, ULS of Iasi, Romania
17. Liviu Dan MIRON - Faculty of Veterinary Medicine, ULS of Iasi, Romania
18. Dumitru MILITARU - Academy of Agricultural and Forestry Sciences, Bucharest, Romania
19. Manuella MILITARU - Faculty of Veterinary Medicine, USAMV of Bucharest, Romania
20. Sorin MORARIU - Faculty of Veterinary Medicine, ULS from Timisoara, Romania
21. Florin MUSELIN - Faculty of Veterinary Medicine, ULS from Timisoara, Romania
22. Domenico OTRANTO - Università degli Studi di Bari Aldo Moro, Italy
23. Gheorghe SAVUŢA - Faculty of Veterinary Medicine, ULS of Iasi, Romania
24. Gheorghe SOLCAN - Faculty of Veterinary Medicine, ULS of Iasi, Romania
25. Marina SPÎNU - Faculty of Veterinary Medicine, USAMV of Cluj-Napoca, Romania
26. Dana TĂPĂLOAGĂ - Faculty of Veterinary Medicine, USAMV of Bucharest, Romania
27. Constantin VLĂGIOIU - Faculty of Veterinary Medicine, USAMV of Bucharest, Romania

SUMMARY

FUNDAMENTAL SCIENCES

CLINICAL SCIENCES

ANIMAL PRODUCTION, PUBLIC HEALTH AND FOOD QUALITY CONTROL

EXPERIMENTAL MEDICINE

FUNDAMENTAL SCIENCES

Scientific Works. Series C. Veterinary Medicine. Vol. LXX (2), 2024
ISSN 2065-1295; ISSN 2343-9394 (CD-ROM); ISSN 2067-3663 (Online); ISSN-L 2065-1295

DOGS' HAIR AND TISSUES AS BIOINDICATORS FOR THE ASSESSMENT OF HEAVY METALS POLLUTION

Gheorghe Valentin GORAN[1], Emanuela BADEA[1], Cristina ȚOCA[2], Camille BELLI[1]

[1]University of Agronomic Sciences and Veterinary Medicine of Bucharest, Faculty of Veterinary Medicine, 105 Splaiul Independentei Street, 050097, District 5, Bucharest, Romania
[2]Institute of Diagnosis and Animal Health, 63 Dr. Staicovici Street, 050557, District 5, Bucharest, Romania

Corresponding author email: gheorghe.goran@fmvb.usamv.ro

Abstract

The study aimed to examine the accumulation pattern and concentrations of heavy metals and minerals in different tissues of dogs (hair, kidney, brain, liver). Additionally, it explored the feasibility of utilizing these samples for identifying potential environmental impacts associated with these pollutants.
ICP-MS was used to analyse the samples for concentrations of heavy metals. The obtained values were assessed considering various factors that could impact the levels of minerals and metals in the organisms of animals, including age, gender, and habitat.
Generally, heavy metals recorded higher levels in the hair, liver and kidneys of dogs living outdoors compared to the ones living indoors. Of all types of samples lead had the highest levels in female dogs, in dogs younger than 5 years and in those living outdoors. The results also show that hair, among all samples, plays a significant role for the evaluation of heavy metals pollution.

Key words*: heavy metals, hair, liver, kidney, brain, dogs, ICP-MS.*

INTRODUCTION

Pollution is the undesirable physical, chemical and biological alterations that occur in air, water and soil following the action of anthropogenic and natural sources. With the alarming growth in global population, the release of potentially toxic substances continues to be one of the greatest challenges the global society has to face.
The widespread use of heavy metals across industrial, domestic, agricultural, medical, and technological sectors has led to their pervasive presence in the environment. Once released, these metals display resistance to natural degradation processes and persist indefinitely in certain organs and body systems, posing significant health risks.
Unlike organic pollutants, heavy metals once introduced into the environment cannot be biodegraded and they persist indefinitely in certain organs and body system causing serious health problems (Adams et al., 2006; Badea et al., 2016a; Hernández-Moreno et al., 2013; Michalak et al., 2012; Poon et al., 2004; Tchounwou et al., 2012). Heavy metals by definition are metals with relatively high densities and high atomic mass. Some of them are essential for human health but they can become toxic in larger amounts or forms. One of the reasons they are so toxic is related to their ability to stop the absorption, metabolism and use of essential minerals, leading to their deficiency (Jaishankar et al., 2014). The accumulation of xenobiotics depends on several factors, especially physiological conditions and habitats (Badea et al., 2017; Goran et al., 2017a; Goran et al., 2017b; Poon et al., 2004).
Dogs represent a very good indicator of the pollution load on the environment because they inhabit the same space with us and are exposed to the same pollutants (Nageeb Rashed & Soltan, 2005; Park et al., 2005). By analysing the different organs and their ability to accumulate heavy metals we can acquire a better understanding of their metabolism and kinetics (Badea et al., 2016b; Badea et al., 2018; Combs et al., 1982; Jafari, 2016; Kolachi et al., 2012; Roug et al., 2015; Singh et al., 2011).
The aim of this study is to investigate the pattern of accumulation and content of some

heavy metals and minerals in various tissues of dogs (hair, kidney, brain, liver) taking into consideration their sex, age and habitat and the possibility of using such samples to biologically monitoring of the environmental pollution.

MATERIALS AND METHODS

Hair, liver, kidney and brain samples were collected from the cadavers of 12 dogs belonging to different breeds, the majority of them being mixed-breed that were raised in the Bucharest area (Table 1). Following the collection of anamnestic data such as sex, age, habitat and the pathological findings while they were still alive, all dogs were evaluated as clinically unhealthy.

Table 1. Studied dogs' samples depending on habitat, age and sex

Habitat	Indoor	4	M	3
			F	1
	Outdoor	8	M	3
			F	5
Age	< 5	6	M	3
			F	3
	> 5	6	M	3
			F	3

The hair samples were collected from the flank region, the liver samples were collected from each lobe, the kidney samples were collected from the medulla and cortical regions and the brain samples were collected in their whole. Each sample was packaged in plastic bags, labelled and transported to the laboratory where they were stored in the freezer. Each sample was numbered and the following data were noted: breed, sex, age, weight, habitat and pathology.

All tissues and hair samples were weighed to 0.01 g and placed in polypropylene tubes. Samples were then disintegrated by cold wet mineralisation, adding to each sample 5 ml of HNO_3 and 1 ml of HCl. After the complete disintegration, ultrapure water was added in each sample up to the volume of 10 ml. The disintegrated samples were analysed by ICP-MS.

Statistical analysis was performed using VassarStats software: Website for Statistical Computation (http://vassarstats.net/). For all samples' mineral concentrations One-Way ANOVA was performed, and when ANOVA generated $p \leq 0.05$, all-pair Tukey HSD Test was carried out for the comparison of the averages.

RESULTS AND DISCUSSIONS

The mean Zn, Pb and Cd contents of hair and tissues samples from the studied dogs depending on habitat, age and sex are presented in Table 2, Table 3 and Table 4, respectively, and expressed as ppm.

The hair of female dogs showed a significantly different higher mean level of Zn than the male dogs' hair samples. In the brain of male dogs, significantly high mean levels of Zn (p=0.03) were detected, compared to those in females (Figure 1).

Table 2. Mean mineral levels in dogs' hair, liver, kidney, and brain samples, depending on habitat (ppm)

Habitat	Indoor				Outdoor			
	H	L	K	B	H	L	K	B
Zn	79.823	18.407	11.803	6.265	84.539	25.728	14.186	6.136
Pb	0.699	0.051	0.052	0.013	2.002	0.609	0.109	0.069
Cd	0.044	0.074	0.323	0.005	0.071	0.046	0.169	0.005

H-hair, L-liver, K-kidney, B-brain

Table 3. Mean mineral levels in dogs' hair, liver, kidney, and brain samples, depending on age (ppm)

Age	<5 years old				>5 years old			
	H	L	K	B	H	L	K	B
Zn	6.113	82.751	83.183	6.245	14.058	23.528	21.142	12.725
Pb	0.102	2.077	1.059	0.012	0.139	0.763	0.082	0.041
Cd	0.006	0.079	0.045	0.004	0.150	0.039	0.071	0.290

H-hair, L-liver, K-kidney, B-brain

Table 4. Mean mineral levels in dogs' hair, liver, kidney, and brain samples, depending on sex (ppm)

Sex	Male				Female			
	H	L	K	B	H	L	K	B
Zn	14.340	21.836	12.600	6.530	83.435	25.360	13.515	5.828
Pb	1.202	0.101	0.058	0.017	1.934	0.744	0.122	0.084
Cd	0.069	0.069	0.293	0.006	0.056	0.041	0.147	0.004

H-hair, L-liver, K-kidney, B-brain

In both liver and kidney samples of female dogs, levels of Zn were not significantly different (p=0.8) compared to liver and kidney samples of males.

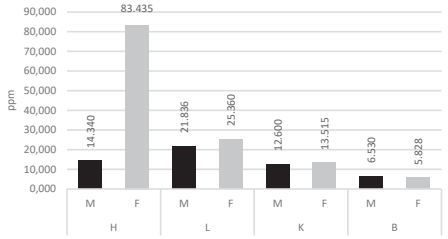

Figure 1. Mean Zn levels in dogs' hair, liver, kidney, and brain samples, depending on sex

In a study on heavy metals concentration in dogs' hair, Zn showed the highest levels, followed by Pb (Tomza-Marciniak et al., 2012). In correlation with the results reported in another study, Zn levels were higher in female dogs than in males (Hayashi et al., 1981), but not significantly different. Most of the minerals, such as Zn, are needed in small quantities in the brain, therefore lower levels of this mineral were detected in the brain compared to hair or the other tissues.

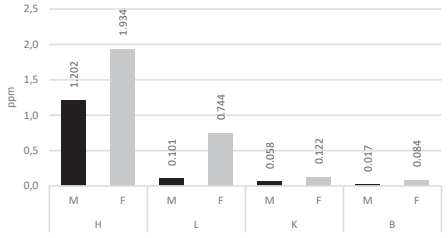

Figure 2. Mean Pb levels in dogs' hair, liver, kidney, and brain samples, depending on sex

In all studied hair and tissues samples of female dogs, mean Pb concentration were higher (p>0.05) than in male dogs, but not significantly different (Figure 2). In correlation with the results reported by Hayashi et al. (1981), Pb levels were higher in female dogs than in males. Due to slow brain excretion, excessive accumulation of Pb is observed in the brain of dogs, similar to what was detected in the rat's cerebral cortex (Li et al., 2015).

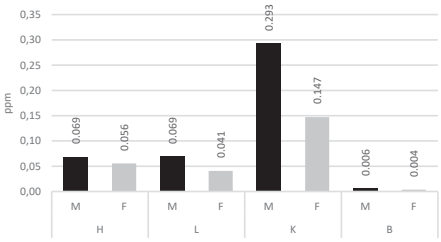

Figure 3. Mean Cd levels in dogs' hair, liver, kidney, and brain samples, depending on sex

The Cd mean levels in the hair and tissues samples from the male dogs were insignificantly different (p>0.05) than in female dogs' samples (Figure 3).

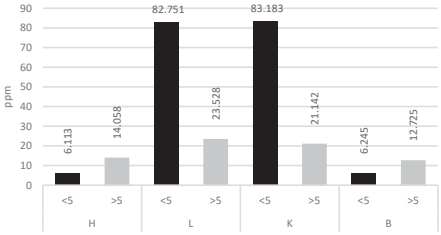

Figure 4. Mean Zn levels in dogs' hair, liver, kidney, and brain samples, depending on age

The hair and brain samples from dogs older than 5 years showed insignificantly higher mean levels of Zn (p>0.05) than younger dogs, while the Zn mean levels of dogs younger than 5 years in liver and kidney samples were insignificantly higher (p>0.05) than in those of dogs older than 5 years (Figure 4). Zn showed a negative correlation between the hair and the age of the dogs as previously reported by Park

et al. (2005). The sex of the animals has only minor impact on the concentrations of the elements in the kidney, as has been observed by Hermoso de Mendoza et al. (2011), but differences depending on age of the animals are observed. Goran et al. (2020) reported that Zn mean levels in hair samples from female cats showed insignificant differences across various health statuses, and in all animals regardless of age or health condition.

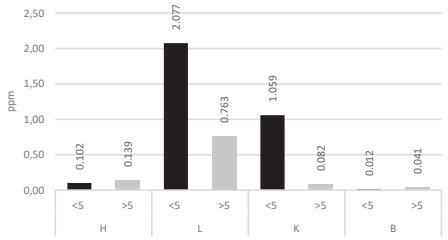

Figure 5. Mean Pb levels in dogs' hair, liver, kidney, and brain samples, depending on age

The hair and brain samples of dogs older than 5 years showed insignificantly higher Pb mean concentrations (p>0.05) than those of younger dogs (Figure 5). In the liver and kidney samples of younger dogs insignificantly higher Pb concentrations (p>0.05) were detected than in those from the older ones. In this study, the concentration of Pb in dog hair is slightly increased with the age as it has been previously observed by Park et al. (2005).

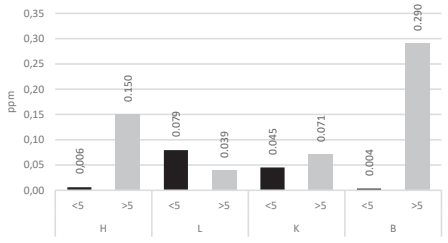

Figure 6. Mean Cd levels in dogs' hair, liver, kidney, and brain samples, depending on age

Cd concentrations were higher in liver samples in young dogs compared to old dogs, and higher in hair, kidney, and brain samples in older dogs compared to young dogs, however the differences were not statistically significant (p>0.05) (Figure 6). In this study, the concentration of Cd in dog hair increases with the age as it has been previously observed by Park et al. (2005). Paßlack et al. (2014) reported that Cd content in the feline liver doesn't show an increase with the animals' age. The hair of dogs living outdoor showed an insignificantly different higher mean level of Zn (p>0.05) than the hair of dogs living indoor. In addition, the highest Zn mean concentration was detected, among all the studied samples types, in hair samples, independent of the habitat (Figure 7). The liver and kidney of outdoor dogs showed insignificant higher Zn levels (p>0.05) than those of indoor dogs. In the brain of dogs living indoor insignificantly different mean levels of Zn (p>0.05) were detected compared to those in the brain of dogs living outdoor, and the lowest Zn mean concentration was detected in this type of sample independent of habitat.

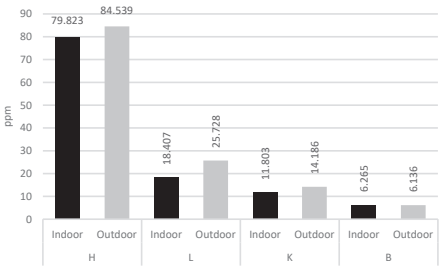

Figure 7. Mean Zn levels in dogs' hair, liver, kidney, and brain samples, depending on habitat

The results from this study show a higher accumulation of Zn in the kidneys compared to Pb and Cd as observed in a previous study on fish from the Arabian Gulf by Ashraf (2005).
In the study on felines by Paßlack et al. (2014), Zn was detected with the highest levels in the liver, followed by the kidneys.

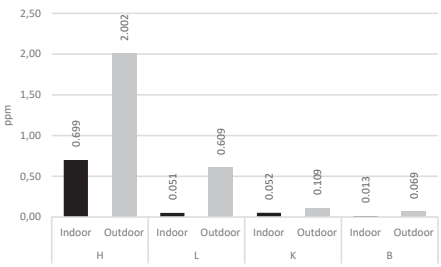

Figure 8. Mean Pb levels in dogs' hair, liver, kidney, and brain samples, depending on habitat

In all types of samples of dogs living outdoor insignificantly different higher Pb mean concentrations (p>0.05) were detected than in dogs living indoor, and, independent of the habitat, the highest Pb mean concentration was detected in hair (Figure 8).
The hair of dogs living outdoor showed insignificantly different Cd mean levels (p>0.05) than indoor dogs. In the liver and kidney samples of indoor dogs an insignificantly different Cd higher mean concentration was detected than in outdoor dogs' liver and kidney samples, and, independent of habitat, the highest Cd mean concentration was detected in kidney samples (Figure 9).

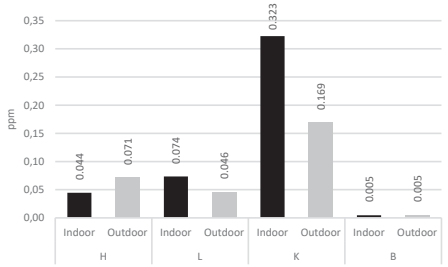

Figure 9. Mean Cd levels in dogs' hair, liver, kidney, and brain samples, depending on habitat

Both indoor and outdoor dogs showed the same Cd mean concentrations in the brain samples.

CONCLUSIONS

Generally, heavy metals recorded higher levels in the hair, liver and kidneys of dogs living outdoors compared to the ones living indoors.
Pb showed higher levels in the hair, liver and kidneys of dogs living outdoor compared to the ones living indoors.
The highest levels of Zn were detected in the liver, kidney and brain of dogs younger than 5 years compared to older dogs, and in the hair of dogs living outdoor.
Zn levels were higher in the hair of female dogs and in the brain samples of male dogs.
Of all types of samples, Pb had the highest levels in female dogs, in dogs younger than 5 years and in those living outdoors.
In all types of samples Pb had the highest levels in female dogs, in dogs younger than 5 years and in those living outdoor.
Male dogs showed higher accumulation of Cd in all studied samples compared to female dogs.
Independent of habitat, the highest Cd mean concentration was detected in kidney samples.
Analysing heavy metals especially in hair, of all the studied samples, may be valuable as a means of biologically monitoring the metallic elements pollution.

REFERENCES

Adams, J. B., Holloway, C. E., George, F., & Quig, D. (2006). Analyses of toxic metals and essential minerals in the hair of Arizona children with autism and associated conditions, and their mothers. *Biological Trace Element Research, 110*, 193-209.

Ashraf, W. (2005). Accumulation of heavy metals in kidney and heart tissues of *Epinephelus microdon* fish from the Arabian Gulf. *Environ Monit Assess., 101*(1-3), 311-316. doi:10.1007/s10661-005-0298-4

Badea, E., Goran, G., & Crivineanu, V. (2016a). Hair Mineral Levels in Dogs with Atopic Dermatitis. *Bulletin UASVM Veterinary Medicine, 73*(2), 451-453.

Badea, E., Goran, G., Matei, E., Rotaru, E., & Crivineanu, V. (2016b). Heavy metal and mineral content in the coat of cats in relationship with kidney failure. *Lucrări Stiinţifice Medicină Veterinară Timişoara, XLIX*(1), 17-28.

Badea, E., Goran, G., Ţoca, C., & Crivineanu, V. (2017). Heavy metals in cat hair depending on keeping conditions. *Lucrări Ştiinţifice Medicină Veterinară Iaşi, 60*(19), 160-166.

Badea, E., Goran, G., Toca, C., & Crivineanu, V. (2018). Assessment of heavy metal and mineral levels in hair samples from dogs with mammary neoplasms. *Bulletin UASVM Food Science and Technology, 75*(1), 1-7.

Combs, D. K., Goodrich, R. D., & Meiske, J. C. (1982). Mineral concentrations in hair as indicators of mineral status: a review. *Journal of Animal Science, 54*(2), 391-398.

Goran, G., Badea, E., & Crivineanu, V. (2017a). Hair mineral content analysis in cats with different liver disorders. *Scientific Works. Series C. Veterinary Medicine, LXIII*(1), 101-108.

Goran, G., Badea, E., Toca, C., & Crivineanu, V. (2017b). The effect of habitat on hair copper, molybdenum, and selenium levels in cats. *Lucrări Ştiinţifice Medicină Veterinară, 60*(3), 325-329.

Goran, G., Badea, E., & Crivineanu, V. (2020). Comparison of zinc hair mineral levels in cats with liver and kidneys disorders. *Scientific Works. Series C. Veterinary Medicine, LXVI*(1), 11-16.

Hayashi, M., Okada, I., Tate, H., Miura, Y., Ohhira, S., & Yamada, Y. (1981). Distribution of environmental pollutants in pet animals. VI. Heavy metals in hair of house-dogs. *Bull Environ Contam Toxicol., 26*(1), 60-64. doi:10.1007/BF01622055

Hermoso de Mendoza García, M., Hernández Moreno, D., Soler Rodríguez, F., López Beceiro, A., Fidalgo Alvarez, L., & Pérez López, M. (2011). Sex- and age-dependent accumulation of heavy metals (Cd, Pb and Zn) in liver, kidney and muscle of roe deer (*Capreolus capreolus*) from NW Spain. *J Environ Sci Health A Tox Hazard Subst Environ Eng., 46*(2), 109-116. doi:10.1080/10934529.2011.532422

Hernández-Moreno, D., de la Casa Resino, I., Fidalgo, L. E., Llaneza, L., Rodríguez, F. S., Pérez-López, M., & López-Beceiro, A. (2013). Noninvasive heavy metal pollution assessment by means of Iberian wolf (*Canis lupus signatus*) hair from Galicia (NW Spain): a comparison with invasive samples. *Environ Monit Assess, 185*, 10421-10430.

Jafari, S. (2016). *Use of pets as indicators of heavy metal exposure across Sydney.* (Thesis), Macquarie University.

Jaishankar, M., Tseten, T., Anbalagan, N., Mathew, B., & Beeregowda, K. (2014). Toxicity, mechanism and health effects of some heavy metals. *Interdiscip Toxicol., 7*(2), 60-72. doi:10.2478/intox-2014-0009

Kolachi, N. F., Kazi, T. G., Afridi, H. I., Kazi, N. G., & Khan, S. (2012). Investigation of essential trace and toxic elements in biological samples (blood, serum and scalp hair) of liver cirrhotic/cancer female patients before and after mineral supplementation. *Clin Nutr., 31*(6), 967-973.

Li, Q., Liu, H., Alattar, M., Jiang, S., Han, J., Ma, Y., & Jiang, C. (2015). The preferential accumulation of heavy metals in different tissues following frequent respiratory exposure to PM2.5 in rats. *Sci Rep., 5*, 16936. doi:10.1038/srep16936

Michalak, I., Chojnacka, K., & Saeid, A. (2012). Relation between mineral composition of human hair and common illnesses. *Chin Sci Bull, 57*, 3460-3465.

Nageeb Rashed, M., & Soltan, M. E. (2005). Animal Hair as Biological Indicator for Heavy Metal Pollution in Urban and Rural Areas. *Environmental Monitoring and Assessment, 110*, 41–53.

Park, S., Lee, M., & Kim, S. (2005). Studies on Cd, Pb, Hg and Cr Values in Dog Hairs from Urban Korea. *Asian-Aust. J. Anim. Sci., 18*(8), 1135-1140. doi:10.5713/ajas.2005.1135

Paßlack, N., Mainzer, B., Lahrssen-Wiederholt, M., Schafft, H., Palavinskas, R., Breithaupt, A., . . . Zentek, J. (2014). Concentrations of strontium, barium, cadmium, copper, zinc, manganese, chromium, antimony, selenium and lead in the equine liver and kidneys. *Springerplus, 3*, 343. doi:10.1186/2193-1801-3-343

Poon, W. T., Ling, S. C., Chan, A. Y. W., & Mak, T. W. L. (2004). Use of hair analysis in the diagnosis of heavy metal poisoning: report of three cases. *Hong Kong Med J, 10*, 197-200.

Roug, A., Swift, P. K., Gerstenberg, G., Woods, L. W., Kreuder-Johnson, C., Torres, S. G., & Puschner, B. (2015). Comparison of trace mineral concentrations in tail hair, body hair, blood, and liver of mule deer (*Odocoileus hemionus*) in California. *Journal of Veterinary Diagnostic Investigation, 27*(3), 295-305.

Singh, R., Gautam, N., Mishra, A., & Gupta, R. (2011). Heavy metals and living systems: An overview. *Indian J Pharmacol., 43*(3), 246-253. doi:10.4103/0253-7613.81505

Tchounwou, P., Yedjou, C., Patlolla, A., & Sutton, D. (2012). Heavy Metals Toxicity and the Environment. *Exp Suppl., 101*, 133-164. doi:10.1007/978-3-7643-8340-4_6

Tomza-Marciniak, A., Pilarczyk, B., Bąkowska, M., Ligocki, M., & Gaik, M. (2012). Lead, cadmium and other metals in serum of pet dogs from an urban area of NW Poland. *Biol Trace Elem Res., 149*(3), 345-351. doi:10.1007/s12011-012-9433-6

Scientific Works. Series C. Veterinary Medicine. Vol. LXX (2), 2024
ISSN 2065-1295; ISSN 2343-9394 (CD-ROM); ISSN 2067-3663 (Online); ISSN-L 2065-1295

ETHOLOGICAL STUDY REGARDING THE DIPSIC BEHAVIOUR CHANGES DURING THE GESTATION PERIOD IN DOMESTIC CATS

Simona NICOLAE, Iuliana CODREANU

University of Agronomic Sciences and Veterinary Medicine of Bucharest, Faculty of Veterinary Medicine, 105 Splaiul Independentei Street, 050097, District 5, Bucharest, Romania

Corresponding author email: iulianacod@yahoo.com

Abstract

The body's water requirement, under normal metabolic conditions, is direct proportional to the metabolic processes' intensity, therefore, gestation can be correlated with the water requirement's physiological variations, which will lead to a series of changes of the dipsic behaviour in domestic cats. For this ethological study, we analysed a group of 8 healthy female cats, monitoring their dipsic behaviour in the gestation period (between day 35 and 55), for 5 consecutive days. Based on the individual values obtained, the average group values of the studied parameters were calculated and statistically compared with the mean results obtained for a group of 10 clinically healthy individuals. Thus, in the studied group of pregnant felines, there was observed the increase of the mean number of waterings/24 hours and of the average duration/watering session, the two parameters were statistically significant ($p<0.05$) higher than the values obtained in the case of the control group. Also, it was recorded an increase of the dipsic behaviour manifestation duration/24 hours ($p<0.01$), as a result of the concomitant increase of the mean number of waterings and the average duration of a watering session.

Key words*: dipsic behaviour, gestation, domestic cats.*

INTRODUCTION

The physiological status intrinsically influences the nutrients intake and, at the same time, the body's water requirements. Since, under basal conditions, the amount of water that the body needs is proportional with the intensity of the physiological processes, gestation can be correlated, as a demanding period, with some physiological variations of the water intake, which will be expressed through a series of dipsic behaviour changes in pregnant cats (Codreanu, 2018; Dawkins, 2003).

In order to determine the impact that gestation has on the main parameters used for quantifying dipsic behaviour in cats, a group of 8 females was formed. The subjects were clinically and ethologically evaluated on the course of the gestation period. The results were then compared to the ones obtained for a group of 10 healthy adult cats.

The dipsic behaviour of the selected patients was monitored at home for 5 consecutive days, between day 35 and 55 of gestation. The monitoring was carried out by video recording means, and the data obtained was used for performing individual and group ethograms – as the ethogram represents the most important tool in assessing and analysing an individual's behaviour (Codreanu, 2022; Stanton et al., 2015).

The intensification of the dipsic behaviour during the gestation period, in this species, was also reported by other researchers (Taylor, 1995; Wichert et al., 2009), and was translated, in our study, by the increase of the values of all the ethological parameters used for quantifying this type of behaviour.

Thus, in the case of the individuals in our study group, we recorded an increase (with statistical significance) of the mean number of watering sessions/24 h. The same findings were noted in the case of the mean duration/ watering session. All the results were statistically analysed and compared with the values of the control group.

Pregnant cats showed, therefore, an increased dipsic behaviour, in correlation with their high metabolic demands, an aspect also reported by other authors in the specialty literature (Alekseeva et al., 2020; Bowen, 2002).

MATERIALS AND METHODS

The study regarding the influence of gestation on dipsic behaviour in cats, was carried out on a group of 8 pregnant females, which were monitored, for 5 consecutive days, constituting

the study group (Table 1). The females were clinical and paraclinical (haematology, blood biochemistry, ultrasonographic exams) evaluated, their clinical status being healthy, before and during gestation. An important component of the clinical evaluation was the neurological exam, in order to exclude any type of behaviour change connected to the occurrence of Toxoplasmosis or other neurological pathologies (Cucoș et al., 2015; Turbatu et al., 2018).

Table 1. The structure of the study group - pregnant females with healthy clinical status

Individuals from the study group		
Patient no.	**Breed**	**Age** (y.o.)
1	European Shorthair	3
2	British Shorthair	4
3	British Shorthair	3
4	British Longhair	2
5	European Shorthair	1.5
6	European Shorthair	5
7	European Shorthair	2
8	Burmese	5

The dipsic behaviour was analysed by means of video recording, this being the most appropriate way of monitoring the individual with accuracy and without causing any type of stress (Codreanu et al., 2022; Nicolae et al., 2023; Nicolae & Codreanu, 2023). Through video monitoring, using the Xiaomi Home portable surveillance camera, it was possible to directly observe the dipsic behaviour (Figure 1). The Xiaomi Mi Home Security video camera can be connected to the smartphone via the mobile app and provide both real-time data and stored video recordings for later analysis in full HD resolution (Nicolae et al., 2023).

For monitoring the dipsic behaviour, the camera was placed to capture the water bowl or automatic water dispenser (Figure 1). The sensors have been set so that the camera activated and recorded (when the cat comes into proximity) a short video, which it then transmitted to the mobile app. Thus, the videos stored were analysed individually, allowing us to assess, with great precision, the duration of the dipsic behaviour, as well as the frequency of manifestation of this type of behaviour, in 24 hours.

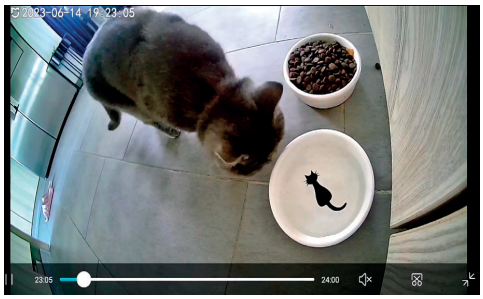

Figure 1. The direct observation of the dipsic behaviour in a patient (British Sh, F, 4 years old) from the study group – using the Xiaomi video camera

The camera has a night mode, due to the integrated invisible infrared LEDs, so that individuals could be properly monitored even during the night, the recordings being clear and conclusive (Figure 2).

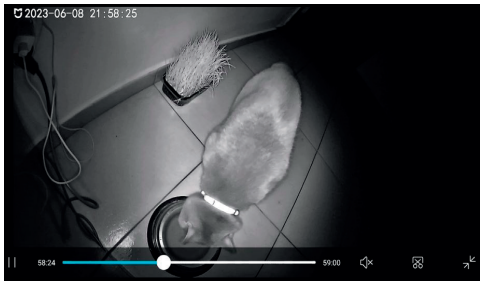

Figure 2. Video recording of the dipsic behaviour, during the night, in a patient (British Sh, F, 3 years old) from the study group – using the Xiaomi video camera night mode feature

The entire process of monitoring, data collection and processing was carried out with the prior written consent of the owners, in accordance with the Romanian and European Union laws regarding the protection of personal data.

The ethograms were drawn up for each individual based on the data obtained. The individual ethogram included data on: time interval in which the dipsic behaviour occurred, watering sessions frequency/24 h, the dipsic behaviour total duration/24 h, the mean duration of a watering session, and data regarding the frequency of approaching the water source without exhibiting dipsic behaviour.

RESULTS AND DISCUSSIONS

The results for each individual were synthetised as group ethograms, which we drawn up for each day of monitoring. Those preliminary data were used for the synthetic data analysis (Table 2).

As concerning the average values obtained for our group of study, they were statistically compared (classic T-test) with the ones obtained in the case of a group of 10 non-pregnant, female adults. The results of the comparative analysis are presented in the graph from Figure 3 and also in Table 3.

Table 2. The average values of the parameters used for evaluating the dipsic behaviour/monitoring period/individual from the study group

No.	**Patient** (breed, age)	**Parameter**			
		Average number of waterings/24 hours	**Average duration of the dipsic behaviour** (sec./24 hours)	**Average duration of a watering session** (sec.)	**Average number of approaches to the water source without displaying dipsic behaviour/24 hours**
1	European Sh, 3 y.o.	2.8	112.09	40.31	0.6
2	British Sh, 4 y.o.	3	118.07	40.09	0.8
3	British Sh, 3 y.o.	3.2	126.74	39.92	0.8
4	British Lh, 2 y.o.	3	119.60	40.28	0.4
5	European Sh, 1.5 y.o.	3	112.83	37.61	0.8
6	European Sh, 5 y.o.	2.4	95.67	40.61	0.4
7	European Sh, 2 y.o.	3.4	127.83	37.78	1.2
8	Burmese, 5 y.o.	3.8	139.86	36.82	1.2
GROUP AVERAGE		**3.08**	**119.08**	**39.18**	**0.77**

Table 3. Comparative results regarding the mean values of the dipsic behaviour indicators, correlated with the physiological status (gestation) in the group of study

DIPSIC BEHAVIOUR INDICATOR	**STUDY GROUP**	
	PREGNANT	**ADULTS – CONTROL GROUP**
Average number of waterings/24 h	3.08*	2.57
Mean duration of dipsic behaviour (sec./24 h)	119.08**	94.05
Average duration of a watering session (sec.)	39.18*	37.06
The average number of approaches to the water source, without the manifestation of dipsic behavior /24 h	0.77	0.57

$p > 0.05$ – non-significant differences
*$p < 0.05$ – significant differences
**$p < 0.01$ - highly significant differences

In the individuals from our study group – pregnant cats (in the second part of the gestation period), we observed a statistically significant *($p<0.05$)* increase of the mean duration/ watering session and of the mean number of waterings/24 h, compared with the control group.

It has been recorded also, an important increase - highly significant *($p<0.01$)* of the mean duration of the manifestation of dipsic behaviour/24 h, being most likely the result of the simultaneous increase of the other parameters monitored.

In the same context, we observed an increase, but without statistical significance ($p>0.05$) of the average values for the number of approaches to the water source, without exhibiting dipsic behaviour/24 h, in the study group.

The results are consistent with the ones reported in the specialty literature, in studies regarding the dipsic and nutritional behaviour changes in different physiological and pathological situations in this species (Kim & Wakshlag, 2023; Houpt, 1991; Bradshaw, 2018).

Although we observed a clear intensification of the dipsic behaviour, which, by any means, indicates an increased water consumption, we can exclude the polydipsia syndrome, as the water intake increase has physiological causes, and the clinical status of the patients does not indicate any sign of underlying pathology (Codreanu M.D., 2017; Cunningham, 2019).

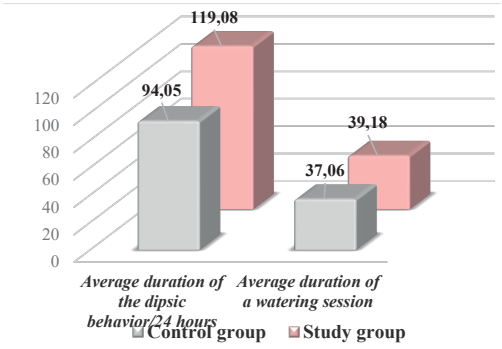

Figure 3. Comparative aspect regarding the influence of the physiological status (gestation) on some quantification parameters for the dipsic behaviour in pregnant cats

CONCLUSIONS

The physiological status (gestation) has an essential impact on the dipsic behaviour in this species.

As concerning the manner in which the physiological status (gestation) influences this behaviour in cats, the ethological indicators used for quantifying this type of behaviour recorded higher mean values (with statistical significance), compared to the healthy adults' group, especially, due to the intensification of metabolic processes and, respectively, water consumption, in the second part of the gestation period.

Pregnant cats presented longer and more often watering session, than adults from the control group, the duration of manifesting dipsic behaviour/24 hours being, therefore, higher.

The changes of the dipsic behaviour are part of the complex ethological features present during pregnancy in this species.

These findings indicate that additional to the special nutritional needs, during gestation, the water requirements are also higher, therefore, ensuring that the female has constant access to a clean, room temperature water supply is mandatory for ensuring the welfare and health of both the mother and future offsprings.

ACKNOWLEDGEMENTS

The present study is part of an extensive research regarding the changes of different behavioural patterns in cats, that has been carried out during the doctoral studies of Dr. Nicolae Simona, DVM, PhD, and are presented in the doctoral thesis "*Research on the physiological and pathophysiological factors involved in the modification of dipsic and urinating behaviour in cat*".

REFERENCES

Alekseeva, G.S., Loshchagina, J.A., Erofeeva, M.N., Naidenko, S.V. (2020). Stressed by Maternity: Changes of Cortisol Level in Lactating Domestic Cats. *Animals (Basel)*, 10(5), 903, doi: 10.3390/ani10050903.

Bradshaw, J.W. (2018). Normal feline behaviour: … and why problem behaviours develop. *J Feline Med Surg.*, 20(5), 411-421, doi: 10.1177/1098612X18771203.

Bowen, J. (2002). *BRAVA manual of canine and feline behavioural medicine*. Gloucester: British Small Animal Veterinary Association.

Dawkins, M. (2003). Behaviour as a tool in the assessment of animal welfare. *Zoology*, 106, 383-387, doi:10.1078/0944-2006-00122.

Codreanu, I., Nicolae, S., Ghiță, M, Anghel, R.M. (2022). Study regarding the adaptation stress impact on the nutritional behavior in domestic cats. *Scientific Works. Series C. Veterinary Medicine*, LXVIII (1), 20-24.

Codreanu, I. (2022). *Tratat de etologie și etopatologie veterinară*. Bucharest, RO: Printech Publishing House.

Codreanu, I. (2018). *Textbook of animal physiology*. Bucharest, RO: Printech Publishing House.

Codreanu, M.D. (2017). *Patologie și clinică medicală veterinară*. Bucharest, RO: Printech Publishing House.

Cucoș, C. A., Ionașcu, I., Mocanu, J., Militaru, M. (2015). Neurological and ocular form of toxoplasmosis in cats. *Scientific Works. Series C. Veterinary Medicine*, LXI, 95-98.

Cunningham, J. (2019). *Textbook of Veterinary Physiology*, *VI*th *Edition*. Saunders Elsevier Inc.

Houpt, K.A. (1991). Feeding and drinking behavior problems. *Vet Clin North Am Small Anim Pract.*, 21(2), 281-98, doi: 10.1016/s0195-5616(91)50033-4.

Kim, H.T., Wakshlag, J.J. (2023). Nutrition and Theriogenology: A Glimpse Into Nutrition and Nutritional Supplementation During Gestation, Lactation, Weaning and Breeding Dogs and Cats. *Vet Clin North Am Small Anim Pract.*, 53(5), 1083-1098, doi:10.1016/j.cvsm.2023.05.003.

Nicolae, S., Reu, I.N., Codreanu, I. (2023). Study regarding the use of modern means of video recording and GPS-tracking in monitoring the dipsic behavior in domestic cats. *Lucrări Ştiinţifice Medicină Veterinară Timişoara*, LVI(2), 168-175.

Nicolae, S., Codreanu, I. (2023). The Age Impact On The Urinary Behaviour In Cats - Comparative Case Study. *Scientific Works. Series C. Veterinary Medicine*, LXIX(1), 31-36.

Stanton, L.A., Sullivan, M.S., Fazio, J.M. (2015). A standardized ethogram for the Felidae: a tool for behavioral researchers. *Appl Anim Behav Sci.*, 173, 3-16.

Taylor, H.R. (1995). Drinking behaviour in cats. *Vet Rec.*, 136(14), 372, doi: 10.1136/vr. 136.14.372-a.

Turbatu, R.M., Fernoaga, C., Tudor, N., Vlagioiu, C. (2018). A Review Of Neurological Examination-Differential Diagnosis For Intracranial Diseases In Cats And Dogs. *Scientific Works. Series C. Veterinary Medicine*, LXIV(2), 88-96.

Wichert, B., Schade, L., Gebert, S., Bucher, B., Zottmaier, B., Wenk, C., Wanner, M. (2009). Energy and protein needs of cats for maintenance, gestation and lactation. *J Feline Med Surg.*, 11(10), 808-815, doi: 10.1016/j.jfms.2009.02.006.

Scientific Works. Series C. Veterinary Medicine. Vol. LXX (2), 2024
ISSN 2065-1295; ISSN 2343-9394 (CD-ROM); ISSN 2067-3663 (Online); ISSN-L 2065-1295

MORPHOLOGICAL PARTICULARITIES OF THE *Lama glama* SKULL

Petronela Mihaela ROȘU, Bogdan GEORGESCU, Cristian Romeo BELU, Adela Ioana MUSTĂȚEA, Sorina Andreea MIHAI, Diana ȘERBĂNESCU, Dana TĂPĂLOAGĂ

University of Agronomic Sciences and Veterinary Medicine of Bucharest, Faculty of Veterinary Medicine, 105 Splaiul Independentei Street, 050097, District 5, Bucharest, Romania

Corresponding author email: adela.mustatea@yahoo.com

Abstract

This study is crucial as it aims to analyze and describe the morphological characteristics of the llama's skull bones. The research provides a series of characteristics crucial for recognizing and differentiating the Lama glama, a domesticated South American camelid. These findings can be applied to identify and study this species accurately. The growth of this species in Europe has gained momentum in recent years. Two skulls, male and female, were selected from the Anatomy discipline collection for this study. The following conclusions emerge from our detailed anatomical descriptions: males' external sagittal and nuchal crests are more developed, and the supraorbital foramen continues rostrally with a reduced groove. Between the frontal, nasal, lacrimal and maxillar bones is a fronto-naso-lacrimo-maxillary foramen. Two foramina open in the orbital hiatus: the optic foramen and the orbitorotundum foramen. Accessory palatine foramina are located caudal to the greater palatine foramen. On the upper arch, at the level of the diastema, in both males and females, there are one or two dental alveoli for the rudimentary first premolar.

Key words: *camelids, Lama glama, morphology, skull.*

INTRODUCTION

The llama (*Lama glama*) is a species in the Order Artiodactyla, suborder Tylopoda, family Camelidae. Several taxonomic studies identified four species: *Lama guanicoe* (Guanaco), *Lama pacos* (Alpaca), *Lama glama* (Llama) and *Vicugna pacos* (Vicuña) (Cabrera & Yepes, 1960), although in other studies, all four species are included in the Lama genre. Studies were carried out on morphological characteristics and behavioural variations but also based on archaeological evidence, which showed that the llama descended from guanaco and the alpaca from the vicuña (Hershkovitz, 1948).

Phylogenomic analysis shows that the llama was domesticated from the guanaco and the alpaca from the vicuña (Fan et al., 2020).

Other genetic studies show a gene flow between llamas and alpaca and genetic crosses between llamas and guanacos (Varas et al., 2020).

Traditionally, morphometric techniques have been used to identify Camelidae species (L'Heureux & Hernández, 2019). However, these methods have proven less effective in differentiating the llama and other species of Camelidae from South America, especially when the differentiation faced the guanaco.

There are studies carried out on camelid`s skulls (Balcarcel et al., 2021; Cartajena, 2009, G.L.; Castañeda et al., 2016; Choudhary et al., 2021; El Allali et al., 2017; Moyano et al., 2022) that provide a detailed description of the skull bones and also of the dentition (Wheeler, 1995).

A clear distinction between the different species of Llama has not yet been made; those species are at the beginning of their domesticated stages, so the differences between their skulls and the skulls of their wild relatives are subtle (Balcarcel et al., 2021).

Morphological studies were carried out on the bones of the thoracic limb in Camelid species (Rosu et al., 2017; Belu et al., 2022; L'Heureux & Hernández, 2019) or on the pelvic limb, including the metatarsophalangeal joint and the digital flexor muscles of the pelvic limb (Constantinescu et al., 2008; Lesbre, 1903). Osteometry studies were also conducted on South American camelids (Izeta, 2010).

This study thoroughly investigated the *Lama glama* skull morphology to generate valuable

characteristics with application in species recognition and differentiation within the South American camelids group.

MATERIALS AND METHODS

The study was conducted in the Anatomy laboratory of the Faculty of Veterinary Medicine in Bucharest. Two skulls, one from an adult female *Lama glama* and one from an adult male of the same species, were used as study material. These skulls belong to the Anatomy Discipline Collection. The morphological aspects of the skull bones were described, and the most exciting aspects were photographed. The description was made according to Nomina Anatomica Veterinaria 2017.

RESULTS AND DISCUSSIONS

The skull of *Lama glama* presents specific morphological particularities, with the maximum width at the orbit level.
High nuchal ridges on the dorsal face, with an caudo-ventral disposition, form by joining a very high external occipital protuberance, drawn caudo-ventrally (Figure 1).

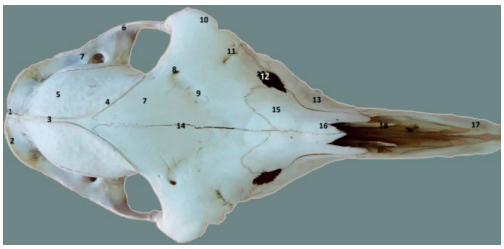

Figure 1. Llama skull (*Lama glama*) - dorsal view (original):
1. External occipital protuberance; 2. Nuchal crest; 3. External sagittal ridge; 4. Temporal line; 5. Parietal; 6. The zygomatic process of the temporal; 7. Retroarticular foramen; 8. The supraorbital foramen; 9. Supraorbital groove; 10. Zygomatic process of the frontal; 11. Supraorbital fissure; 12. Fronto-naso-lacrimo-maxillary foramen; 13. Maxilla; 14. Interfrontal suture; 15. Nasal; 16. Internasal notch; 17. Incisive; 18. Conchal crest

The external sagittal crest is arranged dorso-rostral starting from the external occipital protuberance and is better highlighted in males than females. Rostrally, it is divided into two temporal lines and is well highlighted in the male (Figure 1).
The parietal, elongated rostro-caudal, has a convex surface from one side to the other.
In the rostral extremity of the frontal bone, a subtle depression is observed. The base of the zygomatic processes is perforated by the supraorbital foramen, from which a reduced groove starts rostrally, reaching the frontonasal suture. Before the orbit, slightly dorsolaterally, there is a fronto-naso-lacrimo-maxillary foramen, also present in other wild species (deer, Bactrian camel, dromedary). The nasal bone, end bifid, is short, and an internasal notch is present (Figure 1).
There is a frontal fissure above the orbit, rostrally, slightly oblique medio-laterally.
A complete orbit, an elongated and narrow zygomatic process of the temporal, characterizes the lateral side. The zygomatic bone is divided in the caudal part into two temporal processes, one dorsal and the other ventral. The supraorbital margin has a small incision, which is more evident in the male (Figure 2).

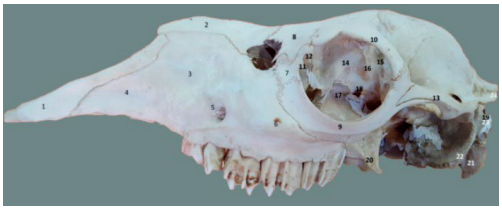

Figure 2. Llama skull (*Lama glama*) - side view (original): 1. Incisive; 2. Nasal; 3. Canine fossa; 4. Maxilla; 5. Infraorbital foramen; 6. Maxillofacial tubercle; 7. Lacrimal; 8. Frontal; 9. Zygomatic; 10. Zygomatic process of the frontal; 11. Lacrimal tubercle; 12. Infratrochlear notch; 13. The zygomatic process of the temporal; 14. Orbital fossa; 15. Temporal fossa; 16. Orbito-temporal crest; 17. Ethmoid fossa; 18. Orbital foramen; 19. External acoustic meatus; 20. Hamulus of the pterygoid; 21. Paracondylar process; 22. Tympanic bulla; 23. Mastoid process; 24. Nuchal crest

At the level of the orbital hiatus, there are two openings: the optic foramen and the orbitorotundum foramen. The ethmoidal fossa is deep and relatively circular, and dorsal to it is the ethmoidal foramen. From the base of the zygomatic process of the frontal, a reduced orbito-temporal crest descends on the orbito-temporal face (Figure 2).

The well-marked mastoid process is on the temporal bone pyramid's lateral face. The external acoustic meatus is reduced and circular, and the obvious tympanic bulla is elongated and flattened in the rostro-caudal direction (Figure 3).
The lacrimal bone has an obvious lacrimal foramen on the orbital face, an apparent infratrochlear notch, and an evident lacrimal tubercle on the lacrimal ridge.
On the external face of the maxilla, there is a facial tubercle, better highlighted in the male. Rostrally, the maxilla shows a small canine fossa, and ventral to it is the infraorbital foramen. An obvious maxillary tuberosity is observed in the caudal extremity of the maxilla.

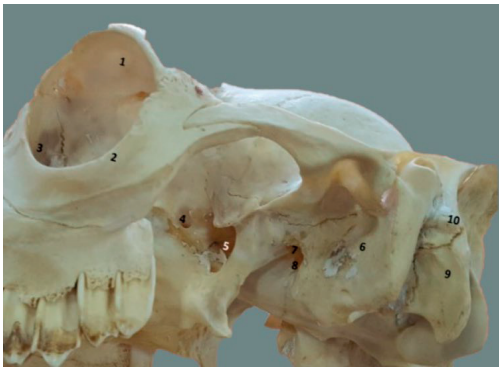

Figure 3. Llama skull (*Lama glama*) - lateral-ventral view (original):
1. Lacrimal gland fossa; 2. Zygomatic; 3. Fossa of the lacrimal sac; 4. Optical foramen; 5. Orbitorotundum foramen; 6. Tympanic bulla; 7. Oval foramen; 8. Spinous foramen; 9. Paracondylar process; 10. Mastoid process of the temporal bone

The pterygopalatine fossa is very elongated dorso-ventrally, and two foramina open at its level: latero-dorsal, the sphenopalatine foramen and latero-ventrally the caudal palatine foramen.
The orbit communicates with the nasal cavity through the incomplete suture between the orbital part of the lacrimal bone and the orbital part of the frontal bone, named frontolacrimal foramen. Under this incomplete suture opens the maxillary foramen (Figure 4).
Two to three evident retroarticular foramina are at the base of the temporal zygomatic process (Figure 4).
On the ventral side, a small muscular process is located at the base of the temporal bone. Ventro-medial to the mastoid process is the stylomastoid foramen. The stylomastoid fossa is very deep.
A deep and elongated ventral condyloid fossa is evident between the occipital condyle and the jugular process. Ventral to the condylar fossa is the hypoglossal canal. Lateral to the basioccipital, in a rostral direction, are three openings: the jugular foramen, the tympano-occipital fissure and the carotid foramen. Rostral to the tympanic bulla are two foramina: the spinous and oval foramen, separated by a small bony blade (Figure 5).

Figure 4. Llama skull (*Lama glama*) – side view (original):
1. Parietal; 2. Occipital; 3. Nuchal crest; 4. Temporal; 5-6. Retroarticular foramina; 7. External acoustic canal; 8. Paracondylar process; 9. Mastoid process; 10. The zygomatic process of the temporal; 11. Ethmoidal foramen; 12. Sphenopalatine foramen; 13. Frontolacrimal foramen; 14. Zygomatic process of the frontal; 15. Zygomatic

The basioccipital has the greatest width in the central portion. At the place of articulation with the basisphenoid, the two muscular tubercles (sphenobasioccipital) are well highlighted, especially in males (Figure 5).
The orbital hiatus crest is evident (Figure 3).
The pterygoid is reduced but shows, caudally, a very prominent hamulus (Figure 4).
The pterygoid fossa is delimited caudo-medially by the hamulus of the pterygoid bone and latero-medially by the pterygoid process of the sphenoid (Figure 3).
The palatine processes of the maxilla are narrower in the central portion and wider in the rostral extremity (Figure 6). The greater palatine foramen continues rostrally with a short palatine groove. On the hard palate, there are two-tree accessory palatine foramina (Figure 5).

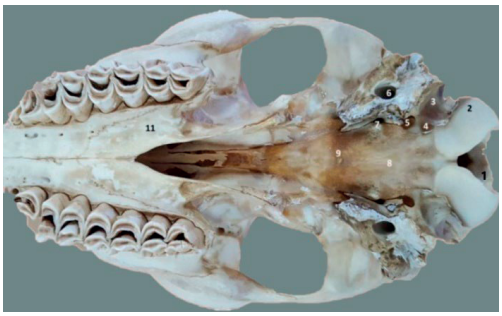

Figure 5. Llama skull (*Lama glama*) - ventral view (original):
1. Foramen magnum; 2. Occipital condyle; 3. Ventral condyloid fossa; 4. Hypoglossal canal; 5. Jugular foramen; 6. Stylomastoid fossa; 7. Carotid foramen; 8. Basioccipital; 9. Muscular tubercles; 11. Horizontal plate of the palatine

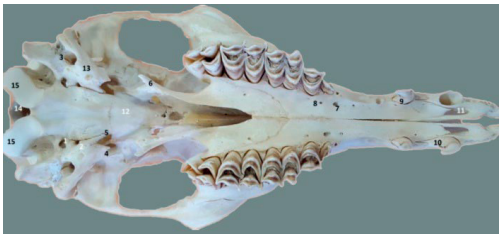

Figure 6. Lama skull (*Lama glama*) - ventral view (original):
1. Jugular foramen; 2. Carotid foramen; 3. Stylomastoid fossa; 4. Oval foramen; 5. Spinous foramen; 6. Hamulus of the pterygoid; 7. Greater palatine foramen; 8. Accessory palatine foramina; 9. Canine; 10. Incisive; 11. Palatine fissure; 12. Basisphenoid; 13. Tympanic bulla; 14. Foramen magnum; 15. Occipital condyles

The diastema on the upper arch is interrupted by the alveolus for the first premolar, both in the male and female. The palatine fissures are oval in shape and very well-defined (Figure 6).
The nuchal face presents a prominent external occipital crest, slightly more developed in the male, which descends dorso-ventrally from the external occipital protuberance to the foramen magnum, dividing this face into two symmetrical parts (Figure 7).
A dorsal condylar fossa is on either side of the external occipital crest, above the occipital condyles. At the base of the jugular process is the mastoid foramen (Figure 7).
The two halves of the mandible are articulated at the body's level by synchondrosis.
The body of the mandible is flattened dorso-ventrally; the diastema is long and presents rostrally the dental alveolus for the canine (Figure 8).
The ventral edge is convex-concave. The dorsal margin presents the alveoli for premolars and molars.

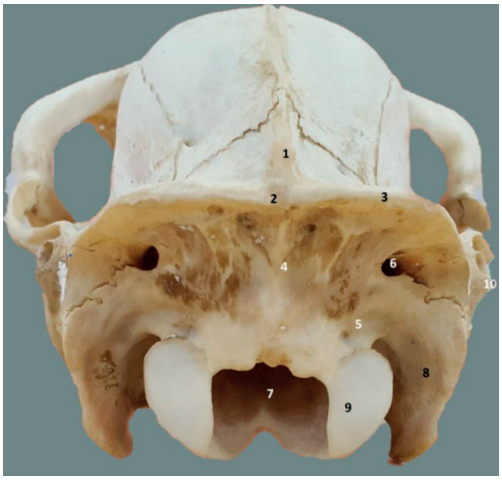

Figure 7. Llama skull (*Lama glama*) - nuchal view (original):
1. External sagittal crest; 2. External occipital protuberance; 3. Nuchal crest; 4. External occipital crest; 5. Dorsal condylar fossa; 6. Mastoid foramen; 7. Foramen magnum; 8. Paracondylar process; 9. Occipital condyles; 10. External acoustic meatus

The mental foramen opens on the lateral surface of the mandibular body, and caudally to it open the two accessory mental foramina. (Figure 8)

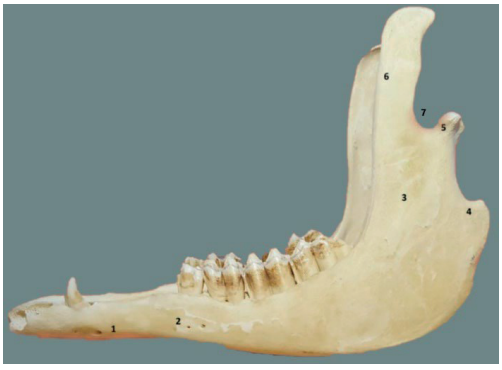

Figure 8. Lama mandible (*Lama glama*) - side view (original):
1. Mental foramen; 2. Accessory mental foramina; 3. Masseteric fossa; 4. Angular process; 5. Condylar process; 6. Coronoid process; 7. Mandibular notch

On the lateral face, the mandibular ramus has a concave-convex from top to bottom masseteric fossa, which is more pronounced in males. On the medial side, the pterygoid fossa is superficial and presents the mandibular foramen in the rostro-dorsal plane.
Caudo-ventrally, the branch shows an obvious angular process, much more robust in males than females. The hook-like process is slightly curved medially.
The coronoid process is highly developed, with a relatively constant width along its entire length. The process has a rounded edge and is curved slightly caudally. The condylar process is short, with a convex surface. The mandibular notch is wide (Figure 8).

CONCLUSIONS

The following conclusions emerge from our detailed anatomical descriptions. The external sagittal crest and nuchal ridges are more developed in the male. The external occipital protuberance is high and drawn caudo-ventrally. The supraorbital foramen continues rostrally with a reduced groove. At the level of the suture between the frontal, nasal, lacrimal and maxilla, there is a fronto-naso-lacrimo-maxillary foramen.
Two-tree retroarticular foramina are located at the base of the zygomatic process of the temporal. There are two openings in the orbital hiatus: the optic foramen and the orbitorotundum foramen.
The mastoid process is highly developed, the external acoustic meatus is reduced, and the tympanic bulla is obvious, elongated and flattened rostro-caudal.
In the pterygopalatine fossa, are two openings: latero-dorsal, the sphenopalatine foramen and latero-ventral, the caudal palatine foramen.
The orbit communicates with the nasal cavity through the frontolacrimal foramen. Ventral to this, the maxillary foramen opens**.**
The spinous foramen and the *foramen ovale* are separated by a small bone blade.
The sphenobasioccipital tubercles are evident, especially in the males.
The external occipital crest is more prominent in the male. Above the occipital condyles, there is a dorsal condylar fossa on either side.
The mandible is characterized by a prominent, robust, hook-like angular process, slightly curved medially. The mandible presents more than one mental foramen. The masseteric fossa is concave-convex from top to bottom, the concavity being more pronounced in males.
On the upper arch, at the level of the diastema, in both males and females, there are one or two dental alveoli for the rudimentary first premolar.

REFERENCES

Balcarcel, A. M., Sánchez-Villagra, M. R., Segura, V., & Evin, A. (2021). Singular patterns of skull shape and brain size change in the domestication of South American camelids. *Journal of Mammalogy*, *102*(1), 220–235.

Belu, C. R., Șeicaru, A., Manolescu, A., Mihai, S. A., Rosu, P. M., Dumitrescu, I., & Sîrbu, M. L. (2022). Morphological aspects of the thoracic limb skeleton in Bactrian camel. *Scientific Works. Series C. Veterinary Medicine.*, *LXVIII*(1).

Cabrera, Á. L., & Yepes, J. (1960). Mamíferos sud americanos. In *Mamíferos sudamericanos* (2nd ed.). Buenos Aires, Argentina, Ediar.

Cartajena, I. (2009). Explorando la variabilidad morfométrica del conjunto de camélidos pequeños durante el Arcaico Tardío y el Formativo Temprano en Quebrada Tulán, norte de Chile. *Revista Del Museo de Antropologia*, *2*.

Constantinescu, G., Reed, S., & Constantinescu, I. (2008). The Suspensory Apparatus and Digital Flexor Muscles of the Llama (Lama glama) 2: The Pelvic Limb. *International Journal of Morphology*, *26*.

Fan, R., Gu, Z., Guang, X., Marin, J., Varas, V., González, B., Wheeler, J., Hu, Y., Li, E., Sun, X., Yang, X., Zhang, C., Gao, W., He, J., Munch, K., Corbett-Detig, R., Barbato, M., Pan, S., Zhan, X., & Dong, C. (2020). Genomic analysis of the domestication and post-Spanish conquest evolution of the llama and alpaca. *Genome Biology*, *21*, 159.

Henry Castañeda, C., Miluska Navarrete, Z., Alberto Sato, S., & Alexander Chávez, R. (2016). Osteometría del cráneo de la alpaca adulta (Vicugna pacos). In *Revista de Investigaciones Veterinarias del Perú,* 27. 403–420.

Hershkovitz, P. (1948). Names of Mammals Dated from Frisch, 1775, and Zimmermann, 1777. *Journal of Mammalogy*, *29*(3), 272–277.

Izeta, A. (2010). Variabilidad Osteométrica de Camélidos de Sitios Arqueológicos del NOA. In *Zooarqueología a principios del siglo XXI: aportes teóricos, metodológicos y casos de estudio* (1st ed., pp. 29–38). Buenos Aires, Argentina, Ediciones del Espinillo.

L'Heureux, L., & Hernández, A. (2019). Geometric morphometrics of large South American camelids and their potential for the taxonomical identification

in archaeological sites of the northern Argentina. *Historical Biology*, *33*, 1–14.

Lesbre, F. X. (1903). Recherches anatomiques sur les camélidés. *Publications du musée des Confluences (pp. 5-195).Lyon, France.*

Moyano, S. R., Aragón, P. N. S., Alvarez, A., Ercoli, M. D., Geronazzo, L. N. L., & Fossati, J. L. G. (2022). Comparative anatomy of the skull of South American camelids. A contribution to their taxonomical identification. *Zoologischer Anzeiger*, *299*, 82–95.

Rosu, P. M., Georgescu, B., Belu, C. R., Dumitrescu, I., RAITA, ȘTEFANIA, Roșu, G. B., & Predoi, G. (2017). The morphological particularities of the thoracic limb bones at lama glama (Linnaeus, 1758) - case study. *SCIENTIFICAL PAPERS: VETERINARY MEDICINE, L(1), 173–183.*

Varas, V., Vásquez, J. P., Rivera, R., Longo, A., Valdecantos, P. A., Wheeler, J. C., Johnson, W. E., & Marín, J. C. (2020). Interbreeding among South American camelids threatens species integrity. *Journal of Arid Environments*, *181*, 104249.

Wheeler, J. C. (1995). Evolution and present situation of the South American camelidae. *Biological Journal of the Linnean Society*, *54*(3), 271–295.

Scientific Works. Series C. Veterinary Medicine. Vol. LXX (2), 2024
ISSN 2065-1295; ISSN 2343-9394 (CD-ROM); ISSN 2067-3663 (Online); ISSN-L 2065-1295

Actinobacillus pleuropneumoniae PREVALENCE AND SEROTYPE DIVERSITY IN ROMANIAN PIG FARMS

Mădălina Iulia SITEAVU[1, 2], Roxana Ionela DRUGEA[1], Elena PITOIU[2], Emilia CIOBOTARU-PÎRVU[1]

[1]University of Agronomic Sciences and Veterinary Medicine of Bucharest, Faculty of Veterinary Medicine, 105 Splaiul Independentei Street, 050097, District 5, Bucharest, Romania
[2]Synevovet, 25 Industriilor Street, Chiajna, Ilfov County, Romania

Corresponding author email: madalinaiuliasiteavu@yahoo.com

Abstract

Actinobacillus pleuropneumoniae is a bacterial porcine respiratory tract pathogen that causes porcine pleuropneumonia, with high economic consequences and distribution all over the world. This study aimed to assess the prevalence of A. pleuropneumoniae in Romanian swine farms by two methods of diagnosis: microbiological examination and Real-time PCR. Serotyping was performed on 28 bacterial isolates from 6 farms. From 1281 number of tested samples by microbiological examination, there were obtained 137 number of isolates with a positive result for A. pleuropneumoniae, with an overall prevalence of 11%. By Real-time PCR, 231 samples were tested and 100 (43%) were positive for A. pleuropneumoniae, 13/81 (16%) lung tissue samples, and 87/150 (58%) oral fluid samples. The serotyping of 28 A. pleuropneumoniae-positive cultures revealed the presence of the following serotypes: 1-9-11, 2, 3, 4, 5, 14, the most frequently encountered being serotype 2, in 10 isolates (36%) and serotype 14, in 7 isolates (25%).

Key words*: A. pleuropneumoniae, swine, prevalence, serotyping.*

INTRODUCTION

Actinobacillus pleuropneumoniae (*A. pleuropneumoniae*) is the causative agent of porcine pleuropneumonia, a disease that leads to severe economic losses in the swine industry all over the world, due to its high morbidity and mortality being one of the most important respiratory diseases in pigs (Vanni et al., 2012; Kucerova et al., 2011; Costa et al., 2011). *A. pleuropneumoniae* is considered a primary pathogen for Porcine Respiratory Disease Complex (PRDC), a multifactorial and polymicrobial disease that involves infectious factors, viral and bacterial, and non-infectious factors, such as genetics, environmental conditions, production system or management (Hansen et al., 2010; Dayao et al., 2014; van Dixhoorn et al., 2021).

The disease has different clinical forms, from peracute to subacute or chronic (Gómez-Laguna et al., 2014). *A. pleuropneumoniae* induces severe and rapidly fatal fibrinohemorrhagic and necrotizing pleuropneumonia, often detected in the postmortem inspection (Kamimura et al., 2016; Yoo et al., 2014). Animals that recover from acute infection and chronically infected animals can carry the pathogen in the nasal cavities and tonsillar crypts, becoming a source of infection and making eradication difficult (Hölzen et al., 2021).

A. pleuropneumoniae is classified as belonging to the family *Pasteurellaceae*, genus *Actinobacillus,* and is a Gram-negative, nonmotile, encapsulated, and facultative anaerobic bacteria (Pascu et al., 2022; Vanni et al., 2012). *A. pleuropneumoniae* isolates are classified based on the nicotinamide adenine dinucleotide (NAD) requirement for *in vitro* growth into biotype I (NAD-dependent) and biotype II (NAD-independent) (Zimmerman et al., 2019). There have been recognized 19 serotypes of *A. pleuropneumoniae*, based on differences in the antigenic properties of the capsular polysaccharides (Hernández-Cuellar et al., 2022; Stringer et al., 2021). Most serovars carry either the ApxI and ApxII toxin genes, which are considered more virulent, or the ApxII and ApxIII toxin genes, and in addition, all serovars carry the ApxIV toxin gene (MacInnes et al., 2008; Frey, 2019). The Apx toxins are serovar-dependent and have haemolytic and cytotoxic effects, leading to the

development of specific necrotic lung lesions (Stringer et al., 2021; Frey, 2019). ApxI is produced by serovars 1, 5a, 5b, 9, 10, 11, 14, and 16 and has strongly haemolytic and strongly cytotoxic effects; ApxII is present in all serovars except for 10 and 14, with weakly haemolytic cytotoxic effects; ApxIII is present in serovars 2, 3, 4, 6, 8, and 15, with strongly cytotoxic effects, but non-haemolytic effects; ApxIV is not characterized with haemolytic or cytotoxic effects (Sassu et al., 2018). The discovery of *A. pleuropneumoniae* toxins improved the diagnostic approaches and vaccine development for the disease (Frey, 2019).

The aim of this study was to assess the prevalence of *A. pleuropneumoniae* and its serotypes by different diagnosis methods originating from Romanian swine farms.

MATERIALS AND METHODS

Sampling. The study was conducted on samples collected between 2017 and 2022, and sent to the Synevovet laboratory. Swabs collected from affected lung tissue were used for microbiology testing. For molecular biology, lung tissues as well as oral fluid samples were analyzed. The farms are located all over the country.

The number of samples included in the study, per method, is presented in Table 1.

Table 1. Number of samples tested, per method

Microbiology	Molecular Biology	Coagglutination Serotyping
1281	**231 (81 lung tissues + 150 oral fluid)**	**28**

Isolation and Identification

Bacteriological examination. For sample culture, chocolate agar and blood agar mediums were used and incubated in anaerobic conditions (CO_2 5% thermostat) at 35-37 °C for 20-24 h. The colonies were selected based on their morphological characteristics and then identified using MALDI-TOF MS (Matrix-assisted laser desorption/ionization time-of flight mass spectrometry) technology.

Molecular biological examination. The samples were analyzed by Real-time PCR in laboratories from Spain, Germany, and from July 2020 in the Synevovet laboratory. In Synevovet laboratory, nucleic acid extraction was performed with the BioExtract Column Kit or the BioExtract Superball Kit (BioSellal, France). The viral identification was obtained using EXOone *Actinobacillus pleuropneumoniae* (Exopol, Spain), according to the manufacturer's instructions. For the amplification it was used the AriaMx Real-Time PCR System (Agilent, United States).

Serotyping. 28 positive cultures from 6 farms were selected for serotyping, which was performed in Spain by the coagglutination method and tested for serotypes 1–15.

RESULTS AND DISCUSSIONS

To assess the prevalence, two methods of diagnosis have been used: microbiological examination, a culture-dependent approach, and DNA identification by Real-time PCR. Bacteriological examination of affected lung tissue was the most frequently used method of diagnosis for this pathogen, and a number of 1281 samples were tested by this method. 137 isolates were positive for *A. pleuropneumoniae*, with an overall prevalence of 11%. The occurrence over the study period is presented in Table 2.

Table 2. Prevalence of *A. pleuropneumoniae* isolates over the study period

	2017	2018	2019	2020	2021	2022	Total
No. of tested samples	102	113	85	252	355	374	**1281**
No. of positive isolates	13	14	10	15	30	55	**137**
%	**13**	**12**	**12**	**6**	**8**	**15**	**11**

From 231 tested samples by Real-time RT-PCR, 100 (43%) were positive for *A. pleuropneumoniae*, 13 of 81 (16%) lung tissue samples, and 87 of 150 (58%) oral fluid samples (Figure 1).

The serotyping of 28 *A. pleuropneumoniae* isolates revealed the presence of the following serotypes: 1-9-11, 2, 3, 4, 5, and 14. The distribution of the serotypes is presented in Figure 2.

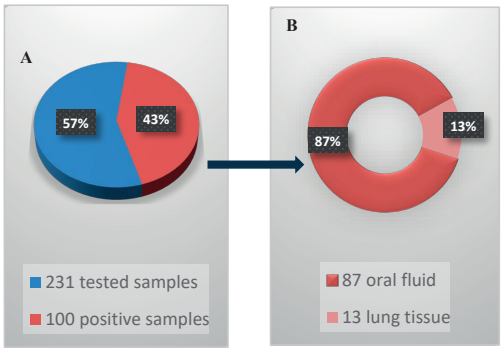

Figure 1. Total prevalence by Real-time PCR (A) and the distribution of positive samples by sample types (B)

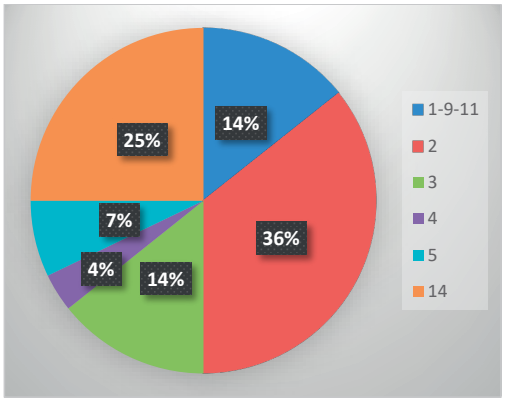

Figure 2. Serotypes revealed by typing the positive *A. pleuropneumoniae* isolates

Serotype 2 was detected in 10 isolates (36%), serotype 14 in 7 isolates (25%), serotypes 1-9-11 and 3 in 4 isolates each (14%), serotype 5 in 2 isolates (7%) and serotype 4 in 1 isolate (4%).

Serotype distribution among the farms is presented in Table 3. Four farms were positive for two or more serotypes, and two farms were positive only for serotype 2.

Table 3. Serotypes distribution among the farms

Farm	A	B	C	D	E	F
Serotype	3 and 14	2 and 1-9-11	2 and 4	2, 5, and 1-9-11	2	2

The overall prevalence was higher by Real-time PCR (43% vs. 11%). The occurrence of *A. pleuropneumoniae* in lung tissue samples was similar by microbiological examination (11%) and Real-time PCR (16%). The highest prevalence was shown in the last year of study.

The comparison of *A. pleuropneumoniae* detection by the same methods used in our study was performed in a study that tested tonsil samples, and positive results were obtained by PCR in all 12 tested pigs, but the isolation was possible in only nine samples by bacteriological examination (Chiers et al., 2002).

The high prevalence in oral fluid samples (58%) indicates a high number of carrier animals; this type of sample is also frequently used for monitoring purposes. For living animals, nasal swabs or tonsillar scraping were considered for bacteriological examination, but *A. pleuropneumoniae* resides deep in the tonsillar crypts, and commensal bacteria tend to overgrow it (Sassu et al., 2018). Bacterial detection to confirm a carrier state is not a method of choice (Gottschalk, 2015).

The distribution of *A. pleuropneumoniae* serotypes is very diverse around the world, and researchers from different countries have revealed data on the presence and prevalence of the corresponding *A. pleuropneumoniae* serotypes. Several studies indicate serotype 2 as the most prevalent in Europe (Sárközi et al., 2018; Soto Perezchica et al., 2023). Similar to our results, in a study from Italy, conducted from 2015 to 2022, the serotypes 9/11 (39.2%) and 2 (28.1%) are the most prevalent, with an increase of up to nine different serotypes isolated in the final study period (Guarneri et al., 2024). Serovar 2 was also the most prevalent (64%) in a study from Germany, followed by serovar 9/11 with about 15% of the isolates, and serovars 5, 6, 7, 8, 12, and 13 together representing 12% of the isolates; serovars 16 and 18 were also reported (Schuwerk et al., 2021). In Hungary, from 91 isolates, serotype 2 (39.5%) and serotype 13 (15.4%) were the most frequent (Sárközi et al., 2018). In Spain, the serotyping of biovar 1 isolates revealed that the most prevalent was serovar 4 (42.1%), then serovars 2 (24.3%), 9 (9.1%), and 5 (8.8%), while after the serotyping of biovar 2, serovar 7 was the most frequently encountered (68.5%), followed by serovars 2 (4.7%), 4 (4.7%), and 11 (1.6%) (Maldonado et al., 2009). Serotypes 2 (41.0%) and 4 (40.2%) were the most prevalent in a different report from Spain (Gutierrezmartin et al., 2006).

In England and Wales, serovar 8 was the most prevalent (71.7%) in the 2008–2014 period, and serovars 2, 6, 7, and 12 were also present in a smaller amount, the distribution of serotypes being similar to the 1995-2007 period (Li et al., 2016).

In a study from Japan, 95% of serovars, in decreasing order, are 2, 1, and 5 (Koyama et al., 2007). In a study from Canada on 142 *A. pleuropneumoniae* isolates, 75% belonged to serotypes 7 and serotype 5; serotypes 12, 2, 1, 8, 15, 6, 13, and 15 were present, in decreasing order (Lacouture & Gottschalk, 2020). Serovar 1 (65.4%) was predominant in Taiwan, followed by serovars 2 (34.1%) and 5 (0.5%), while in Thailand serotypes 1, 9, or 11 were predominantly found (29%), followed by serotypes 3, 6, or 8 and serotype 5a (26% each) (Assavacheep et al., 2003).

The results support the hypothesis that the prevalence of *A. pleuropneumoniae* and its serotypes may vary within pig farms worldwide. Thus, it is important to establish the serotype distribution in the pig population so that the pathogen can be monitored by implementing immunoprophylaxis programs and adding newly recognized serotypes in the construction of new vaccines (Kim et al., 2016).

Therefore, biosecurity protocols, good management practices, implementation of immunoprophylactic vaccination, development of prophylactic strategies for medicines, and good antimicrobial treatment are the main measures to control the incidence of *A. pleuropneumoniae* in pig farms (Kuchiishi et al., 2023).

CONCLUSIONS

This study brings information about the *A. pleuropneumoniae* prevalence and serotype distribution across Romanian swine farms. Two different diagnosis techniques were used for the assessment of *A. pleuropneumoniae* infection: microbiological examination and molecular biological examination, with an overall higher prevalence by PCR (43% versus 11%). Serotypes 1-9-11, 2, 3, 4, 5, and 14 were found. Serotype 2 was encountered most frequently, followed by serotype 14. Regular serotype monitoring is advisable since it provides insights into the epidemiology of *A. pleuropneumoniae* and its pathogenic capacity, the virulence being different among the serotypes. The high prevalence of *A. pleuropneumoniae* strains identified in our study leads to the need for a much larger study for serotype assessment, that includes all the serotypes known up to date, to have a better understanding of the significance of this pathogen on pig health in our country, as well as the need to strengthen the knowledge for proper surveillance and control of this disease.

ACKNOWLEDGEMENTS

We would like to thank Synevovet Laboratory and its team for their contribution to this study.

REFERENCES

Assavacheep, P., Persson, M., Luengyosluechakul, S., Watanaphansak, S., Laohasinnarong, D., Pungkhun, P., & Wallgren, P. (2003). *Actinobacillus pleuropneumoniae* in Thai pig herds. Prevalence of serum antibodies and relation to performance. *Journal of Veterinary Medicine, Series B, 50*(8), 390–395.

Chiers, K., Donné, E., Van Overbeke, I., Ducatelle, R., & Haesebrouck, F. (2002). Evaluation of serology, bacteriological isolation and polymerase chain reaction for the detection of pigs carrying *Actinobacillus pleuropneumoniae* in the upper respiratory tract after experimental infection. *Veterinary Microbiology, 88*(4), 385–392.

Costa, G., Oliveira, S., Torrison, J., & Dee, S. (2011). Evaluation of *Actinobacillus pleuropneumoniae* diagnostic tests using samples derived from experimentally infected pigs. *Veterinary Microbiology*, *148*(2–4), 246–251.

Dayao, D. A. E., Gibson, J. S., Blackall, P. J., & Turni, C. (2014). Antimicrobial resistance in bacteria associated with porcine respiratory disease in Australia. *Veterinary Microbiology, 171*(1–2), 232–235.

Frey, J. (2019). Rtx toxins of animal pathogens and their role as antigens in vaccines and diagnostics. *Toxins*, *11*(12), 719.

Gómez-Laguna, J., Islas, A., Muñoz, D., Ruiz, Á., Villamil, A., Carrasco, L., & Quezada, M. (2014). Infection dynamics and acute phase response of an *Actinobacillus pleuropneumoniae* field isolate of moderate virulence in pigs. *Veterinary Microbiology, 173*(3–4), 332–339.

Gottschalk, M. (2015). The challenge of detecting herds sub-clinically infected with *Actinobacillus pleuropneumoniae*. *The Veterinary Journal*, *206*(1), 30–38.

Guarneri, F., Romeo, C., Scali, F., Zoppi, S., Formenti, N., Maisano, A. M., Catania, S., Gottschalk, M., & Alborali, G. L. (2024). Serotype diversity and

antimicrobial susceptibility profiles of *Actinobacillus pleuropneumoniae* isolated in Italian pig farms from 2015 to 2022. *Veterinary Research, 55*(1), 48.

Gutierrezmartin, C., Blanco, N., Blanco, M., Navas, J., & Rodriguezferri, E. (2006). Changes in antimicrobial susceptibility of *Actinobacillus pleuropneumoniae* isolated from pigs in Spain during the last decade. *Veterinary Microbiology, 115*(1–3), 218–222.

Hansen, M. S., Pors, S. E., Jensen, H. E., Bille-Hansen, V., Bisgaard, M., Flachs, E. M., & Nielsen, O. L. (2010). An investigation of the pathology and pathogens associated with porcine respiratory disease complex in Denmark. *Journal of Comparative Pathology, 143*(2–3), 120–131.

Hernández-Cuellar, E., Guerrero-Barrera, A. L., Avelar-González, F. J., Díaz, J. M., Chávez-Reyes, J., & Salazar De Santiago, A. (2022). Adhesion mechanisms of *Actinobacillus pleuropneumoniae* to the porcine respiratory system and biofilm formation. *Austral Journal of Veterinary Sciences, 54*(3), 93–102.

Hölzen, P., Warnck, T., Hoy, S., Schlegel, K., Hennig-Pauka, I., & Gaumann, H. (2021). Comparison of protectivity and safety of two vaccines against *Actinobacillus pleuropneumoniae* in a field study. *Agriculture, 11*(11), 1143.

Kamimura, S., Sameshima, T., & Ito, H. (2016). Serovar and antimicrobial resistance profiles of *Actinobacillus pleuropneumoniae* isolated in Japan from 2006 to 2011. *Japan Agricultural Research Quarterly, 50*(1), 73–77.

Kim, B., Hur, J., Lee, J. Y., Choi, Y., & Lee, J. H. (2016). Molecular serotyping and antimicrobial resistance profiles of *Actinobacillus pleuropneumoniae* isolated from pigs in South Korea. *Veterinary Quarterly, 36*(3), 137–144.

Koyama, T., To, H., & Nagai, S. (2007). Isolation of *Actinobacillus pleuropneumoniae* serovar 15-like strain from a field case of porcine pleuropneumonia in Japan. *Journal of Veterinary Medical Science, 69*(9), 961–964.

Kucerova, Z., Hradecka, H., Nechvatalova, K., & Nedbalcova, K. (2011). Antimicrobial susceptibility of *Actinobacillus pleuropneumoniae* isolates from clinical outbreaks of porcine respiratory diseases. *Veterinary Microbiology, 150*(1–2), 203–206.

Kuchiishi, S. S., Ramos Prigol, S., Bresolin, E., Fernandes Lenhard, B., Pissetti, C., García-Iglesias, M.-J., Gutiérrez-Martín, C.-B., Martínez-Martínez, S., Kreutz, L. C., & Frandoloso, R. (2023). Brazilian clinical strains of *Actinobacillus pleuropneumoniae* and *Pasteurella multocida*: Capsular diversity, antimicrobial susceptibility (In vitro) and proof of concept for prevention of natural colonization by multi-doses protocol of tildipirosin. *Antibiotics, 12*(12), 1658.

Lacouture, S., & Gottschalk, M. (2020). Distribution of *Actinobacillus pleuropneumoniae* (From 2015 to June 2020) and *Glaesserella parasuis* (From 2017 to June 2020) serotypes isolated from diseased pigs in Quebec. *The Canadian Veterinary Journal = La Revue Veterinaire Canadienne, 61*(12), 1261–1263.

Li, Y., Bossé, J. T., Williamson, S. M., Maskell, D. J., Tucker, A. W., Wren, B. W., Rycroft, A. N., & Langford, P. R. (2016). *Actinobacillus pleuropneumoniae* serovar 8 predominates in England and Wales. *Veterinary Record, 179*(11), 276–276.

MacInnes, J. I., Gottschalk, M., Lone, A. G., Metcalf, D. S., Ojha, S., Rosendal, T., Watson, S. B., & Friendship, R. M. (2008). Prevalence of *Actinobacillus pleuropneumoniae*, *Actinobacillus suis*, *Haemophilus parasuis*, *Pasteurella multocida*, and *Streptococcus suis* in representative Ontario swine herds. *Canadian Journal of Veterinary Research = Revue Canadienne De Recherche Veterinaire, 72*(3), 242–248.

Maldonado, J., Valls, L., Martínez, E., & Riera, P. (2009). Isolation rates, serovars, and toxin genotypes of nicotinamide adenine dinucleotide-independent *Actinobacillus pleuropneumoniae* among pigs suffering from pleuropneumonia in Spain. *Journal of Veterinary Diagnostic Investigation, 21*(6), 854–857.

Pascu, C., Costinar, L., & Herman, V. (2022). Antibiotic resistance of *Actinobacillus pleuropneumoniae* strains in the period 2016-2022 in Romania. *Romanian Review of Veterinary Medicine, 32*(4), 40–46.

Sárközi, R., Makrai, L., & Fodor, L. (2018). *Actinobacillus pleuropneumoniae* serotypes in Hungary. *Acta Veterinaria Hungarica, 66*(3), 343–349.

Sassu, E. L., Bossé, J. T., Tobias, T. J., Gottschalk, M., Langford, P. R., & Hennig-Pauka, I. (2018). Update on *Actinobacillus pleuropneumoniae* -knowledge, gaps and challenges. *Transboundary and Emerging Diseases, 65*, 72–90.

Schuwerk, L., Hoeltig, D., Waldmann, K.-H., Valentin-Weigand, P., & Rohde, J. (2021). Sero- and apx-typing of German *Actinobacillus pleuropneumoniae* field isolates from 2010 to 2019 reveals a predominance of serovar 2 with regular apx-profile. *Veterinary Research, 52*(1), 10.

Soto Perezchica, M. M., Guerrero Barrera, A. L., Avelar Gonzalez, F. J., Quezada Tristan, T., & Macias Marin, O. (2023). *Actinobacillus pleuropneumoniae*, surface proteins and virulence: A review. *Frontiers in Veterinary Science, 10*, 1276712.

Stringer, O. W., Bossé, J. T., Lacouture, S., Gottschalk, M., Fodor, L., Angen, Ø., Velazquez, E., Penny, P., Lei, L., Langford, P. R., & Li, Y. (2021). Proposal of *Actinobacillus pleuropneumoniae* serovar 19, and reformulation of previous multiplex PCRs for capsule-specific typing of all known serovars. *Veterinary Microbiology, 255*, 109021.

van Dixhoorn, I. D. E., Te Beest, D. E., Bolhuis, J. E., Parmentier, H. K., Kemp, B., van Mourik, S., Stockhofe-Zurwieden, N., van Reenen, C. G., & Rebel, J. M. J. (2021). Animal-based factors prior to infection predict histological disease outcome in Porcine Reproductive and Respiratory Syndrome Virus- and *Actinobacillus pleuropneumoniae*-infected pigs. *Frontiers in Veterinary Science, 8*, 742877.

Vanni, M., Merenda, M., Barigazzi, G., Garbarino, C., Luppi, A., Tognetti, R., & Intorre, L. (2012). Antimicrobial resistance of *Actinobacillus pleuropneumoniae* isolated from swine. *Veterinary Microbiology, 156*(1–2), 172–177.

Yoo, A. N., Cha, S. B., Shin, M. K., Won, H. K., Kim, E. H., Choi, H. W., & Yoo, H. S. (2014). Serotypes and antimicrobial resistance patterns of the recent Korean *Actinobacillus pleuropneumoniae* isolates. *Veterinary Record, 174*(9), 223–223.

Zimmerman, J. J., Karriker, L. A., Ramirez, A., Schwartz, K. J., Stevenson, G. W., & Zhang, J. (Ed.). (2019). *Diseases of swine* (*Eleventh edition*). Wiley-Blackwell/American Association of Swine Veterinarians.

CLINICAL SCIENCES

Scientific Works. Series C. Veterinary Medicine. Vol. LXX (2), 2024
ISSN 2065-1295; ISSN 2343-9394 (CD-ROM); ISSN 2067-3663 (Online); ISSN-L 2065-1295

CONSEQUENCES OF NEOSPOROSIS ON EMBRYO TRANSFER IN BUFFALOES: REVIEW

Crina Raluca ANDREI[1, 2], Nicolae Tiberiu CONSTANTIN[1, 2], Florin Petrișor POSASTIUC[1, 3], Alexandru DIACONESCU[1], Mariana IONIȚĂ[1], Ioan Liviu MITREA[1]

[1]University of Agronomic Sciences and Veterinary Medicine of Bucharest, Faculty of Veterinary Medicine, 105 Splaiul Independentei Street, 050097, District 5, Bucharest, Romania
[2]Research and Development Institute for Bovine Balotesti, Bucharest-Ploiesti Road, km 21, 077015, Balotesti, Ilfov, Romania
[3]Department of Internal Medicine, Reproduction and Population Medicine, Faculty of Veterinary Medicine, Ghent University, Salisburylaan 133, 9820, Merelbeke, Belgium

Corresponding author email: andrei_crina_raluca@yahoo.com

Abstract

With a long history and a wide distribution across the globe, the population of buffaloes (Bubalus bubalis) increased by 1.3% annually between 2002 and 2017, suggesting rising interest in this species. The results of assisted reproduction technologies in buffaloes are not as fulfilling as in cows; for this purpose, any other possible inconvenience must be removed. Parasitic and infectious diseases represent the major cause that negatively impact biotechnologies, especially in embryo transfer, since, although the relocation of an embryo from a seropositive donor to a seronegative recipient seems to be disease-free, in 25% of cases abortion occurs. Neosporosis is a parasitosis with effects that interest mainly the female reproduction, being one of the most important abortigenic entities among buffaloes, with an average prevalence in Australia and America of approximately 88%, in Africa 68%, in Asia 54.7-66.7%, and in Europe varying from 9.1% (Czech Republic) to 68.5% (Romania). In.order.to.monitor and control neosporosis, it is imperative that all three existing categories involved in the embryo transfer process (donors, recipients, embryos) should be tested and proved to be free.

Key words*: Neospora caninum, buffalo, embryo transfer, abortion.*

INTRODUCTION

One of the primary factors contributing to abortions in cows is thought to be neosporosis. An apicomplexan parasite called *Neospora caninum* (*N. caninum*) causes abortion and can have major negative economic impact on ruminants worldwide (Reichel et al., 2013). Even if the cattle are the main intermediate affected by this protozoan parasite (Reichel et al., 2020), there are studies that certified neosporosis in small ruminants too (Lindsay & Dubey, 2020a). It seems that the buffaloes have a lower occurrence of abortion even though *N. caninum* has a high seroprevalence (Reichel et al., 2015). *N. caninum* was first found in Norway in 1984 in dogs, in the case of early death of some puppies with myositis and encephalomyelitis (Bjerkas et al., 1984). This parasite was at the beginning confused with *Toxoplasma gondii* (*T. gondii*) because both are tissue-dwelling coccidia, but they have different predominant ways of transmission. *N. caninum* is transmitted predominantly vertical, whereas *T. gondii* has mainly a horizontal transmission (Goodswen et al., 2013).

The three distinct infectious phases of *N. caninum's* life cycle include tachyzoites, tissue cysts, and oocysts. The tachyzoites cause tissue destruction, infection in the whole body of the intermediate host, and are passed through the placenta. Oocysts (10-13/10-11 µm) are shed unsporulated, by the definitive host (dog) in faeces and sporulate outside, in the environment (Lindsay & Dubey, 2020a).

CLINICAL SIGNS

In the adult buffalo females, neosporosis occurs most frequently with abortions, in any month of gestation, starting from the 3rd month until almost the end, although most appear in the 5th-6th months. Fetuses can be stillborn, living and displaying symptoms, dead in utero (resorbed,

mummified, autolyzed), or alive and clinically healthy but permanently diseased (Lindsay & Dubey, 2020a).

Apparently, despite the increased seroprevalence of this protozoan in buffalo, clinical signs (such abortion) appear to be uncommon overall, which has sparked speculation that buffalo may be naturally immune to the negative clinical effects of *N. caninum* infection. (Reichel et al., 2015).

However, this small number of abortions could also be due to poor (ineffective) reporting because they can appear in less developed economies, where it is hence less probable that abortions will be registered or carefully investigated (Reichel et al., 2015).

Clinical signs were identified only in buffalo calves that are less than two months, including neurological indicators (ataxia, diminished patellar reflex, loss of conscious proprioception), underweight, inability to rise, limb flexion or hyperextension, exophthalmos, hydrocephalus, narrowing of the spinal cord (Lindsay & Dubey, 2020a).

DIAGNOSIS

For the certain and definitive diagnosis in a case of suspected neosporosis abortion, both the examination of blood serum from the mother and the histological examination of the abortus are necessary (Lindsay & Dubey, 2020a).

PATHOLOGICAL LESIONS

In an experimental study, buffaloes were inoculated with *N. caninum*, and one day after the females aborted, they were euthanized and the lesions present were analysed. Therefore, serum leakage was observed between the foetal villi and the maternal caruncle and fibrosis, multifocal necrosis, diffuse lymphoplasmacytic infiltration within the maternal caruncle (Chryssafidis et al., 2015a).

The most common histopathological lesions observed in fetuses from the experimentally inoculated animals associated with this parasite are the nonsuppurative infiltration and multifocal necrosis (Chryssafidis et al., 2015b), such as nonsuppurative placentitis, meningoencephalitis, many mononuclear inflammatory foci in several fetal tissues, including the liver (periportal-hepatitis), kidney (interstitial nephritis), heart (epicarditis and myocarditis), and lungs (peribronchiolar interstitial pneumonia) (Konrad et al., 2012).

Compared to spontaneous abortions, epizootic abortions are more likely to result in hepatitis. Additionally, lesions are identifiable in the umbilical cord, but it is very difficult to find parasites (Lindsay & Dubey, 2020a).

IMMUNOHISTOCHEMESTRY

Immunohistochemistry is necessary since autolysing organs often only contain a small number of parasites that are not seen on a normal hematoxylin eosin stained section (Lindsay & Dubey, 2020a).

SEROLOGICAL AND MOLECULAR APPROACHES

Antibodies can be detected by various serological tests, such as Enzyme Linked Immunosorbent Assays (ELISA), Indirect Fluorescent Antibody Assay (IFA), agglutination test for Neospora. The modified ELISA method, by evaluating the avidity, can be used when it is desired to find the moment of infection. Thus, if the avidity is low, it can be considered a recent infection (Lindsay & Dubey, 2020a).

N. caninum DNA was found in the fetuses and placentas of the buffalos that had received the vaccination (Konrad et al., 2012).

The distribution of the immune cells (natural killer cells, T. cell subsets, and CD79αcy cells) in buffalo placentomes were comparable to those previously described in calves that had been experimentally infected with N. caninum during the early stages of pregnancy (Maley et al.,2006). Because of the milder lesions, there may have been fewer abortions in this species after infection (Cantón-et al., 2014).

Pro-inflammatory cytokines, such as interleukin (IL): IL-2, IL-12, and Interferon-γ (IFN-γ) are useful in preventing the growth of *N. caninum* and are necessary for the production of T helper (Th) 1-type responses, but they have the potential to be harmful and may result in the foetus being rejected or aborted (Raghupathy R, 1997). The production of IL-10 by fetal trophoblast cells overwhelms the mother's immune system and locally produces a Th2 cytokine environmental at the.maternal fetal

interface. It is well known that IL-10 inhibits IFN-γ production, which could promote the development of *N. caninum* throughout pregnancy and change the parasite-host equilibrium in their favour (Entrican, 2002).

A definite diagnosis is when antibodies are found in the serum of the foetus, but if the result is negative, this fact does not automatically imply that the foetus is not infected, since the synthesis of antibodies based on the gestational stage, exposure level, and interval between infection and abortion. While peritoneal fluid is not often used for serologic diagnosis, other fluids such as blood or serum from the fetus can be used for serologic diagnosis, peritoneal fluid is most relevant. In calves, serum collected before the first suckling can provide a conclusive congenital infection diagnosis (Lindsay & Dubey, 2020a). Apparently, serum ELISA is much more conclusive than the milk ELISA (Nasir, 2018). When a high prevalence is suspected, evaluating pooled milk samples might be a better option than testing individual milk samples (Enachescu et al., 2014).

TRANSMISSION

INTERSPECIES AND INTRASPECIES TRANSMISSION

Intermediate host: In buffaloes, vertical (transplacentally) transmission is the best known and most likely mode of transmission of neosporosis (Lindsay & Dubey, 2020a), as in the case of cows (Baillargeon et al.,.2001; de Oliveira et al., 2010; Enachescu et al., 2012). Transmission through milk or between adult intermediate hosts is impossible Since *N. caninum* has been found in semen, it seems improbable to be transmitted via sperm or embryotransfer from donor cows. Furthermore, embryotransfer is the preferred approach to avoid vertical (Lindsay & Dubey, 2020a). However, a preliminary test is necessary, in order not to transfer an embryo to a seropositive buffalo. Horizontal transmission occurs through exposure of buffaloes to food and water contaminated with oocysts (from the faeces of infected canids). Not much data is known on the regularity with which dogs in the wild shed *N. caninum* oocysts or the oocysts' resistance (Lindsay & Dubey, 2020a). The high number of oocytes (average of 290,347) produced by dogs that ingested generated by dogs who consumed the brains of adult buffaloes that were naturally infected may suggest that buffaloes are the natural intermediate hosts for *N. caninum* (Rodrigues et al., 2004).

Definitive host: The mechanism by which canids can become infected is not yet well understood. It is assumed that they become ill by ingesting infected tissues. Placental membranes can be a source, as opposed to abortions (Lindsay & Dubey, 2020a).

The dogs from more studies were clinically healthy, but they started to shed oocysts five days after consumption of bovine infected tissue (Gondim et al., 2002; Rodrigues et al., 2004). Moreover, four months after the initial incident, a dog had another oocyst shedding episode (McGarry et al., 2003).

EXPERIMENTAL TRANSMISSION

In experimental studies, from seropositive buffalo dams, in 74% of the calves, the antibodies persisted for 7 months, exhibiting the acquisition of *N. caninum* infection in neonates (Rodrigues et al., 2005). Unlike buffaloes, cows have a shorter period of time (180 days) in which the antibodies remain in bloodstream (Hietala & Thurmond, 1999).

Experimentally, tachyzoites were inoculated intravenously at 70 or 90 days of pregnancy, and until the time of slaughter (28- or 42-days post inoculation), there were no negative effects or clinical symptoms (such as fever or abortions) noted (Konrad et al., 2012).

Several methods of digestive (per os) infection have been tried. Thus, by adding 107 tachyzoites to colostrum/milk replacer, calves were shown to seroconvert, in contrast to the calves fed with placental tissue or with colostrum from *N. caninum* - infected cows (Davison et al., 2001).

ZOONOTIC RISK

It is impossible to overlook *N. caninum* zoonotic potential. It seems that primates and humans cannot be naturally infected. Nonetheless, transplacental transmission and fetal infection occurred when pregnant non-human primates were experimentally inoculated with *N. caninum* isolate from cattle (Lindsay & Dubey, 2020a).

THE IMPACT OF *N. caninum* ON GENERAL CONDITION AND EMBRYO TRANSFER

It seems that in seropositive buffaloes some blood parameters are modified, probably due to the stress that infection causes to the host. Therefore, lower monocyte count and higher blood glucose levels were observed (Nasir, 2018).

An effectively method of controlling the transmission of various pathogens in bovine is suggested by the International Embryo Transfer Society (IETS) and it involves the protection of the early stage embryos by several washing and trypsin treatments (Wrathall & Sutmöller, 1998).

Calves of seronegative recipients that received the embryos from seronegative or seropositive donors were seronegative, resulting in a 0% vertical transmission rate (Baillargeon et al., 2001). Nevertheless, regardless of the donor's status, the progeny becomes infected when recipients test positive for *N. caninum* (Baillargeon et al., 2001; de Oliveira et al., 2010). It also seems that the recipients' response to the hormonal therapy (synchronization) in order to be prepared for embryo transfer is associated with their serologic status (Diniz et al., 2016).

It seems that the incidence of the vertical transmission is directly proportional to the titers of *N. caninum* antibodies during the period of the recipients' gestation (de Oliveira et al., 2010).

SEROPREVALENCE

The global seroprevalence of *N. caninum* infection in buffalo is almost 48%, which is three to four times greater than the seroprevalence of the global herd (16.1% for dairy cattle and 11.5% for beef cattle) (Reichel et al., 2015). In Romania, the seroprevalence of Neosporosis in buffaloes was 68.5% (Bărburaș et al., 2019), and as regards cows, depending on the area of the country, the seroprevalence varied as follows: 34.6% in the Centre (Gavrea et al., 2011), 40.3% in the South (Mitrea et al., 2012) and 27.7% in the West (Imre et al., 2012). Apart from the species, the seroprevalence is also dependent on the age. Therefore, it is reasonable to assume that older animals are more prone to be exposed to oocysts at least once throughout their lifetime, the probability of being serologically positive to *N. caninum* increase by 3.5% per year in the populations of buffalo (Moore et al., 2014). In some studies (Nasir et al., 2011; Sengupta et al., 2012), the highest prevalence was found in groups of animals that were 3-5 years old, in others (Guarino et al., 2000; Fujii et al., 2001), the most infected animals belonged to the 6-8 years old groups. On the other side, Gennari et al. (2005) found no correlation between the age of the buffalos and the incidence of neosporosis. The seroprevalence all over the world during the last 10 years is presented in Table 1 and Figure 1.

Regarding the definitive hosts (Rodrigues et al., 2004) observed that while the elder dogs did not shed oocysts, the younger dogs did.

Table 1. Seroprevalence of *Neospora caninum* in buffaloes from different countries in the last 10 years (2013-2023) (selected reports)

Continent	Country	Method*	Seropositive (%)	Reference
EUROPE	Romania	ELISA	68.5	(Bărburaș et al., 2019)
	Czech Republic	IFAT/ELISA	40/20	(Bártová et al., 2017)
	Italy	ELISA	20.2	(Ciuca et al., 2020)
		ELISA	51	(Auriemma et al., 2014)
AFRICA	Egypt	IgG/IgM	13.52/6.97	(Ibrahim et al., 2021)
AMERICA	Brazil	IFAT	27.5	(A. A. Rodrigues et al., 2022)
		IFAT	35.4	(P.R.F. de Oliveira et al., 2018)
		IFAT	39	(da Silva et al., 2017)
		IFAT	36.4	(Portella et al., 2016)
		IFAT	19.1	(Brasil et al., 2015)
		ELISA	88.02	(Chryssafidis et al., 2015c)
		IFAT/ELISA	48.8/55.55	(da Silva et al., 2014)
	Argentina	IFAT	42.2	(Konrad et al., 2013)
		IFAT	43.3	(Moore et al., 2014)
	Mexico	ELISA	41.2	(Baltazar-Pérez et al., 2022)
		ELISA	44.8	(Salguero-Romero et al., 2021)
		ELISA	24.3	(Romero-Salas et al., 2017)

ASIA	India	ELISA	21.6	(Mahajan et al., 2020)
	Philippines	ELISA	46	(Mingala et al., 2020)
	Laos	ELISA	78.5	(Olmo et al., 2019)
		ELISA	68.9	(Olmo et al., 2018)
	Iran	ELISA	83	(Rezvan et al., 2019)
		ELISA	17.7	(Yagoob et al., 2017)
		ELISA	62.3	(Hamidinejat et al., 2015)
	Israel	IFAT	72.2	(Mazuz et al., 2018)
	Pakistan	Milk/serum ELISA	61.64/76.6	(Nasir, 2018)
		ELISA	42.8	(Nasir et al., 2014)
	Thailand	IFAT	9.1	(Kengradomkij et al., 2015)
	Iraq	ELISA	20	(Al-Amery et al., 2016)
OCEANIA	Australia	ELISA	88.3	(Neverauskas et al., 2015)

*IFAT (Indirect Fluorescent Antibody Test), NAT (Neospora agglutination test), DAT (direct agglutination test)

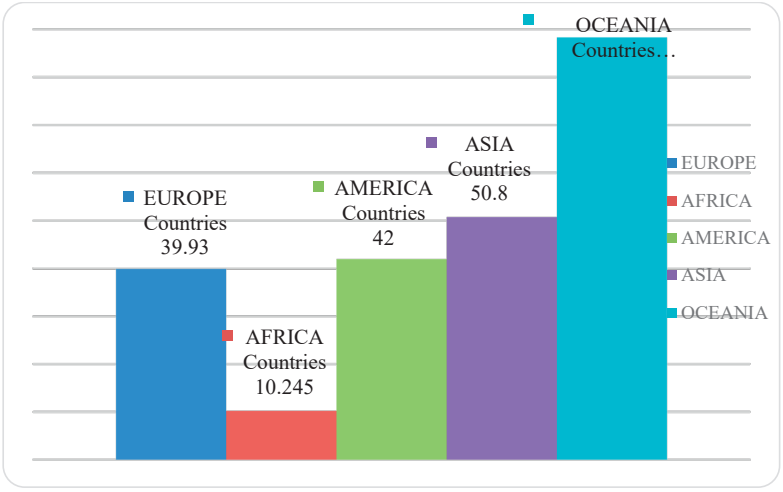

Figure 1. Over the past ten years, the average seroprevalence of *Neospora caninum* in buffaloes from various nations (2013-2023) (selected reports)

METHODS OF CONTROL

Several antimicrobial drugs have been tried *in vitro* (Dubey & Lindsay, 1996; Kim et al., 2002; Lindsay et al., 1997) or *in vivo* in mice (Gottstein et al., 2001). Drugs that eradicate the *N. caninum* bradyzoites found inside tissue cysts do not exist. Although there are no effective ways that can control neosporosis, the most popular approaches to reduce *N. caninum* infection include (Innes et al., 2002; Lindsay & Dubey, 2020b):

(1) reducing/eliminating the possibility of dogs or other possible definitive hosts to contaminate cow feed or water with feces (Mitrea et al., 2013; Paltin et al., 2020);

(2) disposal of dead calves, placentas, and aborted bovine foetuses as soon as possible;

(3) minimizing the number of infected animals that are added to the herd;

(4) culling infected animals (especially the seropositive females and/or calves from seropositive dams in order to reduce the vertical transmission). This is the current best method of prevention, but is impractical if the incidence in a herd is extremely high;

(5) embryo transfer from seropositive buffaloes to seronegative ones.

VACCINE

The creation of suitable attenuated strains that might be used as neosporosis vaccines is of great interest. The advantage of live vaccinations over killed vaccines is that the former are more likely to cause the proper cell-mediated immunity responses in the host animals. On the other hand, there are some disadvantages of the live vaccines, such as cost, limited shelf-life, need for cold storage, and potential for virulence reversal (Innes et al., 2002).

CONCLUSIONS

The recipients' serologic status is related to the risk of the new generation infection. Therefore, it is stated that the most practical manner of producing offspring free of infection with N. caninum at delivery is the transfer of embryos into seronegative recipients, as IETS recommends.

ACKNOWLEDGMENTS

This work was financially supported by the Ministry of Agriculture and Rural Development (ADER 7.2.2 - Bioeconomic solutions for the conservation of the Romanian Buffalo *in situ* through directed breeding and *ex situ* through gametes and embryos obtained using reproductive biotechnologies).

REFERENCES

Al-Amery, A. M., Faraj, A. A., & Faleh, I. B. (2016). Seroprevalence and Histopathological Study of Neosporosis in Water Buffaloes (*Bubalus bubalis*) in Baghdad City, Iraq. *Journal of Animal Health and Production*, *4*(3), 101–104.

Auriemma, C., Lucibelli, M. G., Borriello, G., De Carlo, E., Martucciello, A., Schiavo, L., Gallo, A., Bove, F., Corrado, F., Girardi, S., Amoroso, M. G., Ďegli Uberti, B., & Galiero, G. (2014). PCR detection of *Neospora caninum* in water buffalo foetal tissues. *Acta Parasitologica*, *59*(1), 1–4.

Baillargeon, P., Fecteau, G., Paré, J., Lamothe, P., & Sauvé, R. (2001). Evaluation of the embryo transfer procedure proposed by the International Embryo Transfer Society as a method of controlling vertical transmission of *Neospora caninum* in cattle. *Journal of the American Veterinary Medical Association*, *218*(11), 1803–1806.

Baltazar-Pérez, J., Utrera-Quintana, F., Camacho-Ronquillo, J., González-Garduño, R., Jiménez-Cortez, H., & Villa-Mancera, A. (2022). Prevalence of *Neospora caninum*, *Toxoplasma gondii* and *Brucella abortus* in water buffalo (*Bubalus bubalis*): Climatic and environmental risk factors in eastern and southeast Mexico. *Microbial Pathogenesis*, *173*, 105871.

Bărburaş, D., Györke, A., Ionică, A. M., Bărburaş, R., Mircean, V., & Cozma, V. (2019). Evidence of *Neospora caninum* infection in buffaloes (*Bubalus bubalis*) from Northwestern Romania. *Parasitology Research*, *118*(5), 1667–1671.

Bártová, E., Kobédová, K., Lamka, J., Kotrba, R., Vodička, R., & Sedlák, K. (2017). Seroprevalence of *Neospora caninum* and *Toxoplasma gondii* in exotic ruminants and camelids in the Czech Republic. *Parasitology Research*, *116*(7), 1925–1929.

Bjerkas, I., Mohn, S. F., & Presthus, J. (1984). Unidentified cyst-forming Sporozoon causing encephalomyelitis and myositis in dogs. *Zeitschrift Fur Parasitenkunde Parasitology Research*, *70*(2), 271–274.

Brasil, A. W. de L., Parentoni, R. N., Feitosa, T. F., Bezerra, C. de S., Vilela, V. L. R., Pena, H. F. de J., & Azevedo, S. S. de. (2015). Risk factors for *Toxoplasma gondii* and *Neospora caninum* seropositivity in buffaloes in Paraiba State, Brazil. *Revista Brasileira de Parasitologia Veterinária*, *24*(4), 459–463.

Cantón, G. J., Konrad, J. L., Moore, D. P., Caspe, S. G., Palarea-Albaladejo, J., Campero, C. M., & Chianini, F. (2014). Characterization of immune cell infiltration in the placentome of water buffaloes (*Bubalus bubalis*) infected with *Neospora caninum* during pregnancy. *Journal of Comparative Pathology*, *150*(4), 463–468.

Chryssafidis, A. L., Cantón, G., Chianini, F., Innes, E. A., Madureira, E. H., Soares, R. M., & Gennari, S. M. (2015a). Abortion and foetal lesions induced by *Neospora caninum* in experimentally infected water buffalos (*Bubalus bubalis*). *Parasitology Research*, *114*(1), 193–199.

Ciuca, L., Borriello, G., Bosco, A., D'Andrea, L., Cringoli, G., Ciaramella, P., Maurelli, M. P., Di Loria, A., Rinaldi, L., & Guccione, J. (2020). Seroprevalence and Clinical Outcomes of *Neospora caninum*, *Toxoplasma gondii* and *Besnoitia besnoiti* Infections in Water Buffaloes (*Bubalus bubalis*). *Animals*, *10*(3), 532.

da Silva, J. B., dos Santos, P. N., de Santana Castro, G. N., da Fonseca, A. H., & Barbosa, J. D. (2014). Prevalence Survey of Selected Bovine Pathogens in Water Buffaloes in the North Region of Brazil. *Journal of Parasitology Research*, *2014*, 1–4.

da Silva, J. B., Nicolino, R. R., Fagundes, G. M., Dos Anjos Bomjardim, H., Dos Santos Belo Reis, A., da Silva Lima, D. H., Oliveira, C. M. C., Barbosa, J. D., & da Fonseca, A. H. (2017). Serological survey of *Neospora caninum* and *Toxoplasma gondii* in cattle (*Bos indicus*) and water buffaloes (*Bubalus bubalis*) in ten provinces of Brazil. *Comparative Immunology, Microbiology and Infectious Diseases*, *52*, 30–35.

Davison, H. C., Guy, C. S., McGarry, J. W., Guy, F., Williams, D. J. L., Kelly, D. F., & Trees, A. J. (2001). Experimental studies on the transmission of *Neospora caninum* between cattle. *Research in Veterinary Science*, *70*(2), 163–168.

de Oliveira, V. S. F., Álvarez-Garcia, G., Ortega-Mora, L. M., Borges, L. M. F., & da Silva, A. C. (2010). Abortions in bovines and *Neospora caninum* transmission in an embryo transfer center. *Veterinary Parasitology*, *173*(3–4), 206–210.

Diniz, J., Ochoa, J. , Montoya, L. , Satrapa, R. , Okuda, L. , Pituco, E. , Marcelino, R. , & Oba (2016). Immune-serological identification of infectious agents with influence on bovine embryo transfer in the north of Brazil. *Austral Journal of Veterinary Sciences*, *48*(2).

Dubey, J. P., & Lindsay, D. S. (1996). A review of *Neospora caninum* and neosporosis. In *Veterinary Parasitology*, 67(1-2): 1-59.

Enachescu, V., Ionita, M., & Mitrea, I. (2014). Comparative study for the detection of antibodies to Neospora caninum in milk and sera in dairy cattle in southern Romania. *Acta Parasitologica*, *59*(1):5-10.

Enachescu V., Ionita, M,., Mitrea, I.L. (2012). Serosurveillance of *Neospora caninum* in farm and courtyard cattle. *Scientific Works Series C. Veterinary Medicine*, LVIII (4):136-145.

Entrican, G. (2002). Immune regulation during pregnancy and host-pathogen interactions in infectious abortion. In *Journal of Comparative Pathology* (Vol. 126, Issues 2–3, pp. 79–94).

Fujii, T. U., Kasai, N., Nishi, S. M., Dubey, J. P., & Gennari, S. M. (2001). Seroprevalence of *Neospora caninum* in female water buffaloes (*Bubalus bubalis*) from the southeastern region of Brazil. In *Veterinary Parasitology*, 99(4): 331-334.

Gavrea, R. R., Iovu, A., Losson, B., & Cozma, V. (2011). Seroprevalence of *Neospora caninum* in dairy cattle from north-west and centre of Romania. *Parasite*, *18*(4), 349–351.

Gennari, S. M., Rodrigues, A. A. R., Viana, R. B., & Cardoso, E. C. (2005). Occurrence of anti-*Neospora caninum* antibodies in water buffaloes (*Bubalus bubalis*) from the Northern region of Brazil. *Veterinary Parasitology*, *134*(1–2), 169–171.

Gondim, L. F. P., Gao, L., & McAllister, M. M. (2002). Improved production of *Neospora caninum* oocysts, cyclical oral transmission between dogs and cattle, and *in vitro* isolation from oocysts. *Journal of Parasitology*, *88*(6), 1159–1163.

Goodswen, S. J., Kennedy, P. J., & Ellis, J. T. (2013). A review of the infection, genetics, and evolution of *Neospora caninum*: From the past to the present. *Infection, Genetics and Evolution*, *13*, 133–150.

Gottstein, B., Eperon, S., Dai, W. J., Cannas, A., Hemphill, A., & Greif, G. (2001). Efficacy of toltrazuril and ponazuril against experimental *Neospora caninum* infection in mice. *Parasitol Res*.; 87(1):43-8

Guarino, A., Fusco, G., Savini, G., Di Francesco, G., & Cringoli, G. (2000). Neosporosis in water buffalo (*Bubalus bubalis*) in southern Italy. *Vet Parasitol*.; 91(1-2): 15-21

Hamidinejat, H., Seifi Abad Shapouri, M. R., Namavari, M. M., Shayan, P., & Kefayat, M. (2015). Development of an Indirect ELISA Using Different Fragments of Recombinant Ncgra7 for Detection of *Neospora caninum* Infection in Cattle and Water Buffalo. *Iranian Journal of Parasitology*, *10*(1), 69–77.

Hietala, S. K., & Thurmond, M. C. (1999). Postnatal *Neospora caninum* transmission and transient serologic responses in two dairies. *Int J Parasitol*.; 29(10):1669-76

Ibrahim, H. M., Abdel-Rahman, A. A. H., & Bishr, N. M. (2021). Seroprevalence of *Neospora caninum* and *Toxoplasma gondii* IgG and IgM antibodies among buffaloes and cattle from Menoufia Province, Egypt. *Journal of Parasitic Diseases*, *45*(4), 952–958.

Imre, K., Morariu, S., Ilie, M. S., Imre, M., Ferrari, N., Genchi, C., & Dărăbuş, G. (2012). Serological Survey of *Neospora caninum* Infection in Cattle Herds from Western Romania. *Journal of Parasitology*, *98*(3), 683–685.

Innes, E. A., Andrianarivo, A. G., Bjorkman, C., Williams, D. J. L., & Conrad, P. A. (2002). Immune responses to *Neospora caninum* and prospects for vaccination. *Trends Parasitol*.;18(11):497-504

Kengradomkij, C., Inpankaew, T., Kamyingkird, K., Wongpanit, K., Wongnakphet, S., Mitchell, T. J., Xuan, X., Igarashi, I., Jittapalapong, S., & Stich, R. W. (2015). Seroprevalence and risk factors associated with exposure of water buffalo (*Bubalus bubalis*) to *Neospora caninum* in northeast Thailand. *Veterinary Parasitology*, *207*(1–2), 156–160.

Kim, J.-T., Park, J.-Y., Seo, H.-S., Oh, H.-G., Noh, J.-W., Kim, J.-H., Kim, D.-Y., & Youn, H.-J. (2002). In vitro antiprotozoal effects of artemisinin on *Neospora caninum*. Vet Parasitol.; 103(1-2):53-63.

Konrad, J. L., Campero, L. M., Caspe, G. S., Brihuega, B., Draghi, G., Moore, D. P., Crudeli, G. A., Venturini, M. C., & Campero, C. M. (2013). Detection of antibodies against Brucella abortus, Leptospira spp., and Apicomplexa protozoa in water buffaloes in the Northeast of Argentina. *Tropical Animal Health and Production*, *45*(8), 1751–1756.

Konrad, J. L., Moore, D. P., Crudeli, G., Caspe, S. G., Cano, D. B., Leunda, M. R., Lischinsky, L., Regidor-Cerrillo, J., Odeón, A. C., Ortega-Mora, L. M., Echaide, I., & Campero, C. M. (2012). Experimental inoculation of *Neospora caninum* in pregnant water buffalo. *Veterinary Parasitology*, *187*(1–2), 72–78.

Lindsay, D. S., Butler, J. M., & Blagbum, B. L. (1997). Efficacy of decoquinate against *Neospora caninum* tachyzoites in cell cultures. *Vet Parasitol*.; 68(1-2):35-40

Lindsay, D. S., & Dubey, J. P. (2020a). Neosporosis, Toxoplasmosis, and Sarcocystosis in Ruminants: An Update. *Vet Clin North Am Food Anim Pract*. ;36(1):205-222

Lindsay, D. S., & Dubey, J. P. (2020b). Neosporosis, Toxoplasmosis, and Sarcocystosis in Ruminants: An Update. In *Veterinary Clinics of North America - Food Animal Practice* (Vol. 36, Issue 1, pp. 205–222).

Mahajan, V., Banga, H. S., & Filia, G. (2020). Patho-epidemiological and risk factor studies for detection of *Neospora*-associated abortion in cattle and buffaloes in Punjab, India. *Revue Scientifique et Technique de l'OIE*, *38*(3), 801–808.

Maley, S. W., Buxton, D., Macaldowie, C. N., Anderson, I. E., Wright, S. E., Bartley, P. M., Esteban-Redondo, I., Hamilton, C. M., Storset, A. K., & Innes, E. A. (2006). Characterization of the Immune Response in the Placenta of Cattle Experimentally Infected with *Neospora caninum* in Early Gestation. *Journal of Comparative Pathology*, *135*(2–3), 130–141.

Mazuz, M. L., Alvarez-García, G., King, R., Savisky, I., Shkap, V., Ortega-Mora, L. M., & Gutiérrez-Expósito, D. (2018). Exposure to *Neospora* spp. and *Besnoitia* spp. in wildlife from Israel. *International Journal for Parasitology: Parasites and Wildlife*, *7*(3), 317–321.

McGarry, J. W., Stockton, C. M., Williams, D. J. L., & Trees, A. J. (2003). Protracted Shedding of Oocysts of *Neospora caninum* by a Naturally Infected Foxhound. In *J. Parasitol.,* 89(3):628-30.

Mingala, C. N., Abenoja, J. A., Rivera, C. V, Balbin, M. M., Venturina, V. M., & Villanueva, M. A. (2020). *Trypanosoma evansi* and *Neospora caninum* among water buffaloes (*Bubalus bubalis*) in the Philippines. *Archives of Veterinary Science,* 25(1), 10-19.

Mitrea, I. L., Enachescu, V., & Ionita, M. (2013). *Neospora caninum* Infection in Dogs from Southern Romania: Coproparasitological Study and Serological Follow-Up. *Journal of Parasitology*, *99*(2), 365–367.

Mitrea, I. L., Enachescu, V., Radulescu, R., & Ionita, M. (2012). Seroprevalence of *Neospora caninum* Infection on Dairy Cattle in Farms from Southern Romania. *Journal of Parasitology*, *98*(1), 69–72.

Moore, D. P., Konrad, J. L., San Martino, S., Reichel, M. P., Cano, D. B., Méndez, S., Späth, E. J. L., Odeón, A. C., Crudeli, G., & Campero, C. M. (2014). *Neospora caninum* serostatus is affected by age and species variables in cohabiting water buffaloes and beef cattle. *Veterinary Parasitology*, *203*(3–4), 259–263.

Nasir, A. (2018). Prevalence of *Neospora caninum* using Milk and Serum ELISA and its Hematological Effect in Dairy Buffaloes. *Pakistan Veterinary Journal*, *38*(03), 281–285.

Nasir, A., Ashraf, M., Khan, M. S., Yaqub, T., Javeed, A., Avais, M., & Akhtar, F. (2011). Seroprevalence of *Neospora caninum* in dairy buffaloes in Lahore District, Pakistan. *Journal of Parasitology*, *97*(3), 541–543.

Nasir, A., Ashraf, M., Shakoor, A., Adil, M., Abbas, T., Kashif, M., Younus, M., & Reichel, M. P. (2014). Co-infection of water buffaloes in Punjab, Pakistan, with *Neospora caninum* and *Brucella abortus*. *Turkish Journal of Veterinary and Animal Sciences*, *38*, 572–576.

Neverauskas, C. E., Nasir, A., & Reichel, M. P. (2015). Prevalence and distribution of *Neospora caninum* in water buffalo (*Bubalus bubalis*) and cattle in the Northern Territory of Australia. *Parasitology International*, *64*(5), 392–396.

Oliveira, P. R. F. de, Soares, L. B. F., Borges, J. de M., Mota, R. A., & Pinheiro Junior, J. W. (2018). Prevalence and associated factors with *Neospora caninum* infection in female water buffaloes (*Bubalus bubalis*) from Pernambuco, Brazil. *Revista Brasileira de Parasitologia Veterinária*, *27*(4), 439–445.

Olmo, L., Dye, M. T., Reichel, M. P., Young, J. R., Nampanya, S., Khounsy, S., Thomson, P. C., Windsor, P. A., & Bush, R. D. (2018). Investigation of infectious reproductive pathogens of large ruminants: Are neosporosis, brucellosis, leptospirosis and BVDV of relevance in Lao PDR? *Acta Tropica*, *177*, 118–126.

Olmo, L., Reichel, M. P., Nampanya, S., Khounsy, S., Wahl, L. C., Clark, B. A., Thomson, P. C., Windsor, P. A., & Bush, R. D. (2019). Risk factors for *Neospora caninum*, Bovine Viral Diarrhoea Virus, and Leptospira interrogans serovar Hardjo infection in smallholder cattle and buffalo in Lao PDR. *PLOS ONE*, *14*(8), e0220335.

Paltin, A.C., Ionita, M., Bota, A., Ionescu, E.C., Mitrea, I.L. (2020). A coprological study on gastro-intestinal parasite community in water buffaloes from a Romanian farm. *AgroLife Scientific Journal*, 9(2): *200-205.*

Portella, L. P., Cadore, G. C., Lima, M. de, Sangioni, L. A., Fischer, G., & Vogel, F. S. F. (2016). Antibodies against *Neospora caninum*, *Sarcocystis* spp. and *Toxoplasma gondii* detected in buffaloes from Rio Grande do Sul, Brazil. *Pesquisa Veterinária Brasileira*, *36*(10), 947–950.

Raghupathy R. (1997). Th1-type immunity is incompatible with successful pregnancy. *Immunol Today*. ;*18*(10): 478-82.

Reichel, M. P., Alejandra Ayanegui-Alcérreca, M., Gondim, L. F. P., & Ellis, J. T. (2013). What is the global economic impact of *Neospora caninum* in cattle - The billion-dollar question. *International Journal for Parasitology*, *43*(2), 133–142.

Reichel, M. P., McAllister, M. M., Nasir, A., & Moore, D. P. (2015). A review *of Neospora caninum* in water buffalo (*Bubalus bubalis*). In *Veterinary Parasitology* (Vol. 212, Issues 3–4, pp. 75–79).

Reichel, M. P., Wahl, L. C., & Ellis, J. T. (2020). Research into *Neospora caninum*—What Have We Learnt in the Last Thirty Years? *Pathogens*, *9*(6), 505.

Rezvan, H., Khaki, A., Namavari, M., & Abedizadeh, R. (2019). An investigation of the concurrency of anti-*Neospora* antibody and parasitemia in water buffalo (*Bubalus bubalis*) in northwest of Iran. *Veterinary Research Forum: An International Quarterly Journal*, *10*(1), 79–84.

Rodrigues, A. A., Brito, D. R. B., Kono, I. S., Reis, S. S., Nino, B. de S. L., Nascimento, T. V. C., Barros, L. D. de, Garcia, J. L., & Cunha, I. A. L. da. (2022). Seroprevalence of *Neospora caninum* and risk factors associated with infection in water buffaloes (*Bubalus bubalis*) from Maranhão State, Brazil. *Veterinary Parasitology: Regional Studies and Reports*, *27*, 100661.

Rodrigues, A. A. R., Gennari, S. M., Aguiar, D. M., Sreekumar, C., Hill, D. E., Miska, K. B., Vianna, M. C. B., & Dubey, J. P. (2004). Shedding of *Neospora caninum* oocysts by dogs fed tissues from naturally infected water buffaloes (*Bubalus bubalis*) from Brazil. *Veterinary Parasitology*, *124*(3–4), 139–150.

Rodrigues, A. A. R., Gennari, S. M., Paula, V. S. O., Aguiar, D. M., Fujii, T. U., Starke-Buzeti, W., Machado, R. Z., & Dubey, J. P. (2005). Serological responses to *Neospora caninum* in experimentally and naturally infected water buffaloes (*Bubalus bubalis*). *Veterinary Parasitology*, *129*(1–2), 21–24.

Romero-Salas, D., Alvarado-Esquivel, C., Domínguez-Aguilar, G., Cruz-Romero, A., Ibarra-Priego, N., Barrientos-Salcedo, C., Aguilar-Domínguez, M., Canseco-Sedano, R., Espín-Iturbe, L. T., Sánchez-Anguiano, L. F., Hernández-Tinoco, J., & Pérez de León, A. A. (2017). Seroepidemiology of infection with *Neospora caninum*, *Leptospira*, and Bovine Herpesvirus Type 1 in water buffaloes (*Bubalus bubalis*) in Veracruz, Mexico. *European Journal of Microbiology and Immunology*, *7*(4), 278–283.

Salguero-Romero, J. L., Romero-Salas, D., Cruz-Romero, A., Alonso-Díaz, M. A., Aguilar-Domínguez, M., Sánchez-Montes, S., Lammoglia-Villagómez, M. A., Chaparro-Gutiérrez, J. J., Nogueira-Domingues, L., Pérez-de León, A. A., & Dubey, J. P. (2021). Serosurveillance and risk factors for *Neospora*

caninum infection in water buffaloes (*B. bubalis*) from central and southern Mexico. *Veterinary Parasitology: Regional Studies and Reports*, *26*, 100631.

Sengupta, P. P., Balumahendiran, M., Raghavendra, A. G., Honnappa, T. G., Gajendragad, M. R., & Prabhudas, K. (2012). Prevalence of *Neospora caninum* antibodies in dairy cattle and water buffaloes and associated abortions in the plateau of southern peninsular India. *Tropical Animal Health and Production*, *45*(1), 205–210.

Wrathall, A., & Sutmöller, P. (1998). Potential of embryo transfer to control transmission of disease. *Manual Int Embryo Transfer Soc*, 17–44.

Yagoob, G., Yaghuob, F., & Mohammad, H. A. (2017). Assessment of *Neospora caninum* seroprevalence in buffalo in Tabriz city, north-west of Iran. *Buffalo Bulletin*, 36(2): 379-384.

Scientific Works. Series C. Veterinary Medicine. Vol. LXX (2), 2024
ISSN 2065-1295; ISSN 2343-9394 (CD-ROM); ISSN 2067-3663 (Online); ISSN-L 2065-1295

ANALYSIS OF ETIOLOGICAL, CLINICAL MANIFESTATIONS AND GROSS LESIONS ASSOCIATED WITH YOUNG PIGEON DISEASE IN A PIGEON LOFT OUTBREAK

Andrei Gabriel CĂPRIȚĂ[1], Denise Maria DINA[2], Mihai MĂCINIC[1], Doina DANEȘ[1]

[1]University of Agronomic Sciences and Veterinary Medicine of Bucharest, Faculty of Veterinary Medicine, 105 Splaiul Independentei Street, 050097, District 5, Bucharest, Romania
[2]Emergency University Hospital Bucharest, 169 Splaiul Independentei Street, District 5, Bucharest, Romania

Corresponding author email: c_andrei_gabriel@yahoo.com

Abstract

Young Pigeon Disease Syndrome (YPDS) is a multifactorial condition that poses a significant health challenge to young pigeons, particularly those between the ages of 3 and 12 weeks post-weaning. In rare cases, it can also affect older pigeons. This syndrome is characterized by high morbidity and mortality, leading to considerable losses in the pigeon breeding and racing industries. The primary viral agent responsible for YPDS is pigeon circovirus (PiCV), known for its immunosuppressive effects, which increase susceptibility to secondary infections caused by Escherichia coli and other opportunistic pathogens like Candida albicans and Trichomonas gallinae. Additionally, pigeon aviadenovirus (PiAdV) and Columbid herpesvirus-1 (CoHV-1) are associated with the syndrome, contributing to its complex pathogenesis. Clinical signs of YPDS are non-specific and include lethargy, weight loss, vomiting, diarrhoea, and respiratory distress. The disease is most severe in juvenile pigeons, with rapid progression often leading to death within 3 to 5 days, while adult birds that develop clinical signs may take up to 8 days to die.

Key words*: pigeon, young pigeon disease syndrome, pigeon circovirus, pigeon adenovirus, co-infection.*

INTRODUCTION

Young Pigeon Disease Syndrome (YPDS) represents a significant health challenge in the avian world, particularly affecting young pigeons between the ages of 3 to 12 weeks (Raue et al., 2005). This multifactorial disease is characterized by high morbidity and mortality rates, often leading to severe losses in pigeon breeding and racing industries (Raue et al., 2005). The ethology of YPDS is complex, involving various viral, bacterial, and parasitic infections that can compromise the immune system of affected birds (Raue et al., 2005).

Among the viral agents implicated, the pigeon circovirus (PiCV) has emerged as a primary contributor to the syndrome, due to its immune-suppressive properties, increasing susceptibility to secondary infections and overall poor health outcomes in young pigeons (Sahindokuyucu et al., 2022; Stenzel & Pestka, 2014; Cságola et al., 2011).

Furthermore, there is pigeon aviadenovirus (PiAdV) and Columbid herpesvirus-1 (CoHV-1) that can also contribute to the onset and progression of YPD (Sahindokuyucu et al., 2020; Abdulrasool et al., 2022).

Pigeon circovirus (PiCV) was first identified as a potential cause of YPDS in the early 1990s, prompting extensive research into its role in disease pathogenesis. PiCV is now recognized as globally widespread, frequently detected in flocks with clinical signs of YPDS (Stenzel & Pestka, 2014; Stenzel & Koncicki, 2017). Studies have also documented significant genetic diversity among PiCV strains, suggesting varying levels of virulence and pathogenicity, which complicates both diagnosis and treatment (Cságola et al., 2011; Stenzel et al., 2014).

In addition to viral agents, bacterial pathogens like Salmonella spp. and Escherichia coli contribute to the progression of YPDS. These bacteria can worsen clinical symptoms, leading to severe gastrointestinal and systemic infections in young pigeons (Stenzel et al., 2014; Al-jumaili, 2023). Mixed infections involving multiple pathogens are associated with increased disease severity, highlighting the need for a comprehensive diagnostic approach by veterinarians (Hamouda et al., 2017; Nath et al., 2023).

Among the diverse pathogens associated with YPDS, adenoviruses have emerged as significant contributors to the disease's pathogenesis.
Adenoviruses are non-enveloped, double-stranded DNA viruses that can infect various avian species, including pigeons. Their involvement in YPDS has attracted growing research attention, particularly due to the intricate interactions between adenoviral infections and other co-infecting pathogens, such as bacteria and additional viruses (Vereecken et al., 1998).
The clinical presentation of adenoviral infections in pigeons varies significantly based on the host's age and immune status. In juvenile pigeons, adenovirus infections often result in severe gastrointestinal disturbances, immune-suppression and systemic illness, key features of YPDS. In pigeons older than one year, adenovirus infections typically lead to necrotizing hepatitis (Vereecken et al., 1998).
The clinical manifestations of YPDS range from lethargy and weight loss to severe respiratory and neurological symptoms.
Without prompt intervention, the disease progresses rapidly, often leading to high mortality (Sahindokuyucu et al., 2022; Stenzel & Koncick, 2017).
Effective management of YPDS involves identifying causative agents and implementing preventive strategies, such as vaccination and biosecurity measures, to minimize outbreak risks in pigeon lofts (Stenzel et al., 2012; Stenzel & Koncicki, 2017).
Research has shown that environmental stressors related to racing and breeding can weaken immune responses in young pigeons, increasing their susceptibility to infections and YPDS (Zigo et al., 2017; Zigo et al., 2019). Additionally, the presence of zoonotic bacteria underscores the public health implications of YPDS, beyond its impact on avian health (Teske et al., 2013; Karim et al., 2020).

MATERIALS AND METHODS

Research materials

Samples were collected over one year (2023-2024) from a breeding facility in southwest Bucharest. Ten pigeons 7 males and 3 females were examined, including 7 juveniles (3 to 12 weeks old) and 3 pigeons older than 1 year. All pigeons were closely monitored to prevent external factors or unauthorized medications from affecting the study.
Ante-mortem the pigeons were closely monitored for any sign of illness. Initially, we were looking for birds that refused to eat with all the others, birds that had a bad posture or any respiratory distress. Clinical examination continued without removing the birds from the loft for better understanding their behavior in distress.
The necropsy began with an examination of external signs such as fluid discharge, pectoral muscle condition, and feather abnormalities. Upon entering the coelomic cavity, attention focused on the macroscopic appearance of the viscera, particularly the liver, while all internal organs were examined for notable findings.

Sampling method

Real time PCR was used to identify the viral portion of disease like pigeon circovirus (PiCV), pigeon aviadenovirus (PiAdV), Columbid herpesvirus-1 (CoHV-1) and also for the diagnosis of *Trichomonas galinae*. For RT-PCR testing, cloacal swabs (sterile swabs without medium) were taken, and also pieces of liver, spleen, trachea, heart, lung, kidneys, small and large intestines were preserved in tightly sealed sterile containers and sent. The PCR test was performed in an external laboratory and the sample collection, and transport were done accordingly to the laboratory's recommendations.
Swabs for bacteriological and mycological cultures were collected, and tissue samples from previously excised organs were used for aerobic, anaerobic, and mycological cultures.
For the detection of aerobic bacteria and respiratory tract swabs, Columbia agar, Endo agar, and Chocolate agar were used.
For stool samples, Columbia agar, MacConkey agar, Hektoen agar, and XLD agar were employed. Additionally, XLD and Chromagar were used for the enrichment of *Salmonella* detection.
For the cultivation of anaerobic bacteria, we used Schaedler and Schaedler KV agar plates.
The methodology for mycological cultures varied based on the sample source:
For respiratory tract samples, Sabouraud agar supplemented with chloramphenicol and gentamicin, as well as malt extract agar, were used.

For stool samples, Sabouraud agar with gentamicin and chloramphenicol, along with Chromagar for yeasts, were employed.
Matrix-Assisted Laser Desorption Ionization–Time of Flight Mass Spectrometry (MALDI-TOF MS), a valuable tool in veterinary medicine, was utilized for the identification of various bacterial and fungal species.

RESULTS AND DISCUSSIONS

The general clinical signs observed in all affected birds included depression, lethargy, reluctance to fly, and varying degrees of weight loss, some leading to emaciation (Figure 3). Other symptoms were vomiting, dark-green droppings, diarrhoea, and an enlarged crop exhibiting signs of stasis with undigested food and water. A fluid-filled crop, as described by Rüdiger Raue and Volker Schmidt, was also noted (Raue et al., 2005).
Additionally, respiratory distress and neurological signs, including an abnormal forward position of the head and neck, were observed in rare cases (Figure 1).

Figure 1. Abnormal position of the head without tremor

Clinical signs varied, with pigeons aged 3 to 12 weeks post-weaning experiencing more severe symptoms and faster progression to death, typically within 2 to 5 days. In contrast, adult pigeons could survive up to 7 or 8 days, often showing severe pectoral muscle emaciation. Most fatalities occurred at night, with birds found in secluded areas of the loft, positioned forward with extended necks and wings by their sides. Gross lesions observed during necropsy are detailed in Table 1.

Table 1. Gross lesions observed during necropsy

Organs and systems	Types of gross lesions	Proportion with lesion
Gastrointestinal system	○ Green to yellow fluid in the crop, proventriculus, ventriculus and intestin.	9/10
	○ Enlarged, fluid with mucus filled crop.	5/10
	○ Proventriculitis, with numerous hemorrhagic spots on the entire mucosa.	7/10
	○ Hemorrhages on the ventricular mucosa.	4/10
	○ Enteritis.	9/10
	○ Necrotic hemorrhagic enteritis.	6/10
	○ Elevated gas content.	2/10
	○ Intestinal obstruction due to a granulomatous mass formation.	1/10
Lungs and air sacs	○ Air sacs covered with yellow mucus.	7/10
	○ Fibrinous airsacculitis.	8/10
	○ Accumulation of yellowish serous fluid in thoracic air-sacs.	4/10
	○ Bilateral enlargement of lungs.	4/10
	○ Fibrosed and dark-red in color lungs.	2/10
	○ Pulmonary hemorrhages.	4/10
Liver and pancreas	○ Liver friable with mild to severe enlargement.	7/10
	○ Discoloration of the liver and pancreas from yellow to red-black.	5/10
	○ Liver and pancreas with diffuse punctate to sever hemorrhages.	7/10
	○ Multifocal whitish lesions in pancreas.	4/10
	○ Necrosis of the liver and pancreas.	9/10
Heart	○ Multifocal submiliar white lesions in the myocardium.	2/10
	○ Serous pericarditis with a clear fluid or cloudy yellow liquid.	4/10
Kidneys	○ Diffuse green in colour.	3/10
	○ Diffuse yellow in colour.	2/10
Lymphatic system	○ Splenomegaly.	3/10
	○ Necrotic hemorrhage of the spleen.	4/10
	○ Atrophy of the Bursa of Fabricius, in some cases severe.	4/10

Cloacal feathers were clumped with faecal matter, and some birds exhibited yellow-green secretions from the oral and nasal cavities (Figure 2).

Figure 2. Yellow watery liquid with mucus flowing from the oral cavity post-mortem

Various degrees of emaciation of the pectoral muscles were observed during the external examination (Figure 3 a). Additionally, some birds were in the process of moulting, with new follicles emerging. Post-mortem examination revealed a significant loss of subcutaneous connective adipose tissue and generalized muscle atrophy (Figure 3 a, b).

Figure 3.(a) Deformation of the sternum together with sternal amyotrophy. (b) Sternal amyotrophy

In all examined cases, liver involvement was substantial, with hepatomegaly being the most common finding, accompanied by discoloration, increased friability and haemorrhagic necrosis (Figure 4). In several cases, multifocal whitish lesions were identified in the pancreas (Figure 4).

Focal haemorrhages on the ventricular mucosa (Figure 5) were observed in some cases; however, haemorrhagic proventriculitis, characterized by numerous haemorrhagic spots dispersed across the entire mucosal surface (Figure 5), was more frequently documented. The proventriculus and ventriculus were often filled with a yellow-green fluid and mucus.

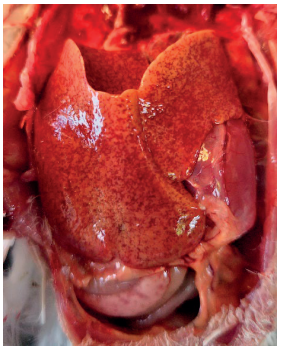

Figure 4. Liver with hepatomegaly, widespread discoloration indicating severe necrosis and diffuse punctate hemorrhages, which can also be observed on the pancreas

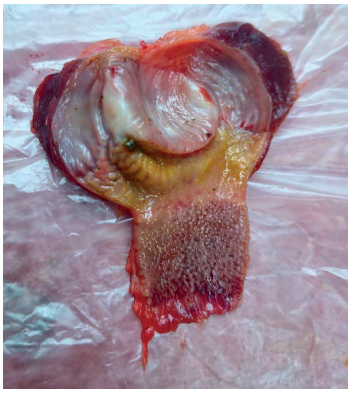

Figure 5. Proventriculitis with numerous hemorrhagic spots on the entire mucosa and focal hemorrhages on the ventricular mucosa

Results following necropsy and laboratory examination are presented in Tabel 2.

Out of 10 pigeons, only 1 was not positive for PiCV and it was a 3 years old female. It showed poor condition for a few weeks without any concrete signs of illness. Once clinical signs appeared, the bird's condition deteriorated rapidly, leading to death within 4 days, marked by progressive weight loss. Some articles suggest that pigeons older than 1 year may be able to clear the infection without exhibiting clinical signs (Abdulrasool et al., 2022).

Table 2. Age-related distribution of pathogens

Pathogen	3-12 weeks old	older than 1 year
PiCV	7/7	2/3
PiAdV	2/7	0/3
CoHV-1	0/7	0/3
Escherichia coli	7/7	3/3
Enterococci	3/7	0/3
Enterobacter hormaechei	1/7	0/3
Chlamydophila spp.	1/7	0/3
Aeromonas caviae	1/7	0/3
Acinetobacter baumannii	1/7	0/3
Candida sp.	4/7	2/3
Aspergillus flavus	0/7	1/3
Mucor sp.	1/7	0/3
Trichomonas gallinae	1/7	0/3
Ascaridia columbae	0/7	2/3

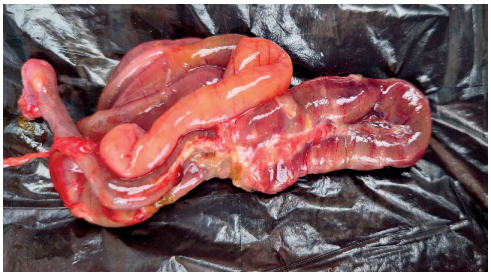

Figure 6. Impacted intestinal tract with *Ascaridia columbae*. Necrotic hemorrhagic enteritis and pancreatitis

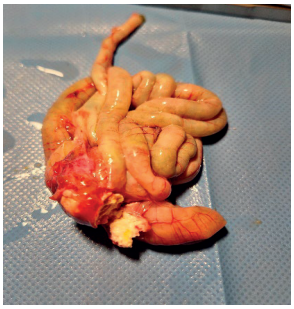

Figure 7. Intestinal tract showing enteritis and elevated gas content with a yellowish white granulomatous mass formation in the duodenum adhering to the cell wall causing obstruction

Haemorrhagic enteritis and pancreatitis (Figure 6) were frequently observed among the lesions. Additionally, the pancreas exhibited necrosis, while intestinal stiffness (Figure 6) was also noted, primarily due to parasitic infestations, including *Ascaridia columbae*.

In one instance, a yellowish granulomatous tumour mass adhering to the intestinal wall (Figure 7) was observed, resulting in intestinal transit obstruction. The intestinal tract was distended with gas, and the intestinal wall appeared thin, displaying signs of inflammation and haemorrhage (Figure 7).

The pericardium, along with the thoracic air sacs, exhibited inflammation, accompanied by moderate to substantial accumulations of transparent or slightly yellowish serous fluid (Figure 8). Furthermore, multifocal submiliary white lesions were observed in the myocardium on two separate occasions.

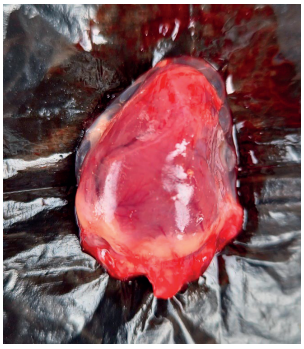

Figure 8. Serous pericarditis with a clear fluid

In relation to the lungs, gross lesions such as mild bilateral enlargement and the presence of a fibrinous covering on the serosal surfaces (Figure 9 a, b) were observed with increased frequency. Additionally, severe bilateral haemorrhages (Figure 9 a, b) were noted, originating centrally and progressively extending radially to involve the entire lung (Figure 9 b).

In one case, pulmonary congestion caused a complete discoloration of the lungs, rendering them dark red internally (Figure 9 a), while a fibrinous layer on the serosal surfaces contributed to a white-grey appearance (Figure 9 a).

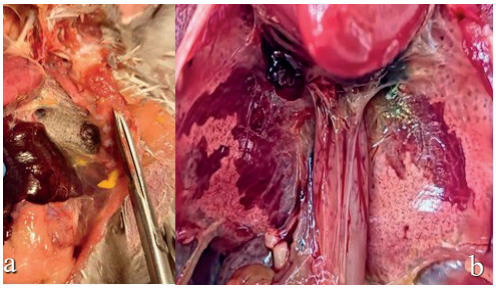

Figure 9. Pericarditis and airsacculitis with a yellowish, fibrinous covering, present on the serosal surfaces of the air sacs and heart. (a) The lung is fibrosed and gray in color on the outside and on the inside the color is dark-red indicating congestion and edema. (b) The lung shows bilateral, extensive hemorrhagic areas, with irregular edges localized predominantly centrally

Together with the liver, the air sacs exhibited the most frequent pathological changes. Predominantly, these alterations included fibrinous aerosacculitis characterized by enhanced adhesion of the air sacs to adjacent cavity organs and the accumulation of yellowish serous fluid (Figure 10). In severe cases, a yellowish, fibrinous exudate was observed on the serosal surfaces of the air sacs and various organs. These lesions are indicative of an *E. coli* infection.

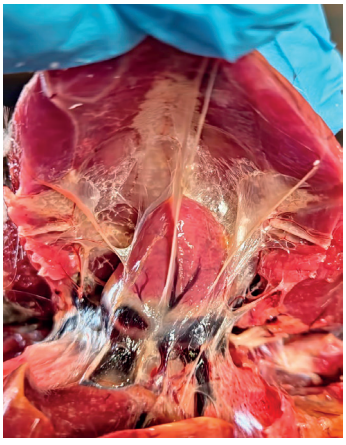

Figure 10. Fibrinous airsacculitis and pericarditis with increased adhesion of the air sacs to cavity organs and accumulation of yellowish serous fluid

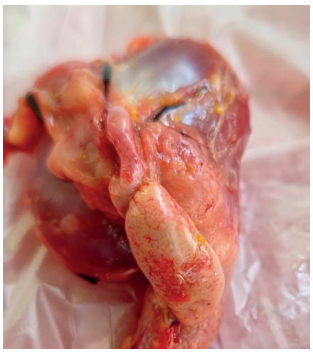

Figure 11. Splenomegaly with discoloration and petechial hemorrhages

The spleen was generally of normal size; however, in some cases, it was observed to be enlarged and exhibited a yellowish-white discoloration, with or without petechial hemorrhages (Figure 11). In certain instances, despite appearing of normal size, necrosis was present.

Examination of the Bursa of Fabricius revealed atrophy, with some cases demonstrating severe atrophy, thereby underscoring the immunosuppressive impact of circovirus.

Figure 12. Opened intestine with underlying hemorrhagic enteritis showing yellowish content and presence of *Ascaridia* worms

Several birds were affected by more than one secondary pathogen, either bacteria, fungi or parasites (Figure 12), highlighting the multifactorial nature of this pathology and its complexity.

CONCLUSIONS

This study confirms that YPDS primarily affects juveniles between 3 and 12 weeks post-weaning, with non-specific clinical signs.

Adults can also develop symptoms, which can sometimes lead to death.

Major stressors such as transportation, overcrowding, and moulting can contribute to the onset and spread of the disease.

PiCV was identified as the primary viral pathogen in 9 out of the 10 cases, sometimes co-infecting with PiAdV, while CoHV-1 was not detected. *Escherichia coli* was the most common co-pathogen, isolated from all samples, while other opportunistic pathogens like *Candida albicans* and *Trichomonas gallinae* suggested a compromised immune system.

The study highlights the multifactorial nature of YPDS, with PiCV playing a key role in its pathogenesis.

REFERENCES

Abdulrasool, M. T. A., Khaleefah, A., & Najem, H. A. (2022). A brief review of pigeon circovirus infection worldwide. *Multidisciplinary Reviews*, *5*(4), 2022018-2022018.

Al-jumaili, M. (2023). Pharmacokinetic profile of norfloxacin in pigeons. *Revista De Ciências Agroveterinárias*, 22(3), 470-474.

Cságola, A., Lőrincz, M., Tombácz, K., Wladár, Z., Kovács, E., & Tuboly, T. (2011). Genetic diversity of pigeon circovirus in hungary. *Virus Genes*, 44(1), 75-79.

Hamouda, E., Mohamed, N., Eid, A., Ismail, A., El-Sisi, M., Hassanin, O., … & Abou-Hashem, N. (2017). Utilization of rt-pcr and restriction enzyme analysis in detection and differentiation of pigeon paramyxovirus-1 and newcastle disease virus in pigeons. *Zagazig Veterinary Journal*, 45(Supplementary 1), 37-47.

Karim, S., Islam, M., Sikder, T., Rubaya, R., Halder, J., & Alam, J. (2020). Multidrug-resistant *Escherichia coli* and *Salmonella* spp. isolated from pigeons. *Veterinary World*, 13(10), 2156-2165.

Nath, B., Das, S., Tidd, N., Das, T., Forwood, J., & Raidal, S. (2023). Lesions and viral loads in racing pigeons naturally coinfected with pigeon circovirus and columbid alphaherpesvirus 1 in australia. *Journal of Veterinary Diagnostic Investigation*, 35(3), 278-283.

Raue, R., Schmidt, V., Freick, M., Reinhardt, B., Johne, R., Kamphausen, L., ... & Krautwald-Junghanns, M. E. (2005). A disease complex associated with pigeon circovirus infection, young pigeon disease syndrome. *Avian Pathology*, *34*(5), 418-425.

Sahindokuyucu, I., Turkmen, M. B., Antepliogˇlu, T., Alcigir, E., YAZICI, Z., Barry, G., ... & Kul, O. (2020). Young Pigeon Disease Syndrome (YPDS) in Turkish Pigeons (*Columba livia domestica*) stemming from coinfection with Pigeon aviadenovirus A and Pigeon circovirus: The first isolation and molecular characterization. *Authorea Preprints*.

Sahindokuyucu, I., Yazıcı, Z., & Barry, G. (2022). A retrospective molecular investigation of selected pigeon viruses between 2018–2021 in turkey. *Plos One*, 17(8), e0268052.

Stenzel, T. and Koncicki, A. (2017). The epidemiology, molecular characterization and clinical pathology of circovirus infections in pigeons – current knowledge. *Veterinary Quarterly*, 37(1), 166-174.

Stenzel, T. and Pestka, D. (2014). Occurrence and genetic diversity of pigeon circovirus strains in poland. *Acta Veterinaria Hungarica*, 62(2), 274-283.

Stenzel, T., Bancerz-Kisiel, A., Tykałowski, B., Smiałek, M., Pestka, D., & Koncicki, A. (2014). Antimicrobial resistance in bacteria isolated from pigeons in Poland. *Polish Journal of Veterinary Sciences*, 17(1), 169-171.

Stenzel, T., Pestka, D., Tykałowski, B., Smiałek, M., & Koncicki, A. (2012). Epidemiological investigation of selected pigeon viral infections in poland. *Veterinary Record*, 171(22), 562-562.

Stenzel, T., Piasecki, T., Chrząstek, K., Julian, L., Muhire, B., Golden, M., … & Varsani, A. (2014). Pigeon circoviruses display patterns of recombination, genomic secondary structure and selection similar to those of beak and feather disease viruses. *Journal of General Virology*, 95(6), 1338-1351.

Teske, L., Ryll, M., Rubbenstroth, D., Hänel, I., Hartmann, M., Kreienbrock, L., … & Rautenschlein, S. (2013). Epidemiological investigations on the possible risk of distribution of zoonotic bacteria through apparently healthy homing pigeons. *Avian Pathology*, 42(5), 397-407.

Vereecken, M., De Herdt, P., & Ducatelle, R. (1998). Adenovirus infections in pigeons: a review. *Avian Pathology*, *27*(4), 333-338.

Zigo, F., Takáč, L., Zigová, M., & Takáčová, J. (2017). Changes in bacterial microflora in young carrier pigeons during the race season. *Int J Avian Wildlife Biol*, *2*, 41-4.

Zigo, F., Ondrašovičová, S., Zigová, M., Takáč, L., & Takáčová, J. (2019). Influence of the flight season on the health status of the carrier pigeons. *Int J Avian & Wildlife Biol*, *4*(2), 26-30.

Scientific Works. Series C. Veterinary Medicine. Vol. LXX (2), 2024
ISSN 2065-1295; ISSN 2343-9394 (CD-ROM); ISSN 2067-3663 (Online); ISSN-L 2065-1295

THE IMPORTANCE OF CLINICAL EXAMINATION FOR THE DIAGNOSIS OF HEART DISEASE AND LEFT CONGESTIVE HEART FAILURE SYNDROME IN DOGS AND CATS - A REVIEW

Maria Beatrice PUSTA (CRISTESCU), Alice Mihaela ISTRATE (RĂDULESCU), Lucian IONIŢĂ

University of Agronomic Sciences and Veterinary Medicine of Bucharest, Faculty of Veterinary Medicine, 105 Splaiul Independentei Street, 050097, District 5, Bucharest, Romania

Corresponding author email: beatricecristescu@yahoo.com

Abstract

The aim of this systematic review is to present the clinical examination of the cardiovascular system in dogs and cats. The heart is an organ deeply interconnected with the hemodynamic of the entire body. Anamnesis and physical examination allow early diagnosis of heart disease. The stages of the examination are represented by inspection, palpation, percussion, auscultation and thermometry. This can establish the treatment schedule, prolonging the patient's life and improving its quality. Important clinical changes in left congestive heart failure syndrome must be quickly and correctly identified: respiratory distress, cough, syncope, heart murmur, or gallop sound. This allows the establishment of emergency therapeutic protocol. Clinical monitoring is still important for both the clinician and the owner. It shows the effectiveness of the action of drugs and the risk of cardiovascular decompensation, requiring adaptation of therapy.

Key words*: clinical, cardiovascular, dyspnea, murmur, heart failure.*

INTRODUCTION

Despite the increasing diversity and complexity of cardiac diagnostic examinations, the information obtained from the medical history and clinical examination have undeniable value. History and clinical examination offer diagnostic clues and guide the initial therapy in emergency situations involving cardiac, respiratory and vascular diseases. This information can allow the diagnosis of cardiac pathology, help to differentiate or associate the condition to respiratory pathology, prioritize diagnostic tests, and provide objective evidence of a therapeutic response.

MEDICAL HISTORY

In the first stage, identifies age, sex and breed (Keene et al., 2019), sometimes referred to as the "signalment". The history (anamnesis) should include key questions that include: (1) the reason for the consultation; (2) the onset of signs; (3) duration of the medical problem; (4) the evolution of signs; (5) the vaccination and heartworm prophylaxis history; (6) current medications and the animal's response to therapy; and finally, (7) the owner's ability to administer the drugs. Additional questions that further define the major problems should also be directed to the owner. For example, useful information about respiratory difficulties might include its relationship to rest or exertion; an onset that is sudden or gradual; and any association with audible respiratory noise that might indicate a major airway obstruction.

Important information highlighted in the medical history report is particularly relevant to the pathology of the cardiorespiratory system. Increased respiratory rate (tachypnea), respiratory distress (hyperpnea or dyspnea), coughing, exercise intolerance, difficulty in sleeping, and general signs of illness are common to both cardiac and respiratory disorders. Abnormal respiratory patterns are usually overlooked by owner and are discussed further under "Clinical Examination".

Further information to determine from the history or direct observation includes: (1) anorexia or decreased appetite; (2) weight loss or cachexia; (3) abdominal distention (hepatomegaly or ascites); (4) diarrhea (from severe right heart failure with intestinal edema and potentially enteropathy with protein loss);

(5) the presence of hemoglobinuria (found in caval syndrome of dirofilariosis); (6) hemoptysis (in pulmonary thromboembolism, pneumonia, coagulation disorders including toxicities, foreign bodies, and neoplasia); (7) exertional collapse, syncope or seizures; and (8) signs of hind leg instability or sudden onset of paresis/paralysis (Smith et al., 2015).

Syncope can be to cardiac, vascular, or respiratory origin. When due to respiratory disorders exertional collapse or syncope is often associated with pulmonary arterial hypertension, severe bronchopulmonary or pleural space diseases, or obstructive upper respiratory diseases (especially in brachycephalic breeds). While less common, syncope in respiratory disease can develop from low arterial oxygen concentration, insufficient cardiac output (pulmonary arterial hypertension), or potentially from activation of reflex bradycardia as with vasovagal syncope (Kittleson, 1998).

Cardiogenic syncope has many causes and some of these might become more relevant based on the history and clinical examination. For example, a cardiogenic mechanism is suggested by signs of reduced cardiac output as in a dog with dilated cardiomyopathy or one with severe mitral regurgitation. Reflex-mediated (vasovagal) syncope can occur in dogs with structural heart disease, especially with sudden excitement or exertion. Cardiac brady- and tachyarrhythmias are a common reason for syncope and might be detected during clinical examination. Examples include sinus arrest, complete atrioventricular block, or sustained ventricular tachycardia. Abnormal auscultation might suggest pulmonary hypertension or a congenital cardiac defect associated with syncope such as subaortic stenosis, pulmonary stenosis, or tetralogy of Fallot (Tilley et al., 2008). Often there are multiple factors, as with ventricular arrhythmia in a dog with dilated cardiomyopathy.

Syncope with a cardiogenic origin is associated with sudden loss of consciousness, short duration (usually less than one minute), and rapid recovery. The syncope is often induced by exercise or excitement/stress. Sometimes the event is preceded by vocalization. Pre- and postictal behavioral abnormalities are absent. Urination can occur although loss of feces is uncommon. Tonic-clonic muscle contractions, facial fits, and hypersalivation are not typical of cardiac syncope. These aspects help to differentiate canine syncope from seizure disorders. Syncope in cats is more challenging to assess and often shares features of neurological disease (Penning V.A., 2009). One useful recommendation is to videorecord the animal during the crisis as it can provide valuable clues which complete the history and physical examination.

Exertional weakness and especially **intolerance to exercise** are sensitive though not specific signs of cardiac disease. Often, the owners do not report exercise intolerance. In some cases, the dog is relatively sedentary, as with many English Bulldogs (Chong, 2017). Cats sleep almost all the time with only short periods of high activity so owners might not identify their clinical signs until they become severe. Furthermore, dogs are excellent athletes and are not commonly stressed to the maximal exercise capacity that might reveal underlying heart disease.

Moreover, these findings with exercise are nonspecific, and can develop with respiratory, musculoskeletal, neurologic, and some systemic diseases. Other conditions that might show intolerance to effort can include anemia, endocrinologic (adrenal diseases, thyroid diseases, diabetes mellitus), and some metabolic diseases (including hypokalemia).

Coughing is probably the most common symptom reported by owners of dogs with heart disease. However, frequently the cough is not due to cardiac disease. Potential etiologies of a "cardiac" cough in dogs include alveolar pulmonary edema and marked compression of the left principal bronchus between the left atrium and the aorta. The importance of bronchial compression is debated, but most studies have either focused on patients undergoing bronchoscopy with a high likelihood of concurrent bronchitis and bronchomalacia, or else relied only on radiographs to exclude bronchitis (which is not sufficient). Clearly many dogs with chronic valve disease also have concurrent tracheal disease, chronic bronchitis, or pulmonary fibrosis which can result in coughing or tachypnea in the absence of cardiac enlargement or failure.

In terms of specific causes of coughing, the following are general guidelines. Canine patients with upper respiratory diseases usually exhibit a chronic, loud cough with high acoustic intensity, paroxysmal bouts, and worsened by exertion of (Martin, 1997). The "cardiac" cough often described as low-intensity and occurs intermittently, being favored by the presence of compression of the main left bronchi by the dilated left atrium. It can be accompanied by dyspnea and nocturnal agitation (Ferasin, 2019). As indicated above, many of these dogs have concurrent airway diseases, including bronchomalacia, that make the source of the cough uncertain. For dogs developing left congestive heart failure any coughing can be associated with tachypnea and possibly dyspnea. In fulminating failure there might be bloody or foamy nasal secretions. Generally, these dogs have acute respiratory effort.

The abnormalities mentioned above are important considerations when evaluating a potential case of cardiac or respiratory disease. Frequently, a complete and correctly highlighted history will guide the veterinarian to the nature of the animal's underlying pathology, often allowing the differentiation of heart disease from other competing problems (Rijnberk, 1995).

GENERAL EXAMINATION

The general appearance of the canine or feline patient, as well as the overall condition of maintenance are observed. The attitude, posture, and behavior of the animal provide clues about the type of pathology and its severity. Vital signs and rapid thoracic auscultation also provide valuable clues. Animals with respiratory distress often require immediate oxygen supplementation and sedation to reduce symptoms and permit a more thorough examination.

General Inspection

Weight loss occurs in chronic, severe heart disease. It is represented by the loss of fat and skeletal muscle mass, despite the maintenance of appetite (Ineson, 2019).

Obesity can restrict ventilation and might precipitate coughing in cases of tracheal collapse. Also, obesity exacerbates the cough associated with lung or heart disease (Slupe et al., 2008).

Posture of an animal can be revealing and often reveals signs of respiratory dysfunction. One that refuses to adopt a decubitus position may have respiratory distress due to pulmonary edema, pleural effusion, pericardial effusion, pneumothorax, diaphragmatic hernia, or another respiratory condition. Dogs often assume a standing or sitting position to minimize their work of breathing; cats typically position in sternal recumbency with abducted elbows. The patient with head in extension, abducted elbows, open mouth breathing, and dilated (flared) nostrils, requires immediate therapy for respiratory distress (Le Boedec et al., 2012). Orthopnea is discussed more fully below.

Vital signs and Thermography

The pulse and respiratory rates, body temperature, and a rapid assessment of mucous membrane color and refill time should be obtained from any patient as part of the initial evaluation (assessment of membranes is discussed later). Ideally, a noninvasive systemic arterial blood pressure also should be also recorded.

Significant changes in body temperature results from a multitude of etiological factors, including changes in metabolic rate, impairment of tissue perfusion, toxic factors, exposure to extreme environmental temperatures, inflammatory or infectious diseases and iatrogenic issues. From a cardiovascular perspective, hypothermia can be induced by the presence of hypotension, bradyarrhythmia or tachycardia (atrial fibrillation, tachycardia or ventricular fibrillation) or cardiogenic shock. Fever or hyperthermia can be associated with infective endocarditis, infection or inflammation of the myocardium or pericardium, or represent increased temperature related to work of breathing, as with upper airway pathology found in brachycephalic dog breeds (Pope, 2009).

A true fever must be distinguished from hyperthermia secondary to anxiety or increased work of breathing. Hyperthermia usually resolves once a dyspneic patient is sedated and the underlying problem is managed. Hypothermia – especially in cats – is often associated systemic arterial thromboembolism or shock. Cardiogenic shock is associated with bradycardia and systemic hypotension.

Initial Auscultation

In patients with signs of respiratory dysfunction, a rapid auscultation assessment of the lungs might reveal important abnormalities such as muffled breath and heart sounds (suggesting a pleural or pericardial fluid accumulation), lung crackles (indicating parenchymal or small airway dysfunction), or sounds of inspiratory (upper airway) or expiratory (lower airway) airway obstruction. Lung ultrasound scanning is complementary to thoracic auscultation. Similarly, a rapid cardiac auscultation can be revealing. For example, the presence of marked sinus arrhythmia along with coughing suggests a primary respiratory problem, even in the presence of the left apical murmur. Conversely, sinus tachycardia with a loud murmur, gallop sounds, or obvious arrhythmia such as atrial fibrillation points to a cardiac cause of respiratory dysfunction. Notably, cardiac findings are often absent in many cats with congestive heart failure, at least during initial examination. More details about auscultation follow under "Cardiorespiratory Examination".

Initial Diagnostic Tests

Diagnostic testing must be performed with great care in patients with symptomatic respiratory or heart diseases. One must avoid aggressive manipulation or performing lower-priority tests (for example, radiography or detailed cardiac ultrasound) (Vulpe et al., 2014). In addition to the initial inspection, recording of vital signs, and rapid auscultation, point-of-care ultrasound should be given priority using a standardized protocol for the practice.

CARDIORESPIRATORY EXAMINATION

The specific clinical examination requires following a rigorous protocol, taking into account that each stage of evaluation can provide valuable information for obtaining a diagnosis. These stages include inspection, palpation, percussion, and auscultation of the heart and lungs.

Evaluation of visible mucous membranes

It is recommended to assess mucous membrane color both at the level of the cephalic extremity (oral mucosa) and caudal (preputial or vaginal mucosa). Assessment of capillary refill time will also be considered. A refill time of more than 2 seconds suggests peripheral vasoconstriction, typically as a response to decreased cardiac output. Pale mucous membranes suggest a diminished cardiac output, shock, or anemia (Ware et al., 2021).

The hyperemic appearance of mucous membranes (plethora) may indicate venous congestion (in right congestive heart failure) or polycythemia (in right-left congenital heart shunts, encountered within the septal ventricular defect or persistence of the arterial duct). Peripheral vasodilation from sepsis or vasodilator drugs are other causes.

Cyanosis is classified as central (low arterial oxygen content) or peripheral (due to intense vasoconstriction from hypotension or reduced perfusion). In most cases cyanosis indicates a low oxygen tension, either centrally or due to obstruction of arterial blood flow. For example, lack of oxygen diffusion at the alveolar level or intrapulmonary shunting can accompany respiratory disease and distress. Similarly, a low arterial oxygen can be due to right-to-left shunting defects at the level of the heart, as with tetralogy of Fallot.

Differential cyanosis affecting the caudal part of the body could indicate a right-to-left ("reversed") patient ductus arteriosus with severe pulmonary hypertension. A similar finding can occur in cat with distal aortic thromboembolism where there is the pale or cyanotic appearance of the affected, ischemic limbs (Smith et al., 2004).

Usually, cyanosis is a late sign in acquired cardiac disease associated with pulmonary dysfunction due to lung edema or atelectasis from pleural effusion. It can also present as a symptom of hypoxemia in dogs with primary or chronic obstructive respiratory diseases.

The assessment of respiratory rate and pattern of ventilation

Respiratory pattern and respiratory rate often change with heart disease: the degree of tachypnea and dyspnea usually reflect the severity of the heart pathology (Dickson, 2018). Normal *respiratory rate* in dogs and cats is less than 30 respiration per minute (rpm). Respiratory frequency exceeding 30 rpm is

considered to be tachypnea (Ohad, 2013; Boswood, 2020). Often but variably changes in respiratory rate or pattern is associated with altered breath sounds detectable during respiratory auscultation (also see Auscultation later).

Tachypnea (increased respiratory rate without distress or increased depth of ventilation) has numerous causes, including lung and pleural space disorders that can arise from congestive heart failure. Tachypnea minimizes the work of breathing when the lung is restricted such that it represents an early sign of pulmonary edema or pleural effusion that might be recognized by the observant client during home monitoring. It is important not to confuse simple tachypnea, or polypnea, due to thermoregulation (in dogs), stress, fever, or pain with tachypnea caused by cardiac, respiratory or systemic pathology or intoxications. This distinction often requires further diagnostic testing such as thoracic ultrasound or radiography.

Dyspnea is the sensation of difficult, sometimes painful, breathing reported by people. In veterinary medicine it is sometimes used to indicate respiratory distress or *hyperpnea* (increased rate and depth of ventilation). Regardless of the terminology used, dyspnea is an important sign of respiratory, cardiac, or systemic disease and requires rapid etiological diagnosis to institute life-saving therapy.

The causes of respiratory distress or dyspnea are numerous and can be tracked from the upper airways, through the bronchopulmonary system, to the pleural space and even the muscles of ventilation. Animals with extra thoracic airway obstruction have a pronounced or more rapid respiratory effort. (Corcoran, 2010) as do dogs with severe abdominal distension from any cause.

Respiratory rate is not significantly increased as long inspiration usually reduces the work of breathing, and exhalation is usually normal (MacPhail, 2014). However, if the dog develops hyperthermia, both increased depth and rate might be detected. Patients with fixed upper airway obstructions tend to have prolonged phases of both inhalation and exhalation.

The most common cardiac cause of dyspnea in dogs is pulmonary edema following left-sided congestive heart failure. In cats, dyspnea of cardiac origin often indicates the presence of pleural effusion and/or pulmonary edema, also associated with congestive heart failure. Edema might be associated with abnormal auscultation, variably louder bronchial sounds or crackles. Pleural effusions result in louder referred tracheal sounds dorsally with muffling of breath and heart sound ventrally (fluid line).

More severe respiratory distress is clinically translated by the presence of discordant or paradoxical pattern of breathing, evidenced by the presence of movement of the chest and abdominal walls inward, due to the diaphragm contraction during inspiration (Little, 2012). It is called paradoxical because it opposes the normal expansion of the thoracic cavity, thus aggravating respiratory failure. The observation of this respiratory type draws attention to the presence of a severe pathology and requires rapid therapeutic action (Cole, 2008).

Progressive, chronic tachypnea or dyspnea also may be associated with right-sided congestive heart failure secondary to ascites or pleural effusion. These signs are also observed in some dogs with cardiac compression due to large pericardial effusions.

Orthopnea in humans indicates an inability to breath comfortably while recumbent. As mentioned under “General Examination” dogs and cats with respiratory distress assume certain breathing positions. Typically, there is stretching and elevation of the neck and head and abducted elbows to open the thoracic inlet and expand the chest cavity. Dogs typically stand or sit; cats assume sternal recumbency. The presence of a frightened facies with flared nostrils and retracted lips often indicates serious pulmonary dysfunction or pleural effusion. These animals have minimal respiratory reserve and the least stress can be fatal (Sigrist, 2011).

Animals alter their pattern of ventilation to minimize the work of breathing. Patients with dynamic upper airway obstructions, such as laryngeal paralysis, can develop respiratory distress that is often worsened by exercise. Aditionally, these animals have prolonged inspiration, as negative intrathoracic pressure tends to collapse the affected area, narrowing the lumen. Obstructive inspiratory sounds are detectable with the stethoscope and frequently audible during observation alone.

Animals with intrathoracic airway obstructions, such as dogs with bronchomalacia or chronic bronchitis or cats with asthma, tend to develop increased respiratory effort during exhalation. Bronchoconstriction usually creates a whistling or high pitched sound (wheeze) during expiration association with contraction of the abdominal muscles that improve the expulsion of air from the lungs (Corcoran, 1995).

Examination of the Jugular Veins

Distention of jugular veins and jugular pulsation extending towards the mandible are clinical signs of right-heart dysfunction. The examination is performed with the animal in a standing position and the head elevated parallel with jaw parallel to the floor. Abnormal pulsations are associated with elevated central venous pressure, vigorous right atrial contraction, tricuspid regurgitation, and arrhythmias causing atrioventricular dissociation. Jugular pulsations might be accentuated during abdominal compression (abdomino- or hepto-jugular reflex).

The jugular pulse identified with right-sided congestive heart failure is often related to tricuspid regurgitation that increases right atrial pressure during systole. In congenital pulmonary stenosis or with pulmonary hypertension the pulse occurs when the right atrium contracts more vigorously in end-diastole against a less compliant, hypertrophied ventricle (Radulescu, 2019). With ventricular tachycardia or complete atrioventricular block the jugular pulse is intermittent associated with atrial contraction on a closed tricuspid valve (cannon waves)

Distention of jugular veins indicates increased systemic venous pressure or obstruction to venous return. It occurs in right heart failure, pericardial effusions, heart base tumors and with large mediastinal masses. It can also be seen with over-infusion of intravenous fluids, especially in cats with otherwise mild cardiac dysfunction or those in volume-retentive states (Ionita, 2000).

Palpation

The cervical region of cats (and dogs) should also be evaluated for the presence of lymphadenopathy and thyroid tumors that in cats are often associated with secondary cardiac changes. In dogs thyroid carcinoma can partially obstruct the airway and often metastasizes to the thorax.

Palpation of the trachea can highlight a collapse, tumor masses or increased sensitivity. A slight pressure exerted from the side inwards of the larynx can exacerbate the inspiratory stridor in dogs with laryngeal paralysis (Ware, 2011).

Palpation of the chest is necessary to identify the point of maximum intensity (PMI) of the heart (apical) beats and recognize precordial vibrations (thrills) of a loud cardiac murmur. The normal cardiac impulse (apical beat) is located at the left side, in the 4^{th} to 6^{th} intercostal spaces, usually at the 5^{th} ICS in dogs. Decrease in intensity can occur with obesity, pleural or pericardial effusions, an intrathoracic mass, pneumothorax, or in cases of depressed cardiac contractility. Increased apical beat intensity occurs in young or thin animals or in setting of a hyperdynamic circulation. Left ventricular dilation can displace the ventricular apex ventrally and caudally. Right ventricular hypertrophy can increase the intensity of the right apical impulse (normally at the 3rd or 4^{th} intercostal space and weaker than the left apical impulse).

Palpation of the abdomen can identify hepatomegaly and ascites in right-sided congestive heart failure. Other abnormalities, such as tumor masses or lymphadenopathy might be found suggesting the presence of lung metastases.

Abdominal palpation to identify ascites or hepato- or splenomegaly is difficult to achieve in obese animals (ultrasound investigation is preferred). In cats, palpation of the kidneys with small dimensions usually indicates chronic kidney disease and can be associated with systemic hypertension (Stepien, 2011). Irregular renal surfaces representing prior infarctions are sometimes identified in cats with cardiomyopathy.

The arterial pulse is palpated and analyzed in standing position, most frequently at the femoral artery. It is analyzed in terms of rate, regularity (rhythm), quality (intensity) and symmetry. In congestive heart failure, tachycardia is noted, translated by an increase in pulse frequency, while in respiratory diseases it is more likely to notice a normal rate of it, or the presence of sinus arrhythmia

(Smith et al., 2015). Pulse deficits are an important indicator of a cardiac arrhythmia (as in atrial fibrillation).

The hypokinetic pulse is characteristic of diseases with low stroke volume, as with heart failure, or impaired ejection dynamics, as with subaortic stenosis. The hyperkinetic (bounding) pulse indicates the presence of a widened pulse pressure between systole (normal to increased) and diastole (lower than normal). Typical causes are left-to-right patent ductus arteriosus, moderate to severe aortic regurgitation, and third degree atrioventricular block with ventricular escape rhythm.

Percussion

Chest percussion is a very efficient method for recognition of large pleural effusions but requires experience and is a lost clinical art. The typical features of pleural effusion are hyporesonant (duller) sounds bilaterally and the presence of a dorsal fluid line. Similar findings can occur with large mediastinal masses (cranially) or pulmonary masses. The area of cardiac dullness is also expanded with large pericardial effusions. Conversely hyperresonance on thoracic wall percussion may indicate the diagnosis of pneumothorax.

Auscultation

Auscultation is the most important stage of the clinical examination for detecting heart disease. Two fundamental abnormalities are identified by auscultation. The first involves the transient (brief) sounds, including the heart sounds. Abnormalities in the number, rate, rhythm, intensity, or character of the transient sounds might be detected. The second major abnormality detected by auscultation is the presence of pathologic cardiac murmur. Some key points regarding cardiac and respiratory auscultation are summarized below.

Technique Proper use of the stethoscope offers valuable clues for detecting cardiac and respiratory diseases. It must be done systematically and with care, with the animal in standing position, so that the heart is anatomically positioned. It is aimed at examining the heart, lungs and pleural space, and the upper respiratory tract (Dennis, 2013).

Auscultation should be done in a quiet environment. The examiner should listen carefully over the four canine heart valves, and over the left craniodorsal base of the heart (over the ascending aorta and pulmonary trunk). These areas should also be palpated for precordial thrills. In cats, auscultation is focused to the sternal edges both apically – near the palpable beat – and cranially (Fox, 1999).

For small dogs and cats it is recommended to use the pediatric stethoscope, mainly the diaphragm, because heart sounds of animals are best detected with this chest piece. Lower frequency sounds, especially the ventricular gallop in dogs and soft murmurs of aortic regurgitation are sometimes heard better with the stethoscope bell.

The left apical beat is initially identified by palpation. It represents the ventral part of the listening area for the mitral valve and corresponds to the intercostal space (ICS) 5 in most dogs, ventral to the costochondral junction. Mitral sounds project ventrally down the solid structure of the left ventricle towards the apex (Murmurs from the mitral valve are often loud at the apex as well as dorsal the mitral valve itself). From here, the stethoscope moves one intercostal cranially and dorsally to the aortic valve area (ICS 4); ventral and cranial to the aortic valve is the pulmonary valve (ICS 2-3). Murmurs from both semilunar valves project dorsally above the costochondral junction (Strickland et al., 2008).

Special attention is required to auscultation of the left axillary region, especially in young animals, for the detection of the continuous murmur of PDA.

Heart Sounds. The systolic heart sound S1 (generated by the vibrations around closure of the atrioventricular valves) is loudest over the mitral valve and left apical region. The second sound (indicating the onset of diastole) is generated by vibrations around the closure of the semilunar valves); it is most prominent over the aortic and pulmonary valve areas.

The intensity of the cardiac sounds may be diminished, suggesting the presence of pleural, pericardial effusion, tumor masses or pneumothorax. Depressed contractility from dilated cardiomyopathy is an under-recognized cause of soft heart sounds. The intensity of the first sound increases with progressive

cardiomegaly in primary (degenerative) mitral valve disease (Häggström, J., 1995).
Increased heart rate (tachycardia) is most often due to sympathetic activation. It can be seen as a physiological response (exertion, fear) or secondary to disease (fever, pain, anemia, hypovolemia, or heart failure).
Normal values for heart rate (Ettinger et al., 2017):

- Dogs: 70-160 (adult dogs); 60-140 (giant breeds); 80-180 (toy breeds); up to 220 in puppies;
- Cats: 140-240 (hospital measurement); 100-120 (home environment).

A decrease of the heart rate (bradycardia) is physiologically found in sighthounds (such as greyhounds), working athletic breeds (such as the border collie), and in the context of various organ or systemic pathologies, including hypothyroidism, hyperkalemia, hypothermia, and acute renal failure. Iatrogenic causes include sedatives and tranquilizers, beta-adrenergic blockers, and some antiarrhythmic drugs (Abbott, 2001) (Smith et al., 2008).
Cardiac rhythm disturbances might be recognized by auscultation. Dogs normally have sinus arrhythmia, typically associated with respiration. Exercise will usually resolve this, at least briefly. Exaggerated sinus arrhythmia might be noted in the setting of respiratory diseases; conversely, it is usually absent in heart failure (Bonagura et al., 1999). Pathologic rhythms can be intermittent and challenging to identify. For example, the pause after a single premature beat can mimic a sinus block or a sinus arrest. The same thing does not happen in the case of atrial fibrillation, which can be easily recognized by the presence of heart beats of different intensity accompanied by a noncyclical, chaotic rhythm.
Abnormal transient sounds usually indicate pathology. Splitting S1 or S2 sounds in dogs is usually caused by a conduction delay as with bundle branch block or ventricular ectopy. Splitting of S2 is mainly due to delayed closure of the pulmonary valve, which can also occur in pulmonary stenosis, ventricular septal defect or severe pulmonary hypertension.
An S3 (ventricular filling) or S4 (atrial contraction) sound is considered pathologic in dogs and in cats. These “gallops” are indicative of diastolic dysfunction, most often some form of cardiomyopathy or of congestive heart failure (Vancheri, 1989). Systolic clicks or additional sounds are generally due to valvular disease. The systolic click is most often attributed to the presence of mitral valve prolapse (de Madron, 2000). In most cases, isolated mitral and tricuspid valve systolic clicks are signs of mild valvular disease. However, gallops and systolic clicks in younger cats are especially concerning because they often indicate hypertrophic cardiomyopathy.
important indication for the presence of heart disease (Saponaro, 2023)

Cardiac murmurs are generated by the vibration of the cardiac anatomical structures under the influence of the blood flow that generates turbulence under certain conditions. Most often a murmur is associated with an increased ejection velocity (as with functional or physiologic murmurs) or a high velocity turbulent jet (as with most pathologic murmurs). High velocity jets are associated with valvular regurgitation and stenosis, restrictive ventricular septal defects, and left-to-right shunting PDA. However, there are other reasons for murmurs, including reduced blood viscosity (anemia), ejection into dilated great vessels, and sudden changes in the diameter of a flow pathway including fixed and dynamic obstructions (Côté et al., 2015).
The timing of the murmur in the heart cycle classifies it as systolic, diastolic, or continuous. Systolic murmurs are most common and occur during ventricular contraction. These include mitral and tricuspid regurgitation, ventricular septal defect, increased pulmonary flow of atrial septal defect, (sub)aortic and pulmonic stenosis, and those physiologic/innocent/functional murmurs not associated with cardiac disease. Timing can be subdivided into early (proto-), middle (meso-) or late (tele-) systole. Loud murmurs of ventricular septal defect and of mitral and tricuspid regurgitation (from myxomatous disease) are usually holosystolic. Some distinguish between holosystolic, where the second heart sound is still heard, and pansystolic where only the cardiac murmur is audible (for example - ventricular septal defect); however, this is less common today.

Diastolic murmurs are heard after S2; these are rare to uncommon in small animals. The most common example is the decrescendo diastolic murmur of aortic regurgitation caused by infective (bacterial) endocarditis (Smith et al., 2015). Stenosis of the mitral or tricuspid valve or inlets are rare.

Continuous murmurs are present throughout systole and diastole, as happens with persistence of the arterial duct (PDA). In this congenital heart defect, there persistent difference in pressure in between the aorta and the pulmonary artery generates a continuous murmur. Thus, one can hear a higher intensity murmur in systole (when the pressure differences are greatest) and a lower intensity murmur in the diastole. Should pulmonary hypertension develop, the diastolic murmur becomes softer or inaudible; this is often the case in cats.

The combination of systolic and diastolic murmurs can mimic a continuous murmur. In dogs this situation is most common with subaortic stenosis with moderate to severe aortic regurgitation, ventricular septal defect with secondary aortic insufficiency, and pulmonary stenosis accompanied by severe pulmonary regurgitation (or with pulmonary hypertension).

Phonocardiography – the graphical recording of heart sounds and murmurs – can specify the timing and the "shape" of a heart murmur, although this is not routinely done. For example, the crescendo-decrescendo (diamond-shaped) murmur of pulmonary or aortic stenosis contrasts with the more constant intensity ("plateau"-shaped) murmurs of mitral regurgitation and ventricular septal defect. This distinction is difficult to appreciate when listening with the stethoscope (Fonfara, 2015), especially when murmurs are loud.

The *point of maximal intensity* (PMI) of a murmur and its timing in the cardiac cycle are the most important clinical features distinguishing heart murmurs. Firstly, the typical PMI for different murmurs are over the respective valve areas.

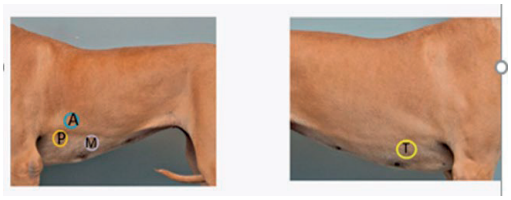

A B

Figure 1. Representation of cardiac ascultation areas for the left (A) and right hemithorax (B) (after Englar R.E., 2017, modified)
(M - mitral valve area auscultation; A - aortic valve area auscultation; P - pulmonary valve area auscultation; T - tricuspid valve area auscultation)

Additionally, mitral regurgitation is heard at the left apex and radiates dorsally (and to the right if loud). Tricuspid regurgitation is over the right thorax (3-4 ICS) above the sternum, whereas, a typical murmur of VSD is loudest over the right sternal border (Englar R.E., 2017). Murmurs of (sub)aortic and pulmonic stenoses radiate cranially and for PS dorsally into the main pulmonary artery at the left-craniodorsal cardiac base. Subaortic stenosis also radiates towards the apex and into the right thorax (ascending aorta) when loud (Allen et al., 1998).

The murmur of PDA is also heard best over the left craniodorsal cardiac base because the high-velocity jet enters the pulmonary artery. Functional (physiologic) murmurs in dogs are nearly always soft, proto-mesosystolic in timing, and loudest over the aortic valve, pulmonic valve, or left craniodorsal cardiac base. In cats these functional murmurs are soft to moderate and typically due to sympathetic activation. The PMI in cats is over the left or the right cranial sternal edges.

Murmur intensity is most often classified into six grades, using a modified Levine grading scale:

- Grade 1 – faint, perceived after a few minutes of listening in a very quiet room. These are usually localized murmurs.
- Grade 2 – soft but immediately perceptible; usually focal, at the level of a single valve or listening area.

- Grade 3 – moderate intensity murmur that radiates to other adjacent listening areas.
- Grade 4 – loud, but not accompanied by a precordial vibration or thrill. Radiates widely.
- Grade 5 – loud murmur with a precordial thrill.

  Grade 6 – loud murmur audible without a stethoscope in some cases or with the chest piece off the thorax; always accompanied by a precordial thrill.

Numerous modifications of murmur grading appear in the veterinary literature with none following the exact original description of Levine (Cote, 2015). Some suggestions relate loudness of a murmur to intensity of heart sounds; others have condensed the scale to five or four grades of murmurs (Rishniw, 2018). There is no veterinary consensus at this point.

The murmur intensity does not always correlate with the severity of the disease. In some heart conditions there is this direct correlation, for example, in aortic stenosis and pulmonary stenosis the intensity and time of peak do correlate – louder and later are worse. In primary mitral valve disease of dogs, soft murmurs indicate mild disease and murmurs with precordial thrills have a greater likelihood for cardiac remodeling, but the "middle grades" have much overlap in terms of severity. In other heart diseases, the intensity of the murmur is not directly proportional to the severity: ventricular septal defect, mitral regurgitation associated with dilated cardiomyopathy, or murmurs in feline cardiomyopathy are good examples that correlate poorly (Visser, 2018).

Respiratory auscultation is performed at the level of the specific areas of each segment.

Normal breath sounds include tracheal sounds (from panting) in dogs, and bronchovesicular sounds over the thorax. There are both inspiratory and expiratory components to these sounds. Tracheal sounds are loudest over the cervical region and have a distinct "pause" between the phases. These usually radiate to the thorax where they are misinterpreted as pathologic "harsh" sounds (a description of no medical relevance). Tracheal sounds can help to exclude pleural effusions if well-heard from dorsal to ventral, bilaterally. Otherwise they are a nuisance that obscure other breath sounds.

Bronchovesicular sounds include contributions from both the lungs (vesicular) and larger airways (bronchial). There is little separation between phases with normal breathing. With respiratory disease, the sounds are often more intense during expiration. Accentuation is generally not a sign of high specificity for the presence of respiratory diseases. Asymmetry of bronchial sounds can develop if different lung lobes are affected; sometimes sounds become louder in diseased lungs but at other times they are attenuated, especially if there is bronchial obstruction. Attenuation of bronchovesicular sounds is also associated with obesity, atelectasis, pleural fluid, or thoracic masses. Adventitious respiratory sounds include stridor, wheezes, rhonchi, crackles (rales) and friction rubs. Critical upper airways obstructions are usually audible without the need for a stethoscope.

The perception of an increased sound or noise in upper airway auscultation (over the larynx and cervical trachea) suggests an obstructive upper respiratory condition. Respiratory *stridor* has high intensity, and accompanies the turbulent passage of air to the larynx or upper bronchial airways. It can occur both in fixed obstructions (it is evident in inspiration and exhalation) and in dynamic ones located at the upper airways (it appears only during inspiration).

Respiratory *stertor* is a low-toned noise, similar to snoring produced in the nasopharyngeal or pharyngeal pathway, generated by obstruction in one of these zones. It is most often due to soft palate redundancy and entrapment and frequently associated with stenotic phenomena of brachycephalic breeds. Increased nasal resistance usually accentuates the obstructive sounds. It is present during inspiration but might also be evident with exhalation (Dupré, 2016).

Abnormal respiratory sounds originating in the bronchial tree include *rhonchi* and *wheezes*. The rhonchus is similar in quality to stertor but localized to the thorax. It indicates fluid or mucous in larger bronchi. Wheezes are high-pitched expiratory sounds typical of bronchial narrowing as observed with feline bronchial asthma. Wheezes are also common when there is lobar or mainstem bronchial collapse or compression.

The detection of lung *crackles* (previously termed "rales") has distinct pathological relevance, being present in the inspiration and early expiration. In the setting of congestive heart failure it is a sign of severe pulmonary edema (Ettinger et al., 2016). However, the loudest crackles are frequently detected with pulmonary fibrosis or other primary lung disease that result in explosive opening of the smallest airways as this loose radial traction. Thus crackles cannot be assumed to be fluid.

CONCLUSIONS

Going through the stages of the clinical examination facilitates the establishment of the diagnosis of cardiac pathology, its differentiation or association with a respiratory pathology, as well as the evaluation of the proposed therapeutic response. Depending on the patient's condition, the emergency therapeutic conduct is instituted, or, if this allows, the paraclinical investigations with diagnostic value are continued.

ACKNOWLEDGEMENTS

This article work was carried out with the support of John D. Bonagura, DVM, MS, DACVIM (Cardiology, Internal Medicine), Adjunct Professor, Department of Clinical Sciences, College of Veterinary Medicine, North Carolina State University Professor Emeritus, Veterinary Clinical Sciences, The Ohio State University

REFERENCES

Abbott, J. (2001). Auscultation: What type of practice makes perfect? *Journal of Veterinary Internal Medicine*, *15*(6), 505-506.

Allen, D. G., & Kruth, S. A. (1988). *Small animal cardiopulmonary medicine*. BC Decker Inc.

Baisan, R. A., Condurachi, E. I., & Vulpe, V. (2020). Short-term heart-rate variability in healthy small and medium-sized dogs over a five-minute measuring period. *Journal of Veterinary Research*, *64*(1), 161.

Bonagura, J. D., Lehmkuhl, L. B., Fox, P., Sisson, D., & Moise, N. (1999). Textbook of Canine and Feline Cardiology.

Boswood A, Gordon SG, Häggström J, Vanselow M, Wess G, Stepien RL, Oyama MA, Keene BW, Bonagura J, MacDonald KA, Patteson M, Smith S, Fox PR, Sanderson K, Woolley R, Szatmári V, Menaut P, Church WM, O'Sullivan ML, Jaudon JP, Kresken JG, Rush J, Barrett KA, Rosenthal SL, Saunders AB, Ljungvall I, Deinert M, Bomassi E, Estrada AH, Fernandez Del Palacio MJ, Moise NS, Abbott JA, Fujii Y, Spier A, Luethy MW, Santilli RA, Uechi M, Tidholm A, Schummer C, Watson P.(2020). Temporal changes in clinical and radiographic variables in dogs with preclinical myxomatous mitral valve disease: The EPIC study. J Vet Intern Med. 2020 May;34(3):1108-1118.

Chong, L. Y., & YiJun, L. (2017). *Cat owners'perception towards feline heart disease: a behavioural study.* Veterinary sciences, 90.

Cole, S. G., & Drobatz, K. J. (2008). Emergency management and critical care. In *Manual of canine and feline cardiology* (pp. 342-355). WB Saunders.

Corcoran, B. M. (2010). Respiratory pathophysiology. In *BSAVA Manual of Canine and Feline Cardiorespiratory Medicine* (pp. 108-111). BSAVA Library.

Corcoran, B. M., Foster, D. J., & Fuentes, V. L. (1995). Feline asthma syndrome: a retrospective study of the clinical presentation in 29 cats. *Journal of Small Animal Practice*, *36*(11), 481-488.

Côté E, Edwards NJ, Ettinger SJ, Fuentes VL, MacDonald KA, Scansen BA, Sisson DD, Abbott JA (2015). Management of incidentally detected heart murmurs in dogs and cats. *J Vet Cardiol*., 2015 Dec; 17(4): 245-61.

de Madron, E. (2000). Textbook of Canine and Feline Cardiology: Principles and Clinical Practice. *The Canadian Veterinary Journal*, *41*(3), 246.

Dennis, S. (2013). Sound advice for heart murmurs. *Journal of Small Animal Practice*, *54*(9), 443-444.

Dickson, D., Little, C. J. L., Harris, J., & Rishniw, M. (2018). Rapid assessment with physical examination in dyspnoeic cats: the RAPID CAT study. *journal of small animal practice*, *59*(2), 75-84.

Dupré, G., & Heidenreich, D. (2016). Brachycephalic syndrome. *Veterinary Clinics: Small Animal Practice*, *46*(4), 691-707.

Englar, R. E. (2017). *Performing the Small Animal Physical Examination*. John Wiley & Sons.

Ettinger, S. J., Feldman, E. C., & Cote, E. (2016). *Textbook of Veterinary Internal Medicine-Inkling E-Book*. Elsevier health sciences.

Ferasin, L., & Linney, C. (2019). Coughing in dogs: what is the evidence for and against a cardiac cough? *Journal of Small Animal Practice*, *60*(3), 139-145.

Fonfara, S. (2015). Listen to the sound: what is normal? *Journal of Small Animal Practice*, *56*(2), 75-76.

Fox, P. R. (1999). Canine and feline cardiology. *Cardiovascular Pathology*, 817-844.

Ineson, D. L., Freeman, L. M., & Rush, J. E. (2019). Clinical and laboratory findings and survival time associated with cardiac cachexia in dogs with congestive heart failure. *Journal of veterinary internal medicine*, *33*(5), 1902–1908. https://doi.org/10.1111/jvim.15566

Ioniță, L. (2000). *Patologie şi clinică medicală veterinară*. Universitatea de Ştiinţe Agronomice şi Medicină Veterinară Bucureşti.

Keene, B. W., Atkins, C. E., Bonagura, J. D., Fox, P. R., Häggström, J., Fuentes, V. L., ... & Uechi, M. (2019). ACVIM consensus guidelines for the diagnosis and treatment of myxomatous mitral valve disease in dogs. *Journal of veterinary internal medicine*, *33*(3), 1127-1140.

Kittleson, M. D., & Kienle, R. D. (1998). *Small animal cardiovascular medicine*. Mosby; 195-217

Häggström, J., Kvart, C., & Hansson, K. (1995). Heart sounds and murmurs: changes related to severity of chronic valvular disease in the Cavalier King Charles spaniel. *Journal of veterinary internal Medicine*, *9*(2), 75-85.

Le Boedec, K., Arnaud, C., Chetboul, V., Trehiou-Sechi, E., Pouchelon, J. L., Gouni, V., & Reynolds, B. S. (2012). Relationship between paradoxical breathing and pleural diseases in dyspneic dogs and cats: 389 cases (2001–2009). *Journal of the American Veterinary Medical Association*, *240*(9), 1095-1099.

Little, S. E. (2012). The cat: clinical medicine and management, Saunders Elsevier, St. *Louis, Missouri, USA*.

MacPhail, C. (2014). Laryngeal disease in dogs and cats. *Veterinary Clinics: Small Animal Practice*, *44*(1), 19-31.

Martin, M. W., & Corcoran, B. M. (1997). *Cardiorespiratory diseases of the dog and cat*. Blackwell Science Ltd..

Ohad DG, Rishniw M, Ljungvall I, Porciello F, Häggström J. (2013). Sleeping and resting respiratory rates in dogs with subclinical heart disease. *J Am Vet Med Assoc*. 2013 Sep 15; 243(6): 839-43. doi: 10.2460/javma.243.6.839. PMID: 24004231.

Penning VA, Connolly DJ, Gajanayake I, McMahon LA, Luis Fuentes V, Chandler KE, Volk HA. (2009). Seizure-like episodes in 3 cats with intermittent high-grade atrioventricular dysfunction. *J Vet Intern Med*., 2009 Jan-Feb; 23(1): 200-5.

Pope, E. R., & Constantinescu, G. M. (2009). Brachycephalic Upper Airway Syndrome. *Kirk's Current Veterinary Therapy XIV. St. Louis: Saunders Elsevier*, 619-21.

Radulescu, A., Cristescu, B., Harrigan, P., & Ionita, L. (2019). Reversal of cardiac pathology by echocardiography in a dog with severe pulmonary hypertension secondary to heartworm disease-case report. *Scientific Works. Series C. Veterinary Medicine*, *65*(1), 79-88.

Rishniw M. (2018). Murmur grading in humans and animals: past and present. *J Vet Cardiol*., 2018 Aug; 20(4): 223-233.

Rijnberk, A., & De Vries, H. W. (Eds.) (1995). *Medical history and physical examination in companion animals*. Springer Science & Business Media.

Saponaro V, Mey C, Vonfeld I, Chamagne A, Alvarado MP, Cadoré JL, Chetboul V, Desquilbet L. (2023). Systolic third sound associated with systolic anterior motion of the mitral valve in cats with obstructive hypertrophic cardiomyopathy. *J Vet Intern Med*., 2023 Sep-Oct; 37(5): 1679-1684.

Sigrist, N. E., Adamik, K. N., Doherr, M. G., & Spreng, D. E. (2011). Evaluation of respiratory parameters at presentation as clinical indicators of the respiratory localization in dogs and cats with respiratory distress. *Journal of veterinary emergency and critical care*, *21*(1), 13-23.

Slupe, J. L., Freeman, L. M., & Rush, J. E. (2008). Association of body weight and body condition with survival in dogs with heart failure. *Journal of veterinary internal medicine*, *22*(3), 561-565.

Smith, F. W., Tilley, L. P., Oyama, M., & Sleeper, M. M. (2015). *Manual of canine and feline cardiology*. Elsevier Health Sciences.

Smith, F. W., Tilley, L. P., Oyama, M., & Sleeper, M. M. (2015). *Manual of canine and feline cardiology*. Elsevier Health Sciences.

Smith, S. A., & Tobias, A. H. (2004). Feline arterial thromboembolism: an update. *Veterinary Clinics: Small Animal Practice*, *34*(5), 1245-1271.

Stepien, R. L. (2011). Feline systemic hypertension: diagnosis and management. *Journal of feline medicine and surgery*, *13*(1), 35-43.

Strickland, K. N., Tilley, L. P., Smith, F. W. K., Oyama, M. A., & Sleeper, M. M. (2008). *Manual of canine and feline cardiology*.

Tilley, L. P., Smith Jr, F. W. K., Oyama, M. A., & Sleeper, M. M. (2008). *Manual of canine and feline cardiology*. 4th ed., Saunders.

Vancheri, F. E. D. E. R. I. C. O., & Gibson, D. E. R. E. K. (1989). Relation of third and fourth heart sounds to blood velocity during left ventricular filling. *Heart*, *61*(2), 144-148.

Visser, L. C. (2018). Feline hypertrophic cardiomyopathy. *Textbook of Small Animal Emergency Medicine*, 349.

Vulpe, V., Meomartino, L., Daraban, C., Șerban, C. M., Tipișcă, V., Baisan, R. A. (2014). Radiologie veterinară - manual practic. Ed. Performantica, Iași.

Ware, W. (2011). *Cardiovascular disease in small animal medicine*. CRC Press.

Ware, W. A., Bonagura, J. D., & Scansen, B. A. (2021). Abnormal Mucous Membrane Color. In *Cardiovascular Disease in Companion Animals* (pp. 247-252). CRC Press

Scientific Works. Series C. Veterinary Medicine. Vol. LXX (2), 2024
ISSN 2065-1295; ISSN 2343-9394 (CD-ROM); ISSN 2067-3663 (Online); ISSN-L 2065-1295

ENDOSCOPIC TRANSCERVICAL INSEMINATION: A METHOD FOR SUCCESSFUL CANINE ARTIFICIAL INSEMINATION

Cătălin MICŞA[1], Maria Roxana TURCU[1], Nicolae Tiberiu CONSTANTIN[1, 2], Dorin ŢOGOE[1], Alexandru DIACONESCU[1]

[1]University of Agronomic Sciences and Veterinary Medicine of Bucharest, Faculty of Veterinary Medicine, 105 Splaiul Independentei Street, 050097, District 5, Bucharest, Romania
[2]Research and Development Institute for Bovine Balotesti, Bucharest-Ploiesti Road, km 21, 077015, Balotesti, Ilfov County, Romania

Corresponding author email: catalin_micsa@yahoo.com

Abstract

Artificial insemination (AI) is one of the most frequently implemented assisted reproductive technologies for animals. The dog-breeding industry is extremely dependent on artificial insemination (AI), which enables the successful transfer of genetic material over large distances and its indefinite storage for future use in breeding programs. When natural reproduction is not possible due to male incapacity, receptivity, or physical impairment, AI may also be utilised. The manner in which AI is put into practice in canines differs and is dependent on the variety of sperm utilised. In particular, with preserved or fresh sperm, intrauterine insemination is performed through transcervical catheterization using an endoscope. Endoscopic TCI for frozen sperm offers the advantage of obtaining comparable or superior results while avoiding the requirements and potential risks associated with general anaesthesia and surgery. Undoubtedly, the capacity to perform all inseminations with fresh or refrigerated semen increases the conception rates. This article will centre on the endoscopic transcervical insemination (TCI) method of canine artificial insemination (AI).

Key words*: artificial insemination, endoscopy, reproduction, TCI.*

INTRODUCTION

Transcervical catheterisation (insemination), or TCI, is a minimally invasive technique that involves inserting a tool through the vagina and cervix into the uterus. In large animals, this procedure is possible due to their size and the ability to control the cervix through the rectum (Thomassen et al., 2006; Fontbonne, 2006; Blendinger, 2007b). However, this was not feasible in small animals until about 25 years ago. Scandinavian veterinarians were successful in modifying a fox transcervical catheter for use in female dogs (Linde-Forsberg et al., 2001), which led to the subsequent documentation of a procedure involving the insertion of a catheter into the cervix of a dog using a cystourethroscope designed for humans (Johnston et al., 2001; Santos et al., 1997). The use of a human ureteroscope modified for dogs has enhanced canine transcervical insemination (TCI), enabling more effective cervical manipulation and faster procedures (Silva et al., 1995; Silva et al., 1996).

The TCI procedure, which utilizes advanced equipment, is becoming a standard technique in canine artificial insemination due to its ability to enhance fertility, particularly when using frozen or low-quality semen, as well as overcome the obstacle of a closed cervix that occurs near the end of estrus, when oocytes are still capable of being fertilized (Sum et al., 2009; Rodrigues et al., 2002).

The limited use of transcervical insemination (TCI) in cats has resulted in ineffective attempts to perform the procedure due to the small size of the feline vaginal entrance, which complicates endoscopic exams. Moreover, the procedure of gathering feline seminal material is more difficult compared to dogs, leading to a reduced need for intrauterine deposition of seminal material in cats. However, despite the challenges, TCI manoeuvres have been documented in cats (Feldman et al., 2004; Levy et al., 2007).

When it comes to canine reproduction, using frozen-thawed semen for intrauterine semen deposition has been considered (Nizanski, 2006; Wilson, 1993). However, the outcomes

may be affected by the low quality of the semen after thawing (Fukushima et al., 2010; Meyers-Wallen, 2007). Additionally, the offspring produced using this method are generally smaller compared to those acquired by inseminations using fresh semen (Linde-Forsberg et al., 1999). Intrauterine artificial insemination is a viable option when both the male and female are unable to reproduce naturally due to conditions such as vaginal strictures, orthopaedic issues including fractures, a history of refusing to mate or allow mating, or behavioural factors (Silva et al., 2003).

This study aimed to examine the specific characteristics and challenges associated with performing the endoscopic transcervical intrauterine technique in canines. Additionally, another object of this study was to determine whether challenges in performing the endoscopic transcervical intrauterine artificial insemination (AI) procedure can be resolved through equipment manipulation and practical experience.

It is crucial to determine the most suitable timing for AI performance in female dogs, as the proestrus, oestrus, and ovulatory phases can be lengthy and unpredictable (Arbeiter et al., 1991; Concannon et al., 1989; England et al., 2002). The LH surge is considered the most significant phase of the oestrous cycle as it is closely associated with all reproductive processes, ranging from ovulation to parturition. Research indicates that the LH surge takes place when progesterone levels reach approximately 2 ng/ml (de Gier et al., 2006). Clinical and reproductive parameters, vaginal cytology, hormonal tests, and ovarian ultrasonography are all methods that can be employed to ascertain ovulation (Jackson et al., 1979; Wright, 1990).

MATERIALS AND METHODS

This study included five healthy female Golden Retrievers, three of which had given birth multiple times (pluriparous) and two of which had never given birth (nulliparous). The age of the dogs ranged from 24 months to 6 years, and their weight ranged from 26.8 to 33.2 kg. The female dogs had a detailed medical history of their reproductive system.

Three mature (1.5-3 years old) male Golden Retrievers with confirmed fertility were chosen based on an examination of their reproductive health, in accordance with the kennel's breeding programme and the quality of their semen. All animals, both females and males, included in this study are from a commercial kennel and are subjected to identical environmental, nutritional, and management circumstances.

The timing of insemination was determined using vaginal cytology, serum progesterone concentrations, and vaginoscopy (Macedo et al., 2012; Pretzer et al., 2006).

All female dogs were brought to the clinic for their initial evaluation 5 to 7 days after the owner noticed swelling or discharge in their vaginal area. Vaginal smears were obtained by inserting a dampened cotton swab into the posterior part of the vagina. Subsequently, swabs were delicately rotated onto glass microscope slides and dyed using Diff Quick (Blendinger, 2007a). Vaginal smears were examined during the initial appointment to determine the stage of the menstrual cycle. Vaginal smears were only evaluated for concerns about the cycle not proceeding as expected, as indicated by progesterone fluctuations (Hase et al., 2000; Hori et al., 2005).

The blood samples were obtained by drawing blood from cephalic veins. The blood was collected and sent to the laboratory for detection of serum progesterone levels. The serum progesterone concentration was measured during the initial visit and then every 3 to 4 days until the LH surge was identified, which is indicated by a progesterone value exceeding 2 ng/mL (Volkman, 2006). Following the LH surge, the concentration of progesterone in the blood was measured every 24 to 48 hours until ovulation was considered to have finished. After determining ovulation based on a progesterone concentration of 2-6 ng/mL, vaginoscopic investigations were started (Jeffcoat et al., 1989). Insemination was only carried out if ovulation was considered complete, indicated by a progesterone concentration over 6 ng/mL. Measurement of serum progesterone was discontinued after reaching a concentration higher than 10 ng/mL (Kim et al., 2007; Kutzler et al., 2003).

Reproductive monitoring began with the completion of anoestrus and the onset of proestrus. The proestrus and oestrous phases were identified by observing behaviour and reproductive factors, as well as analysing vaginal cytology and doing serum progesterone assays. During the proestrus phase, female dogs exhibited signs of male attraction, swelling of the vulva, a discharge of blood-tinged fluid from the vagina, and a reluctance to be mounted by males (Concannon, 2005). In contrast, during the oestrus phase, female dogs displayed male attraction, a discharge of blood-tinged fluid from the vagina, willingness to be mounted by males, and a deviation of the tail. The female dogs were assessed at intervals of 24 to 48 hours until the first artificial insemination was carried out in each dog.

RESULTS AND DISCUSSIONS

The initial artificial insemination (AI) procedure was conducted during the period when the female dogs were sexually receptive to males, as shown by a vaginal cytology with more than 80% superficial cells and a progesterone concentration exceeding 6 ng/mL. The semen was collected just prior to artificial insemination using digital manipulation. This involved acquiring both the first and second ejaculate fractions (Nizanski, 2006).

Following collection, the sperm's total and progressive motility, speed, and morphology were assessed using bright-field microscopy at a magnification of 100x. The concentration of sperm was measured using a hemocytometer, and the morphology of the sperm was analysed using phase contrast microscopy at a magnification of 1000x (Kustritz, 2007). The semen collected from the male canines in this investigation exhibited a total motility of over 80% and a sperm speed exceeding 4 with CASA System (Computer Assisted Sperm Analysis).

A rigid endoscope with a cover and catheter port or working channel is preferable for vaginal examination in bitches compared to a flexible endoscope. Rigid endoscopes enhance vaginal navigation and facilitate the insertion of flexible catheters and brushes. Regardless of their size, rigid endoscopes can be used for the majority of dogs. Typically, an endoscope should have a length of at least 30 cm to reach the cervix in medium to large dogs. It should also have a tiny diameter to pass through the cranial section of the vagina in small and medium dogs. Authors typically suggest an optical angle ranging from 6° to 30° in order to enhance the visualisation of the cervical aperture. A commonly used instrument for the assessment of vaginal and transcervical insemination (TCI) is a cystoscope with an enlarged urethra and a diameter of 3.5 mm (Concannon, 2004; Linde-Forsberg, 1991).

During the AI procedure, the female dog was placed in a standing position on a table with an antiskid surface and manually restrained by the owner. The front part of the table was inclined at an angle of around 30 degrees towards the ground, causing the hindquarters of the female dog to rest on the higher section of the table.

Typically, the procedures of vaginal examination and intrauterine insemination are generally well-tolerated by individuals without the need for anaesthesia. On average, these procedures may be conducted on female canines while they are positioned upright on a veterinary examination table. Under some circumstances, such as anoestrus and/or limited lumen, an anxious female dog, or vestibulitis/vaginitis, it may be appropriate to provide sedation (e.g., medetomidine, 10-20 μg/kg IV) or general anaesthesia in order to reduce the risk of vaginal trauma and/or damage to equipment (Macedo et al., 2012).

After external cleaning of the vulvar area, the cervix was visualised using a TCI cystoscope (Karl Storz, Tuttlingen, Germany) that had a xenon cold light source and camera. The images were shown on a monitor. Vaginal insufflation was accomplished using a rectal insufflation bulb. A CH-5 transcervical catheter was inserted through the cervix into the uterine body, and semen was gradually introduced for insemination. Following the introduction of semen, the catheter was filled with 1 ml of air to facilitate the deposition of the remaining semen. After the AI procedure, the hindquarters were kept raised for 10 minutes to reduce the possibility of backflow, and manual stimulation was applied to the perineal region (Linde-Forsberg, 2001).

Each female dog was artificially impregnated two times during their reproductive cycle, with

a 24-hour gap between each insemination. Only fresh semen that had been collected beforehand was utilised, as frozen-thawed semen was not suitable due to its low quality after thawing (data not provided). A volume of 5.4 ml was used during insemination in order to reduce backflow.

The entire duration of the procedure, from the introduction of the endoscope to its withdrawal after AI, and the time taken for catheter introduction from the endoscope introduction through the vulva to the introduction in the cervical os, did not exceed 10 to 15 minutes.

The diagnosis of pregnancy was conducted through abdominal palpation and ultrasonographic examination between 25 and 30 days after the estimated LH surge (Fontbonne et al., 2006; Taverne et al., 1985).

There were no observable clinical indications of infection in any of the female dogs during the pregnancy diagnosis. Four out of five female dogs became pregnant, resulting in a conception rate of 80%. The litter size varied from 7 to 11 puppies, and all of them were delivered via caesarean section. Due to the absence of pregnancy in one female dog (the oldest one being 6 years old), a statistical analysis was not conducted. Nevertheless, there were no discernible variations in age, parity, serum P4 concentrations during LH surge and TCI, or sperm quality between the female dogs that successfully conceived and the one that did not conceive.

CONCLUSIONS

Precise identification of the ovulatory phase is crucial for determining the specific days for insemination. Hence, it is essential to conduct a methodical monitoring of the oestrous cycle utilising various techniques.

Furthermore, in the current study, progesterone levels were measured every two days, as suggested by other researchers, in addition to observing any changes in behaviour. Therefore, it was feasible to determine the exact day of the LH spike, enabling the identification of ovulation. The female dogs were artificially impregnated when the concentration of progesterone in their bodies exceeded 6 ng/mL. This was done to ensure that they were impregnated during their fertile phase, which includes the time of ovulation and maturation of the eggs.

In this investigation, the intrauterine insemination technique was conducted following the method described by Wilson (2003). However, the bitches were restrained on an antiskid surface table with an inclination of approximately 30 degrees to enhance the movement of semen to the upper uterine horns.

The difficulty in catheterizing the cervical canal, which was seen in certain animals, was due to factors such as the placement of the deep cervical tubercle and increased movement, but we achieved success in cervical transposition. This involved the simultaneous manipulation of both the endoscope and catheter, with the catheter positioned precisely in front of the cervical os.

In this study, it was found that all five artificial insemination (AI) procedures were able to successfully perform cervical catheterization in all female dogs. However, the level of difficulty varied across the procedures. Nevertheless, Wilson (1993) provided evidence of changes in the position of the cervical os during the progression of oestrus, likely due to dehydration and contraction of the vaginal folds. It was not feasible to insert a catheter in all the female dogs in that study, especially those with a lengthy vagina and a cervix that was out of reach of the equipment. Some of the dogs had a cervix that was positioned towards the front, while others had a cervix that was positioned towards the front and to the side (Wilson, 2003).

One additional aspect that hindered the process of inserting a catheter into the cervical os in this study was the presence of serosanguinous vaginal discharge. This discharge made it difficult to see the cervical os in certain female dogs. While serosanguinous vaginal discharge was present in the majority of female dogs during vaginoscopy prior to intrauterine artificial insemination (AI), it was only necessary to aspirate the discharge in 15% of the AI procedures. In this study, the recommended method of vaginal discharge aspiration, was successfully performed using a urinary catheter.

The technique is fundamentally simple but requires a significant amount of time, patience, and experience to achieve expertise. It

necessitates a comprehensive understanding of the reproductive tract's anatomy, and examining anatomical specimens is quite beneficial.

Attaching a video camera to the endoscope enables direct instruction under the guidance of a skilled operator, as it provides a visual representation of the ongoing procedure. The obstetrician is able to mentally perceive and comprehend the desired outcome.

Many people consider inserting the catheter into the os to be a difficult task, but it can be accomplished with confidence in a relatively short amount of time. However, it takes longer to become proficient in handling the unique characteristics of different breeds and sizes.

In order for the procedure to be widely embraced, it is crucial that it can be effectively administered to all, or at least the majority, of female dogs. Additionally, given the costly nature of the equipment, it is imperative that a significant number of female dogs can be inseminated by applying the exact same endoscope. Considering the wide variety of breeds available in terms of size and shape, it may appear improbable, but it is actually mostly feasible.

Understanding the constraining variables for each step of the procedure is crucial.

By visualising the cervix, it is absolutely certain that the catheter is inside the uterus. By continuously observing the insemination process, we can ensure that the semen is deposited in the uterus without any backflow. The use of a video camera allows both the client and the operator to witness the intrauterine deposition of the semen.

Overall, by assessing the behaviour and reproductive indicators, conducting serial serum progesterone assays, and examining vaginal cytology, it was possible to determine the LH surge day and ovulation. These procedures proved to be efficient in identifying the optimal time for performing artificial insemination (AIs).

There are precautions taken to keep the procedure as clean as feasible, but it is rarely aseptic. No infections associated with vaginal endoscopy have been identified (Stasi et al., 2001).

The challenges associated with performing the endoscopic transcervical intrauterine artificial insemination procedure in female Golden Retrievers were successfully and resolved by skilful equipment management and practical expertise. The specific characteristics of the technique, such as the challenge of cervical os catheterization, the resistance encountered during semen intrauterine deposition, and the occurrence of backflow, were consistent among the five artificial insemination methods examined in the female dogs that were tested.

One significant constraint of this investigation was identified. The findings of this study were validated through the use of ultrasound to examine the foetuses and gestational sac. However, the exact number of puppies was not established through visual examination. Hence, it remains ambiguous if this approach yields a typical duration of pregnancy and regular deliveries.

Furthermore, the accuracy of the confirmed number of foetuses using ultrasonography may not be as precise as those observed upon delivery. Hence, it is imperative to investigate the duration of pregnancy, the process of giving birth, and the quantity of offspring per birth in forthcoming studies.

The endoscope should not be seen as an exclusive procedure, such as artificial insemination, but rather should be utilised in all relevant circumstances in order to improve experience and proficiency.

Endoscopic vaginal endoscopy is a rapid, non-invasive procedure that can provide additional diagnostic information regarding the phase of the oestrous cycle and to conduct transcervical artificial insemination

REFERENCES

Arbeiter, K., Dobretsberger, M., Muller, E. and Holzmann, A., 1991. *Indirect detection of ovulation and fertilization in the dog by progesterone level testing.* Zentralbl. Veterinarmed. A 38: 696–701.

Blendinger, K., 2007a. *Physiology and pathology of the estrous cycle of the bitch*. In 56th Congresso Internazinale Multisala SCIVAC, Rimini. Proceedings of the 56th SCIVAC Congress, pp. 73–77.

Blendinger, K., 2007b. *Techniques of artificial insemination by fresh, chilled and frozen semen*. In: 56th Congresso Internazinale Multisala SCIVAC, Rimini. Proceedings of the 56th SCIVAC Congress, pp. 87–89.

Chapwanya, A., Clegg, T., Stanley, P., et al., 2008. *Comparison on the Immulite and RIA assay methods*

for measuring peripheral blood progesterone levels in Greyhound bitches. Theriogenology 70, 795–799.

Concannon, P.W., 2004. *Canine breeding management and artificial insemination: techniques and caveats*. In: 29th World Congress of the World Small Animal Veterinary Association, Rhodes. Proceedings (online). Available from: Access 14/12/08.

Concannon, P.W., McCann, J.P., Temple, M., 1989. *Biology and endocrinology of ovulation, pregnancy and parturition in the dog*. Journal of Reproduction and Fertility 39s, 3–25.

Concannon, P.W., 2005. *Understanding and monitoring canine pregnancy*. In: 30th World Congress of the World Small Animal Veterinary Association, Mexico City. Proceedings... (online). Available from: Access 15/01/2009.

de Gier, J., Kooistra, H. S., Djajadiningrat-Laanen, S. C., Dieleman, S. J. and Okkens, A. C., 2006. *Temporal relations between plasma concentrations of luteinizing hormone, follicle-stimulating hormone, estradiol-17beta, progesterone, prolactin, and alpha-melanocyte-stimulating hormone during the follicular, ovulatory, and early luteal phase in the bitch*. Theriogenology 65: 1346–1359.

England, G., Concannon, P.W., 2002. *Determination of the optimal breeding time in the bitch: Basic considerations*. In: Concannon, P.W., England, G., Verstegen, J., et al. (Eds), Recent Advances in Small Animal Reproduction. International Veterinary Information Service, Ithaca, New York.

Feldman, E.C., Nelson, R.W., 2004. *Canine and Feline Endocrinology and Reproduction*, third ed. Saunders Company, Philadelphia.

Fontbonne, A., 2006. *How to perform transcervical catheterization in the bitch*. In: 31st World Congress of the World Small Animal Veterinary Association, Sidney. Proceedings, pp. 721–722. Available from: Access 01/15/2009.

Fontbonne, A., Malandain, E., 2006. *Ovarian ultrasonography and follow-up of estrus in the bitch and queen*. Waltham Focus 16, 22–29.

Fukushima, F.B., Malm, C., Henry, M., et al., 2010. *Site of intrauterine artificial insemination in the bitch does not affect sperm distribution within the uterus.* Reproduction in Domestic Animals 45, 1059–1064.

Hase, M., Hori, T., Kawakami, E. and Tsutsui, T., 2000. *Plasma LH and progesterone levels before and after ovulation and observation of ovarian follicles by ultrasonographic diagnosis system in dogs*. J. Vet. Med. Sci. 62: 243–248.

Hori, T., Hagiuda, K., Kawakami, E. and Tsutsui, T., 2005. *Unilateral intrauterine insemination with prostatic fluid-sensitized frozen caudal epididymal sperm in beagle dogs.* Theriogenology 63: 1573–1583.

Jackson, P. G. and Nicholson, J. M., 1979. *The use of ultrasound to monitor fetal life in a pregnant bitch*. Vet. Rec. 104: 36

Jeffcoate, I.A., Lindsay, F.E.F., 1989. *Ovulation detection and timing of insemination based on hormone concentrations vaginal cytology and the endoscopic appearance of the vagina in domestic bitches*. Journal of Reproduction and Fertility 39s, 277–287.

Johnston, S.D., Kustritz, M.V.R., Olson, P.N.S., 2001. *Breeding management and artificial insemination of the bitch*. In: Johnston, S.D., Kustritz, M.V.R., Olson, P.N.S. (Eds.), Canine and Feline Theriogenology. Saunders Company, Philadelphia.

Kim, Y., Travis, A.J., Meyers-Wallen, V.N., 2007. *Parturition prediction and timing of canine pregnancy.* Theriogenology 68, 1177–1182.

Kustritz, R., 2007. *The value of canine semen evaluation for practioners.* Theriogenology 68, 329–337.

Kutzler, M.A., Mohammed, H.O., Lamb, S.V., et al., 2003. *Accuracy of canine parturition date prediction from the initial rise in preovulatory progesterone concentration*. Theriogenology 60, 1187–1196.

Lévy, X., Fontbonne, A., 2007. *Determining the optimal time of mating in bitches: particularities*. Revista Brasileira de Reprodução Animal 31, 128–134.

Linde-Forsberg, C., 1991. *Achieving canine pregnancy by using frozen or chilled extended semen*. Veterinary Clinics of North America – Small Animal Science 21, 467–485.

Linde-Forsberg, C., 2001. *Intra-uterine insemination in the dog using the scandinavian trans-cervical catheter and a comparison with other methods*. In: Concannon, P.W., England, G., Verstegen, J. (Eds), Recent Advances in Small Animal Reproduction. International Veterinary Information Service, Ithaca, New York.

Linde-Forsberg, C., Holst, B.S., Govette, G., 1999. *Comparison of fertility data from vaginal vs intrauterine insemination of frozen–thawed dog semen: A retrospective study*. Theriogenology 52, 11–23.

Macedo, S. P., Malm, C., Henry, M. R., Telles, L. F., Figueiredo, M. S., Fukushima, F. B., Neves, M. M., de Oliveira Cavalcanti, G. A., Chaves, M. S., Mascarenhas, R. M., de Albuquerque Lagares, M. and Gheller, V. A. 2012. *Endoscopic transcervical intrauterine artificial insemination in Labrador Retriever bitches*. Res. Vet. Sci. 92: 494–500.

Meyers-Wallen, V.N., 2007. *Unusual and abnormal canine estrous cycles*. Theriogenology 68, 1205–1210

Nizański, W., 2006. *Intravaginal insemination of bitches with fresh and frozen-thawed semen with addition of prostatic fluid: use of an infusion pipette and the Osiris catheter.* Theriogenology 66: 470–483.

Pretzer, S.D., Lillich, R.K., Althouse, G.C., 2006. *Single, transcervical insemination using frozen–thawed semen in the Greyhound: a case series study*. Theriogenology 65, 1029–1036.

Rodrigues, B.A., Rodrigues, J.L., 2002. *Endocrinologia reprodutiva na cadela*. Clínica Veterinária 40, 50–58.

Santos, S.E.C., Vannucchi, C.I., 1997. *Inseminação artificial em cães*. Clínica Veterinária 2, 22–24.

Silva, A.R., Cardoso, R.C.S., Silva, L.D.M., 2003. *Principais aspectos ligados à aplicação da inseminação artificial na espécie canina*. Revista Portuguesa de Ciências Veterinárias (RPCV) 98, 53–60.

Silva, L.D.M., Onclin, K., Lejeune, B., et al., 1996. *Comparisons of intravaginal and intra-uterine insemination of bitches with fresh or frozen semen*. Veterinary Record 17, 154–157.

Silva, L.D.M., Onclin, K., Snaps, F., et al., 1995. *Laparoscopic intrauterine insemination in the bitch*. Theriogenology 43, 615–623.

Stasi, K. and Melendez, L. 2001. *Care and cleaning of the endoscope*. Vet. Clin. North Am. Small Anim. Pract. 31: 589–603

Sum, S. and Ward, C. R. 2009. *Flexible endoscopy in small animals*. Vet. Clin. North Am. Small Anim. Pract. 39: 881–902.

Taverne, M. A., Okkens, A. C. and van Oord, R., 1985. *Pregnancy diagnosis in the dog: a comparison between abdominal palpation and linear-array real-time echography*. Vet. Q. 7: 249–255.

Thomassen, R., Sanson, G., Krogenaes, A., et al., 2006. *Artificial insemination with frozen semen in dogs: a retrospective study of 10 years using a non-surgical approach*. Theriogenology 66, 1645–1650.

Volkmann, D.H., 2006. *The effects of storage time and temperature and anticoagulant on laboratory measurements of canine blood progesterone concentrations*. Theriogenology 66, 1583–1586.

Wilson, M.S., 1993. *Non-surgical intrauterine artificial insemination in bitches using frozen semen*. Journal of Reproduction and Fertility 47s, 307–311.

Wilson, M.S., 2003. *Endoscopic transcervical insemination in the bitch*. In: Concannon, P.W., England, G., Verstegen III, J., Linde-Forsberg, C. (Eds). Recent Advances in Small Animal Reproduction. International Veterinary Information Service, Ithaca, New York.

Wright, P.J., 1990. *Application of vaginal cytology and plasma progesterone determinations to the management of reproduction in the bitch*. Journal of Small Animal Practice 31, 335–340.

Scientific Works. Series C. Veterinary Medicine. Vol. LXX (2), 2024
ISSN 2065-1295; ISSN 2343-9394 (CD-ROM); ISSN 2067-3663 (Online); ISSN-L 2065-1295

CLINICAL AND BACTERIOLOGICAL STUDY REGARDING A DEEP CHRONIC GOAT'S DERMATITIS

Adrian MIHAI, Nicoleta Andreea MINCĂ, Bogdan Alexandru TAȘBAC , Carmen IONIȚĂ, Roxana Mariana IGNĂTESCU, Daniela BRĂSLAȘU, Letiția PURDOIU, Lucian IONIȚĂ

University of Agronomic Sciences and Veterinary Medicine of Bucharest, Faculty of Veterinary Medicine, 105 Splaiul Independentei Street, 050097, District 5, Bucharest, Romania

Corresponding author email: ionitacarmen63@yahoo.com

Abstract

Our study reveals the association between a chronic local-generalized clinical hard-skin infection in a 2-year-old Sannen goat and pathogens identified from lesions. The particular infection consists of a deep haemorrhagic-purulent, non-contagious, ineffectively treated dermatitis. The open skin lesions were infected with a mixed microbial flora. It was therefore difficult to identify the actual pathogenic microorganism necessary for effective and specific treatment. By conventional bacteriological examinations, we identified three bacterial pathogens: a haemolytic strain of Staphylococcus, a non-haemolytic strain of Corynebacterium and a haemolytic and highly proteolytic strain of Trueperella pyogenes. We also isolated many other germs, including Gram negatives that do not ferment lactose. For Staphylococcus and Corynebacterium, we assessed antibiotic susceptibility by the Kirby-Bauer diffusimetric method. Through local and general antibiotic treatment (beta-lactams, aminoglycosides), associated with a stimulation of the immune system and prevention of possible secondary liver disease, an improvement in housing conditions also improved clinical condition, appetite, livability and wound healing rate.

Key words*: dermatitis, goat, Staphylococcus, Corynebacterium, Trueperella.*

INTRODUCTION

Many bacterial infections can be distinguished in the pathology of small ruminants. Some of them affect all tissues - generalized infections, others are localized. For local skin infections, with deep and multiple, disseminated lesions, the pathogenic ability of the bacteria to synthesize and release enzymes/exotoxins affects the clinical condition: weakness, altered appetite, functional impairment of milk production, etc.

In goat pathology, staphylococcal infections, *Corynebacterium* infections, also Grips bacillus infections (*Trueperella pyogenes*), including mixed infections can be identified.

Staphylococcus infectious are frequent and dangerous, a real problem in veterinary medicine. Patogenic *Staphylococcus* strains cause clinically various forms, more or less aggressive, such: pustules, haemorrhagic lesions or discrete lesions. In goats, *Staphylococcus* infections can be secondary to contagious pustular dermatitis (e.g. parapox viral infection), or the integumentary infections involves the different predisposing factors. Acute clinical mastitis is associated with *Staphylococcus aureus* (Arteche-Villasol et al., 2022; Lima et al., 2020). Staphylococcal exotoxin production appeared to be a consequent event inducing the evolution to gangrenous mastitis (Rainard et al., 2018).

Staphylococcus aureus and *Corynebacterium* are responsible for liver abscesses, thus being a possible common complication in small ruminants (Rosa et al., 1989; Tadayon et al. 1980). One of the most recognizable signs of liver dysfunction in most species is icterus. However, ruminants often do not become jaundiced even when there is severe hepatocellular dysfunction (Fetcher, 1983).

The studies shown that majority of *S. aureus* with the highest rate of resistance to penicillin (Mechesso et al., 2021). Several studies support enrofloxacin therapy, being the right choice in this case (Polveiro et al., 2021).

Trueperella pyogenes is an opportunistic, but hardly pathogen, that causes suppurative deep infections in animals. Also, it can do the complications of a minor wound. Similar with *Trueperella*, *Corynebacterium* pathogenic

strains can cause persistent pyogenic infections, difficult to treat without a specific diagnostic.
In this paper, we propose a complex analysis, by clinical and paraclinical tests, of a goat with a particular deep and severe skin infection, located on the metapodial areas; thick crusts are also present on the mammary tegument and on the external pinna of the ears.

MATERIALS AND METHODS

Our clinical and microbiological analysis were realized in November-December 2023.
Clinical examination was permanently associated with paraclinical tests on this patient: complete blood count, cytology, and microbiological diagnostic.
All animals from the farm, including the goat, were up to date with preventive actions (vaccinations, internal-external deworming). For monitoring the herd, we took blood samples from several individuals. Only one animal has shown this pathology.

Clinical examination

Normally, the skin is constantly exposed to different microorganisms - real pathogenic, opportunistic, non-pathogenic (Figure 1). Different injuries of the skin barrier allow bacteria or other microbes to proliferate and penetrate deep into the lower layers of the skin (Faccin, 2023).
Our clinical examination included an epidemiological investigation involving risk factors, epidemiological data, feed and shelter analysis.
Also, the clinical study included determination of age, body weight, body temperature, assessment of dehydration, appearance of mucous membranes and clinical examination.

Figure 1. Metapodial skin lesions of exterminated goat

Paraclinical diagnostic analysis

1. *Haematology and biochemistry tests.* Blood samples were collected from jugular vein puncture, using 21 G needles, heparin and K3EDTA vacutainers.
Haematological and biochemical tests were performed using the haematology analyser Abacus Junior Vet 5 (SUA) and the biochemistry analyser Arkray Spotchem EZ SP4430 (Japan) (Figure 2).
The results were compared to the available relevant literature data.

Figure 2. Abacus Junior Vet 5 and the biochemistry analyser Arkray Spotchem EZ SP4430

2. *Microbiology analysis.* The biologic samples were represented by thick crusts from the skin lesions, introduced in a sterile test-tube. Because the crusts were dry, we added into recipient sterile physiologic solution, and shacked on vortex for decompose the primary hard crust's structure.
About the microbiological diagnostic, we applied two conventional steps. The first was represented by a direct bacterioscopic exam of the pathological sample, on smears stained by Gram method, also by blue methylene simple variant. In the second part, we made cultural analysis, using special and usual culture media: Columbia sheep blood agar plates, MacConkey lactosed agar plates, Brain Hearth Infusion broth, coagulated horse serum blood tubes, nutrient agar and nutrient simple broth.
We inoculated the liquid samples on Columbia sheep blood agar, incubated at 37°C, in normal atmosphere, for 24-48 hours, but we continued the exam of the prime cultures - maintained on room temperature, during other few days.
From Columbia sheep blood agar, we selected the isolated colonies, especially the smooth haemolytic ones, also the non-haemolytic rough type colonies, transferred on sterile fresh culture media, for the secondary pure cultures. The pure cultures were examined macro- and microscopic, also few biochemical-enzymatic tests for establish the particular pathogenic properties of isolated strains.

We detected the haemolytic activity, also proteolytic properties on coagulated serum blood.
On secondary pure cultures we established the bacteria cells morphology, correlated with the macroscopic aspects, for obtain the typical germs properties.
Using the secondary cultures, decimal diluted, we performed the bacterium sensitivity test, by the antibiotesting, Kirby-Bauer method.

Local and general infection treatment
Although systemic and topical treatments have their usefulness, it is essential to manage risk factors to stop recurrences.
Supportive therapy was also provided together with a conservative two steps treatment. Therapy was initiated according to the antibiogram results.
We applied a two-step conventional therapy. The first was an injectable treatment with penicillin G procaine (Penstrep) in doses of 8 mg/kg penicillin and 10 mg/kg dihydrostreptomycin for 3 days, after which we decided to initiate treatment with enrofloxacin (Enroxil 5%) a daily dose of 50 mg/kg for a minimum of 5 days. To prevent secondary liver damage, dehydration and apathy, we resorted to fluid therapy and liver support.
For the secondary part of the treatment (local treatment) we chose neomycin spray and chlorhexidine washes twice a day. Complete healing was achieved after 62 days.
The first choice was penicillin for 3 days, then enrofloxacin to which both *Staphylococcus* and *Corynebacterium* were sensitive. Enrofloxacin is a fluoroquinolone, which acts by inhibiting DNA gyrase which causes bacterial cell division to be blocked. They are also known to have direct effects on the immune system.
As abscesses are known to occur in internal organs, with specificity in small ruminants for the liver area, secondary to *Corynebacterium*.

RESULTS AND DISCUSSIONS

Clinical examination
We identified the next general aspects of our case: approximate age of 2 years, body weight 23 kg, temperature 38.2°C, degree of dehydration > 12%, sticky whitish mucous membranes. Clinical examination on machines indicated increased intensity of cardiac noises, vesicular murmur at pulmonary auscultation, reaction to abdominal palpation on the hepatic projection area, ruminal noises present, defecation and normal urination. Decreased appetite and temperature were the most important indications for chronic secondary systemic involvement.
Multiple nodular lesions were identified on the skin, with active bleeding, pungent smell and myasis. The lesions tend to desquamation, with the extension of the proliferation area to the udder, posterior portion and ears. Open lesions showed numerous thick bloody scabs, especially on the limbs. In our case we included a mastitis with bacterial origin, in asymptomatic stage, most likely consecutive to chronic evolution.
The particular infection consists of a deep haemorrhagic-purulent, non-contagious, ineffectively treated dermatitis.
In conclusion, clinical examination revealed a deteriorated general condition, pronounced weakness, inadequate maintenance, chronic bad-smelling haemorrhagic lesions on the hind limbs. The goat showed multifocal alopecia with ulcers, erosions and scabs, predominantly on the dorsal portion. The skin lesions were pruritic, firm, demarcated, haemorrhagic and pigmented.
Cytology and biochemical results
Complete blood count showed ***chronic neutrophilia***, ***lymphocytic reaction*** and ***increased blood platelets***.
On the basis of these diagnostic tools, the diagnosis of chronic inflammatory skin disease complicated with recurrent bacteria was established. In these cases, the most important diagnostic test is the microbiological one.
Microbiology analysis results
The general appearance of the hydrated sample showed the presence of grey-greenish portions mixed with red parts (Figure 3). The odour was repulsive, ihorous.
Macroscopic aspects of primary cultures
The primary culture on Columbia sheep blood agar was very abundant, mixed: (1) a large number of medium size colonies, pigmented - grey-withe-yellow, smooth surface, circular edges, convex to flat profile, surrounded by a complete haemolysis; (2) many tiny colonies, rough surface, flat, non-haemolytic, grey

colour, with a medium to high consistence. After few days, we detected the presence of (3) the very small colonies, smooth type, surrounded by a narrow weak beta haemolysis area. We appreciated that the all three types mentioned colonies represent the codominant microflora. For other colonies types, we considered they correspond with saprophytic microbes.

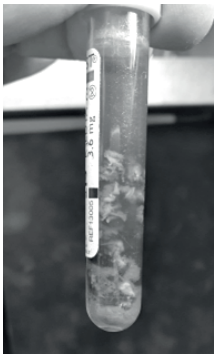

Figure 3. Biological sample, hydrated and mixed

On MacConkey lactosed agar, the cultures showed an abundant flora, with medium (a) and little (b) size colonies, smooth type; all of them are lactose-negatives.

Macroscopic aspects of secondary cultures

On pure secondary cultures, we observed the characteristic aspects of yellowish pigmented Staphylococcus on nutrient agar, and a thin ring and low turbidity in nutrient broth, that correspond with type (1) colonies; rough type, non-pigmented, opaque colonies, and a pellicule, medium to low turbidity - for type (2) colonies, on simple culture media; a low turbidity, a medium to large pulverulent sediment, non-adherent, on Brain Hearth Infusion broth, after few days of incubation, for type (3) colonies (Grips bacillus).

For lactose negative strains, from MacConkey agar plate, we obtained on nutrient slant agar smooth type, non-pigmented colonies, medium (a), and little (b) size, respectively, with a medium to high turbidity on nutrient broth. For (a) type, we observed a pellicule on the broth surface.

Microscopic analysis

The direct analysis of the samples, by Gram staining method, revealed: (1) many *Corynebacterium*-like Gram-positive polymorphic cocobacilli, arranged typically diplo V shape, and Chinese characters; (2) Gram-positive cocci, bunch of grapes arranged; (3) Gram-negative medium size isolated cocobacilli were also present, but in low number; (4) cellular debris, and the pycnotic nucleus of leucocytes.

In blue methylene staining method, we remarked similarities with the Gram stained smears, but a particular aspect of the *Corynebacterium*-like cells was significant: a specific irregular aspect of stained cytoplasm, by the presence of disseminated inclusion, and the biggest ones were at the extremity of bacterium, constantly.

We examined smears, staining by two methods, from the secondary pure cultures, too.

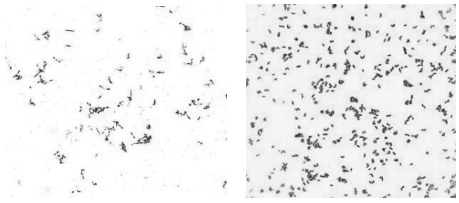

Figure 4. *Trueperella pyogenes* bacteria cells (left), *Corynebacterium* (right), Gram staining method, 1000x

The morphology of stained *Staphylococcus* revealed the Gram positive cocci, specifically arranged. For *Corynebacterium*, and *Trueperella*, Gram-positive bacteria, we detected many similarities, but *Trueperella* cells were more polymorphic, thin cells, with many cytoplasmic inclusions, and the dominant arrangement was Chinese characters (Figure 4).

Biochemical-enzymatic properties

The proteolytic character of small haemolytic beta colonies was very intense on coagulated serum blood cells. Indeed, within a short time - one day at 37°C, another few days at laboratory temperature, the serum was transformed almost entirely into a liquid consistency (Figure 5). One can easily correlate this breakdown of total serum proteins with the high pathogenicity of *Trueperella pyogenes*, as it can similarly break down proteinaceous tissues, such as the deep integument, *in vivo* layers. We add other enzymatic previous test - haemolysis.

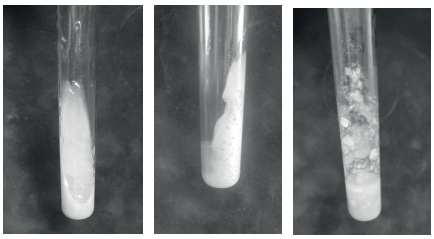

Figure 5. Intense proteolytic action of *Trueperella pyogenes* on coagulated blood from horse serum

By antibiotic susceptibility testing, we determined the susceptibility of *Staphylococcus* and, separately, *Corynebacterium* to some antibiotics (Figure 6).

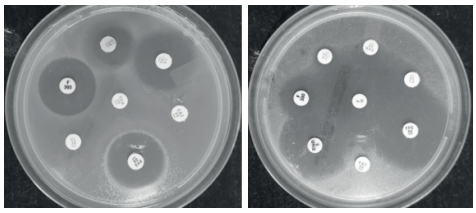

Figure 6. Antibiotic testing by Kirby-Bauer method

The *Staphylococcus* strain exhibited (Table 1) full resistance to Methicillin, which includes similar properties to the antibiotic beta-lactams. We obtained good susceptibility to fluoroquinolones as well as piperacillin, rifampicin, florfenicol and nitrofurantoin. A medium sensitivity to oxytetracycline was a good result, as it can be used directly on infected areas. The same important information corresponds with nitrofurantoin, as it can be used directly on infected tissues.

Table 1. Antibiotic test results for *Staphylococcus*

	ANTIBIOTIC SUBSTANCES	THE RESULTS
1.	METHICILLIN	R
2.	AMPICILLINE-SULBACTAM	R
3.	CEFALEXINE	R
4.	CEFTAZIDIME	R
5.	CEFUROXIM	R
6.	**PIPERACILIN**	**S**
7.	**RIFAMPICINE**	**S**
8.	OXYTETRACYCLINE	MS
9.	LINCOSPECTINE	MS
10.	**ENROFLOXACINE**	**S**
11.	**PEFLOXACINE**	**S**
12.	**OFLOXACINE**	**S**
13.	**FLORFENICOL**	**S**
14.	**NITROFURANTOINE**	**S**

Antibiotic testing of *Corynebacterium* strain (Table 2) showed many opportunities, such as susceptibility to penicillin, similar enrofloxacin, neomycin, bacitracin and nitrofurantoin.

Table 2. Antibiotic test results for *Corynebacterium*

	ANTIBIOTIC SUBSTANCES	THE RESULTS
1.	**PENICILLIN**	**S**
2.	AMPICILLINE-SULBACTAM	R
3.	CEFALEXINE	R
4.	CEFTAZIDIME	R
5.	CEFUROXIM	R
6.	**PIPERACILIN**	**S**
7.	**FLORFENICOL**	**S**
8.	OXYTETRACYCLINE	R
9.	LINCOSPECTINE	R
10.	ERITROMICINE	R
11.	**ENROFLOXACINE**	**S**
12.	**NEOMICINE**	**S**
13.	POLIMIXINE B	R
14.	**BACITRACINE**	**S**
15.	**NITROFURANTOINE**	**S**

We highlighted the possibility of a local antimicrobial therapy in combination with systemic antibiotics. Another aspect to be mentioned is the respect of common antibiotic susceptibility for both bacterial strains.

Treatment results

After microbiological diagnosis, response to therapy was initially rapid, followed by a period of slow healing. Peak clinical response was generally observed within 2 weeks of starting treatment.

Because microbiological diagnosis is complicated and involves different bacteria, we developed a continuity treatment plan by combining antibiotics to which they are sensitive. This animal was isolated from the others, then removed from the breeding plan and milked.

The clinical response to enrofloxacin was rapid but long-term and chronic pathology was associated with dramatic clinical signs. Although the animal was diagnosed at a very advanced stage, the efficacy of treatment was confirmed from the first day, with an improvement in general condition identified.

Healing was slow, possibly due to chronic pathology and multiple bacterial skin diseases.

Healing was complete 62 days after the start of treatment.

CONCLUSIONS

Through complex diagnostic tools we can provide some relevant conclusions:

1. The clinical exam is essential for establish the character of the disease.
2. The cytological exam and the blood tests provide many important data regarding the immunologic reactions of the patient.
3. Microbiology can identify the pathogenic microorganism involved in the dermatitis lesions. Also, a specific therapy can be correctly conducted according to the antibiotic sensitivity testing results.
4. Both topic and general complex treatment are required in this type of dermatitis for a good management of the case.

ACKNOWLEDGEMENTS

Diagnosis of chronic inflammatory skin disease complicated by bacteria was carried out with the help of the Department of Microbiology, the Department of Parasitology and the Department of medical clinic, the Faculty of Veterinary Medicine of Bucharest.

REFERENCES

Arteche-Villasol, N., Fernández, M., Gutiérrez-Expósito, D., & Pérez, V. (2022). Pathology of the Mammary Gland in Sheep and Goats. *Journal of comparative pathology*, 193, 37–49. https://doi.org/10.1016/j.jcpa.2022.02.007

Faccin, M., Wiener, D. J., Rech, R. R., Santoro, D., & Rodrigues Hoffmann, A. (2023). Common superficial and deep cutaneous bacterial infections in domestic animals: A review. *Veterinary pathology*, 60(6), 796–811. https://doi.org/10.1177/03009858231176558

Fetcher A. (1983). Liver diseases of sheep and goats. The Veterinary clinics of North America. Large animal practice, 5(3), 525–538. https://doi.org/10.1016/s0196-9846(17)30061-7

Lima, M. C., de Barros, M., Scatamburlo, T. M., Polveiro, R. C., de Castro, L. K., Guimarães, S. H. S., da Costa, S. L., da Costa, M. M., & Moreira, M. A. S. (2020). Profiles of *Staphyloccocus aureus* isolated from goat persistent mastitis before and after treatment with enrofloxacin. *BMC microbiology*, 20(1), 127. https://doi.org/10.1186/s12866-020-01793-9

Mechesso, A. F., Moon, D. C., Ryoo, G. S., Song, H. J., Chung, H. Y., Kim, S. U., Choi, J. H., Kim, S. J., Kang, H. Y., Na, S. H., Yoon, S. S., & Lim, S. K. (2021). Resistance profiling and molecular characterization of *Staphylococcus aureus* isolated from goats in Korea. *International journal of food microbiology*, 336, 108901. https://doi.org/10.1016/j.ijfoodmicro.2020.108901

Moga Manzat R. (2001). *Boli infectioase ale animalelor domestice. Bacterioze.* 394-400, Timisoara, RO: Brumar Publishing House.

Perianu T. (2001). *Boli infectioase ale animalelor domestice. Bacterioze.* 382, 389-390, Timisoara, RO: Brumar Publishing House.

Polveiro, R. C., Granja, M. M. C., Roldão, T. C. B., Da Silva Lopes, I., Vidigal, P. M. P., Lima, M. C., & Moreira, M. A. S. (2021). Multilocus sequence analysis reveals genetic diversity in *Staphylococcus aureus* isolate of goat with mastitis persistent after treatment with enrofloxacin. *Scientific reports*, 11(1), 17252. https://doi.org/10.1038/s41598-021-96764-z

Rainard, P., Gitton, C., Chaumeil, T., Fassier, T., Huau, C., Riou, M., Tosser-Klopp, G., Krupova, Z., Chaize, A., Gilbert, F. B., Rupp, R., & Martin, P. (2018). Host factors determine the evolution of infection with *Staphylococcus aureus* to gangrenous mastitis in goats. *Veterinary research*, 49(1), 72. https://doi.org/10.1186/s13567-018-0564-4

Rosa, J. S., Johnson, E. H., Alves, F. S., & Santos, L. F. (1989). A retrospective study of hepatic abscesses in goats: pathological and microbiological findings. The *British veterinary journal*, 145(1), 73–76. https://doi.org/10.1016/0007-1935(89)90012-2

Tadayon, R. A., Cheema, A. H., & Muhammed, S. I. (1980). Microorganisms associated with abscesses of sheep and goats in the south of Iran. *American journal of veterinary research*, 41(5), 798–802.

Tasbac, B. (2018). *Microbiologie veterinara generala. Lucrari practice ilustrate. Editia a doua,* 34-87, 88-116, 158, 166-168, Campulung Muscel, RO: Larisa Publishing House.

Tasbac, B. (2022). *A color handbook of special bacteriology. The Gram positive bacteria*. 1-6, 37-39, 47-78, Campulung Muscel, RO: Larisa Publishing House.

Vasiu C. (2011). *Tratat de boli infectioase ale animalelor domestice. Bacterioze. 699-700, 703, 707-708, I,* Iasi, RO: Brumar Publishing House

Scientific Works. Series C. Veterinary Medicine. Vol. LXX (2), 2024
ISSN 2065-1295; ISSN 2343-9394 (CD-ROM); ISSN 2067-3663 (Online); ISSN-L 2065-1295

HEMATOLOGICAL AND BIOCHEMICAL INVESTIGATIONS IN CASE OF ACETAMINOPHEN ADMINISTRATION IN HORSES

Dalma PIVARIU[1], Mircea MIRCEAN[2], Nechita-Adrian OROS[1], Alexandra MUREȘAN[2], Zsofia DARADICS[2], Robert STĂNILĂ[1], Naomi LATIȘ[1], Melania Ioana CRIȘAN[3], Sabrina ARDELEAN[4]

[1]Department of Toxicology, Faculty of Veterinary Medicine, University of Agricultural Sciences and Veterinary Medicine Cluj-Napoca, Calea Manastur 3-5, 400372, Cluj-Napoca, Romania
[2]Department of Internal Medicine, Faculty of Veterinary Medicine, University of Agricultural Sciences and Veterinary Medicine Cluj-Napoca, Calea Manastur 3-5, 400372, Cluj-Napoca, Romania
[3]Department of Physiology, Faculty of Veterinary Medicine, University of Agricultural Sciences and Veterinary Medicine Cluj-Napoca, Calea Manastur 3-5, 400372, Cluj-Napoca, Romania
[4]Department of Clinical Sciences, Ross University School of Veterinary Medicine, Basseterre P.O. Box 334, Saint Kitts and Nevis

Corresponding author email: melaniacrisan@gmail.com

Abstract

Acetaminophen is one of the most used analgesic agent for the relief of acute and chronic pain in humans. Equine analgesia poses a common challenge to clinicians, so acetaminophen could be considered as an alternative to common non-steroidal anti-inflammatory drugs used in horses.

The purpose of this research was to observe the safety of treatment with acetaminophen, and it was carried out at the USAMV Cluj-Napoca. In order to initiate treatment with acetaminophen, a dose of 20 mg/kg was administered orally, once every 12 hours, for a period of 14 days, in two horses of approximately 500 kg, aged 16 and 17 years, from Lipizzan breed. We administered the commercial product Paracetamol Terapia, containing 500 mg acetaminophen each tablet, for human use. The horses in this study were monitored throughout the treatment, from a clinical point of view, and complementary examinations were made (the gastric mucosa was monitored with gastroscopy). The haematological analyses were performed with the Abacus Junior Vet5, and for the biochemical analyses a Skyla vb1+ analyser was use. In this study during the treatment, no significant haematological or biochemical changes were observed after acetaminophen administration.

Key words*: acetaminophen, pain, anti-inflammatory drug, exams.*

INTRODUCTION

Pain management in horses represents a real challenge encountered often by clinicians. In human medicine, acetaminophen is used for its analgesic and antipyretic effect, therefore emerged an alternative to replace non-steroidal anti-inflammatory drugs (NSAID) that are so commonly used in horses. The studies that have already been completed are pointing out that acetaminophen has a high absorption rate in horses and because of its mechanism of action, there were no signs of side effects when it was used in the correct doses. Acetaminophen, used in horses that showed different sort of pain-inducing diseases showed encouraging results, becoming more a current topic, as the pain from an orthopaedic condition is different from an abdominal pain (Jones E. et al., 2007). Moreover, when used as an adjuvant, it proved to enhance the analgesic effect of other drugs.

The purpose of the research carried out under the guidance of the department of Toxicology and Internal Medicine, from the University of Agricultural Sciences and Veterinary Medicine of Cluj-Napoca, is to observe the safety of acetaminophen treatment in horses. The horses monitored in this research were clinically evaluated before the acetaminophen administration, haematological, and biochemical analyses were carried out.

Acetaminophen, often known as paracetamol, is a medicine used to treat fever and moderate pain. It was synthesized in 1873, by reducing p-

nitrophenol in acetic acid medium. Its therapeutic properties were not recognised at the time of its discovery, until Bernard Brodie and Julius Axelrod discovered that the metabolite, acetanilide had the analgesic effect.
The relatively large safety margins make it a drug of choice in the management of moderate pain in humans (Graham et al., 2013). This substance gained interest as an alternative to non-steroidal anti-inflammatory drugs because its mechanism of action has fewer gastrointestinal side effects compared to NSAIDs. It has been found, that when administered together with other non-steroidal anti-inflammatory drugs, especially COX-2 inhibitors, acetaminophen potentiates their analgesic and anti-inflammatory action compared to their solitary use (Latimer et al., 2011).
Recently there have been studies proving the effectiveness of acetaminophen treatment in horses, acetaminophen is reported to have 91% bioavailability (Neirinckx et al., 2010). Its use is cited both as a single agent, especially in cases of lameness, West et al., in 2011, has demonstrated efficacy as an adjunct treatment for laminitis in one pony and in combination with NSAIDs for pain control in general, it is an effective analgesic agent when combined with NSAIDs in a model of inducible foot pain (Foreman et al., 2016). Recent research on this protocol makes this topic novel, making acetaminophen a serious candidate for equine analgesic medication. In this paper, we want to present data's on the adverse effects of acetaminophen and see it's safety in adult horses.

MATERIALS AND METHODS

Acetaminophen was administered to two horses of approximately the same weight (500-550 kg) presenting normal body score. Both horses are belonging to the Lipizzan breed, a 16-year-old male (Siglavy-Capriola XX-25) and a 17-year-old female (Maestoso XLVII-27). Before starting the treatment with acetaminophen, the horses were examined from a clinical and paraclinical point and performed biochemical and haematological analyses. Following the examinations performed, the horses were declared clinically healthy.
In our protocol, we administered acetaminophen, in a dose of 20 mg/kg, orally once every 12 hours for 14 days. Considering that there is no approved commercial product containing acetaminophen, for veterinary use, we used Paracetamol Terapia 500 mg tablets, for human use. Prior to administration the tablets were ground in a mortar to obtain a powder. This pulvis was mixed with a 3% glucose solution and was administered orally with a 20 mL syringe whose tip was previously removed.
To perform the haematology examination, the blood was collected on day 0, before the first administration of acetaminophen, on day 7, and day 14, which was also the last day of the treatment. Blood sample collection was performed by puncturing the left jugular vein, after performing antisepsis and a light manual haemostasis. The collected blood was stored in vacutainers with a purple and green lid. The haematological analyses were performed using an Abacus Junior Vet 5 device.
Blood biochemistry was performed using a Skyla vb1+ device. The serum is introduced inside the rotor with reagents, where the chemical reactions take place, then at the end of the process the results of the biochemical analyses are displayed. A single sample is sufficient for the analysis of several biomarkers in a panel.

RESULTS AND DISCUSSIONS

Before starting the treatment protocol with acetaminophen, we carried out a series of analyses at the department of Pathology and Clinical Medicine of Faculty of Veterinary Medicine in Cluj-Napoca. The obtained values and required parameters are shown in the Table 1, below.
We observed slightly elevated values of urea, total protein, serum glucose and triglycerides. These values can be attributed to the advanced age of the horses, to the diet or to some conditions existing before the research was carried out. We administered acetaminophen to older horses, with the approximately same age, breed, and weight, to have a picture of the effects of acetaminophen in this category, where we found no studies.

Table 1. The biochemical values before starting the treatment protocol

The analysed parameters	Mollys results	Samans results	Reference interval
Urea (mg/dL)	51.9	44.2	18-42
Creatinine (mg/dL)	1.19	0.91	0.79-1.808
Total bilirubin (mg/dL)	1.43	3.43	<2.63
Total proteins (g/dL)	7.14	7.28	5.3-6.5
Albumin (g/dL)	2.12	2.23	1.8-2.73
Globuline (g/dL)	1.62	1.67	1.32-2.14
Glucose (mg/dL)	121.0	100.4	50-90
Triglycerides (mg/dL)	87.6	76.4	8.75-35
Phosphorus (mg/dL)	3.68	3.45	3.1-5.26
Calcium (mg/dL)	9.15	10.1	8-13
Gamma-glutamyltransferase (U/L)	43.3	46.2	10-60

The patients were clinically healthy during the administration of the substance, their appetite and peristalsis was also normal.

The haematological and biochemical analyses did not reveal significant changes or detect a liver dysfunction attributed to a potential hepatotoxicity resulting from the administration of acetaminophen. Compared to the results presented in other studies, which demonstrate a decrease in the value of platelets during treatment, in this study the blood platelets decreased too, possibly due to platelet aggregation. In humans, Fischereder et al. (1994) reported thrombocytopenia in 3.4% of humans, presenting acute acetaminophen toxicity in a retrospective evaluation suspecting a direct toxic effect on platelets. More studies are needed to the changes in platelet counts. Maintenance of serum protein values close to the upper limit or even slightly exceeding this threshold, has also been reported in other studies (Mercer, 2018) where the same treatment protocol was used. Thus, an interaction between the mechanism of action of acetaminophen and protein production can be considered.

Table 2. Haematological analyses

HAEMATOLOGY ANALYSES	MOLLY				SAMAN			
	Day 0	Day 7	Day 14	Ref. int.	Day 0	Day 7	Day 14	Ref. int.
Erythrocyte (RBC) 10^{12}/l	6.08	6.38	7.14	6.8-12.9	7.18	6.95	6.89	6.8-12.9
Hemoglobin (HGB) g/dL	10.6	11.8	13.5	11-19	12.2	12.2	11.5	11-19
Hematocrit (HCT) %	37.27	39.31	43.06	32-53	40.54	39.29	38.06	32-53
VEM / MCV Fl	61	62	60	37-59	56	57	55	37-59
MCH Pg	17.5	18.5	18.9	12.3-19.7	16.9	17.5	16.7	12.3-19.7
MCHC g/dL	28.5	29.9	31.4	31-39	30.0	31.0	30.2	31-39
Platelet 10^9/l	108	61	59	100-400	127	88	111	100-400
Leukocyte (WBC) 10^9/l	10.16	13.14	11.25	5.4-14.3	11.02	10.04	9.80	5.4-14.3
Limphocyte (LYM) 10^9/l	5.05	4.85	5.27	1.5-7.7	3.87	3.64	3.18	1.5-7.7
Monocyte (MON) 10^9/l	0.44	0.55	0.06	0-1.5	0.01	0.22	0.23	0-1.5
Neutrophil (NEU) 10^9/l	4.14	7.46	5.55	2.3-9.5	6.08	5.48	5.85	2.3-9.5
Eozinophil (EO) 10^9/l	0.49	0.26	0.34	0.1-1	0.95	0.64	0.49	0.1-1

The blood tests from Molly on day 0 reveals a mild, microcytic, hypochromic and regenerative anaemia, probably due to a post haemorrhagic background. On the 7th and 14th day of treatment, the values normalized, thus suggesting the presence of a pre-existing condition. At the end of the treatment, the erythrogram values were within reference

intervals. The values displayed in the leukogram did not show significant changes during the treatment, being within normal limits at each test (Table 2).

The parameters of the erythrogram did not show significant changes in any value in case of Saman. The only changes reported were in the case of platelets, on day 7, when the displayed value dropped below the normal limits of the species, most likely due to platelet agglutination. The values displayed in the leukogram showed no significant changes throughout the treatment, being within normal limit at each test (Table 2).

The biochemical analyses of Molly showed that the albumin and glucose level remained within the normal limits, the total proteins were close to the upper limit. The liver enzymes represented by ALP, AST and GGT did not show values outside of the reference ranges during treatment. The GLDH enzyme was measured only at the end of the research, but its value was also within the reference limits of the species (8.8 U/L, Ref. int 0-20 U/L). The value of creatine kinase, an enzyme with importance in the metabolism of skeletal muscles, produced by the metabolism of creatine-phosphate in muscles in a constant rate, depending on the muscle mass (Jose H. Salazar, 2014) did not suggest damage throughout the administration of acetaminophen. The role of serum urea is to measure renal dysfunction, also providing information about the liver function or the dietary protein intake (Jose H. Salazar, 2014). In this study urea showed values above the normal limits on day 0 (30.8 mg/dL) and on day 7 (36.4 mg/dL) but on day 14 dropped to 24.4 mg/dL, situating between the normal range (10.0-30.0 mg/dL). The creatinine values were maintained in the reference range throughout the treatment. There were also no significant changes in the electrolytes throughout the treatment, they were constantly within normal limits. As an observation, we noticed an apparently low value of serum calcium, but that can be attributed to the reference range of the device, this value is only relatively low, compared to other kits (8-13 mg/dL), yet in other similar studies calcium decrease was observed too, may have been due to improvement in protein binding from rising total protein concentrations, or to increased dietary intake with supplemental feeding provided during the study period (Mercer et al., 2018)

The analyses in case of Saman showed that the total proteins were above the reference limits, characteristic of the species (5.6-7.9 g/dL), with a value of 8.1 g/dL on the first day, respectively 8.2 g/dL on day 7, following which on day 14 it normalized (6.9 g/dL), so mild hyperproteinaemia is noted at the start of acetaminophen administration, with serum total protein values subsequently normalizing. Comparing these results with the results presented in other articles based on the same protocol, it confirms a potential correlation between the administration of acetaminophen and the increase of total protein values. The value of serum albumin decreased gradually during the study period but was always within the biological limits (2-4.30 g/dL). The glucose value did not undergo significant changes, neither the hepatic enzymes, or creatine kinase, remaining constant within the reference range, as in a pilot study, made by Mercer et al., in 2018. The value of total bilirubin decreased gradually during the treatment. As in the first patient, the glutamate dehydrogenase value was only measured on day 14 of treatment and it was found also within the normal reference intervals (4.5 U/l, Ref. int 0-20 U/L). The serum urea values were normal on day 0 and day 7, but on day 14 they increased, yet the creatinine situated between the normal limits, also the electrolytes. The data is presented in Tabel 3.

Table 3. Biochemical analyses

BIOCHEMICAL ANALYSES	MOLLY				SAMAN			
	Day 0	Day 7	Day 14	Ref. int.	Day 0	Day 7	Day 14	Ref. int.
Albumin (ALB) [g/dL]	3.0	2.6	2.8	2.1-4.3	3.2	2.9	2.7	2.1-4.3
Total proteins (TP) [g/dL]	7.6	7.5	7.6	5.6-7.9	8.1	8.2	6.9	5.6-7.9
Glucose (GLU) [mg/dL]	81	66	84	63-136	85	87	72	63-136
Alkaline phosphatase (ALP) [U/L]	191	159	165	0-326	240	203	165	0-326
Aspartate-aminotransferaze(AST)[U/L]	434	306	342	92-610	390	299	334	92-610
Gamma-glutamyltransferaze (GGT) [U/L]	14	16	16	0-42	13	16	17	0-42
Total bilirubin (TBIL) [mg/dL]	1.5	1.5	2.9	0.0-3.5	2.9	2.3	1.5	0.0-3.5
Creatinkinaza(CPK) [U/L]	272	217	258	0-350	205	160	221	0-350
Uree(BUN) [mg/dL]	30.8	36.4	24.4	10.0-30.0	25.2	24.1	31.7	10.0-30.0
Creatine (CREA) [mg/dL]	1.24	1.38	1.00	0.70-2.00	0.91	0.83	1.23	0.70-2.00
Serum bicarbonate (tCO2) [mmol/L]	26.3	27.6	33.6	20.0-33.0	27.1	29.9	29.2	20.0-33.0
Calcium (Ca) [mg/dL]	10.3	9.6	10.2	11.5-14.2	9.9	9.9	9.6	11.5-14.2
Sodium (Na) [mmol/L]	135	138	138	126-146	132	139	138	126-146
Potassium (K) [mmol/L]	3.6	3.6	3.5	2.5-5.2	2.7	2.4	3.5	2.5-5.2

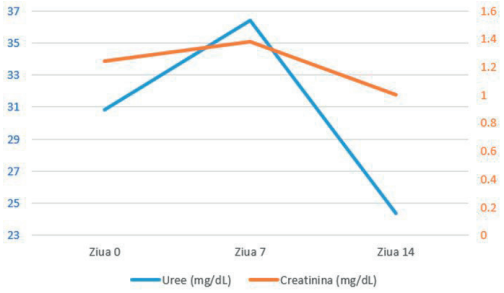

Figure 1. The uree value analyses in Day 0, 7 and 14 (Molly)

The urea value from Molly's blood according to the biochemical analyses was elevated in day 7 but it dropped to the normal limits in day 14, we could observe slightly increased creatinine values too in day 7 (Figure 1).

In Saman case both urea and creatinine were elevated in day 14, but after another 7 days after stopping the administration of acetaminophen both normalized (Figure 2).

The urea and creatinine elevations in both cases, raise questions about the metabolization and elimination of acetaminophen in elder horses, because these modifications were not reported in middle-aged horses.

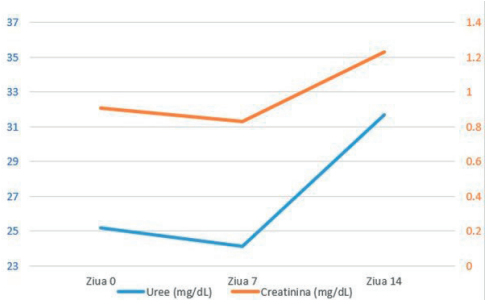

Figure 2. The uree value analyses in Day 0, 7 and 14 (Saman)

CONCLUSIONS

In this study during the treatment, no significant haematological changes were observed after acetaminophen administration in a dose of 20 mg/kg, orally once every 12 hours, for 14 days. The decrease in platelets may be attributed to platelets aggregation, and further investigation is needed to see the correlation.

The biochemical analyses revealed a slight increase in proteinemia during treatment, these results were seen in other studies too, probably the increase is a consequence of acetaminophen mechanism of action.

The increased values of urea and creatinine could be seen probably due to the age of the patients or nutrition factors, these increases were not reported in other studies, so they need to be investigated.

The liver function was not affected during the treatment. The horses did not show clinical signs indicating a hepatopathy (as weight loss, jaundice, colic, photosensitivity, etc.) and the liver enzyme values remained within the physiological ranges. Thus, following the use of this protocol, no cases of hepatotoxicity have been reported.

Acetaminophen can be recommended for elderly horses with chronic conditions for its anti-inflammatory and analgesic effect. This could be an option in case of chronic laminitis, chronic osteoarticular conditions or in case of conditions that do not allow venous access (phlebitis, severe dehydration, etc.).

Following this study, we showed that acetaminophen has a high bioavailability in horses with chronic conditions, without the presence of adverse reactions in the administered dose. It can be administered instead of non-steroidal anti-inflammatory drugs, or a combined protocols could be used.

Further multi-way studies are needed to be able to correlate the action of acetaminophen with the changes in proteinemia and platelet count. Due to the lack of research acetaminophen is not recommended to administer to pregnant mares, and to sport horses participating in the equestrian competitions.

ACKNOWLEDGEMENTS

We want to thank Ing. Chimist Elena Zinveliu for her dedicated work and help.

REFERENCES

Fischereder M, Jaffe JP. (1994). Thrombocytopenia following acute acetaminophen overdose. *Am J Hematol* ; 45: 258-259.

Foreman J, Foreman C, Bergstrom B. (2016) Acetaminophen/Paracetamol Efficacy in a Reversible Model of Equine Foot Pain. *AAEP Annual Convention;* 295-296.

Graham G.G., Davies M.J., Day R.O. et al. (2013). The modern pharmacology of paracetamol: therapeutic actions, mechanism of action, metabolism, toxicity and recent pharmacological findings. Inflammopharmacology.

Jones E, Viñuela-Fernandez I, Eager R.A., et al. (2007). Neuropathic changes in equine laminitis pain. Pain. 132(3): 321-331. doi: 10.1016/j.pain.2007.08.035. Epub 2007 Nov 1. PMID: 17935886.

Jose H. Salazar (2014). Overview of Urea and Creatinine.

Latimer N., Lord J., Grant R.L., et al. (2011). Value of Information in the Osteoarthritis Setting. *PharmacoEconomics*.

Melissa Ann Mercer, Harold C. McKenzie, Chair, Jennifer L. Davis, Bridget J. McIntosh, Katherine E. Wilson, David R. Hodgson (2018). Pharmacokinetics and Safety of Acetaminophen in Horses.

Neirinckx E, Vervaet C, De Boever S, et al. (2010). Species comparison of oral bioavailability, firstpass metabolism and pharmacokinetics of acetaminophen. *Research in Veterinary Science*; 89: 113-119.

West E, Bardell D, Morgan R, et al. (2011). Use of acetaminophen (paracetamol) as a short-term adjunctive analgesic in a laminitic pony. *Veterinary Anaesthesia and Analgesia*; 38: 521- 522. 22.

Scientific Works. Series C. Veterinary Medicine. Vol. LXX (2), 2024
ISSN 2065-1295; ISSN 2343-9394 (CD-ROM); ISSN 2067-3663 (Online); ISSN-L 2065-1295

PERITONEO-PERICARDIAL DIAPHRAGMATIC HERNIA IN A MINIATURE SCHNAUZER: CASE REPORT

Alina ȘTEFĂNESCU, Cristian Ionuț FLOREA, Crina Alexandra BOANCĂ, Andrei RĂDULESCU, Alexandru Bogdan VIȚĂLARU

University of Agronomic Sciences and Veterinary Medicine of Bucharest, Faculty of Veterinary Medicine, 105 Splaiul Independentei Street, 050097, District 5, Bucharest, Romania

Corresponding author email: alexandrumv@yahoo.com

Abstract

A five-months-old female Miniature Schnauzer dog, was referred with persistent vomiting and history of inappetence, lack of appetite, abdominal distention, tachypnea, and progressive weight loss. During clinical examination, the patient presented a defense reaction in the epigastric region upon deep palpation, auscultation of left side of the lungs found enhanced respiratory noises. Cardiac auscultation, revealed diminished heart sounds and intermittent borborygmi on the right hemithorax. At abdominal focused assessment with sonography in trauma, intestines were slightly distended by gas and liquid content and motility was reduced. The X-rays revealed enlarged cardiac silhouette and abnormal topography of the intestinal mass, with the cranial displacement especially on the projection area of the right heart. The radiological aspect suggests a peritoneo-pericardial hernia with the involvement of the small intestine. Peritoneo-pericardial hernia is a malformation which allows the protrusion of abdominal organs into the pericardial sac. Surgical repair was performed by herniorrhaphy with a polypropylene suture. Antibiotics were administered before and after surgery. Following herniorrhaphy, an abdominal exploration was performed. The only treatment for peritoneo-pericardial hernias is surgical and the main tool for diagnosis is radiography.

Key words*: peritoneo-pericardial, hernia, dog, surgery.*

INTRODUCTION

Peritoneo-pericardial diaphragmatic hernia (PPDH) is the end result of dysembryogenesis, wherein a connection stays among the pericardial and peritoneal cavity, permitting the displacement of stomach viscera into the pericardium (Banz, et al., 2010; Bjorck et al., 1970; Evans et al., 1980).

Peritoneo-pericardial diaphragmatic hernia has additionally been proposed to end result from the malformation of the septum transversum and pleuroperitoneal folds for the duration of embryonic development (Bolton et al., 1969; Less, R. D. et al., 2000).

This could be a result of a teratogen, genetic defect, or prenatal injury.

Peritoneo-pericardial diaphragmatic hernia appears to be a common incidental finding, and a breed predilection in Weimaraners and Cocker Spaniels.

Organs herniated into the pericardial sac may include the liver, the gallbladder, falciform ligament, omentum, spleen, stomach, small intestine, and colon (Hunt et al., 2003; McClaran et al., 2023).

Radiographic findings associated with PPDH include cardiomegaly, convex projection of the caudal cardiac silhouette, abdominal organs identified within the pericardial sac, and a confluent silhouette between the diaphragm and the heart. Diagnosis may be difficult with herniation of solid organs such as the liver or spleen as they will lack radiographic contrast (Park et al., 2002; Chalkley et al., 2006).

Treatment includes surgical herniorrhaphy, however, medical management or conservative treatment is commonly used, particularly in the absence of clinical signs or in the presence of medical conditions limiting surgical repair (Banz et al., 2010; Evans et al., 1980; Burns et al., 2008).

MATERIALS AND METHODS

A five-months-old intact female Miniature Schnauzer dog, was referred for a general consultation on the 24th of August, 2023. In the

last 24 hours the dog was presenting 6 episodes of vomiting after she was groomed. Vomit was consistent with undigested food content. The dog was presented with the following symptoms: lethargy, appetite loss, dehydration (5-7%, considerable loss of skin turgor), body temperature of 38.5ºC and sticky mucous membranes.

The complete blood count (CBC) was performed on Vetscan HM5 Hematology (5-part Differential) and determined: white blood cells (WBC), lymphocytes (LYM), monocytes (MON), neutrophils (NEU), eosinophils (EOS), basophils (BAS), LYM%, MON%, NEU%, EOS%, BAS%, red blood cells (RBC), hemoglobin (HGB), hematocrit (HCT), mean corpuscular volume (MCV), mean corpuscular hemoglobin (MCH), mean corpuscular hemoglobin concentration (MCHC), red blood cell distribution width-coefficient of variation (RDWc), red blood cell distribution width-standard deviation (RDWs), platelet (PLT), mean platelet volume (MPV), plateletcrit (PCT), platelet distribution width-coefficient of variation (PDWc) and platelet distribution width-standard deviation (PDWs).

Serum biochemistry was done on Vetscan VS2 Chemistry Analyzer with a comprehensive diagnostic panel that determined: albumin (ALB), alkaline pshophatase (ALP), alanine aminotransferase (ALT), amylase (AMY), total bilirubin (TBIL), blood urea nitrogen (BUN), calcium (CA), phosphorus (PHOS), creatinine (CRE), glucose (GLU), sodium (NA+), potassium (K+), total proteins (TP) and globulin (GLOB).

Blood pressure was evaluated with VET BP Doppler with manometer.

Ultrasound exam was performed on Easote My Lab 7.

Rehydration was established by fluid therapy with Ringer continuous rate of infusion (CRI), (rate and dosage: 10 ml/kg/h) and electrolyte rebalancing and partial parenteral nutrition based on levo-amino acids (rate and dosage: 6 ml/kg/24 h, 0.6-0.8 g amino acids/kg/24 h).

The amount of energy required for maintenance is best expressed as a function of the animal's metabolic weight, rather than its bodyweight. The RER (Resting energy requirement) is the basic energy requirement unit, around which the energy requirements of the various stages of health and illness can be calculated. This is the amount of energy (measured in kilocalories) required per day for maintaining current bodyweight (and avoiding catabolism of body tissues) while a patient rests quietly in a stress-free, non-fasted, thermo-neutral environment. RER was calculated for this patient using the following formulae:

RER = (30 x bodyweight in kg) + 70

For parenteral nutrition was used Intralipid 20% 1000 ml infusible emulsion contains purified soybean oil 200 g and excipients, anhydrous glycerol 22 g, purified egg phospholipids 12 g, sodium hydroxide (up to pH approximately 8), water for injections up to 1000 ml. Energy content: 8.4 MJ (2000 kcal)/1000 ml (Figure 1).

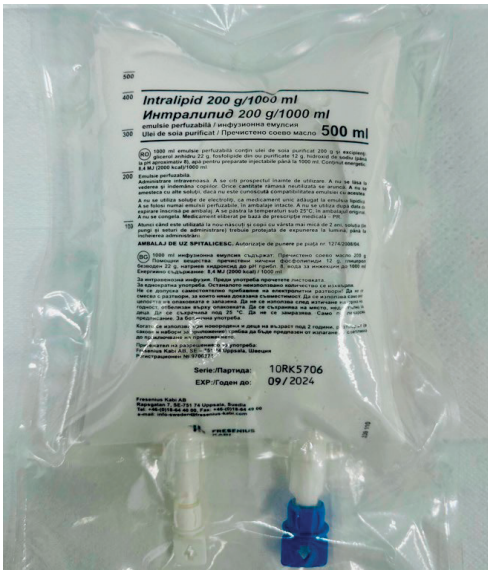

Figure 1. Intralipid 200 g/1000 ml used for patient's parenteral nutrition

Electrocardiogram (ECG) recording and monitoring was performed using Poly-Spectrum 8 Vet Rhythm, 4 clip electrodes with 6-lead ECG.

Electrodes must be positioned as follows: the red one with the inscription RA positioned on the right forelimb, the black one with the inscription RL positioned on the right hind limb, the yellow one with the inscription LA positioned on the left forelimb, the green one with the inscription LL positioned on the left hindlimb.

RESULTS AND DISCUSSIONS

On the 24th of August 2023, blood biochemistry revealed: BUN 12 (RR: 7-25 mg/dL), CREA 0.5 (RR: 0.4-1.4 mg/dL), K^+ 4.4 (RR: 3.4-5.6 mmol/L), CA 11.3 (RR: 8.6-11.8 mg/dL), PHOS 6.6 (RR: 2.9-6.6 mg/dL). Results from complete blood cell count (CBC) showed HCB 14.1 (RR: 12-18 g/dl), HCT 43.93 (RR: 37-55%), MCHC 32.1 (RR: 31-39g/dl) and RDWc 15.7 (RR: 14-20%). Based on the blood work results the patient shows normal values taking into account age and condition. Point of care ultrasound revealed: urinary bladder in semireplation state, distended by anechoic fluid content, and thin wall; spleen with regular outline, parenchyma without changes, dimensions of 0.68 cm in hilum; left kidney with regular outline, appropriate ratio between the renal cortical and renal medullary, shows renal microlithiasis, dimensions: 3.93/2.17 cm; right kidney appearance as the left kidney, dimensions 4.02/1.99 cm; stomach was distended with abundant liquid and gaseous content, absent motility at the time of examination, parietal reaction present; intestines with reduced motility at the time of examination, distended by liquid and gas content, slight parietal reaction present; liver with no pathological changes; gall bladder pre-prandial appearance devoid by transsonic content, without stones, thin wall. On the cross section, in the right intercostal window it is reveled intestinal appearance distended by gas in the close proximity of the heart, image consistent with peritoneo-pericardial hernia diagnosis of susceptibility.

For gold standard diagnosis, radiographs were taken with the following incidents: latero-lateral (Figure 2) and ventro-dorsal (Figure 3) view of the chest and abdomen.

Description of the radiological report was as follows: the cardiac silhouette with an enlarged appearance, especially on the projection area of the right heart, tubular structures with a gaseous content can be observed.

Topographic changes that involved part of the intestinal mass, with their cranial displacement were observed at that time.

The radiological aspect suggests a peritoneo-pericardial hernia with the involvement of at least the small intestine.

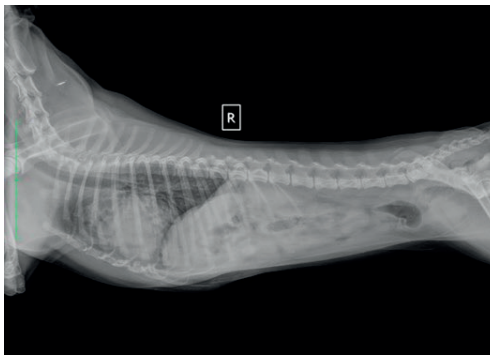

Figure 2. Patient's latero-lateral exposure on the day of primary assessment of the case

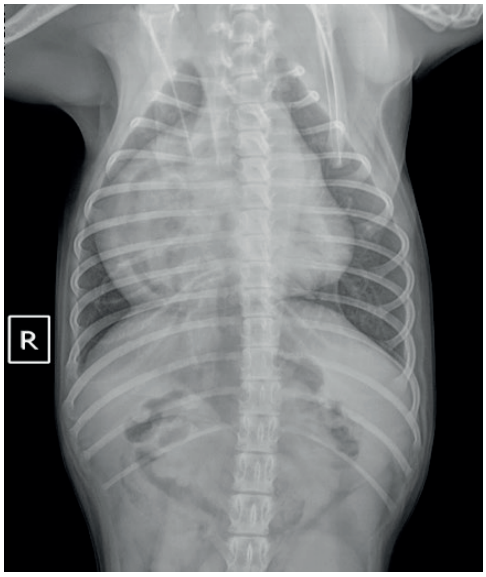

Figure 3. Patient's ventro-dorsal exposure on the day of primary assessment of the case

The patient was admitted to intense care unit for intravenous fluid therapy for electrolyte rebalancing and partial parenteral nutrition based on levo-amino acids and treatment with maropitant and pantoprazol to stop vomiting episodes.

On the 25th of August 2023 the patient started treatment with Intralipid 20% due to the fact that it had no appetite for more than 24 hours, so it was decided to start a parenteral nutrition plan according to the calculated RER. The plan consisted in intravenous administration of Intralipid 20% in three administrations per 24 hours at a rate of 0.2 ml/kg/min for 60 minutes.

On the 26th of August 2023 the patient's condition was considered optimal for surgery. The preoperatory examination revealed the following aspects of blood pressure: 160-170 mmHg, systolic, Doppler method, the patient presented agitation throughout the pre-anesthetic examination. Rhythmic-arrhythmic rate on heart auscultation. Bilateral femoral pulse present, normodynamic and synchronous with the heartbeat. Vesicular murmur present bilateral on auscultation. EKG: respiratory sinus arrhythmia (Figure 4). Pre-operative blood glucose: 88 mg/dL.

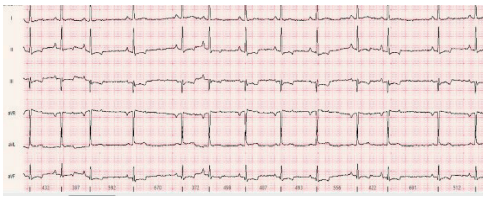

Figure 4. Electrocardiogram of the patient at the time of the preoperative anaesthetic examination

Surgical repair was made through a midline celiotomy (Figure 5). Another important factor is that the patient needs to be assisted with positive-pressure ventilation during the surgical procedure. To evaluate all internal organs, a thorough exploration of the abdominal cavity was conducted before correcting the herniated organs. After evaluating the abdominal cavity, an inspection of the entire diaphragm was performed to assess if there are tears or rents in the musculature.

To perform a safe extraction of incarcerated organs, a slight debridement of hernia ring was performed, it was directed ventrally to avoid trauma to herniated organs, lungs, vena cava, phrenic nerve, and oesophagus.

The herniated organs were represented by segments of the small intestine. Before performing sutures on the diaphragm, the pulmonary parenchyma was evaluated. Because the pericardial sac is joined with the diaphragmatic defect, suturing was performed with a polypropylene monofilament 3/0 absorbable wire with round needle, and the surgical approach was to suture the pericardial sac dorsal to ventral for a better closure of the hernia.

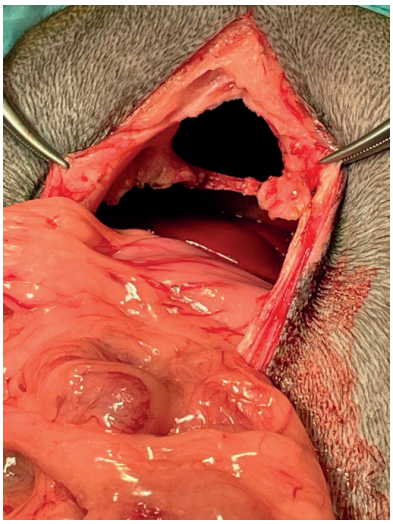

Figure 5. Intra-operative image of the peritoneopericardial defect with herniated structures of the small intestine

Patient was stable during anesthesia and had vital functions within the physiological parameters as it follows: patient had spontaneous breathing and mechanical ventilation (IPPV type) with a respiratory rate between the values: 10-12 rpm. EtCO2 was between the values: 33-45 mmHg. SpO2 was between values: 90-99%. Femoral pulse was present bilaterally and synchronous with the heartbeat: 95-106 bpm. The patient presented transient hypotension, responsive to fluid therapy: 126/85-166/131 mmHg, oscillometry. The patient presented mild transient hypothermia, responsive to medication and external heating operations: the patient's body temperature ranged from 35.8°C to 36.7°C. The patient benefited both intra and post-operatively from high loco-regional anesthesia. Patient had a rapid awakening, without any notable events from the anesthetic point of view, the patient was transferred to the intensive care unit with additional oxygen, heating and monitoring of vital functions.

On the following days, the patient was kept in the intensive care unit for vital functions monitoring general condition of the patient based on the following aspects: water and food appetite, urination, defecation, daily ultrasound rechecks for motility evaluation, post-operative treatment, both systemic and local.

After 48 hours in the intensive care unit, the patient showed a favorable evolution and it was discharged with the following post-operative treatment at home: a broad spectrum antibiotic from class 3 cephalosporin, probiotic to combat intestinal dysmicrobism and ensure a healthy and balanced intestinal transit, CBD oil 3% for anxiety reduction and anti-inflammatory effect, non-steroidal anti-inflammatory drugs cyclooxygenase-2 (COX-2) inhibitors for postoperative pain management and gastro-intestinal food diet.

On the 4th of September 2023, the patient was referred for the first post-operative re-check. During the anamnesis and the patient's medical history, the owner stated that the patient had no changes in general behavior, normal food appetite and normal water intake. During clinical examination the integrity and appearance of the incision line were evaluated. There were no pathological modifications. Healing stage of the incision line was favorable. Abdominal ultrasound reveled the continuity of the diaphragm and the lack of changes of the surgical intervention.

The rest of the organs in the abdominal cavity did not show significant changes during the ultrasound examination.

The following re-check on the 4th of October 2023, thoracic radiography with latero-lateral (Figure 6) and ventro-dorsal (Figure 7) exposures were performed.

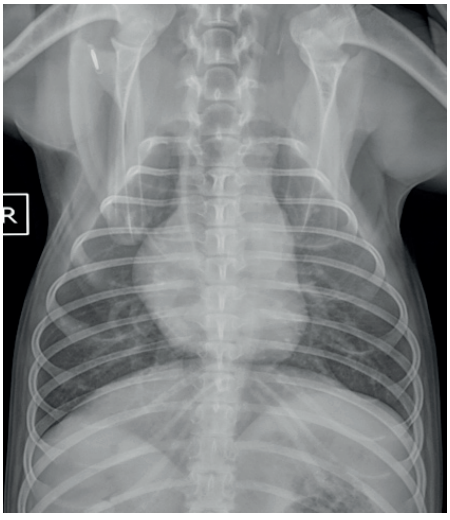

Figure 6. Ventro-dorsal exposure
of the patient at 30 days after the surgery

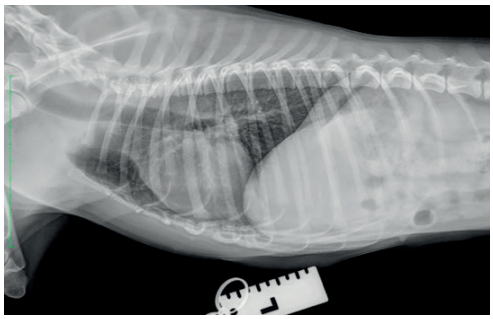

Figure 7. Latero-lateral exposure
of the patient at 30 days after the surgery

On the radiography report there were no pathological modifications noted of abdominal or thoracic viscera and the diaphragm muscle is intact.

CONCLUSIONS

Peritoneo-pericardial diaphragmatic hernia (PPDH) results from embryonic developmental anomalies involving the pericardial and peritoneal cavities, possibly due to teratogens, genetic defects, or prenatal injuries.

Peritoneo-pericardial diaphragmatic hernia is often an incidental finding but patients may present symptoms such as vomiting, lethargy, and dehydration. Diagnosis involves radiographic imaging revealing characteristic findings like cardiomegaly and herniated abdominal organs within the pericardial sac.

Highlighting thorough preoperative assessment, encompassing Doppler blood pressure measurement, blood work, and glycaemia, proves crucial. This thorough examination ensures surgical preparedness, enabling timely interventions and mitigating potential complications.

Surgical herniorrhaphy is the mainstay treatment for PPDH. Preoperative stabilization, including fluid therapy and nutritional support, is often necessary to optimize patient condition for surgery.

Successful surgical repair of PPDH requires careful postoperative management, including intravenous fluid therapy, nutritional support, and monitoring of vital functions.

Follow-up assessments involve imaging studies to confirm the integrity of the diaphragm and evaluate the healing process.

Long-term prognosis of PPDH is generally favorable.

REFERENCES

Banz, A.C., Gottfried, S.D. (2010). Peritoneopericardial diaphragmatic hernia: a retrospective study of 31 cats and eight dogs. *J Am Anim Hosp Assoc*; 46:398-404.

Bjorck, G.R., Tigerschiold, A. (1970). Peritoneopericardial diaphragmatic hernia in a dog. *J Small Anim Pr*act.; 11: 585-590.

Bolton, G.R., Ettinger, S., Rousch, J.C. (1969). Congenital peritoneopericardial diaphragmatic hernia in a dog. *J Am Vet Med Assoc*.; 55:723-730.

Burns, C.G., Bergh, M.S., McLoughlin, M.A. (2013). Surgical and nonsurgical treatment of peritoneopericardial diaphragmatic hernia in dogs and cats: 58 cases (1999-2008). *J Am Vet Med Assoc*.; 242:643-650.

Chalkley, J., Salinardi, B.J., Bulmer, B.J., (2006). What is your diagnosis? Peritoneopericardial diaphragmatic hernia (PPDH). *Journal of the American Veterinary Medical Association*, 228: 695-69.

Evans, S.M., Biery, D.N. (1980). Congenital peritoneopericardial diaphragmatic hernia in the dog and cat: a literature review and 17 additional case histories. *Vet Radiol*.; 21: 108-116.

Hunt, G.B., Johnson, K.A. (2003). Diaphragmatic, pericardial and hiatal hernia. In: *Textbook of Small Animal Surgery*, 3e (ed. D.H. Slatter), 471–487. Philadelphia, PA: WB Saunders.

Less, R.D., Bright, J.M., Orton, C.E. (2000). Intrapericardial cyst causing cardiac tamponade in cat. *J Am Anim Hosp Assoc*.; 36:115-119.

McClaran, J.K. (2023). Diaphragmatic and Peritoneopericardial Diaphragmatic Hernias. In *Small Animal Soft Tissue Surgery*, E. Monnet (Ed.)

Park, R.D. (2002). The diaphragm. In: *Textbook of Veterinary Diagnostic Radiology*, 4e (ed. D.E.Thrall), 359 -375 . Philadelphia, P: WB Saunders.

Scientific Works. Series C. Veterinary Medicine. Vol. LXX (2), 2024
ISSN 2065-1295; ISSN 2343-9394 (CD-ROM); ISSN 2067-3663 (Online); ISSN-L 2065-1295

PENILE AMPUTATION IN A DOG WITH SEVERE NECROTIC LESIONS DUE TO PARAPHIMOSIS - A SHORT CASE PRESENTATION

Dorin ȚOGOE, Nicoleta Andreea MINCĂ, Roxana Maria TURCU

University of Agronomic Sciences and Veterinary Medicine of Bucharest, Faculty of Veterinary Medicine, 105 Spaiul Independentei Street, 050097, District 5, Bucharest, Romania

Corresponding author email: nicoleta_andreea_m@yahoo.ro

Abstract

Paraphimosis it is an emergency which represent the inability to retract the penis into the preputial sheets. Paraphimosis may be congenital resulting from preputial hypoplasia and small preputial orifice or could be acquired resulting from constriction of preputial orifice with hair, trauma, masturbation or coitus with persistent glans engorgement. The treatment goal is to reduce the dimensions of the glans, allowing it to be replaced into the sheets, before any severe damage appear. Poor management can lead to penile amputation due to ischemia, gangrenous necrosis, self-trauma with urethral lesions which impair urination. The study presents a severe case of paraphimosis, due to self-masturbation and preputial hair rings, with extensive necrotic lesions due to ischemia and self-mutilation lesions of a 2,8 years old Mioritic Shepard intact male. The severity of the vascular changes with irreversible damage of the penis and the extent of the self-mutilation injuries, required the scrotal urethrostomy and the amputation of the penis, with satisfactory results even if minor surgical complications were observed in the immediate postoperative period.

Key words*: paraphimosis, penile amputation, penile trauma, dogs.*

INTRODUCTION

Paraphimosis is defined as the inability to withdraw the penis into the sheath and is frequently found in young, intact males as a result of excessive sexual activity. Secondly, the withdrawal of the penis into the sheath can be prevented by low-manifestation abnormalities of the preputial orifice, dysfunctions of the preputial muscles or entanglement of the preputial hairs around the erect penis and circular compression followed by hemodynamic changes in it (Kustritz & Olson, 1999; Ritson et al., 2023).

The prognosis and therapeutic options in paraphimosis are dependent on the clinical symptoms, duration and severity of the course. In the early stages, penile tissue has a normal appearance and is painless. When circulatory changes are severe, changes in the colour of the glans and loss of sensation occur. As a rule, in this advanced stage, males lick and bite their glans exposed to the external environment, inducing self-mutilation lesions (Taylor & Smeak, 2021). Depending on the extent of the changes or induced self-mutilation trauma, partial or complete amputation of the penis may be indicated. Complete amputation of the penis and foreskin can be combined with scrotal urethrostomy (Fossum, 2013; Coomer, 2013).

Knowing and understanding in detail the urethral and vascular anatomy of the dog's penis is very important for planning an intervention of this type.

The penis is structured in three distinct regions: the root of the penis, the body and the penile glans.

The urethra extends from the level of the ischial arch along the entire length of the three segments of the

of the penis and is surrounded by spongy tissue. At the level of the glans, the urethra adopts a ventral position, being housed in the urethral groove of the

penile bone and ends at the level of the external urethral orifice at the tip of the penis. The vascular supply of the penis is provided by three vascular branches that derive from the internal pudendal artery, namely the penile bulb artery, the deep penile artery and the superficial penile artery. The vascularization of the sheath derives from the superficial penile artery, the external pudendal artery and the

superficial epigastric artery. All these vascular branches anastomosis to each other so that special attention must be paid to haemostasis during surgery (Evans & Lahunta, 2013; Zamirbekova et al., 2024).

MATERIALS AND METHODS

At the University Emergency Hospital of the Faculty of Veterinary Medicine in Bucharest, a 2.8-year-old male of the Mioritic Shepherd breed was urgently presented with clinical manifestations of dysuria, bloody urination and lack of appetite. At the general clinical examination, the male was present, alert, body temperature 38.1 C, CRT 2 sec with mild tachypnoea and heart rate 150 bpm.
The penile glans was completely exposed, with extensive necrosis and specific self-mutilation lesions. It was not possible to identify the penile urethra for the purpose of the probe.

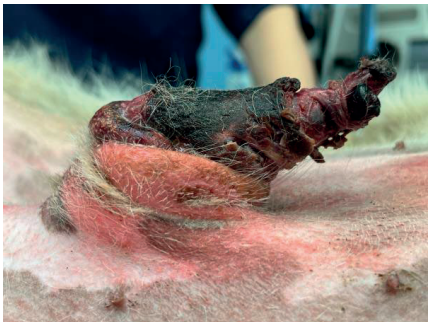

Figure 1. Paraphimosis with extensive necrotic lesions at the level of the penile glans

The blood investigations carried out did not reveal changes in the metabolic profile except for the level of urea (BUN) possibly associated with manifestations such as dysuria. The haematological examination identified a whole series of changes, in accordance with the type and severity of lesions of the external urogenital segment. Immediately after the general clinical examination, the patient was sedated with Dexmedetomidine 3 mcg/kg plus Methadone 0.2 mg/kg and Ketamine 2 mg/kg. Induction was performed with propofol at a dose of 2-3 mg/kg and maintenance throughout the surgery was performed with isoflurane.
The patient was placed in the supine position and the intervention area was prepared aseptically. The first surgical stage required the performance of orchidectomy with ablation of the scrotal pouches and the urethrostomy at this level.
For this purpose, the elliptical incision of the skin around the scrotum was made, with the long axis oriented craniocaudally.
Haemostasis was ensured by forcepress or transfixic ligation with polydioxanone 3/0. Ligation of the testicular cords was performed circularly with polydioxanone 0 then the dissection of the subcutaneous tissues was continued until the complete removal of the scrotal pouches.

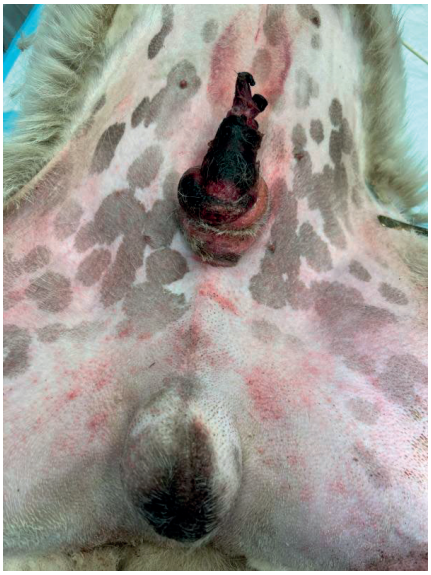

Figure 2. Paraphimosis with extensive necrotic lesions

The penile retractor muscle was carefully dissected and removed laterally from the ventral surface of the urethra. An incision was made in the ventral urethral wall which was later extended with scissors for a distance of 3.5-4 cm to ensure a sufficiently wide orifice. A suture pattern in separate stitches with 2/0 resorbable monofilament thread was used for the apposition of the urethral wall at the cutaneous edge, on each side of the stoma. A 2-way Foley catheter, CH 16 was inserted and secured into the bladder, attached to a urinary bag to provide closed urinary drainage throughout the intervention.
A second elliptical skin incision was made around the external genital segment, taking care that there was a distance of at least 1-2 cm

between the anterior edge of the urethrostomy and the caudal aspect of the penile amputation area. Particular attention was paid to the identification and ligation of the superficial epigastric branches, with polydioxanone 3/0, then the penis continued to be separated from the ventral abdominal wall in a caudal direction to the base of the penile bulbs. A circular ligation was made in an optimal region for amputation behind the base of the penile bone with polyglycolic acid (Vicryl) 0 to control any bleeding from the dorsal artery of the penis.
After sectioning, the penile abutment was evaluated for the presence of haemorrhages and was allowed to retract caudally between the connective tissues. The subcutaneous connective tissue was approached by a continuous suture pattern with resorbable monoflation thread and the skin was closed with non-resorbable thread (Nylon) no. 0, at separate points.

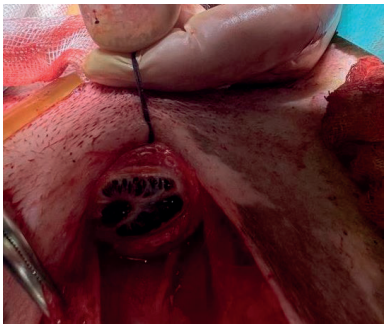

Figure 3. Paraphimosis - image from surgery

Postoperatively, it was recommended to use an Elizabethan collar until the sutures were removed to prevent self-mutilation of the operated area. Postoperative therapy was continued for 5 days with Amoxicillin + clavulanic acid (Synulox) 20 mg/kg/day and analgesia was provided for 3 days postoperatively by Meloxicam 0.2 mg/kg/day. A slight haemorrhage was observed in the first 3 days postoperatively from the urethrostomy, especially after urination, very easily controlled only by manual compression.

RESULTS AND DISCUSSIONS

Penile trauma is less common in the canine species and usually manifests itself because of congenital deficiencies or due to prolonged erection, masturbation or circular hair rings around the preputial orifice, which prevent the penis from retracting into the sheath.
The literature describes a whole series of non-surgical and surgical techniques for correcting congenital paraphimosis, highlighting the fact that partial or total amputation of the penis remains a restricted option for cases in which necrotic changes are very extensive and hinder functional recovery, respectively the ability to urinate and the preservation of reproductive function (Papazoglou, 2001).
The location for the amputation of the penis is dictated by the affected area and the extent of the circulatory lesions. Subtotal penile amputation usually includes the space between the penile fornix and the anterior edge of the ischium and includes resection of the free portion of the penis along with the foreskin, adjacent scrotal tissue, and external genitalia, respectively the testicles. As a rule, a scrotal urethrostomy is associated with this technique, to ensure a viable urinary tract.
The literature does not provide a validated system for assessing the results obtained after total or partial amputation of the penis in dogs. The immediate criteria for evaluating the surgical success were closely related to the animal's capacity for voluntary urination, its comfort during rest periods, possible local complications during the healing process until the removal of the threads. The only complication, cited in the literature, was represented by the reduced intensity of bleeding during urination from the scrotal urethrostomy in the first 3 days postoperatively. Its control did not require specific medication and did not influence the healing of surgical wounds.

CONCLUSIONS

Even if penile trauma is very rare condition in male dogs, the paraphimosis remains a true provocation because of the complex vascular anatomy of dog penis and urethra.
The permanent prevention of this emergency can be achieved simply by sterilizing males that are not intended for reproductive activity or by carefully monitoring them during periods of sexual activity of female dogs.

ACKNOWLEDGEMENTS

The diagnosis of paraphimosis was made with the help of the Reproduction Department of the Faculty of Veterinary Medicine Bucharest.

REFERENCES

Coomer, A. R., 2013. Male reproductive and penile surgery. World Small Animal Veterinary Association, World Congress Proceedings, URL: https://www.vin.com/doc/?id=5709894

Evans, H. E., & de Lahunta, A., 2013. The urogenital system. In W. B. Saunders (Ed.), *Miller's anatomy of the dog* (4th ed., pp. 376–382). Saunders.

Fossum, T. W., 2013. Surgery of The Male Reproductive Tract, In: *Small Animal Surgery*, Ed: Fossum T.W., Dewey C.W., Horn C.V., Johnson A.L., Radlinsky M.G., Schulz K.S., Mac Phail C.M., Willard M.D., 4th edition, Elsevier, Mosby, Missouri, p. 849-853.

Kustritz, M. V., Olson, P. N., 1999. Theriogenology question of the month. Priapism or paraphimosis. *J Am Vet Med Assoc*, 214, 1483–1484.

Papazoglou, L. G., 2001. Idiopathic chronic penile protrusion in the dog: a report of six cases. *J Small Anim Pract*, 42(10), 510-513. https://doi.org/10.1111/j.1748-5827.2001.tb02459.x

Ritson, K., Bird, F., Stefanidis, G., Brissot, H., 2023. The indications, complications and outcomes of dogs undergoing partial penile amputation: 10 cases (2014-2021). *J Small Anim Pract*, 64(2), 103-110. https://doi.org/10.1111/jsap.13564.

Taylor, C. J., Smeak, D. D., 2021. Perineal urethrostomy in male dogs - Technique description, short and long-term results. *Can Vet J*, 62(12), 1315.

Zamirbekova, N., Parlak, K., Satici, I., Ergin, H., Yazici, S., Eris, E. M., Yildiz, M., Alkan, F., 2024. Surgical treatment of Paraphimosis in dogs: 4 Cases. *Eurasian J Vet Sci*, 40(1), 041-046.

Scientific Works. Series C. Veterinary Medicine. Vol. LXX (2), 2024
ISSN 2065-1295; ISSN 2343-9394 (CD-ROM); ISSN 2067-3663 (Online); ISSN-L 2065-1295

CLINICAL, NEUROLOGICAL AND MAGNETIC RESONANCE ASPECTS IN MYELOMALACIA IN DOGS - 10 CASES

Alexandru-Gabriel NEAGU, Raluca Mihaela TURBATU, Marius-Mihai BĂDULESCU, Cristina FERNOAGĂ, Niculae TUDOR, Constantin VLĂGIOIU

University of Agronomic Sciences and Veterinary Medicine of Bucharest, Faculty of Veterinary Medicine, 105 Splaiul Independentei Street, 050097, District 5, Bucharest, Romania

Corresponding author email: neagualex29@yahoo.ro

Abstract

The diagnosis and understanding of myelomalacia in dogs rely heavily on clinical, neurological, and magnetic resonance imaging (MRI) aspects. A study conducted at the Faculty of Veterinary Medicine Bucharest reviewed medical records from 10 cases, selected based on their clinical history, neurological evaluation, and MRI findings. The clinical and neurological signs varied depending on the location and severity of the spinal cord injury, with common symptoms including limb weakness or paralysis, coordination issues, walking difficulties, pain, and changes in posture. MRI plays a vital role in diagnosing myelomalacia by providing detailed images of the spinal cord, offering crucial insights into the condition. The cases were classified into three types based on their cause: traumatic (6 cases), degenerative (3 cases), and vascular (1 case), all affecting the thoracolumbar spinal cord. In conclusion, the combination of clinical assessment, neurological examination, and MRI is essential for accurately diagnosing myelomalacia in dogs and determining appropriate treatment options.

Key words: *dog, imaging diagnosis, MRI, myelomalacia.*

INTRODUCTION

In veterinary medicine, the term myelomalacia is used in the case of hemorrhagic infarction of the spinal cord that can occur following an acute (traumatic), degenerative (progressive myelomalacia), or vascular injury (Platt and Garosi, 2012).

The leading cause of traumatic myelomalacia is intervertebral disc extrusion, where a significant amount of disc material disperses along the vertebral canal, creating intense pressure on the spinal cord. Over time, this severe compression results in degeneration due to the death of nerve cells (De Risio et al., 2009; Cordle et al., 2023).

In degenerative myelomalacia, the death of the tissue at the level of the spinal cord occurs progressively over time and can be ascending or descending at the spinal cord. The exact cause is not fully understood, but it is thought to be multifactorial. It is often associated with abnormalities of the spine, including vertebral malformations, instability, or compression of the spinal cord. Genetic, nutritional, and biomechanical factors may also play an important role (Schweizer-Gorgas, 2018; Lin et al., 2023).

Vascular myelomalacia can occur due to a fibrocartilaginous embolus through the formation of blood clots that reduce blood flow to the spinal cord. Other vascular accidents or conditions that compromise blood flow to the spinal cord are implicated, such as vasculitis or arterial dissection (Lu et al., 2002).

Clinical signs of myelomalacia can include loss of proprioception in the pelvic limbs, tail, and anus, flaccid paraplegia, absence of deep pain perception, weakened abdominal muscles, and a depressed mental state (Fingeroth et al., 2015). While the clinical signs of myelomalacia are typically seen within the first 24 hours after paraplegia begins, they may sometimes only become apparent during the postoperative period or even several days after paraplegia starts (Platt and Garosi 2012; Schweizer-Gorgas, 2018).

Although myelomalacia itself may not be a common condition that can lead to it, such as intervertebral disc disease (IVDD) or traumatic injuries, are seen relatively frequent in veterinary practice, particularly in certain breeds predisposed to spinal problems such as

dogs from the Dachshund or German Shepherd breed (Olby, 2010).

Due to its severity and potential for irreversible damage to the spinal cord, myelomalacia requires prompt diagnosis and appropriate management to minimize neurological deficits and improve the dog's quality of life. The aim of this study was to describe the clinical, neurological, and imaging characteristics, using magnetic resonance, of dogs affected by myelomalacia with different causes.

MATERIALS AND METHODS

Medical records during the period 2018-2024 from the University Emergency Veterinary Hospital "Prof. Dr. Alin Bîrtoiu", were evaluated from clinical, neurological, and imaging points of view.

The criteria for inclusion in the study were based on the anamnestic data provided by the owners, followed by the clinical and neurological data as well as the imaging data by a specific protocol (Fernoaga et al., 2020; Rebecca and Fernoaga, 2021).

For each case, age, breed, sex, and body weight were documented, along with the time elapsed between the onset of clinical signs reported by the owner and the imaging examination. Additionally, it was noted whether decompressive surgery was performed and the timing of the onset of clinical signs of progressive myelomalacia.

As part of the inclusion criteria, all dogs underwent general anesthesia to be evaluated by magnetic resonance imaging (MRI). This study utilized a specialized veterinary MRI device, the VET MR GRADE with a 0.3 Tesla power (ESAOTE, Italy), featuring a permanent magnet and region-specific coils. The imaging protocols included T1 Spin Echo (SE) and T2 Fast Spin Echo (FSE) sequences in two planes (sagittal and transverse), with a slice thickness of 2-3 mm. Post-contrast images were obtained in the T1 sequence following intravenous administration of a contrast agent (Clariscan, 0.2 ml/kg). During the MRI exam, the animals were positioned in left lateral recumbency (Neagu et al., 2018).

The following protocol was used: premedication was administered with Butorphanol at 0.2 mg/kg IV, followed by induction with Propofol at 3-5 mg/kg IV. After intubation, anesthesia was maintained using Isoflurane and 100% oxygen. Spontaneous or intermittent positive-pressure ventilation (IPPV) was provided using a volume-cycled ventilator delivering 12-15 breaths per minute, targeting an end-tidal CO_2 of 35-45 mmHg. Oxygen flow initially started at 2 L/min, with the vaporizer adjusted to reach an end-tidal concentration of 2.0% isoflurane within 10 minutes of induction. Once the target concentration was achieved, oxygen flow was reduced to (500 + 10/kg) L/min, and the isoflurane concentration was consistently maintained at 1.5 vol.% for all cases (Tudor et al. 2019; Pavel et al., 2021).

RESULTS AND DISCUSSIONS

After analyzing the medical files, 10 cases with signs compatible with myelomalacia were identified, represented by: French Bulldog (3 cases), Pug (2 cases), Pomeranian (1 case), Chow-chow (1 case), Bichon (1 case), English Bulldog (1 case) and Golden Retriever (1 case). Of whom 4 females and 6 males, aged between 4 and 9 years. They were divided into three categories: post-traumatic myelomalacia following intervertebral disc extrusion (6 cases), degenerative myelomalacia caused by changes in vertebral alignment (3 cases), and vascular myelomalacia caused by a fibrocartilaginous embolism (1 case). The neurological examination established the localization of the disease at the level of the thoracolumbar segment of the spinal cord.

In the case of myelomalacia produced by disc extrusion, the neurological signs were correlated with the degree of compression of the spinal cord and nerve roots, adjacent to the affected area. The evolution of the injuries was superacute, with the immediate onset of nerve deficits, respectively in the first 24-48 hours after the incident.

Thus, in the 6 cases, the pain was observed, both when palpating the spine on the thoracolumbar region, and when initiating movements (different degrees of pain). The neurological evaluation revealed the following abnormalities: kyphosis and scoliosis (as changes in posture) (4/6); proprioceptive deficits of varying degrees on the hind limbs

(6/6); proprioceptive ataxia and walking paraparesis (6/6); normal spinal reflexes, but in 2 cases flexion was delayed; panniculus was reduced (6/6), caudal to the lesion. Neurological signs were symmetrical or lateralized.

For degenerative myelomalacia, the neurological signs were present or blurred. The evaluated patients presented: kyphosis and scoliosis (3/3); proprioception deficits of varying degrees on the hind limbs (3/3); proprioceptive ataxia (3/3), paresis (2/3), plegia (1/3); normal spinal reflexes, but with incomplete (2/3) or absent (1/3) flexion. In these patients, no pain was detected when palpating the spine or while walking.

The patient with fibrocartilaginous embolism (vascular ischemia) presented intense pain at the time of injury, triggered by play activity/jumping in the yard. The neurological deficits appeared acutely and evolved progressively in the first 24 hours. Afterwards, the pain was no longer present. Neurological signs were symmetrical or lateralized to one side. Proprioceptive deficits of various degrees, proprioceptive ataxia and walking paraparesis, normal spinal reflexes, and reduced panniculus, behind the lesions, were observed; deep pain perception was reduced. This patient did not present pain when palpating the spine and while walking.

Regardless of the cause that determined the myelomalacia (traumatic, degenerative, and vascular), in patients with neuro-localization on the T3-L3 vertebral segment, the urinary bladder was spastic (9/10), and in those with localization on the L4-S3 segment, the urinary bladder was flaccid (1/10).

After the neurological examination and neuro-localization, the MRI examination was used to confirm the lesion.

In the case of traumatic myelomalacia, the aim was to identify and locate the intervertebral disc extrusion and highlight the imaging characteristics. The MRI examination localized the disc extrusion in the T11-L5 segment (Figure 1). Imaging signs included hyperintensity on T2 sequences and isointensity on T1 sequences, without contrast enhancement at the level of the spinal cord. The extramedullary disc extrusion was visible as T2 hypointensity located dorsally in the vertebral canal, compressing the spinal cord. The intramedullary change was identified around the extruded disc fragment.

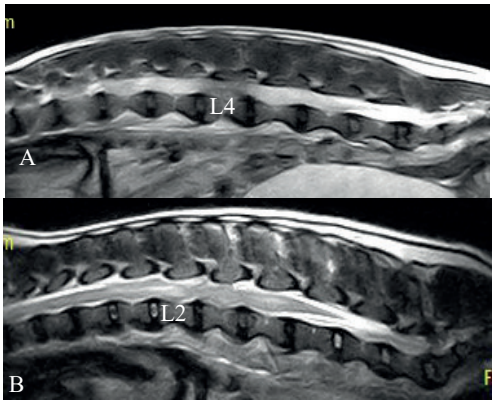

Figure 1. Sagittal planes of the thoracolumbar spine, showing a T2 hyperintensity of the spinal cord ascending and descending from disc extrusion L4-L5 (A), respectively L2-L3 (B)

In 2 of the 6 cases, the extent of the spinal cord injury was both cranial and caudal to the extrusion site. The most likely cause of this effect is the long time elapsed between the onset of the event and the MRI scan. Another cause may be the delay of the surgical intervention (Castel et al., 2017; Castel et al., 2019), mainly due to the hesitation of the owners.

Disc extrusion in the lumbar area can be a risk factor for the occurrence of myelomalacia (Castel et al., 2017; Castel et al., 2019). Previous reports show that disc extrusion, complicated with myelomalacia, is more frequently encountered at T12-T13, T13-L1, and L1-L2 (De Risio et al., 2009). In the present study, disc extrusion was detected on the T11-L5 segment, which led to the extension of the spinal cord injury.

In 3 cases, the presence of degenerative myelomalacia was established, based on the anamnestic signs corroborated with the neurological and imaging ones (Figures 2 and 3).

The evolution of the patient over time was also followed. The patients presented changes in vertebral alignment, as a result of congenital vertebral anomalies, which led to the alteration of the structure of the spinal cord, represented by T2 hyperintensity in the adjacent area. A recent study carried out on French Bulldog

dogs in the thoracolumbar segment, showed that changes in the spine alignment, caused by the presence of congenital vertebral anomalies, lead to swelling of the spinal cord (Fernoaga et al., 2021).

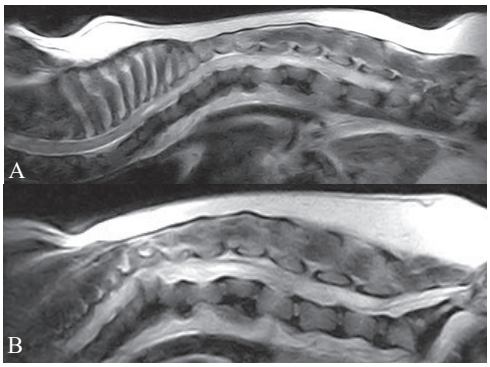

Figure 2. Sagittal planes of the thoracolumbar spine (A and B), showing a T2 hyperintensity of the spinal cord with abnormal vertebral alignment

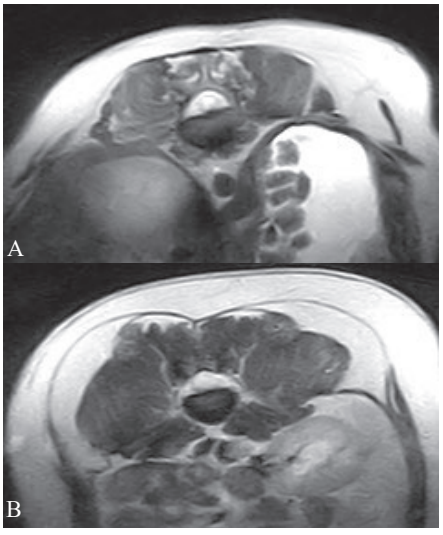

Figure 3. Transversal planes of the thoracolumbar spine (A and B), showing a T2 hyperintensity of the spinal cord

In one case, the presence of changes in the spinal cord, represented by hyperintensity in T2, without the presence of disc extrusion or congenital vertebral anomalies, was found, which led to the suspicion of vascular myelomalacia (Figure 4).

The main cause of vascular myelomalacia is medullary intraparenchymal arterial obstruction, following the embolization of fibrocartilaginous material, which leads to the appearance of local ischemic lesions (Schweizer-Gorgas, 2018). This material is histologically and histochemically similar to the nucleus pulpous, but its origin and appearance mode in the bloodstream are not yet elucidated (De Risio, 2015). Other causes include thrombi, parasites, bacteria, fat embolism, or neoplastic embolism (Schwezer-Gorgas, 2018).

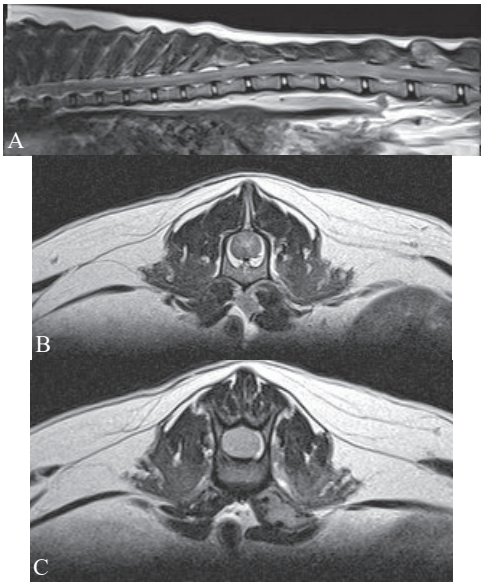

Figure 4. Sagittal plane (A) and transversal planes (B and C) showing reduced T2 hyperintensity on the spinal cord - most probably asses as a vascular ischemia (fibrocartilaginous embolus)

It was noted that the prognosis for dogs in the study with myelomalacia varied significantly based on the underlying cause and the extent of spinal cord damage. In some instances, with timely and proper treatment, dogs were able to recover partial or full mobility within 2 to 6 weeks after the onset of the condition (Olby, 2010; Fingeroth et al., 2015).

CONCLUSIONS

The MRI findings in collaboration with clinical sign and neurological evaluation are important methods in the diagnosis of progressive myelomalacia. The imaging finding of the appearance as a hyperintense signal in the T2 sequences of the spinal cord was associated with progressive myelomalacia.

REFERENCES

Castel A., N.J. Olby , C.L. Mariani, K.R. Munana, and P.J. Early (2017). Clinical Characteristics of dogs with Progressive Myelomalacia following acute Intervertebral Disc Extrusion. *Journal Vet. Intern Med*., 31, 1782–1789.

Castel A., N.J. Olby , C.L. Mariani, K.R. Munana, and P.J. Early (2019). Risk factors associated with progressive myelomalacia in dogs with complete sensorimotor loss following intervertebral disc extrusion: a retrospective case-control study. *BMC Vet. Res.*, 15: 433.

Cordle K. J., Seiler, G. S., Barnes, D., & Olby, N. J. (2023). MRI features can help to confirm a diagnosis of progressive myelomalacia, but may not be accurate in dogs lacking characteristic clinical signs at the time of imaging. *Veterinary Radiology & Ultrasound*, 64(2), 283–293.

De Risio, L., Adams, V., Dennis, R., & McConnell, F. J. (2009). Association of clinical and magnetic resonance imaging findings with outcome in dogs with presumptive acute noncompressive nucleus pulposus extrusion: 42 cases (2000-2007). *Journal of the American Veterinary Medical Association*, 234(4), 495–504.

De Risio, L. (2015). A review of fibrocartilaginous embolic myelopathy and different types of peracute non-compressive intervertebral disk extrusion in dogs and cats. *Frontiers in Veterinary Sciences*, 2(24): 1-9.

Fernoagă C., Turbatu R.M., Neagu A.G., Tudor N. (2021). Clinical and imaging aspects in French Bulldogs with thoracic congenital vertebral malformations. *Lucrări Ştiinţifice Medicină Veterinară*, vol. LIV(4), 45-52.

Fernoagă C., Turbatu R.M., Neagu A.G., Tudor N., Vlăgioiu C. (2020). Diagnosis and treatment outcome of a dog with meningoencephalitis of unknown origin using a combination of prednisolone and cytosine arabinoside: A case study. *AgroLife Scientific Journal*, 9(2), 112-117.

Fingeroth J.M., Lahunta A. (2015). Ascending/Descending Myelomalacia Secondary to Intervertebral Disc Herniation. Advances in Intervertebral Disc Disease in Dogs and Cats. Wiley-Blackwell and ACVS Foundation, Oxford, 115-20.

Lin, A., Lampe, R., Bandt, C., Vieson, M., & Park, J. Y. (2023). Case report: Clinical and pathological findings in a canine patient with intervertebral disk extrusion resembling progressive myelomalacia. *Frontiers in veterinary science*, 10, 1122566.

Lu D., C.R. Lambm, P. Tarcett (2002). Results of myelography in seven dogs with myelomalacia. *Veterinary Radiology & Ultrasound*, 43(4), 326-330.

Neagu, A. G., Săvescu, M., Tudor, R. G., Tudor, N., & Vlăgioiu, C. (2018). MRI findings of the cervical spine in three beagle dogs. *AgroLife Scientific Journal*, 7(1), 92-96.

Olby N. (2010). The pathogenesis and treatment of acute spinal cord injuries in dogs. The Veterinary clinics of North America. *Small animal practice*, 40(5), 791–807.

Pavel, R. G., Neagu, A. G., Turcu, R., Predoi, G., & Costea, R. (2021). Perianaesthetic management of canine patients that underwent hemilaminectomy for medullar compression. *Scientific Works. Series C. Veterinary Medicine.* Vol. LXVII(1), 108-113.

Platt, S., and Garosi, L. (2012). Small Animal Neurological Emergencies (1st ed.). CRC Press.

Rebecca A.P., Fernoagă C. (2021). *Ghid practic de neurologie şi neuropatologie la câine şi pisică*. Editura Ex Terra Aurum, Bucureşti.

Schweizer-Gorgas, D. (2018). Ischemic myelopathy, spinal cord hemorrage, myelomalacia. Ch.7. In: Mai, W. (Ed.). (2018). *Diagnostic MRI in Dogs and Cats* (1st ed.). CRC Press

Tudor, R., Degan, A., Neagu, A. G., Carstinoiu, L., & Predoi, G. (2019). Hemilaminectomy for T11-T12 medullar compression-perianaesthetic management of a geriatric dog. *Scientific Works. Series C. Veterinary Medicine*. Vol. LXV(1), 94-95.

Scientific Works. Series C. Veterinary Medicine. Vol. LXX (2), 2024
ISSN 2065-1295; ISSN 2343-9394 (CD-ROM); ISSN 2067-3663 (Online); ISSN-L 2065-1295

MAGNETIC RESONANCE IMAGING OF INTERVERTEBRAL DISC DISEASE ON CERVICAL SPINE IN DOGS - 12 CASES

Marius-Mihai BĂDULESCU, Alexandru-Gabriel NEAGU, Raluca Mihaela TURBATU, Ruxandra Georgiana PAVEL, Niculae TUDOR, Constantin VLĂGIOIU

University of Agronomic Sciences and Veterinary Medicine of Bucharest, Faculty of Veterinary Medicine, 105 Splaiul Independentei Street, 050097, District 5, Bucharest, Romania

Corresponding author email: marius.badulescu@fmvb.usamv.ro

Abstract

Intervertebral disc disease (IVDD) results from the degeneration and dehydration of intervertebral discs, a natural process that occurs as animals age. These degenerative changes can lead to various clinical and pathological issues, including disc extrusions and protrusions. A review of the medical records of 12 dogs presented at the Faculty of Veterinary Medicine in Bucharest with neurological deficits was conducted. The animals underwent magnetic resonance imaging (MRI) for evaluation. The MRI results identified intervertebral disc disease, with 5 cases classified as Hansen Type I (extrusion) and 7 cases as Hansen Type II (protrusion), all causing spinal cord compression. MRI proved to be a valuable, safe, and non-invasive method for assessing the spinal cord in the cervical segment.

Key words*: discopathy, dog, imaging diagnosis, MRI.*

INTRODUCTION

Discopathy is among the most prevalent spinal conditions in dogs, characterized by the dehydration and degeneration of intervertebral discs. It is typically observed in older dogs or those from chondrodystrophic breeds (da Costa et al., 2012; da Costa et al., 2020). The condition is characterized by two forms of evolution, represented by an acute form, called intervertebral disc extrusion (Hansen type I), and a chronic form, or intervertebral disc protrusion (Hansen type II) (Bergknut et al., 2013).

In the case of disc extrusion, a herniation of the calcified nucleus pulposus occurs through the annulus fibrous ring and it penetrate the vertebral canal. This condition occurs predominantly in chondrodystrophic breeds, with young dogs being more affected, and was clinically manifested by acute hyperesthesia up to paraplegia (Smolders et al., 2013; da Costa et al., 2020; Argent et al., 2022). Disc protrusion is the slow, progressive, focal extension of the annulus fibrosus and dorsal ligament into the spinal canal.

The condition is often seen in non-chondrodystrophic breeds, particularly geriatric dogs, and clinically manifests as slow-onset hind limb paresis and ataxia (Smolders et al., 2013).

Radiographic examination and myelography were the most used methods for the diagnosis of disc diseases (da Costa et al., 2020). With the evolution of technology and the increasing use of magnetic resonance imaging (MRI), the exact differentiation between extrusion and protrusion has been facilitated, a decisive factor in the application of appropriate therapy. MRI diagnosis is considered a modern and non-invasive diagnostic method that, in addition to differentiating the two conditions, also provides important data regarding the integrity of the spinal cord, and the other structures at the vertebral level (Kranenburg et al., 2013; Murthy et al., 2014). This study aimed to identify and localize disc diseases in dogs of different breeds.

MATERIALS AND METHODS

The study was conducted at the University Veterinary Emergency Hospital "Prof. Dr. Alin Bîrțoiu" from Bucharest, on a number of 12 dogs (French Bulldog, Pekingese, Beagle, Shih-Tzu, Crossbreed, German Shepherd), which present neurological signs specific to intervertebral discopathy. The criteria for inclusion in the study following clinical examinations were: the presence of pain in the cervical spine with sudden onset, the presence of tetraplegia, and proprioceptive deficits.

Patients were examined by clinical and neurological examination, followed by recommendations for further investigations.
The MRI scan was carried out using a VET MR GANDE machine with a 0.3 Tesla strength, utilizing a permanent magnet and specialized coils. T1 Spin Echo and T2 Fast Spin Echo sequences were applied in sagittal and transverse planes, with a slice thickness between 2.5 to 3 mm. Contrast medium (Clariscan) images were captured following intravenous administration at a dosage of 0.2 ml/kg. The animals were positioned in sternal and left-lateral recumbency during the procedure
The animals were scanned under general anesthesia. Premedication consisted of Butorphanol at 0.2 mg/kg IV, with Propofol administered intravenously at 3-5 mg/kg for induction. Following intubation, anesthesia was sustained with Isoflurane and 100% oxygen. Spontaneous or intermittent positive-pressure ventilation (IPPV) was managed via a volume-cycled ventilator, delivering 12-15 breaths per minute to maintain an end-tidal CO_2 level between 35-45 mm Hg. Initially, oxygen was supplied at 2 L/min, with the vaporizer adjusted to achieve an end-tidal isoflurane concentration of 2.0% within 10 minutes of induction. Once the target was met, the oxygen flow rate was reduced to (500 + 10/kg) L/min, while the isoflurane concentration remained steady at 1.5 vol.% throughout the procedure (Tudor et al., 2019; Pavel et al., 2021).

RESULTS AND DISCUSSIONS

Patients included in the study belonged to chondrodystrophic breeds (2 cases - French Bulldog, 3 cases - Pekingese, 1 case - Beagle, 2 cases - Shih-Tzu) and non-chondrodystrophic (3 cases - Crossbreed, 1 case - German Shepherd), of different ages and both sexes. The clinical examination followed changes in head and gait. In the case of patients with disc extrusion, acute pain in the cervical segment was also found. By correlating the clinical examination with the anamnesis, regarding the onset of the conditions, symptoms, and evolution, it was found that in most cases no changes were detected, except for the pain manifested when moving the head and neck, as well as when walking.
Neurological examination revealed a normal or altered pain status and normal behaviour, gait evaluation revealed tetraparesis, and proprioceptive deficits varied according to the degree of spinal cord compression. Spinal reflexes, cranial nerve, perianal reflex and panniculus assessments were all normal. As a result, the neuroanatomical localization was identified at the C1-C7 spinal segment. Based on the VITAMIND acronym, the considered etiologies included inflammatory, degenerative and traumatic causes. After the neurological evaluation, both radiographic and MRI examinations of the C1-C7 cervical segment were recommended. The radiographs of this region showed no detectable abnormalities in the vertebrae, intervertebral spaces, or vertebral canal.
During the MRI examination, the following aspects were identified: 5 cases presented disc extrusion (Hansen type I) - 3 cases with disc extrusion present on the C2-C3 segment (Figure 1), and 2 cases at the level of the C3-C4 segment (Figures 2 and 3), respectively 7 cases of disc protrusion (Hansen type II) – one case of protrusion on the C3-C4 segment (Figure 4), 2 cases at the level of the C5-C6 segment and 4 cases that presented C6-C7 location.

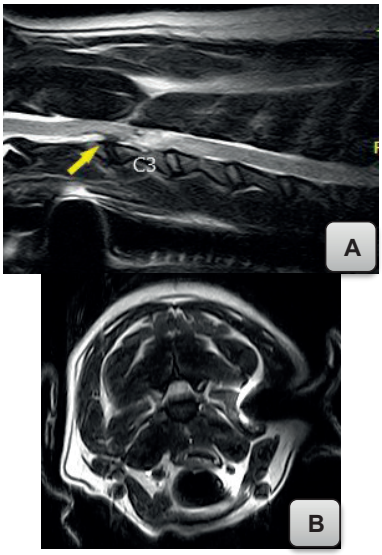

Figure 1. Sagittal plane images - T2 sequences (A) and transverse plane images - T2 sequences (B), at the C2-C3 intervertebral space, demonstrate an irregular distribution of disc material within the vertebral canal, visible as a T2 hypointense signal, resulting in significant dorsal spinal cord compression (A and B). Additionally, a diffuse T2 hyperintense area at C3 indicates secondary edema due to the compression

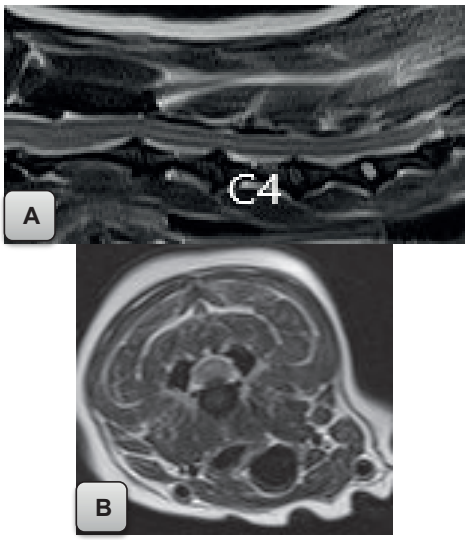

Figure 2. Sagittal T2 sequence images (A) and transverse T2 sequence images (B), at the C3-C4 intervertebral space, reveal a focal, well-defined disc material within the vertebral canal, appearing as a T2 hypointense signal, causing significant dorsal compression of the spinal cord (A and B)

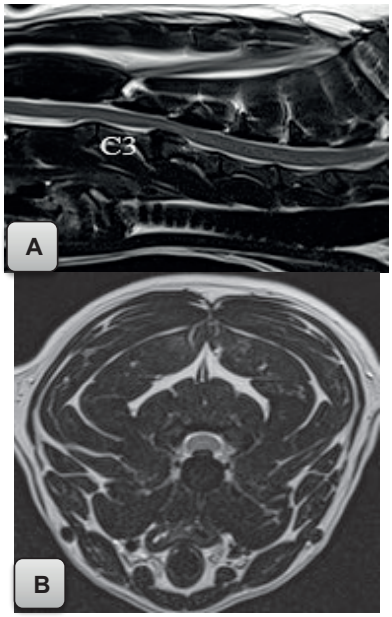

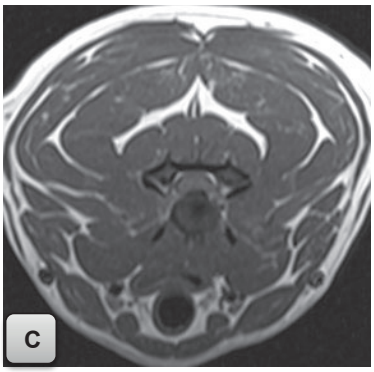

Figure 3. Sagittal T2 sequence images (A), transverse T2 sequence images (B) and transversal T1 sequence images (C), at the C3-C4 intervertebral space, showing a focal, well-delimitated disc material migrated caudally in the vertebral canal as a T2 and T1 hipointensity signal with severe dorsal compression of the spinal cord (A, B and C)

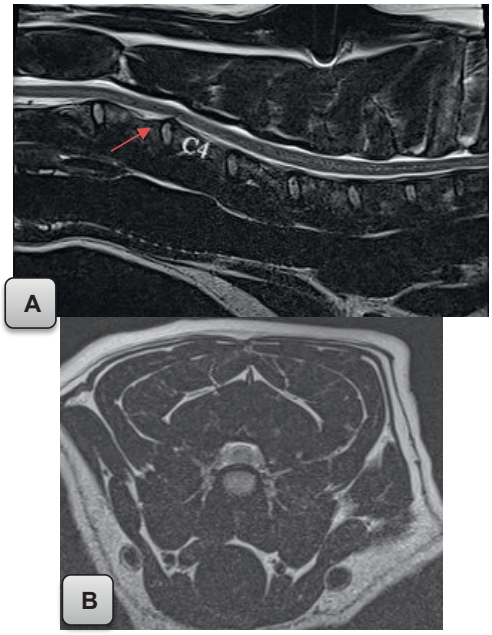

Figure 4. Sagittal T2 sequence images (A) and transverse T2 sequence images (B), at the C3-C4 intervertebral space, display a mild to moderate disc protrusion, resulting in mild to moderate compression of the spinal cord (A and B)

Literature data show differences in the occurrence of disc degeneration in dogs depending on the type of breed, with chondrodystrophic breeds being more predisposed to this condition (Bergknut, 2013; Da Costa et al., 2020). Our study carried out on a smaller number of cases (n=12), highlights the presence of these changes in both categories of dogs (66.57% in chondrodystrophic breeds and 33.33% in non-chondrodystrophic breeds).

Chondrodystrophic patients were between 2 and 9 years old, with an average age of 5.6 years, while non-chondrodystrophic breeds ranged from 3 to 8 years, with a mean age of 6 years. A study by Kranenburg et al. (2013) found no significant age differences among the evaluated subjects, reporting an average age of 6.5 years for chondrodystrophic breeds and 6.6 years for non-chondrodystrophic breeds. More recently, Argent et al. (2022) identified disc disease in patients aged 1 to 17 years, with an average age of 8.41 years, a variation likely due to the larger sample size in the study, which included 119 dogs.

IVDD is a common cause of cervical spine pain and neurological issues in dogs (Lappalainen et al., 2001), with the severity of clinical symptoms varying based on the type and location of the condition (Kranenburg et al., 2013).

In this study, disc extrusion was predominantly recorded in the C2-C3 segment (3 cases), similar to those previously published (da Costa et al., 2020; Neagu et al., 2018). Kranenburg et al. (2013), highlight that the cervical spine segment, was the most affected region in the case of disc extrusion, being found in 17 out of 49 cases, resulting an increased risk of Hansen disc herniation type I in the cervical segment.

In addition, it was found that the location of the disc extrusion in the C2-C3 segment affects small dogs, while the location of C5-C6 and C6-C7 is more frequent in large dogs (Cherrone et al., 2004; Hakozaki et al., 2015; da Costa et al., 2020).

Regarding disc protrusion, in the present study, it was identified at the C6-C7 level, followed by C5-C6 and C3-C4, consistent with previous studies by Hakozaki (2015).

The clinical manifestations expressed by the animals taken in the study confirm the results of other studies, where, secondary to intervertebral disc damage, neurological signs such as ataxia, and delayed proprioception in the forelimbs, which can evolve into paresis or paralysis, appeared (Itoh et al., 2008; Neagu et al., 2018).

CONCLUSIONS

The presence of symptoms such as cervical pain, delayed proprioception in the front limbs, ataxia, and paralysis of the hind limbs can be signs of a spinal condition, where an appropriate therapeutic protocol can be established based on the neurological and imaging diagnosis.

To confirm the suspected neurological diagnosis, the imaging examination (MRI) remains the easiest, non-invasive diagnostic method to confirm the structural changes of the intervertebral discs, being able to exclude other pathologies with similar manifestations.

REFERENCES

Argent V., Perillo R., Jeffery N., Freeman P. (2022). Recurrence of signs consistent with cervical intervertebral disc extrusion in dogs. *Journal of Small Animal Practice*, 63, 454-459.

Bergknut N., Meij B.P., Hagman R. et al. (2013). Intervertebral disc disease in dogs - Part 1: a new histological grading scheme for classification of intervertebral disc degeneration in dogs. *Veterinary Journal*, 195, p. 156-163.

Cherrone, K. L., Dewey, C. W., Coates, J. R., & Bergman, R. L. (2004). A retrospective comparison of cervical intervertebral disk disease in nonchondrodystrophic large dogs versus small dogs. *Journal of the American Animal Hospital Association*, 40(4), 316-320.

Da Costa R.C., Echandi R.L., Beauchamp D. (2012). Computed tomography myelographic findings in dogs with cervical spondylomyelopathy. *Veterinary Radiology & Ultrasound*, 53, p. 64-70.

Da Costa, R. C., De Decker, S., Lewis, M. J., Volk, H., & Canine Spinal Cord Injury Consortium (CANSORT-SCI) (2020). Diagnostic Imaging in Intervertebral Disc Disease. *Frontiers in veterinary science*, 7.

Hakozaki, T., Iwata, M., Kanno, N., Harada, Y., Yogo, T., Tagawa, M., & Hara, Y. (2015). Cervical intervertebral disk herniation in chondrodystrophoid and nonchondrodystrophoid small-breed dogs: 187 cases (1993–2013). *Journal of the American Veterinary Medical Association*, 247(12), 1408-1411.

Itoh, H., Hara, Y., Yoshimi, N., Harada, Y., Nezu, Y., Yogo, T. & Tagawa, M. (2008). A retrospective study of intervertebral disc herniation in dogs in Japan: 297 cases. *Journal of Veterinary Medical Science*, 70(7), 701-706.

Kranenburg, H. J. C., Grinwis, G. C., Bergknut, N., Gahrmann, N., Voorhout, G., Hazewinkel, H. A., & Meij, B. P. (2013). Intervertebral disc disease in dogs–Part 2: Comparison of clinical, magnetic resonance imaging, and histological findings in 74 surgically

treated dogs. *The Veterinary Journal*, 195(2), 164-171.

Neagu, A. G., Săvescu, M., Tudor, R. G., Tudor, N., & Vlăgioiu, C. (2018). MRI findings of the cervical spine in three beagle dogs. *AgroLife Scientific Journal*, 7(1), 92-96.

Pavel, R. G., Neagu, A. G., Turcu, R., Predoi, G., & Costea, R. (2021). Perianaesthetic management of canine patients that underwent hemilaminectomy for medullar compression. *Scientific Works. Series C. Veterinary Medicine.* Vol. LXVII(1), 108-113.

Smolders, L. A., Bergknut, N., Grinwis, G. C., Hagman, R., Lagerstedt, A. S., Hazewinkel, H. A., Meij, B. P. (2013). Intervertebral disc degeneration in the dog. Part 2: chondrodystrophic and non-chondrodystrophic breeds. *The Veterinary Journal*, 195(3), 292-299.

Tudor, R., Degan, A., Neagu, A. G., Carstinoiu, L., & Predoi, G. (2019). Hemilaminectomy for T11-T12 medullar compression-perianaesthetic management of a geriatric dog. *Scientific Works. Series C. Veterinary Medicine*. Vol. LXV(1), 94-95.

Scientific Works. Series C. Veterinary Medicine. Vol. LXX (2), 2024
ISSN 2065-1295; ISSN 2343-9394 (CD-ROM); ISSN 2067-3663 (Online); ISSN-L 2065-1295

SURGICAL APPROACH OF RENAL CALCULI IN A MIXED BREED FEMALE DOG: CASE REPORT

Alexandru Bogdan VIȚĂLARU, Cristian Ionuț FLOREA, Crina Alexandra BOANCĂ, Andrei RĂDULESCU, Alina ȘTEFĂNESCU

University of Agronomic Sciences and Veterinary Medicine of Bucharest, Faculty of Veterinary Medicine, 105 Splaiul Independentei Street, 050097, District 5, Bucharest, Romania

Corresponding author email: alexandrumv@yahoo.com

Abstract

A 5-year-old mixed breed female dog was diagnosed with renal calculi and recurrent cystitis and referred for second opinion. The patient presented lack of appetite, abdominal distention, progressive weight loss, dysuria and haematuria. During clinical examination, temperature, heart rate, blood pressure and respiratory rates were slightly elevated. Blood biochemistry revealed elevated creatinine and blood urea nitrogen. Using abdominal ultrasound examination, two ellipsoidal structures compatible with uroliths were visualized in the left kidney and proximal ureter. Abdominal radiography showed an irregular radiopaque calculus in the pelvis of the left kidney, confirming the ultrasound diagnosis, unilateral nephroureterolithiasis. Urinalysis confirmed struvite. Urolithiasis is a general term referring to aggregates of crystalline that can lead to ureteral obstruction, deterioration of renal function, bacterial urinary tract infection, haematuria and pain. Ureteral obstruction is a common indication for surgical intervention in small animals. Following abdominal radiography, nephrolithotomy and ureteral stenting were performed. Ureteral stenting is frequently performed following ureterotomy or ureteral anastomosis in order to reduce the risk of ureteral stricture. Ureteral stenting is the surgical treatment providing a direct communication between the bladder and kidney.

Key words*: calculi, dog, surgery, lithiasis, kidney.*

INTRODUCTION

Uroliths are polycrystalline concretions consisting mainly of organic or inorganic crystalloids along with smaller quantities of organic matrix. Uroliths generally consist of one or more types of minerals. These minerals can be present in a pure form, layered, or mixed throughout the urolith. Additionally, certain drugs can crystallize within the urinary tract and become part of the urolith. Magnesium ammonium phosphate crystals are observed most frequently whereas, the relative incidence of calcium oxalate, cystine, and ammonium urate tends to vary (Senior & Finlayson, 1986; Koehler et al., 2009).

The response of the body to a blockage in the ureter is intricate, occurring both before and after the blockage is resolved. Studies involving healthy dogs have indicated that the pressure in the ureter increases as soon as an obstruction occurs and may take over 24 hours to return to normal after the obstruction is relieved (Wen et al., 1999). Following the increase in pressure, renal blood flow decreases to 40% of its normal level within the initial 24 hours and subsequently drops to 20% of normal within the following two weeks. The heightened pressure is transmitted to the nephron, resulting in a decline in the glomerular filtration rate (GFR) due to the release of vasoactive mediators, the influx of leukocytes, and eventual fibrosis (Coroneos et al., 1997; Wilson, 1977). In response, the contralateral kidney will undergo an increased GFR. Irreversible effects are based on the severity and duration of the obstruction. A study involving healthy dogs demonstrated that after 7 days of obstruction, the GFR was permanently reduced by 35%, and after two weeks of obstruction, the GFR was reduced by 54%. Many individuals encounter partial blockage while also experiencing concurrent renal impairment, such as chronic kidney disease (CKD). Aggressive management and resolution of the obstruction are advised to enhance the overall outcome (Berent, 2011).

At the time of diagnosis, azotaemia is frequently observed, with 83% of cats and 50% of dogs showing azotaemia in cases of

unilateral obstruction (Berent, 2011). Historical information varies, depending on whether the stone has caused obstruction or whether concurrent infection is present. Nephroureteroliths are often found incidentally. Clinical signs can be intermittent, especially if the animal has received antibiotic treatment. Typical signs include stranguria, hematuria, and pollakiuria. Uncommon signs might involve abdominal discomfort and hypersalivation (Fossum et al., 2019)

The preferred method for diagnosing ureteral obstructions is a combination of radiographs and ultrasound. Radiographs are beneficial for documenting the size, number, and location of stones, as well as the presence of concurrent nephrolithiasis (Berent, 2011).

Surgical intervention is necessary when a ureterolith is causing recurrent urinary tract infections due to its immobility. Other factors to consider before surgery are the patient's overall kidney function, the presence of other stones in the urinary tract, the position of the ureterolith within the ureter, and the patient's general systemic health (Snyder et al., 2005).

The typical double-pigtail ureteral stent is a catheter with multiple openings and a pigtail loop at both ends. The first loop is placed inside the renal pelvis, while the catheter's shaft is located within the ureteral lumen, and the second loop ends inside the urinary bladder. By guiding urine from the renal pelvis directly into the urinary bladder through and around the stent, the double-pigtail stent effectively bypasses the ureteral obstruction (Berent et al., 2011).

Unilateral or bilateral ureteral stents are used to bypass obstruction, especially in cats, regardless of where the obstruction is or the number of stones that reside in the kidney or ureter. Stents enable passive ureteral dilation, restoration of urine flow, and potential recovery of the affected kidney. The placement of ureteral stents can be done endoscopically with cystoscopic and/or fluoroscopic guidance, and the stent can be placed through the ureterovesicular junction or from a ventral midline approach. Using an open approach, stents can be placed normograde via pyelocentesis, retrograde via cystotomy through the ureterovesicular junction, or retrograde through ureterotomy incision. Complications related to ureteral stents include stent migration, stent fracture, recurrent obstruction, recurrent UTI, and chronic urinary tract disease (Fossum et al., 2019).

The presence of urinary calculi or uroliths in the kidneys, ureters, bladder, or urethra is referred to as urolithiasis. Nephrolithiasis or ureterolithiasis specifically denote the condition of having renal or ureteral calculi (e.g., nephroliths or ureteroliths). Removal of renal calculi from the renal pelvis through an incision in the kidney parenchyma is called nephrolithotomy. Making an incision into the renal pelvis and proximal ureter is known as pyelolithotomy. The removal of calculi from the ureter by making an incision is referred to as ureterolithotomy (Fossum et al., 2019).

In dogs, the most frequently encountered types of uroliths are struvite (magnesium ammonium phosphate) and calcium oxalate. Additional types consist of urate, silicate, cystine, and mixed stones (Fossum et al., 2019).

Whether all renal or ureteral stones should be removed is controversial. Removal should be considered if renal stones are associated with refractory infection or hematuria, or if ureteral stones are causing complete obstruction. The removal of kidney stones that are not infected could potentially cause more harm than the stones themselves. Other factors to be considered in deciding surgery includes the effectiveness of medical therapy in dissolving the stone, renal function in the affected and contralateral kidney, the animal's overall health, and the presence of obstructive uropathy (e.g., hydronephrosis, hydroureter, or renal failure) (Fossum et al., 2019).

Ureteral stenting is the preferred choice for managing ureteral calculi that are difficult to remove by ureterotomy in dogs. It is commonly carried out following ureterotomy or ureteral anastomosis to reduce the likelihood of ureteral stricture development (Nicoli et al., 2012).

Urinary tract infection (UTI) caused by bacteria is a prevalent condition in dogs and frequently results in the use of antimicrobial medications. UTI occurs when infectious agents attach to, reproduce, and remain in the urogenital system, leading to inflammation and and related clinical signs (Harrer & Dorsch, 2020).

MATERIALS AND METHODS

A 5-year-old, 7.6 kg, canine mixed breed sterilized female was diagnosed with cystitis and nephroureterolithiasis and has undergone a surgical procedure for excision of the calculus that was located in the ureter, at another veterinary clinic. During the procedure, it was observed that the urolith has migrated and a purulent collection was drained. In the previous clinic, a urine culture sample was sent to a microbiology laboratory and the result was positive for *Proteus mirabilis* (>10.000 colony-forming unit - CFU). A wide spectre antibiotic was initiated according to the antibiogram result. The patient was referred for a second opinion nephrology consult on the 13th of October, 2022. Owner reported that the patient presented lack of appetite with progressive weight loss, abdominal distension, dysuria and haematuria. At the time the patient presented for the second opinion nephrology consult, the patient was on day 20 of antibiotic treatment for *Proteus mirabilis*.

During clinical examination, the following findings were noted: body temperature of 39.0°C, respiratory rate of 30 rpm, heart rate of 110 bpm, and body condition score of 3 with a mild muscle loss and a moderate painful sensitivity and defensive reaction to deep palpation of the abdomen. Arterial blood pressure showed slightly elevated values.

The complete blood count (CBC) was performed on Vetscan HM5 Hematology (5-part Differential) and determined: white blood cells (WBC), lymphocytes (LYM), monocytes (MON), neutrophils (NEU), eosinophils (EOS), basophils (BAS), LYM%, MON%, NEU%, EOS%, BAS%, red blood cells (RBC), haemoglobin (HGB), haematocrit (HCT), mean corpuscular volume (MCV), mean corpuscular haemoglobin (MCH), mean corpuscular haemoglobin concentration (MCHC), red blood cell distribution width-coefficient of variation (RDWc), red blood cell distribution width-standard deviation (RDWs), platelet (PLT), mean platelet volume (MPV), plateletcrit (PCT), platelet distribution width-coefficient of variation (PDWc) and platelet distribution width-standard deviation (PDWs).

Serum biochemistry was performed on Vetscan VS2 Chemistry Analyzer with a comprehensive diagnostic panel that determined: albumin (ALB), alkaline phosphatase (ALP), alanine aminotransferase (ALT), amylase (AMY), total bilirubin (TBIL), blood urea nitrogen (BUN), calcium (CA), phosphorus (PHOS), creatinine (CRE), glucose (GLU), sodium (NA^+), potassium (K^+), total proteins (TP) and globulin (GLOB).

Blood gases and electrolytes were performed on EPOC (electrolyte point of care).

Urinalysis was performed on Vetscan UA Urine Analyzer and determined leukocytes, ketones, nitrites, urobilinogen, bilirubin, glucose, protein, specific gravity, pH, blood, ascorbic acid, microalbumin, calcium, creatinine and protein/creatinine.

Abdominal ultrasound of the right kidney did not show any alteration of the structure. Two ellipsoidal structures (1: 1/0.6 cm, 2: 0.95/0.7 cm) compatible with uroliths were visualized in the left kidney (5.9/3.1 cm) and proximal ureter (0.95 cm). Furthermore, the left ureter was dilated and the left kidney showed signs of hydronephrosis. The renal pelvis was extended to 1.07/0.51 cm (hydronephrosis grade 1 to 2).

Assessment of hydronephrosis typically involves visual examination and categorization into five levels, which span from a slight enlargement of the renal pelvis to significant hydronephrosis accompanied by cortical thinning in advanced stages of the condition (Hansen, K.L., Nielsen, M.B., & Ewertsen, C., 2015).

Abdominal radiography showed irregular radiopaque calculi in the pelvis of the left kidney, confirming the ultrasound diagnosis, unilateral nephroureterolithiasis (Figure 1a, 1b, 1c).

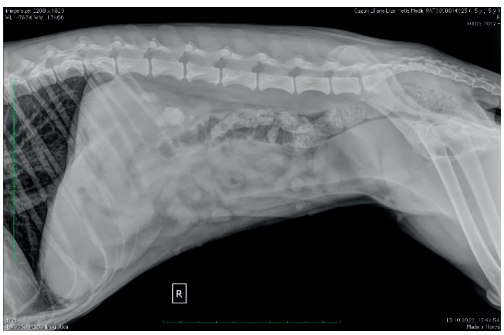

Figure 1a - Right latero-lateral exposure

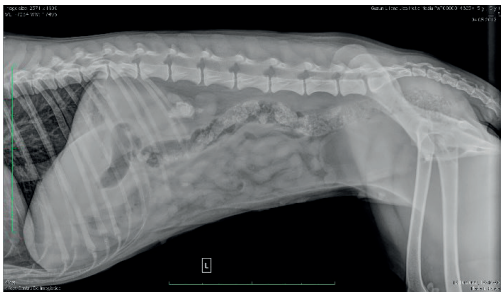

Figure 1b - Left latero-lateral exposure

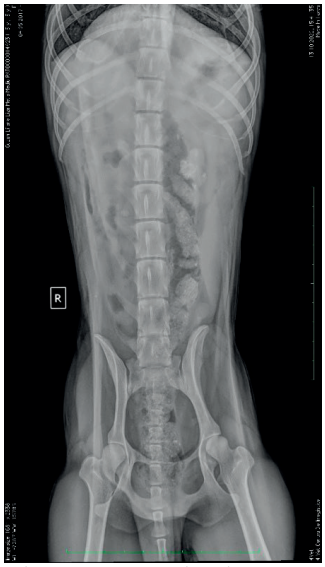

Figure 1c - Ventro-dorsal exposure

The patient was hospitalized and stabilized in order to be submitted to a nephro-uretero-litothomy surgical procedure.

Rehydration and electrolyte rebalancing were established by continuous rate of infusion (CRI) with Ringer solution (rate and dosage: 7 ml/kg/h) and partial parenteral nutrition based on levo-aminoacids was administered (rate and dosage: 0.6-0.8 g amino acids/kg/24 h). The active ingredients in the levo-aminoacids solution are: L-isoleucine, L-leucine, L-lysine monoacetate, L-lysine, L-methionine, L-phenylalanine, L-threonine, L-tryptophan, L-valine, L-arginine, L-histidine, L-alanine, N-acetyl-L-cysteine, L-cysteine, Glycine, L-proline, L-serine, L-tyrosine, N-glycine-L-tyrosine dehydrate, N-glycine/L-tyrosine. It contains a total of 100g/L amino acids.

In the following days leading up to the surgical procedure, the patient was given the following treatment: a potent and selective antagonist of the neurokinin (NK-1) receptor and a proton pump inhibitor. Nutritional supplements based on amino acids combined with a peptide that supports kidney functions and supplements that help maintain and support the urinary tract (based on DL-methionine) were introduced as adjuvants in the therapy. Analgesia was ensured with the use of methadone.

During hospitalization, the patient did not present food appetite. In addition to the ongoing medication and treatment protocol, suppository with mirtazapine was added and administered by intra-rectal route for three days consecutively.

On the day of the surgical procedure the cardiology exam revealed respiratory sinus arrhythmia with elevated ST segment.

Following stabilization, the patient was prepared for the surgical procedure. The approach of uroliths was done at the level of the left ureter by performing an ureterotomy through a small longitudinal incision. Afterwards, an indwelling Double J Catheter Stent of 6.0 French (Fr) and 26 centimetres (Figure 2) was placed by cystoscopy (retrograde) approach.

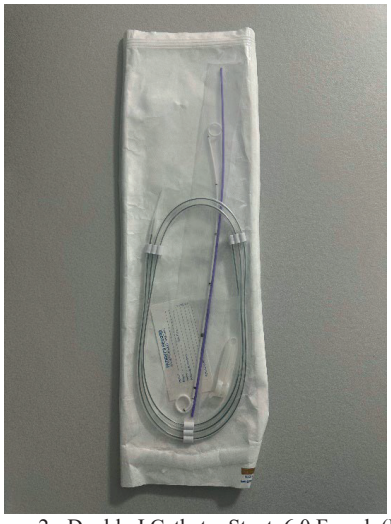

Figure 2 - Double J Catheter Stent, 6.0 French (F)

Ureteral stents are usually available in a Double-J or double-pigtail design and extend from the renal pelvis to the bladder along the length of the ureter. The most prevalent types of ureteral stents used in dogs and cats are currently made from a solid polymer, featuring

a double-pigtail configuration and multiple fenestrations. Temporary and permanent urethral stents place in dog patients have been proven effective as treatment options. Temporary urethral stents are placed less frequently than permanent ones. Basic versions of temporary stents are generally crafted from rubber or polyurethane.

Temporary stents may serve as a temporary solution before permanent stenting. They can be used until a permanent stent is available or to determine if stenting will facilitate with urine drainage in a specific patient. In dogs, temporary stents are also considered when there is suspicion of reflex dysynergy or functional obstruction of urethral outflow. In these cases, permanent stenting may not be able to resolve the urethral obstruction, so temporary stents are used to assess the potential success of stenting (Palm et al., 2021).

Following the surgical procedure, the treatment protocol was modified in the following manner: a broad-spectrum antibiotic was initiated and a non-steroidal anti-inflammatory drug (NSAID) from the coxib class, which has a strong preference for the cyclooxygenase-2 (COX-2) enzyme (Kongara & Chambers, 2018).

The patient received renal diet.

RESULTS AND DISCUSSIONS

On the 13th of October 2022, the patient had the following serum biochemistry modifications: AMY 1365 U/L (RR: 200-1200 U/L), BUN 66 mg/dL (RR: 7-25 mg/dL), CRE 4.3 mg/dL (RR: 0.3-1.4 mg/dL), GLU 117 mg/dL (60-110 mg/dL). There were no changes regarding the complete blood count (CBC). Urine sediment showed leukocytes 10-15 high power field (HPF) (RR: 0-8 HPF) and magnesium ammonium phosphates (struvites). Urinalysis was performed from urine obtained through ultrasound guided cystocentesis and the following results were obtained: slightly turbid urine with a pH of 7 (RR: 6-7.5), specific gravity of 1.012 (RR: 1.015-1.045), leukocytes 25 Leu/uL and proteins 30 mg/dL. A urine culture sample was submitted to a microbiology laboratory and the result was negative (0 colony-forming unit - CFU).

Following the first night of hospitalization, serum biochemistry was re-evaluated and the following modifications occurred: ALB 2.5 g/dL (RR: 2.5-4.4 g/dL), BUN 50 mg/dL (RR: 7.0-25.0 mg/dL), CRE 2.1 mg/dL (0.3-1.4 mg/dL) and GLU 145 mg/dL (RR: 60-110 mg/dL).

After 72 hours of therapy, the serum biochemistry was: ALP 310 U/L (RR: 20-150 U/L), BUN decreased to 30 mg/dL (7-25 mg/dL), CRE slightly decreased to 1.7 mg/dL (0.3-1.4 mg/dL) and GLU slightly decreased to 124 mg/dL (RR: 60-110 mg/dL).

The following day, serum biochemistry results showed ALB 2.4 g/dL (RR: 2.5-4.4 g/dL) and ALP increased to 394 U/L (RR: 20-150 U/L).

On the day of the surgical procedure an electrolyte point of care (EPOC) analysis was performed and no parameters other than BUN, CRE, ALP and ALB were modified.

On the day of the surgical procedure the cardiology exam revealed respiratory sinus arrhythmia with elevated ST segment. Heart rate was between 80-90 beats per minute (bpm). Pimobendane was administered with a dose of 0.25 mg/kg. The heart rate slightly increased between 94-100 bpm.

During the pre-anaesthetic evaluation, heart rate was between 100-110 bpm, systolic blood pressure values were between 120-130 mmHg. No heart murmur was heard with a rhythmic-arrhythmic rate. Femoral pulse was present bilaterally, normodynamic and synchronous with the heartbeat. Vesicular murmur was present bilaterally. The patient's mucous membranes were pink and the capillary refill time was less than 2 seconds. The body temperature was 38.2°C and the Body Condition Score was between 4 and 5.

According to the American Society of Anesthesiologists (ASA) risk classification, the patient was graded score 3, indicating the presence of moderate systemic disease that limits normal function. Animals with an ASA score of 3 or higher are over 10 times more likely to experience peri-anaesthetic complications than animals in ASA scores of 1 or 2. Assigning an ASA score accurately is a reliable method for identifying at-risk patients. To assign the correct ASA status, a comprehensive pre-anaesthetic evaluation is essential (Duke-Novakovski et al., 2016).

The premedication protocol consisted of midazolam (0.2 mg/kg) IV, methadone

(0.3 mg/kg) IV and ketamine (0.3 mg/kg) IV. For induction, propofol was used in a dose of 8 mg/kg IV.
Loco-regional anaesthesia consisted of incisional and peritoneal blocks.
A constant rate infusion (CRI) of fentanyl-lidocaine-ketamine was used as part of the partial intravenous anaesthesia (PIVA).
Isoflurane, administered together with oxygen, was used as an inhalant anaesthetic for maintenance of the anaesthesia during the surgical procedure.
The surgical procedure that the patient had undergone was a nephro-uretero-litothomy.
Ureterotomy is occasionally performed to remove obstructive calculi, but it carries risks such as postoperative leakage and stricture formation, necessitating careful execution. Calculi removal is recommended when obstruction occurs or is anticipated (e.g., in cases of hydroureter or hydronephrosis). Although ureteral mucosa can regenerate around a stent if not entirely disrupted, the use of stenting catheters remains controversial due to potential risks of stricture formation and infection. When stents are used, they should be smaller than the diameter of the ureter. In some cases, ureteral stents may be placed to exit through the urethral orifice and are sutured externally (Fossum et al., 2019).
The patient did not present any complications in the following weeks regarding the urethral stenting.
The following surgery process steps were performed:

- the patient was placed in dorsal recumbency;
- the abdomen was prepared for a ventral midline incision. The prepared area was extended from above the xyphoid to caudal to the pubis;
- a longitudinal incision in the dilated left ureter proximal to the urolith;
- removal of the urolith;
- through the longitudinal incision, with a surgical Kocher clamp, it was possible to reach the nephrolith (the nephrolith was not embedded within the renal pelvis of the left kidney that was presented with hydronephrosis);
- a small soft rubber catheter was placed into the ureter proximal and distal to the incision, through which warm fluid was flushed;
- the incision was closed with a simple interrupted pattern with 6/0 absorbable suture;
- the Double J 6.0 Fr catheter was inserted through a cystoscopy (retrograde) approach.

Abdominal radiography was repeated the following day (Figure 3a and 3b).

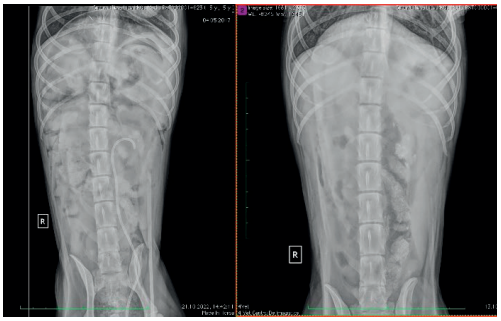

Figure 3a - Radiographs taken before (right) and after (left) the surgical procedure

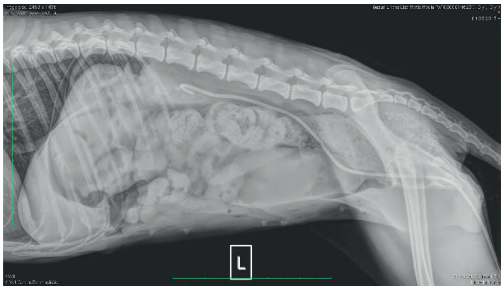

Figure 3b - Latero-lateral incidence of the patient taken after the surgical procedure

The patient was unstable during the procedure and it required specific medication support and special intra-operative monitoring. The heart rate decreased to 50-60 bpm. The patient was responsive to aggressive fluid therapy and inotropic medication. The patient was mechanically ventilated with SIMV-VC and IPPV.
After 24 hours, the bloodwork was re-evaluated and the following parameters were increased: ALB 2.1 g/dL (RR: 2.5-4.4 g/dL), ALP 315 U/L (RR: 20-150 U/L), BUN 42 mg/dL (RR: 7.0-25.0 mg/dL) and CRE 1.6 mg/dL (0.3-1.4

mg/dL). The CBC revealed an increase in WBC 26.69 10^9/l (RR: 6-17 10^9/l) and NEU 24.11 10^9/l (RR: 3-12 10^9/l).

On discharge day, serum biochemistry values showed: ALB 2.1 g/dL (RR: 2.5-4.4 g/dL), ALP 306 U/L (RR: 20-150 U/L), BUN 37 mg/dL (RR: 7.0-25.0 mg/dL) and CRE 1.4 mg/dL (0.3-1.4 mg/dL). The CBC showed a decrease on WBC with 19.39 10^9/l (RR: 6-17 10^9/l) and NEU 15.50 10^9/l (RR: 3-12 10^9/l). The patient was discharged with the following recommendations:

- nutritional supplements based on amino acids combined with a peptide (2000 mg every 12 hours) and supplements that help maintain and support the urinary tract (based on DL-methionine - 250 mg TID);
- calcium carbonate-based phosphorus binders (300 mg every 12 hours);
- supplements for enteric dialysis;
- first-generation cephalosporin antibiotic (22 mg/kg every 12 hours for 14 days);
- a selective proton pump inhibitor (20 mg every 24 hours for 7 days);
- pimobendane 1.25 mg, for 30 days with reassessment;
- probiotic food supplement (every 24 hours for 30 days);
- supplement for liver function support;
- renal diet.

Fourteen days after discharge, CBC, serum biochemistry, urinalysis and abdominal ultrasound were reassessed. There were no abnormalities on the CBC. Serum biochemistry revealed a mild elevation of ALP 160 U/L (RR: 20-150 U/L), ALT 145 U/L (RR: 10-118 U/L), AMY 1242 U/L (200-1200 U/L), CRE 1.5 mg/dL. Abdominal ultrasound of the right kidney revealed a regular contour with a suitable cortico-medullar ratio and renal pelvis dilation of grade 1 to 2. The left kidney has a regular contour with renal pelvis dilatation of grade 1 to 2. The urine sample was obtained by ultrasound guided cystocentesis and urinalysis showed leukocytes +3500 cell/uL, with a specific gravity of 1.030 and a pH of 5.0. Urine sediment did not present any crystals but numerous leukocytes and bacteria. A urine culture sample was submitted to a microbiology laboratory and the result was positive for *Escherichia coli* (>100.000 CFU). The antibiotic of choice was a broad spectrum antibiotic from the aminopenicillin class of penicillin family. The owner was informed that after 28 days of antibiotic treatment, another urine culture sample will have to be sent again for microbiology.

The indwelling Double J Catheter Stent was removed after 14 days since the surgical procedure.

Twenty-eight days after the last check-up, another urine culture sample was sent to a microbiology laboratory and the result was positive for *Klebsiella pneumonia* (>100.000 CFU). An antibiotic from the class of fluoroquinolones was chosen and administered for the next 28 days. Urinalysis showed leukocytes +2125 cell/uL, specific gravity of 1.030 and pH of 5.0. Urine sediment did not present any crystals but numerous leukocytes and renal tubular epithelial cells. Renal tubular epithelial cells, located in the tubulointerstitium, are recognized for their important functions in acute kindey injury (AKI) and CKD (Hong et al., 2020). Abdominal ultrasound showed the right kidney with a regular contour with a suitable cortico-medullar ration and renal pelvis dilatation of grade 1. The left kidney had a regular contour with renal pelvis dilatation of grade 1 to 2 with a calculus of approximately 0.4 cm. The urinary bladder presented multiple hyperechoic particles in suspension with dimensions of about 4.5 cm.

The following re-check, urine sediment showed leukocytes, renal tubular epithelial cells, struvite (magnesium ammonium phosphate) and bacteria. Ultrasound of the left kidney showed a severely altered architecture with renal pelvis dilatation of grade 1 to 2 and ureter dilation due to the presence of a 0.5 cm urolith. The right kidney showed a characteristic architecture with a suitable cortico-medullar aspect ratio and no dilation of the proximal pelvis. The result for urine culture was positive for *Escherichia coli* (>100.000 CFU) with sensitivity to broad spectrum synthetic antibiotic. The antibiotic was administered for 28 days.

Every 30 days, a complete CBC, serum biochemistry, urinalysis and urine sediment, urine culture and abdominal ultrasound were

re-evaluated. Over the following 12 months after discharge, a total of 11 urine cultures were determined. The patient had two negative urine cultures and nine tested positive for *Escherichia coli* (>100.000 CFU).

Since the surgical procedure, serum biochemistry values are as follows: BUN 31 mg/dL (RR: 7.0-25.0 mg/dL) and CRE 2.0 mg/dL (0.3-1.4 mg/dL). Urinalysis revealed a specific gravity of 1.030 and pH of 6.0. Urine sediment did not show any crystals but rare renal tubular epithelial cells.

UTIs in dogs and cats, with female dogs and cats at higher risk, are typically caused by a single pathogen in 75% of cases. In dogs, Escherichia coli is responsible for about half of all infections, followed by Staphylococcus, Proteus and Klebsiella species. Several factors such as incomplete bladder emptying due to neurological disease, the presence of urolithiasis, urinary incontinence and immunosuppression have been associated with an increased risk of UTI (Byron, 2019).

CONCLUSIONS

Stenting of the urinary tract is a minimally invasive and highly effective method of restoring the flow of urine and relieving the pressure in the kidney.

After stenting, regular monitoring is crucial to detect any complications that may necessitate the removal or replacement of the stent.

The combined use of radiology and ultrasonography is recommended to assess the upper urinary tract, as this approach offers greater diagnostic sensitivity than using each method independently.

Monthly clinical evaluation, laboratory tests, medication and a balanced diet can offer a good prognosis for patients diagnosed with nephroureterolithiasis that underwent nephrolithotomy intervention.

REFERENCES

Berent A. C. (2011). Ureteral obstructions in dogs and cats: a review of traditional and new interventional diagnostic and therapeutic options. *Journal of veterinary emergency and critical care (San Antonio, Tex.: 2001)*, *21*(2), 86–103.

Berent, A. C., Weisse, C., Beal, M. W., Brown, D. C., Todd, K., & Bagley, D. (2011). Use of indwelling, double-pigtail stents for treatment of malignant ureteral obstruction in dogs: 12 cases (2006-2009). *Journal of the American Veterinary Medical Association*, *238*(8), 1017–1025.

Byron J. K. (2019). Urinary Tract Infection. *The Veterinary clinics of North America. Small animal practice*, *49*(2), 211–221.

Coroneos, E., Assouad, M., Krishnan, B., & Truong, L. D. (1997). Urinary obstruction causes irreversible renal failure by inducing chronic tubulointerstitial nephritis. *Clinical nephrology*, *48*(2), 125–128.

Duke-Novakovski, T., de Vries, M., Seymour, C., (2016). *BSAVA Manual of Canine and Feline Anesthesia and Analgesia* (3rd Ed.), Published by British Small Animal Veterinary Association

Fossum W. Theresa, et al. (2019). *Small Animal Surgery*, 5th Edition. Elsevier.

Harrer, J., & Dorsch, R. (2020). Bakterielle Harnwegsinfektion und subklinische Bakteriurie des Hundes: eine aktuelle Übersicht [Bacterial urinary tract infection and subclinical bacteriuria in the dog: a current review]. *Tierarztliche Praxis. Ausgabe K, Kleintiere/Heimtiere*, *48*(4), 270–284.

Hong, S., Healy, H., & Kassianos, A. J. (2020). The Emerging Role of Renal Tubular Epithelial Cells in the Immunological Pathophysiology of Lupus Nephritis. *Frontiers in immunology*, *11*, 578952.

Koehler, L. A., Osborne, C. A., Buettner, M. T., Lulich, J. P., & Behnke, R. (2009). Canine uroliths: frequently asked questions and their answers. *The Veterinary clinics of North America. Small animal practice*, *39*(1), 161–181.

Kongara, K., & Chambers, J.P., 2018). Robenacoxib in the treatment of pain in cats and dogs: safety, efficacy, and place in therapy. *Veterinary medicine (Auckland, N.Z.)*, *9*, 53–61.

Nicoli S, Morello E, Marano M, et al. Double-J ureteral stenting in nine cats with ureteral obstruction. *Vet J*, 2012; 194:60-65.

Palm, C. A., Canvasser, N. E., & Culp, W. T. N. (2021). Stenting of Malignant Urinary Tract Obstructions in Humans and Companion Animals. *Veterinary sciences*, *9*(1), 13.

Senior, D. F., & Finlayson, B. (1986). Initiation and growth of uroliths. *The Veterinary clinics of North America. Small animal practice*, *16*(1), 19–26.

Snyder, D. M., Steffey, M. A., Mehler, S. J., Drobatz, K. J., & Aronson, L. R. (2005). Diagnosis and surgical management of ureteral calculi in dogs: 16 cases (1990-2003). *New Zealand veterinary journal*, *53*(1), 19–25. https://doi.org/10.1080/00480169.2005.36464).

Wen, J. G., Frøkiaer, J., Jørgensen, T. M., & Djurhuus, J. C. (1999). Obstructive nephropathy: an update of the experimental research. *Urological research*, *27*(1), 29–39.

Wilson DR. (1977). Renal function during and following obstruction. *Ann Rev Med*; 28: 329–339.

Scientific Works. Series C. Veterinary Medicine. Vol. LXX (2), 2024
ISSN 2065-1295; ISSN 2343-9394 (CD-ROM); ISSN 2067-3663 (Online); ISSN-L 2065-1295

THE IMPORTANCE OF NUTRITION AND THE USE OF ANTI-INFLAMMATORY DRUGS IN THE TREATMENT OF DERMATITIS IN CARNIVORES

Ionuț Răzvan DOBRE, Nicoleta CIOCÎRLIE

University of Agronomic Sciences and Veterinary Medicine of Bucharest, Faculty of Veterinary Medicine, 105 Splaiul Independentei Street, 050097, District 5, Bucharest, Romania

Corresponding author email: razvan.dobre@fmvb.usamv.ro

Abstract

Dermatitis of various causes is one of the most common pathologies encountered in carnivores, especially from May to September. Our study focused on 19 cases of carnivores (11 dogs and 8 cats) which presented to a veterinary clinic with dermatitis of different aetiologies, with both auricular and skin localization. During the anamnesis, we noted the hyperproteic diet, as one of the most important factors favouring these conditions. The highest incidence was food allergic otitis in dogs (36.84%), followed by parasitic otitis in cats (31.57%), parasitic dermatitis in dogs (21.05%), and allergic dermatitis in cats (10.52%). Treatment included a hypoallergenic diet for 8-12 weeks. Dexamethasone or Prednisolone was associated, with therapy, ensuring the success of the therapeutic approach. The success of the treatment was decisively favoured by the hypoallergenic diet and the combination of anti-inflammatory drugs.

Key words*: food, anti-inflammatory drugs, dermatitis, therapy.*

INTRODUCTION

In veterinary clinics, around 20% of case reports present dermatological conditions, where the diagnosis is based on recognizing the type of lesion and etiological agent. It is essential to differentiate primary lesions from secondary ones for the correct diagnosis of dermatitis. Primary lesions are the result of the action of the pathological/etiological agent, while secondary lesions are complications that arise against the background of the pre-existing primary lesion that are caused either by the patient's action or by environment (Grant, 2005; Goth, 2022).

Among these, alopecia is an inflammation expressed by damaging the hair follicle, with a chronic evolution that leads to hair loss in the case of parasitic, fungal, endocrine, and nutritional diseases, as well as organopathies (hepatic and/or renal failure) (Coyer, 2020; Rhodes, 2011). Demodicosis, located in the hair follicle and sebaceous glands, is found mostly in dogs, less frequently in cats, and proliferates in immunosuppressed animals. Sarcoptic mange, most often found in dogs, is expressed by intensely itchy lesions prone to hyperkeratinization and secondary infection of the skin (Bourguignon, 2013).

Our study aimed to monitor the incidence of these conditions in parallel with the effectiveness of the treatment, improved by combining anti-inflammatory drugs and a hypoallergenic diet (Dobre, 2019; Goran, 2016).

MATERIALS AND METHODS

The study was carried out on 19 clinical cases, 11 dogs and 8 cats (Tables 1 and 2), which were presented to a veterinary clinic with dermatitis of different ethology and location.

After diagnosis, the same therapeutic protocol was applied to all cases.

The diagnosis was made by microscopic examination of secretions, crusts, and/or hairs. The collected material was displayed on a microscope slide, the staining was performed after drying. Microscopic examination is a simple and effective method that guides the diagnosis and helps in selecting the appropriate treatment. We also used the otoscope, and the skin scraper on the affected areas (Figures 1 and 2).

Figure 1. Haema rapid staining solutions /Quick-Diff

Figure 2. Riester otoscope

Table 1. Cases of dogs studied

ID	Breed	Sexe	Age (y.o.)	Weight (kg)
1	Mixed	♀	9	15
2	Bulldog	♂	3	21
3	Bichon	♀	2	6
4	Bichon	♂	4	7
5	French bulldog	♂	3	10
6	Mixed	♀	1	9
7	Pug	♂	0.66	6.5
8	Bichon	♂	9	7.5
9	Cocker	♀	2	11
10	German Shepherd	♂	1	33
11	Chihuahua	♀	3	2

Table 2. Cases of cats studied

ID	Breed	Sexe	Age (y.o)	Weight (kg)
1	European	♀	0.16	3
2	British short hair	♀	0.33	3
3	European	♀	1	2.5
4	Persian	♂	1	5
5	Sfinx	♂	0.66	3.5
6	Main Coon	♀	2	4
7	European	♂	1	2
8	British	♂	0.58	3

After a thorough clinical, microbiological and otoscopic examination, the patients were classified into one of four types of dermatitis, based on the ethology and the affected anatomical area: food allergic otitis in dogs - 7 cases, parasitic otitis in cats - 6 cases, parasitic dermatitis in dogs - 4 cases and allergic dermatitis in cats - 2 cases, as shown in Figure 3.

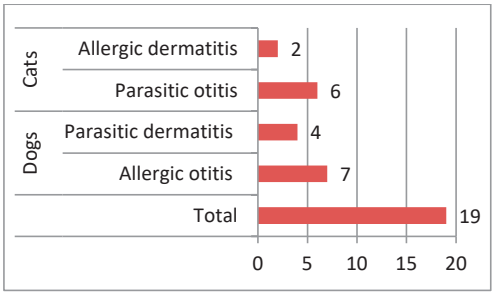

Figure 3. Distribution of different types of dermatitis in dogs and cats

After diagnosing and classifying each patient in a specific dermatitis category, individualized treatment was established. As previously noted, local hygiene of the affected area is essential. For this, we used Specialist® Shampoo for dogs (bathing every 2-3 days) and/or Epiotic® for ear cleaning.

In cases involving bacterial and/or fungal agents, Alfaderm Plus® spray was applied twice a day to the affected area for 7 days. Surolan® otic solution was used in the ear for the same purpose, to combat the etiological agent and reduce inflammation. In both cases, the anti-inflammatory effect is achieved due to the prednisolone content in these medications.

Given the major contributing factor of a hyperprotein diet, a crucial step was implementing a hypoallergenic diet for a continuous period of at least 8-12 weeks

To control ringworm, we used Iver-mite otic® (2-5 drops) and Bravecto® chewable tablets were administered to control ticks and fleas.

RESULTS AND DISCUSSIONS

The treatment was administered for 7-10 days, with follow-up check at 7 days. The anti-allergic medication (e.g. Histamine Control®) was given for 21 days, in parallel with the hypoallergenic diet.

All the cases included in the study showed favourable progress starting from the 7th day, confirming the effectiveness of the treatment. The incidence of the types of dermatitis was as follows: 37% for allergic otitis in dogs, 21% for parasitic dermatitis in dogs, 31.6% for parasitic

otitis in cats, and respective 10.5% for allergic dermatitis in cats, as shown in Figure 3.
Regarding the incidence based on the sex of the animals, we observed a slightly higher incidence in males (52.6%), compared to in females (47.4%), as shown in Figure 4.

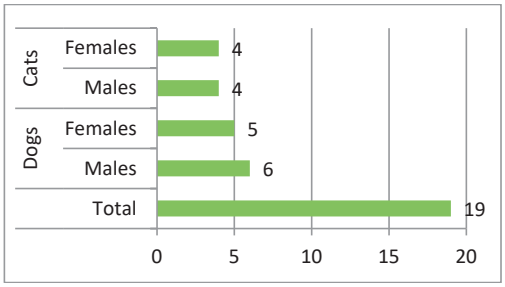

Figure 4. Incidence of Dermatitis in dogs and cats by sex

The optimization of nutrient intake, intestinal microbiota and its immune function could represent an excellent strategy to promote the beneficial effects on health in general, including the decrease of clinical signs of allergic skin diseases (Guidi et al., 2021).
Previous studies in human medicine have shown that the gut microbiota in early childhood is associated with age of onset, severity, remission, exacerbation and even phenotypes of atopic dermatitis (Lee S.-Y. et al., 2018).
In many patients' environmental allergens absorbed epicutaneously function as important triggers. According to this opinion, the removal of allergens on a routine basis in association with hypoallergenic products - oral and topical glucocorticoids - improve the skin barrier (Olivry et al., 2015).

CONCLUSIONS

The incidence of dermatitis was higher in dogs than in cats, with allergic otitis being the most common condition.
The highest incidence was recorded by allergic otitis, at approximately 37%, while allergic dermatitis had the lowest incidence, at only 10.5%.
The main clinical signs in patients were alopecia, pruritus, erythema, and unpleasant odour in the ear.
Combining topical treatments with systemic drugs resulted faster improvement and resolution of symptoms.
The association of anti-inflammatory drugs (prednisolone) and a hypoallergenic diet significantly promoted healing and contributed to the overall therapeutic success.

REFERENCES

Bourguignon, E., Guimaraes,L.D., Fereira, T.S., Favarato, E.S. (2013). *Dermatology in Dogs and Cats,* https://www.intechopen.com/chapters/43169, DOI: 10.5772/53660.

Coyer, K.S. (2020). *Clinical Atlas of Canine and Feline Dermatology*, Willey Blackwell.

Crivineanu, M, Palamaru, F., Nicorescu, V. (2017). Clinical and therapeutic aspects in some skin diseases in dogs and cats. *Scientific Works. Series C. Veterinary Medicine*. Vol. LXIII(1), pg. 67-70

Dobre, I.R. (2019). *Toxicologie veterinară*, Printech Publishing House

Dobre, I.R., Alexandru, D.M., Crivineanu, M. (2019). Study on changes in haematological parameters following administration of NSAIDs in dogs, *Scientific Works. Series C. Veterinary Medicine*. Vol. LXV(1), pg.37-41.

Goran, G.V., Crivineanu, V. (2016). *Toxicologie*. Printech Publishing House.

Goth, G.M. (2022). *Canine and Feline Dermatology*. Atlas, 2nd Edition, Servet.

Grant, D.I. (2005). *Skin diseases of dogs and cats*, 2nd Edition, Blackwells Scientific Publications.

Guidi, E. E.A, Gramenzi, A,, Persico, P., Di Prinzio, R., Di Simone, D., Cornegliani, L. (2021). Effects of feeding a hypoallergenic diet with a nutraceutical on fecal dysbiosis index and clinical manifestations of canine atopic dermatitis - Animals (Basel), doi: 10.3390/ani11102985.

Lee S.-Y., Lee E., Park Y.M., Hong S.-J. (2018). Microbiome in the gut-skin axis in atopic dermatitis doi: 10.4168/aair.2018.10.4.354

Olivry, T., De Boer, D.J,, Favrot, C., Jackson, H.A., Mueller, R.S., Nuttall, P., Prelaud, P. (2015). Treatment of canine atopic dermatitis 2015 updated guidelines from the International Committee on Allergic Diseases of Animals, *BMC Vet Res*, 11, 210.

Rhodes, K.H., Werner, A.H. (2011). *Blackwell's five minutes consult - Small animal dermatology*, 2nd Edition, Willey Blackwell.

Scientific Works. Series C. Veterinary Medicine. Vol. LXX (2), 2024
ISSN 2065-1295; ISSN 2343-9394 (CD-ROM); ISSN 2067-3663 (Online); ISSN-L 2065-1295

DIFFERENTIATION BETWEEN FELINE INTESTINAL T-CELL LYMPHOMA FROM INFLAMMATORY BOWEL DISEASE BY POLYMERASE CHAIN REACTION FOR ANTIGEN RECEPTOR REARRANGEMENI (PARR)

Maria-Mihaela IFROSE, Emilia CIOBOTARU-PÎRVU

University of Agronomic Sciences and Veterinary Medicine of Bucharest, Faculty of Veterinary Medicine, 105 Splaiul Independentei Street, District 5, Bucharest, Romania

Corresponding author email: maria_mihaela99@yahoo.com

Abstract

Intestinal lymphoma is a very common malignancy in cats, classified in low-grade intestinal T-cell lymphoma and high-grade intestinal T-cell lymphoma. Even the exact cause of the intestinal lymphoma remains uncertain, there may be a connection between persistent intestinal inflammation, such as inflammatory bowel disease (IBD), and the development of this tumor. Thus, differentiation between inflammation and low-grade lymphoma is always a challenge. This study included 22 cats with digestive syndrome featured by recurrent vomiting and diarrhea which have been also unresponsive to treatment. Full thickness intestinal biopsies from living animals and tissue samples from dead animals have been considered for routine cytopathological and histopathological diagnosis. Polymerase chain reaction for antigen receptor rearrangement (PARR) for T-cell CD3 region of the TCRy chain was used to differentiate lymphoma from non-lymphoma lesions. Cytological and histological findings have been represented by a residual heterogeneous population consisting of neutrophils, eosinophils and small mature lymphocyte, to which is added a dominant contingent of small- to medium-sized or large lymphocytes. Mesenteric lymph nodes contain characteristic cells which were consistent for incipient malignant lymphoid proliferation. PARR test discriminated 11 cases of T-cell lymphoma showing strong performance for discrimination of lymphoma from IBD.

Key words: *intestinal bowel disease, lymphoma, PARR.*

ABBREVIATIONS

EATL II- Feline enteropathy-associated T-cell lymphoma, type II
FFPE- formalin-fixed and paraffin-embedded
FNA- fine needle aspiration
HGITL- high grade intestinal T-cell lymphoma
IHC- immunohistochemistry
IgG1- immunoglobulin G1
IgG2- Immunoglobuline G2
IgH- immunoglobulin heavy chain
IgM- immunoglobulin M
LGITL- low-grade intestinal T-cell lymphoma
LPE- lymphoplasmacytic enteritis
PARR- polymerase chain reaction (PCR) to assess antigen receptor gene rearrangements
PBS- phosphate buffered saline
QC- quality check
TCL- T-cell lymphoma
TCR -T cell receptor
TRB- T cell receptor betta
TRD- T cell receptor delta
PCR- Polymerase chain reaction
V(D)J gene- genetic diversity joining

INTRODUCTION

The gastro-intestinal tract is the most frequently affected by neoplastic and inflammatory process in cats with an 80 percent of malignancy (Andrews, 2016). Gastric tumors in cats are highly common and varied in embryologic origin, including leiomyosarcomas, lymphomas, adenocarcinomas, intestinal mast cell tumors, gastro-intestinal stromal tumors (GISTs), plasma cell tumors, leiomyomas, adenomatous polyps, and adenomas (Kehl, 2022; Moulton, 2009; Peter 2005; Roth, 1990; Valli, 2000).
Lymphoma remains the single most frequent type of cancer experienced by cats as well as the most common feline gastric neoplasm (Richter, 2003).
Intestinal lymphoma is classified in low-grade intestinal T-cell lymphoma (LGITL) and high-grade intestinal T-cell lymphoma (HGITL), including an un- controlled proliferation of lymphocytes (Barko, 2023; Mc Lear, 2003; Kiupel, 2011).

Throughout maturation, lymphocytes generate specific antigens receptors by re-modelling the V(D)J sections of T-cell and B-cell receptor genes (TCR ɣ [T-cell receptor gamma gene] and immunoglobulin heavy- chain gene [IGH]), thus making them polyclonal at these genetic loci (Hardy, 1981; Van Dongen, 2003).

In T-cell lymphoproliferative disorders, the neoplastic T-cell population shares the same TCR rearrangement pattern and serves as a marker for monoclonality (Burnet, 1976; Richter, 2003). Lymphomas, on the other hand, are caused by the clonal expansion of an individual progenitor cell, and it has a monoclonal receptor loci (Burnet, 1976; Mazur, 1983; Mosli, 2014). The lymphocyte receptors are oligoclonal or monoclonal in low grade lymphomas in cats (Andrews, 2016; Cheroutre, 2004; Kiselow, 2008).

Another cause of lymphoma in cats is the viral infection, such as the feline leukemia virus infection (FeLV), which causes lymphoid and myeloid tumors in domestic cats (Marsilio, 2023; Maunder, 2016; Moore, 2012; Vail, 1998).

There are two main hypotheses on the origin of variation of tumor cells: different sub-clones originate from different tissue stem cells and have their own transformation pattern (polyclonal concept), or different clones develop from the initial clone due to genetic or epigenetic changes during evolution (monoclonal concept) (Marusyk, 2010).

Monoclonal rearrangements reveal limited intra-tumoral heterogeneity in their beginning stages, which rises with tumor size, in comparison with polyclonal population which has substantial intra-tumoral heterogeneity initially, but become more homogeneous as they grow due to clonal growth (Ibragimova, 2017). In polyclonal rearrangements, the formation of a dominant clone proceeds afterwards followed by a decrease in clonal diversity due to the replacement of minor clones. This clone divergence and the generation of dominant clones with minor clones' substitution may occur concurrently in a tumor (Janiszewska, 2015; McLear, 2003).

Polyclonal lymphocyte population's origin refers to cells that have undergone several modifications in their early stages, which may remain or be removed, representing intra-tumoral heterogeneity. The establishment of a dominant clone occurs later, being followed by a decrease in clonal diversity (Kreso, 2013).

Molecular analysis of monoclonal and polyclonal rearrangements of lymphocytes cells is an important key to diagnose the intestinal lymphoma, because morphologically, the intestinal tumors frequently include a polymorphous cell groups with different sizes (Ibragimova, 2017).

PARR has been created for the diagnosis of lymphoid neoplasia, being characterized by clonal proliferation of tumor cells with a rearranged immunoglobulin heavy chain (IgH) or T cell receptor gamma (TCR ɣ) gene in B-cell and T-cell lymphoid malignancies. It represents a major component of the diagnostic algorithm having the interest to differentiate feline inflammatory bowel disease from intestinal lymphoma, amplifying the T-cell receptor γ, but not having the role to determine the phenotype of lymphocytes involved in the processes (Andrews,2016; Jeffrey, 1993; Roth, 1990). PARR is an efficient and extremely sensitive approach (Holmberg, 1976; Van Dongen, 2003). The lymphocyte lineage determines antigen receptor loci rearrangement, which follows a precise sequence. T cells rearrange the T-cell receptor delta (TCR δ) locus first, followed by the TCR ɣ locus (Montañés, 2019; Valli,1981).

Routine microscopical investigation is a challenge, because of coexistence between lymphoma and inflammatory process or because of the progression of chronic inflammatory enteropathy to low-grade intestinal T-cell lymphoma (Moore, 2012).

MATERIALS AND METHODS

This study has considered 22 cats (Table 1) of different breeds and ages. The age of individual ranged between 9 and 14 years, all cats presenting digestive syndromes featured by recurrent vomiting and diarrhea (n=18). The patients presented also weight loss (n=19), icterus (n=2), pales mucous membranes (n=13), abdominal distension (n=6), and peripheral lymph nodes hypertrophy (n=12). Another clinical change observed as polyphagia was noted (n=3).

The weight of the cats included in this study was between 3,2 kg and 5,6 kg.
Abdominal ultra-sound has been used for all patients. Aditionally, blood complementary tests, ELISA for FeLV and FIV diagnosis, serum cobalamin test, cytopathological and histopathological exams, PCR for antigen receptor rearrangement (PARR), DNA extraction, genomic analysis, immunohistochemistry for CD3 T-cell expression, and clonality assessments have been applied.
The abdominal ultrasound examination was performed in all 22 cases, and the standardized images were realized with a linear transducer with high frequency (15 MHz).
Standard necropsy has been done in dead or euthanized animals (n=7) followed by gross examination and by tissue sampling for microscopical investigations. The mesenteric lymph-nodes and intestinal segments were sampled and fixed in 10% neutral buffered formalin for 48 hours. Sections of 4 μm thickness were stained with Hematoxylin and Eosin (HE stain).
Cytological examination was significant in association with histological examinations, distinguishing the lymphoma from inflammatory process. Fine needle aspiration and full thickness intestinal biopsies have been sampled from living animals (n=12) of intestine (duodenal, ileal or jejunal mucosa) and mesenteric lymph nodes. Surgical resection of the jejunum and mass with 5 cm margins and an end-to-end anastomosis were performed (n=3). After smear preparation, the slides were air-dried and dyed with Diff-Quick staining protocol.
Histopathological investigations have been used for both categories of samples (intestinal segments and mesenteric lymph nodes), as well as for the intestinal loops removed by enterectomy, using a routine protocol of staining and examination, with hematoxylin and eosin staining for histological sections imbedded in paraffin. Following necropsy, surgical resections, the intestinal and mesenteric lymph-nodes components were frozen at -20°C in small containers with formal saline CH_2O:NaCl (10:0.9)%, before realizing PARR, histopathological and immunohistochemistry examinations, and before the treatment administration.
PARR test was used for the definitive diagnosis of T-cell lymphoma, with the interest to differentiate lymphoma from non-lymphoma lesions, in all of 22 patients, in concordance with primer sets, and TCR γ.
The interest to use the two methods in PARR evaluation was to develop a classification algorithm to distinguish proteomic signatures of lymphocytic-plasmacytic inflammatory lesions in intestinal lymphoma in cats. Therefore, PARR was based on the distinction of monoclonal lymphomas from polyclonal benign or reactive tissues (Andrews, 2016; Rychlick, 2007).
The examination of ePARR on FFPE samples was realized before and after applying DNA QC method, the FFPE method being significantly faster and more efficient, using the technique analysis performed with microcapillary electrophoresis (Pareek, 2011).
For FFPE method in PARR analyze, the samples of 4 μm thickness were dissected and prepared in 10% neutral buffered formalin, being maintained 70 hours. The final samples were placed in pure toluene, and after in a mixed solution with 50% toluene and 50% paraffin for one hour. In PARR evaluation, the flow cytometry pellets method was used for all 22 cases, to analyze and differentiate the tumoral cells and the smears passing through one or more lasers while suspended in PBS solution, utilizing cell sorter that purified and identified the lymphocyte population which are tumoral, and after, it neutralized these lymphocytes into isotonic saline liquid containing 10% bovine serum. The final preparation with suspended cells was combined with 20 μL of antibody solution, allowing quick quantitative and qualitative expression of lymphocyte population.

CD3 immunophenotyping analysis

The methodology of immunostaining was used to identify the immune-phenotype T, the morphology of T-cells, and to make the difference between this immune-phenotype (T) and from B-cells, this test being applied in all 22 cases. To perform immunophenotyping of CD3 expression, on tissues simples, 5 μm sections from FFPE preparation tissues simples were cut and immune-stained with antibodies that recognize the CD3 antigen stain T cells.

Clonality assessment

The examination of ePARR on FFPE samples was realized before and after applying DNA QC method. Every tissue sample was homogenized, and DNA was extracted following the manufacturer's instructions of QIAamp DNA Mini Kits. T cell clonality was determined by PCR in all 22 cases. Each sample with a polyclonal or oligoclonal population of T cells was tested for B cell clonality using PCR.

To confirm the specificity and reliability (monoclonality, oligoclonality, polyclonality) of the all 22 samples, the PCR reactions from all of these were visualized applying electrophoresis method analysis, and the primer sets tests were used. The PCR products have been separated according to melting rather than the differences between N sequences at the V-J joining, resulting in a very accurate genetic imprint for each TCR-V rearranged allele. Genomic DNA was obtained using the DNA FFPE kit in conformity with the manufacturer's instructions. The quality, quantity, and efficiency of extracted DNA were determined using the extraction of genomic DNA from the lymph-node biopsy samples, frozen pellet cohort, Diff-Quik stained FNA imprints, according to the DNA mini Kit instructions.

The primers from PCR reactions have been analyzed with DNA protocol, after DNA amplification using PARR primers in parallel. The primers from 1 to 10 have been optimized, and fluorescently marked using an identification for alignment to the feline IGH and TRG genomic parts.

To assess sample DNA quality, control primer sets Cμ and γ-actin were applied.

Table 1. Sampling methods in the 22 patients

Breed	Number	Gender	Sampling methods
European Cats	7	Sterilized females	Intestinal biopsies
	3	Sterilized males	Intestinal biopsies
Siberian Cats	2	Sterilized females	Intestinal biopsies
European Cats	3	Sterilized males	Surgical resection
European Cats	5	Sterilized males	Necropsy
	2	Sterilized females	Necropsy

RESULTS

The integration of clinical signs, complementary blood exams, abdominal ultrasound examination, gross evaluations, cytological and histopathological investigations, PARR test, Immunohistochemistry, and clonality assessment data were necessary at multiple stages to distinguish tumoral process from the inflamematory process, being important to minimizing misdiagnoses.

A completed blood count test revealed an average approximative as: a-regenerative anemia (Htc = 20%) in 2/22 cats, regenerative anemia in 4/22 patients, hyperglobulinemia in 2/22 cats, neutrophilia 19.000/μL (reference ranges 10.000-30.000/μL), eosinophilia 2.270/μL (reference ranges 0.170-1.570/μL), monocytosis 10.270/μL (reference ranges 0.050-0.670/ μL), a lymphocytosis was revealed in 13/22 cats, and a thrombocytopenia in 4/22 cats. A serum biochemical profile revealed hypoalbuminemia (2.0 g/dl; reference ranges, 2.7-3.8 g/dl) due to chronical diarrhea, hyperglobulinemia (5.9 g/dl; reference ranges, 2.8-5.1 g/dl) all of these in 16/22 cats, and increased values of hepatic enzymes ALAT (220U/L, 10-130 U/L reference ranges) and PAL (440, 24-147 U/L reference ranges) and a hypercalcemia (7 mg/dL, 4.5-5.3 mg/dL reference ranges) in 6 of 22 patients. ELISA test for feline leukemia virus and feline immunodeficiency virus was tested in all of 22 patients and it presented negative results.

The echography examinations revealed in 10/22, thickening of the ileum and jejunal wall, and 12/22 reduction of luminal diameter of jejunum, 17/22 increased lymph nodes, 3/22 and gastric ulcerations, all of these being associated with clinical signs of gastro-intestinal disorders. In 2/22 patients, at the echography examination no modification at gastro-intestinal tract was observed.

Group I was represented by 11 of 22 cats diagnosed with IBD, whereas Group II is represented by 11 cats diagnosed with intestinal T-cell lymphoma. In Group II, 4 out of 11 patients were identified with HGITL, while 7 had been identified with LGITL.

Macroscopic alterations were observed during enterectomy surgery in duodenum, jejunum and ileonum in 5 cats from Group I and in another 7

from Group II, indicating a diffuse wall thickness of the intestinal tract, and an extended reddened fold in 3 out of Group I and in 7 out of Group II (LGITL) (Figure 2, Table 2).

The sizes of the jejunal lymph nodes were varied in cats diagnosed with LGITL (between 3.5 and 5.5 cm length, 0.3-4.8 cm length reference ranges and between 1-2.5 cm width, width reference ranges 0.2-1.0 cm width reference ranges), whereas the mesenteric lymph nodes were clearly enlarged (3 cm length, 0.1-2.0 cm length reference ranges, and 0.6 cm width, 0.1-1.0 cm width reference ranges) in 3 out of 4 cats with HGITL and in 3 out of 7 LGITL (Figure 3, Table 2).

During the necropsy, the evident lesions were severe with multifocal ulcerations of ileum (n=9 of Group II), of jejunum and duodenum (n=3), and nodular ulcerative masses and plaques were identified in duodenum and jejunum in 7 patients out 11 of Group II, having multifocal lesions aspects, spreading to mesenteric lymph-nodes, and determined multiple intestinal perforations (Figure 4, Table 2). The adjacent digestive mucosa reduced due to loss of mucosal folds. Among the 7 out of 11 patients diagnosed with LGITL, 5 had infiltration in the jejunum only, 3 had infiltration in the two areas of jejunum and the ileum, and 1 had infiltration just in the ileum.

In the necropsies, it was observed that in some cases of fibrinous peritonitis, the chronicity of the lesion with the formation of adhesions was found (n=3 HGITL).

Multiple malignant tumors were identified in the intestines (duodenum, jejunum), kidneys, urinary bladder, and lungs (n=4 HGITL), splenomegaly and hepatomegaly being remarked in lymphomas patients (Group II). In 4 out 11 lymphoma patients, the livers had a pale and a friable gross structure.

In HGITL cases, it was observed a necrotic tissue in jejunal wall, with an irregular surface, bowel ischemia in 3 out 4 cases. In 2 out of 4 HGITL patients, fusiform intramural jejunal and ileal lesions developed outward while the invaded muscle atrophied. All relevant described macroscopic lesions are illustrated in Table 2, including the localization of gastrointestinal segments.

Table 2. Macroscopic features of IBD and gastrointestinal lymphoma

Diagnosisis	Localization	Gross lesions
IBD	Duodenum Jejunum	thickened wall reddened folds
LGITL	Jejunum-Duodenum	thickened wall, small exophytic growth
	Mesenteric lymphnodes	enlarged mesenteric lymp-node
HGITL	Jejunum-ileum	adenopathy, ulcerating nodules, fusiform intramural lesion, bowel ischemia
	Mesenteric lymph-nodes	adenopathy, necrotic tissue plaques

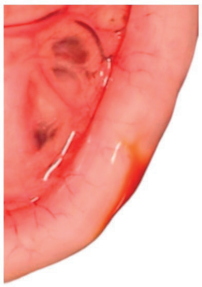

Figure 1. Enlarged intestinal segment

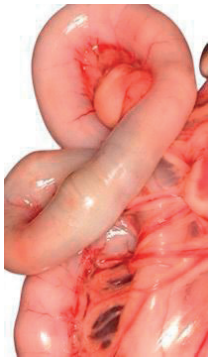

Figure 2. Enlarged small intestinal loops region in a 9 years old cat

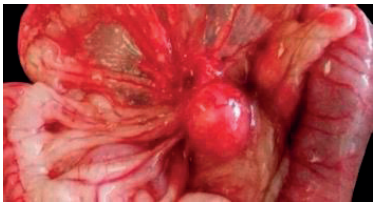

Figure 3. Enlarged mesenteric lymph node (central)

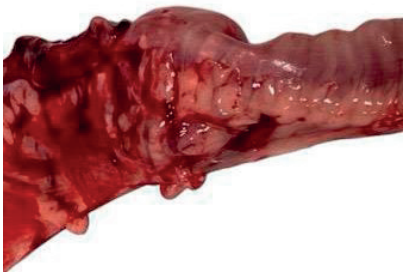

Figure 4. Massive enlarged and ulcerative jejunum mass

In all 22 cases, the cytologic diagnosis was in accordance with the gross and histopathologic examinations. Chronic enteritis was present in 11/22 cases, representing Group I, 6 patients of Group I were diagnosed with lymphocytic plasmacytic enteritis (LPE), while the rest of 5 cases of Group I had eosinophilic enteritis.

The grading system for the degree of inflammatory process was based on lymphocyte population sizes, presence of inflammatory cells, as follows, these being indicator for transition from inflammatory process to intestinal lymphoma lesions: mild inflammation had a few lymphocytes, the moderate inflammation which consisted in nests lymphocytes, and severe inflammation represented by the presence of small lymphocytes, in comparison with neutrophil size or with large lymphocytes (Table 3).

LPE was detected in 6/11 IBD cases and it was characterized by a moderate lymphocytic presence. Eosinophilic enteritis (EE), identified in 5/11 IBD cases, was characterized by a mild lymphocyte identification including eosinophils higher than 5 cells per 400x field. The mild inflammation comprised a few lymphocytes cells with numbered from 0 to 4 cells per 400x field, whereas the moderate inflammatory process consisted on a population of 5 to 20 lymphocytes per 400x field. The severe lesions included more than 20 lymphocytes per 400 × field. Low grade intestinal lymphoma was suspected in the sample which had homogenous and monomorphic population of small-medium-sized mature lymphocytes (Figure 5), an eccentric nucleus being noticed and representative in 7/11 cases, diagnosed with LGITL. The chromatin of the nucleus is less condensed that in the chromatin of mature lymphocytes. The nucleoli are indistinct or are missing. A moderately basophilic cytoplasm with several optically empty vacuoles, that extended to the nucleus regions were noticed. A small population of eosinophils was seen, and a few cells included fine azurophilic cytoplasmic granulations in small number, similar to chromaffin cells or potentially poorly granular mast cells (Figure 7). High-grade intestinal lymphoma was characterized by more than 30% homogenous cellular lymphocyte population. The population of medium to large round cells, well individualized, with a high nucleocytoplasmic ratio allowed lymphoid cells to be recognized, with spherical nucleus (Figure 6). This population is monomorphic, despite varied blast sizes and the presence of nucleolus, and the process was associated with neoplastic lesions, as identified in Figure 6. The lymphocyte's nuclei contained a fine stippled chromatin, with one or more small to medium-sized, spherical nucleoli, and a lightly reduced and basophilic cytoplasm, with azurophilic granulations, which indicated a raised fragility, and it was remarked at examination with magnification x1000.

Table 3. Cytological modifications in IBD, LGITL, HGITL

Diagnosis	Cytological modifications
IBD	LPE: -moderate lymphocyte infiltration; absence of eosinophils or mast cells EE: moderate lymphocyte infiltration; presence of eosinophils or mast cells
LGITL	-homogenous and monomorphic population -small matures lymphocytes -small-medium sized round and eccentric nucleus -less condensed chromatin - absent or distinct nucleoli -moderate basophilic cytoplasm
HGITL	-lymphocytic population -intermediate-large lymphocytes -medium-sized, round, irregular nuclei -multiple small-medium sized proeminant nucleoli -lightly to high basophilic cytoplasm

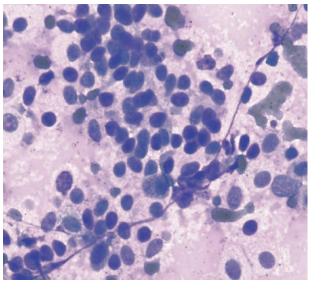

Figure 5. Small lymphocyte population (Diff-Quick staining, x1000)

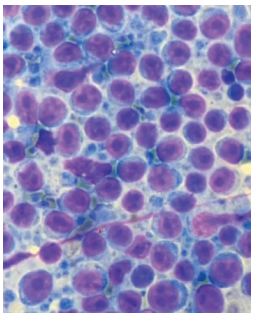

Figure 6. Population of granular lymphocytes, with anysokorya, giant nuclei, basophilic cytoplasm, and sometimes clear areas near the nucleus (May, Grünwald, Giemsa; X1000)

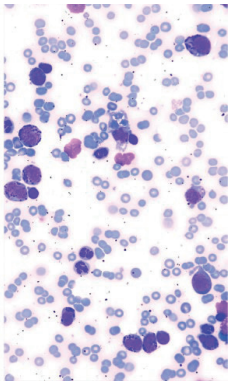

Figure 7. Ileum cells with azurophilic cytoplasmic granulations (Diff-Quick staining, x1000)

Histological examination of duodenal, jejunal, and ileal segments established a diagnosis of inflammatory bowel disease, low-grade or high-grade intestinal lymphomas, in correlation with cytologic and macroscopic analysis and findings for all patients. LPE was identified in the duodenal and jejunal samples, represented by non-neoplastic population of lymphocytes, being framed as mild in one cat, moderate in four cats, and severe in one cat. In the mild lesions of LPE, the histology structure of intestines was not modified. In the cases with moderate lesions, a marked and diffuse to severe focal agglomeration of lymphocytes was observed, with an unchanged histological structure of intestine. Eosinophilic enteritis was identified as with mild infiltration of eosinophils and dominant lymphocytic population. Some transmural eosinophilic infiltrates and muscle hypertrophy were detected in jejunum and ileum segments.

Low-grade intestinal lymphoma was marked by infiltration of small lymphoid T-cells population in the jejunal and ileal segments (Figure 8). In LGITL samples, the cellular group is represented by small T-cells groups arranged in plates, localized inside the villous epithelium. The regions revealed significant lymphocytic cryptis (6 out 7 LGITL) and neutrophilic cryptis in 5 out 7 LGITL patients. Villous atrophy was identified in all 7 LGITL patients. A discrete reactive follicular hyperplasia was noticed, and no invasion of the lymph-node parenchyma or peripheral tissue was observed.

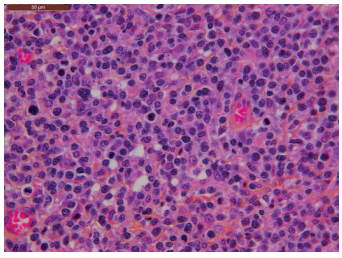

Figure 8. Duodeno-jejunal segment- Diffuse infiltrate with tumoral lymphocytes (Hematoxylin and Eosin staining, x300)

Specific to high-grade intestinal lymphoma were transmural lesions, which affected tunica muscularis along with severe perivascular lymphocytic infiltration, involving tunica muscularis and spreading into the serosa (Figure 10). High-grade intestinal lymphoma had determined the severe mucosal alterations, including blunt villi, and crypt effacement (Figure 10). In 3 out 4 HGITL patients, the lymphoid infiltrates comprised large lymphocytes, in the remaining case, the infiltrate was composed of small to intermediate-sized lymphocytes (Figure 9).

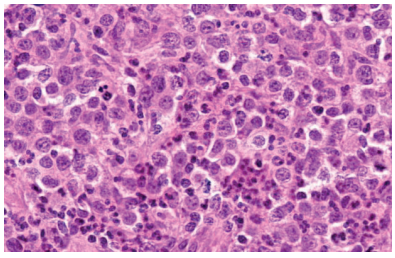

Figure 9. Infiltration with small-intermediate sized lymphocytes (Hematoxylin and Eosin staining, x300)

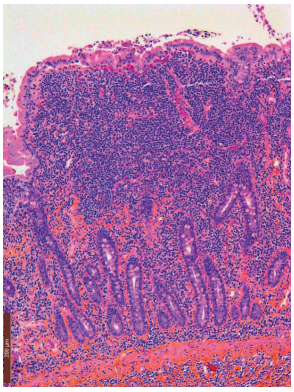

Figure 10. High grade intestinal invasive lymphoma-jejunal and ileal segments (Hematoxylin and Eosin staining, x200)

The PARR test was performed to identify T-cell lymphoma versus non-lymphoma, by monoclonal properties of T-cells population. Table 4 and Figure 11 summarized the PARR performance (sensitivity, specificity, and accuracy) in all 22 cases, in concordance with QC, and DNA extraction. Each DNA sample was amplified using various PARR primers simultaneously, however only QC (quality control) pass resulted in a high percentage of accuracy: in FFPE method, 100% ePARR negative in all 11 IBD cases, 100% ePARR positive in 11 lymphomas out 22. In Flow cytometry pellets method, the accuracy was calculated at 81% e-PARR negative in 9/11 IBD, and 90%-ePARR positive in 10/11 lymphomas. DNA for FFPE method was optim for PARR accuracy evaluation, having a high quality. The polymerase chain reaction for antigen receptor rearrangement (PARR) for the T-cell CD3 region of the TCRγ, utilized in all 22 cases, had as results 11 out 22, diagnosed with inflammatory bowel disease classified in Group I and 11 out 22 cases with intestinal lymphoma, comprised in Group II.

PCR test was performed in all 22 samples. In 11 out 22 samples, the PCR for B-cells identified polyclonal population, the presence of B-cells being significative. The final diagnosis was non-neoplastic lesions. For the rest of 11 cases, the PCR for the B-cells was negative, while the T-cells were dominant. Of 11 samples with monoclonal T-cell population, one sample had the dual clonality for T and B-cells, influenced by a polyclonal background, but the final diagnosis was given as T-cell intestinal lymphoma, being based on correlation with immunohistochemistry (CD3) and on primer sets peak's tests.

By DNA extraction, the values of each sample were ranged from 1 (degraded DNA) to 10 (intact DNA), the results from primer sets 1-10, in combination with Qc and Cμ revealed 11 out 22 samples scored with rang 10, represented by T-cell primer sets, being diagnosed with T-cell lymphoma. The rest of 11 revealed less than rang 3 of DNA input. The presence of B-cells was identified in 2 out 11 (non-lymphomas samples) graded with rang 3 and 2 of DNA. The recombination of genes identified that in 11 out 22 cases, the lymphoma processes provided between V and J genes.

The clonal primer sets improved the diagnosis in concordance with TRG genomic regions. TRGγ primers determined higher monoclonal peaks (1-10) in 11 out 22 cases, the final result being scored as lymphoma lesions. The polyclonal rearrangements had the patterns of Ig genes and TRGγ genes in 11 out 22 cases, being considered as non-lymphoma processes.

In the 11 lymphoma samples, the primer of sequences the both V and J primers for TRGγ genes, which influenced the sensibility and accuracy for this final diagnosis.

The monoclonal rearrangements were represented in 11 out 22 samples by a bigger size band in width with 1 or 2 evident sharp bands with the same size, in comparison with polyclonal populations, the test being realized with electropherograms method. The polyclonal samples had one or multiple small size in width bands with a normal distribution in electropherogram test, with clearer size regions, in the rest of 11 samples, non-lymphoma lesions. In one out 22 cases, the electrophoresis method assessment has shown a monoclonal sample with taller and bigger size band in width, having a few polyclonal peaks localized basal, with variable sizes, representing oligoclonality.

The primer sets from 1 to10 were analyzed with implemented QC method based on adequate input DNA, having a final result 10 out 22 T-cell specific primer sets, and 11 out 22 polyclonal primer sets, while 1 out 11 lymphomas presented T-cell primer sets on a polyclonal background, with 1 to 3 peaks.

The primer sets from 11-14 checked in concordance with γ-actin method revealed 11 T-cell intestinal lymphoma out 22 samples.
The CD3 exam matched with IgH and TCR γ, identifying the antigen region of T-cell receptor in 11 out 22 samples containing the T-cell receptor sequence. The lymphoma cells were positive for cytoplasmic CD3 (Figure 12), with medium sized atypical lymphocytes.

Table 4. PARR performances

Methods control primer/ Diagnostic	IBD	Lymphomas
DNA QC pass - FFPE	Sensitivity:100%- ePARR negative in 11/11 IBD Specificity: 100%- ePARR negative in 11/11 IBD Accuracy: 100%- ePARR negative in 11/11 IBD	Sensitivity:100%- ePARR positive in 11/11 lymphomas Specificity: 100%- ePARR positive in 11/11 lymphomas Accuracy: 100%- ePARR positive in 11/11 lymphomas
DNA QC pass- Flow cytometry pellets	Sensitivity: 90%- ePARR negative -in 10/11 IBD Specificity: 81%- ePARR negative -in 9/11 IBD Accuracy: 81%- ePARR negative in 9/11 IBD	Sensitivity: 90%- ePARR positive in 10/11 lymphomas Specificity: 81%- ePARR positive in 9/11 lymphomas Accuracy:90%- ePARR positive in 10/11 lymphomas

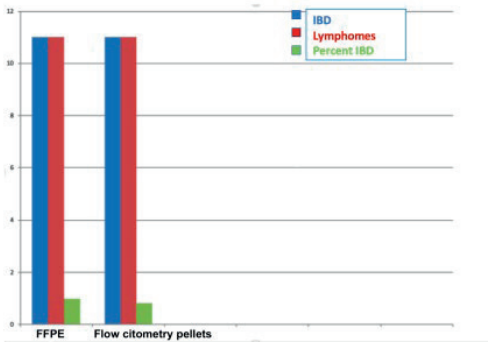

Figure 11. Accuracy of ePARR assay with FFPE and Flow cytometry methods

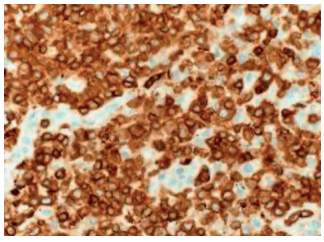

Figure 12. CD3 cytoplasmic positivity for T-cell lymphoma (x300)

DISCUSSIONS

The present study showed that the correlation between clinical, cytological, histological, macroscopically and complementary examinations as PARR test and clonality evaluation, in correlation estimate diagnosis, prognosis, and therapy in IBD and intestinal lymphoma in felines.
Previous studies have indicated that thickening of the small intestine in felines is a significant indicator for distinguishing inflammatory bowel disease and lymphoplasmacytic gastrointestinal inflammation from high-grade intestinal lymphoma (Freiche, 2021). In our study, the difference of thickness of different intestinal segments was significative and representative for IBD, LGITL and HGITL. Researches in the main pathogen causes related to IBD and feline intestinal lymphoma permit greater comprehension of the same illness in humans, showing diagnostic and prognostic indicators (Paulin, 2018).
Increased clonality analysis in human medicine developed from expanding the variety of targeted loci to include TRβ, TRδ, TRγ among others, to compensate for the reduced sensitivity of individual analyses. In veterinary medicine, assays for different objectives have not been used and described for the moment in many studies. The standardization of clonality testing across institutions was a significant advancement in human medicine. Current researches in veterinary medicine demonstrated that LPE processes are often polyclonal, while LGITL patients with percent bigger than 90 illustrated clonal or oligoclonal TCRγ gene rearrangement (Moore, P., F., 2005, Keller, 2016). In our study, the clonality analysis was used in all 22 patients, within 11/22 showing polyclonal rearrangement and the rest of 11/22 monoclonal rearrangement, but just one has shown oligoclonal arrangement.
Polymerase chain reaction for receptor antigen rearrangement is currently the only one technique that can be applied to FFPE tissue samples, and thus it is the most often conducted procedure for cats with enteritis.

CONCLUSIONS

The PARR test is an important method for a definitive diagnosis of monoclonal lymphomas in intestinal neoplasms in cats, versus polyclonal benign or reactive tissues and it revealed in 11/22 the presence of monoclonal rearrangement of the T-cell ɣ receptor gene.
A successful amplification of a control primer quality was observed in FFPE method, having 100% accuracy in diagnosis of lymphomas.
The jejunum and ileum were the most frequently affected regions in all cases of study.
The predominant intestinal cells in 11/22 cases are represented by T-cells, being compatible with Type II Enteropathy in cats.
This article reinforces the importance of PARR laboratory method to accurately diagnose the intestinal lymphoma.
The improvements in immunohistochemical and clonality examinations have increased our therapeutic and results assurance, after a closer diagnosis, as follows: 10/11 of Group I were completely healed after a variable period of treatment, and 3/11 of Group responded to chemotherapic treatment.

REFERENCES

Andrews, C., Operacz, M., Maes, R., &. Kiupel, M. (2016). Cross lineage rearrangement in feline enteropathy-associated T-cell lymphoma.*Veterinary Pathology*, 53,559-562.

Barko, P.C., Williams, D.A., Wu, Y.A., Steiner, J.M., Suchodolski, J.S., Gal, A., & Marsilio, S. (2023). Chronic Inflammatory Enteropathy and Low-Grade Intestinal T-Cell Lymphoma Are Associated with Altered Microbial Tryptophan Catabolism in Cats. *Animals (Basel),* 14(1), 67.

Burnet, F.M. (1976). A modification of Jerne's theory of antibody production using the concept of clonal selection. *Australian Journal of Forensic Sciences*, 26(2), 119-21

Cheroutre, H., & Madakamutil, L. (2004). Acquired and natural memory T cells join forces at the mucosal front line. *Nature Reviews Immunology*, 4(4), 290–300.

Freiche, V., Paulin, V., M., et al. (2021) Histopathologic, phenotypic, and molecular criteria to discriminate low-grade intestinal T-cell lymphoma in cats from lymphoplasmacytic enteritis; *Journal of Veterinary Internal Medicine,* 35(6), 2673-2684.

Hardy, W. (1981). Hematopoietic tumors of cats. *c*,17,921-940.

Holmberg, C.A., Manning, J.S., & Osburn, B.I. (1976). Feline malignant lymphomas: Comparison of morphologic and immunologic characteristics. *American Journal of Veterinary Research*, 37, 1455-1460.

Ibragimova, M., K., Tysganov, M., M., Litviakow, N., T. (2017). Natural and chemotherapy-Induced clonal evolution tumors. *Biochemestry Moscow*, 82(4), 413-425.

Janiszewska, M., Polyak, K. (2015) Clonal evolution in cancer: a tale of twisted twines, *Cell Stem Cell*, 16, 11-12.

Jeffrey, S. D.; Kruger, J. M., Mullaney, T. P. (1993). Lymphocytic/plasmacytic colitis in cats: 14 cases, *Journal of the American Animal Hospital Association,* 202(2), 313-8.

Kehl, A., Torner, K., Jordan, A., Lorenz, M., Schwittlick, U., Conrad, D., Steiger, K, Schusser, B., & Auperte-Lemmbach, H. (2022). Pathological findings in gastrointestinal neoplasms and polyps in 860 cats and a pilot study on miRNA analyses. *Veterinary Science*, 9(9), 477.

Keller, S.M.; Vernau, W., & Moore, P.F. (2016). Clonality Testing in Veterinary Medicine: A Review with Diagnostic Guidelines. *Veterinary Pathology*, 53(4), 711-25.

Kiupel, M., Smedley, R. C., Pfent, C., Xie Y., Xue, Y., Wise, A. G., DeVaul, J.M., & Maes, R.K. (2011). Diagnostic algorithm to differenciate Lymphoma from inflammation in feline small intestinal biopsy samples. *Veterinary Pathology*, 48(1), 212-222.

Kiselow, M.A., Rassnick, K.M., McDonough, S.P.,Goldstein, R.E., Simpson, K.W., & Weinkle, T.K. (2008). Outcome of cats with low- grade lymphocytic lymphoma: 41 cases. (1995–2005). *Journal of the American Animal Hospital Association*, 232(3), 405–10.

Kreso, A., O'brien, C. A., van Galen, P., Gan, O. I., Notta, F., Brown, A. M., Ng, K., Ma, J., Wienholds, E., Dunant, C. (2013). Variable clonal repopulation dynamics influence chemotherapy response in colorectal cancer, *Science.* 339, 543-548.

Marsilio, S., Freiche, V., Johnson, E., et al. (2023). ACVIM consensus statement guidelines on diagnosing and distinguishing low-grade neoplastic from inflammatory lymphocytic chronic enteropathies in cats. *Journal of Veterinary Internal Medicine*, 37(3), 794-816.

Maunder, C. L., Reynolds, Z. F., Peacock, L., Hall, E. J., Day, M. J., & Cogan T. A. (2016). Campylobacter species and neutrophilic inflammatory bowel disease in cats. *Journal of Veterinary Internal Medicine,* 30(4), 996- 1001.

Marusyk, A., Polyak, K. (2010) Tumor heterogeneity: causes and consequences, *Biochim. Biophys. Acta*, 1805, 105-117.

Mazur, M.T., & Clark, H.B. (1983). Gastric stromal tumors. Reappraisal of histogenesis. *The American Journal of Surgical Pathology*, 7(6),507–519.

McLear, R.C., Drobatz, K.J., & Sorenmo, K.U. (2003). Feline epitheliotropic intestinal malignant lymphoma: 10 cases (1997-2000). *Journal of Veterinary Internal Medicine*, 17(3), 326–31.

Moore, P.F., Rodriguez-Bertos, A., & Kass, P.H. (2012). Feline gastrointestinal lymphoma: mucosal

architecture, immunophenotype, and molecular clonality. *Veterinary Pathology*, 49(4), 658–68.

Moore, P., F., Woo, J., C., Vernau W, et al. (2005). Characterization of feline T cell receptor gamma (TCRG) variable region genes for the molecular diagnosis of feline intestinal T cell lymphoma. *Veterinary Immunology and Immunopathology Journal,* 106, 167-178.

Moulton, J.E., & Harvey, J.W. (2009). Tumors of the lymphoid and hemato- poietic tissues. *Withrow& MacEwen's Small Animal Clinical Oncology*, 699-784.

Montañés, A., Vila X., Roura L., Santos A., Canturri J., Verdés L., Martín C., Díaz-Bertrana A., & Lloret. (2019). Gastrointestinal stromal tumors (GIST): retrospective study of 6 dogs. *AVEPA,* 39 (3), 155-161.

Mosli, M., Bhandari, A., Nelson, S. A., D'Haens, G.,Eagan, B. G., Baker, A. K., Sandborn, W. S., Zou, G.Y., MacDonald, J.K., & Levesque, B.G. (2014). Histologic scoring indices for evaluation of disease activity in ulcerative colitis. *Cochrane Database of systematic reviews*, 25; 5(5).

Paulin, V., M., Couronnée L., et al. (2018). Feline low-grade alimentary lymphoma: an emerging entity and a potential animal model for human disease. *BMC Veterinary Research,* 14-306.

Pareek C.S., Smoczynski R., Tretyn A. (2011). Sequencing technologies and genome sequencing. *Journal of applied. Genetics*, 52: 413–435.

Peter F., Moore, Jennifer C. Woo, William Vernau, Sandra Kosten, & Petra S Graham. (2005). Characterization of feline T cell receptor gamma (TCRG) variable region genes for the molecular diagnosis of feline intestinal T cell lymphoma. *Veterinary Immunology and Immunopathology Journal*, 106(3-4), 167-78.

Richter, K.P. (2003). Feline gastro intestinal lymphoma. *Veterinary Clinics of North America: Small Animal Practice,* 33(5), 1083-1098.

Roth, L., Leib M.S., & Davenport, D.J. (1990). Comparisons between endoscopic and histologic evaluation of the gastrointestinal tract in dogs and cats: 75 cases (1984-1987). *Journal of American Veterinary Medicine Association*, 196(4), 635-638.

Rychlick, A., Nishacka, R., Kander, M., Depta, A., Nowicki, M., & Santi, K. (2007). Usefulness of endoscopic examination for the diagnosis of inflammatory bowel disease in the dog. *Polish Journal of Veterinary Sciences*, 10(2), 113-118.

Vail, D.M., Moore, A.S., Ogilvie, G.K., & Volk, L.M. (1998). Feline lymphoma (145 cases): proliferation indices, cluster of differentiation 3 immunoreactivity, and their association with prognosis in 90 cats. *Journal of Veterinary Internal Medicine*, 12(5), 349–54.

Valli, V.E., McSherry, B.J., & Dunham, B.M. (1981). Histocytology of Lymphoid tumors in the dog, cat, and cow. *Veterinary Pathology*, 18(4), 494- 512.

Valli, V.E., Jacobs, R.M., Norris, A., Couto, C.G.,& Morrison, W.B. (2000). The histologic classification of 602 cases of feline lympho- proliferative disease using the National Cancer Institute working formulation. *Journal Veterinary Diagnostic Investigation*, 12(4), 295–306.

Van Dongen, J.J., Langerak, A.W., & Bruggemann, M., et al. (2003). Design and standardization of PCR primers and protocols for detection of clonal immunoglobulin and T-cell receptor gene recombinations in suspect lymphoproliferations: report of the BIOMED-2 concerted action BMH4-CT98-3936. *Leukemia Journal*, 17(12), 2257-317.

Scientific Works. Series C. Veterinary Medicine. Vol. LXX (2), 2024
ISSN 2065-1295; ISSN 2343-9394 (CD-ROM); ISSN 2067-3663 (Online); ISSN-L 2065-1295

REMOTE CHEMICAL IMMOBILIZATION AND ANESTHESIA FOR ORCHIDECTOMY IN A PLAINS ZEBRA (*Equus quagga*)

Ioana ENE[1], Ovidiu ROȘU[2], Mario CODREANU[1]

[1]University of Agronomic Sciences and Veterinary Medicine of Bucharest,
59 Marasti Blvd, District 1, Bucharest, Romania
[2] ARCA Association - Animal Rescue and Care, 61-63 Ion Ionescu de la Brad Blvd,
District 1, Bucharest, Romania

Corresponding author email: ene.m.ioana@gmail.com

Abstract

This case study evaluates the remote chemical immobilization protocol for a reproductive surgical procedure of a free-ranging male Plains Zebra (Equus Quagga), 11 years old, 400 kg body weight. The zebra was darted twice in the gluteal muscles (first from a distance of 30 meters, succeeded after 25 minutes by the second dart, from 15 meters), as the first dart was not fully discharged. Each syringe contained a 5 ml total volume of the combination: 1000 mg Ketamine, 50 mg Medetomidine, 10 mg Butorphanol, and 5 mg Midazolam. The induction time calculated from the last dart until the animal gained lateral recumbency was 8 minutes. A bilateral locoregional intratesticular block was performed using a total dose of 2mg/kg Lidocaine. The maintenance phase lasted 54 minutes ensuring optimal anesthesia and analgesia, necessary for the procedure. Atipamezole 0,15mg/kg was used for antagonization, intravenously and was effective in 1 minute. The patient was classified with a final recovery score of 1 and assisted into a standing position, presenting stable coordination and reduced ataxia. During anesthesia clinical monitoring was continuous, without any complications recorded.

Key words*: zebra, chemical, immobilization, Ketamine, Medetomidine.*

INTRODUCTION

The plains zebras that roam throughout much of sub-Saharan Africa's savannah are known for their unique physical traits. Zebras are specialized grazers and require regular access to water and grass (Landman & Kerley, 2001).

This study aims to evaluate the remote chemical immobilization, monitorization, and recovery protocol for a free-ranging male Plains Zebra (*Equus quagga*), from Africa. Immobilization of feral free-roaming animals can be complicated and many immobilization methods have been described over the years.

Butorphanol-Azaperone-Medetomidine (BAM) immobilization is the most commonly used in zebras (Stemmet et al., 2018), as an adaptation from horses (Balko et al., 2022), and as an alternative to Etorphine-Azaperone (EA) (Stemmet, 2018). The main change in physiological parameters with the EA protocol is related to oxygen metabolization, as severe hypoxia or hypoxemia may occur, as well as a prolonged recovery time (Stemmet, 2018).

Another alternative to EA, also described in zebras, is the Ketamine-Butoprhanol-Medetomidine (KBM) method (Stemmet et al., 2019). The KBM method may reduce the severe hypoxemia produced by EA and balance the severity of hypoxemia, as well as the mean time of ataxia and recovery (Stemmet et al., 2019). Even if the recovery time was longer with KBM, immobilization was done effectively in boma-habituated zebras (Stemmet et al., 2019).

Pre-immobilization evaluation can be a visual assessment of each animal's behavior. As a part of evolutionary factors associated with long-term hunting by humans, a reaction in behavior was studied, comparing the occurrence or non-occurrence of habituation in feral horses *(Equus caballus ferus)* and Plains Zebras *(Equus quagga)*, with the help of Flight Initiation Distances (FID), which was analyzed for 87 equids and resulted in a bigger value in zebras, which suggests that approaching free-roaming zebras may be more difficult than approaching free-roaming horses (Brubaker & Coss, 2015).

Chasing equids can also affect muscle cells, and capture myopathy can occur in free-roaming zebras (Paterson, 2014) that are darted, with clinical signs such as cardiac dysfunction and dyspnea (Breed et al., 2019).

Reproduction control in a free-ranging equid population (King et al., 2022), indicates that no difference in body condition or mortality was found after the orchiectomy, and geldings continued to exhibit the same behaviors as before the orchiectomy, even maintaining similar levels of aggression and still protecting the harem from which they come from.

MATERIALS AND METHODS

The authors propose an alternative combination for the KBM method in immobilizing free-roaming feral zebras, adding the benzodiazepine Midazolam. For remote chemical immobilization, a combination of Ketamine (Ketamine dry powder 2 g, Kyron Laboratories, Johannesburg, South Africa), diluted with Medetomidine (Medetomidine 20 mg/ml, 20 ml vial Kyron Laboratories, Johannesburg, South Africa), Butorphanol (DOLOREX® 10 mg/ml, Merck Animal Health, Germany) and Midazolam (Midazolam 5 mg/ml, 2 ml vial, PFIZER INC., NY) was utilized and referred to as the KBMM method. The substances were delivered with a compressed air tranquilizer dart-gun Pneu-Dart® X-Caliber using a single disposable 5 ml Pneu-Dart® Remote Delivery Device (RDD) Type U. The formula used for calculating the combination (available for two RDDs) was Ketamine dry powder 2000 mg mixed with 100 mg Medetomidine, 20 mg Butorphanol, and 10 mg Midazolam. One RDD was filled with 1000 mg Ketamine + 50 mg Medetomidine + 10 mg Butorphanol + 5 mg Midazolam.

The dental formula was visually evaluated and, after induction, based on the eruption and replacement of incisor and molar teeth (Smuts, G. L., 1974), age was determined. As hypsodont mammals, with a sharper dental crown and different enamel proportion, initial wear of the tooth crown and abrasion and attrition were evaluated (Winkler D. E., & Kaiser T. M., 2015). Also, differences between free-roaming and captive equids were taken into consideration, as less abrasion-dominated tooth wear is usually encountered more in captive equids rather than their free-ranging conspecifics (L. A. Taylor, 2014).

Body weight was documented based on the average weight of male zebras and muscle mass by visual estimation (Bray & Edwards, 1999). Body condition score (BCS) was assigned using a BCS chart adapted to a numerical scoring system for captive (zoo) equids, including zebras (Bray & Edwards, 1999).

A bilateral locoregional intratesticular block was performed using a total dose of 2 mg/kg Lidocaine.

The stallion received the following treatment postoperatively: antibiotic as an injectable aqueous suspension of procaine penicillin and benzathine penicillin, intramuscularly (Duplocillin® LA) 20 mL/animal, injectable NSAID - Ketoprofen, intravenously (Ketofen®), 10 mL/animal and a tetanus toxoid intramuscular shot (Zoetis Inc.).

To assess the efficacy of the immobilization, physiological parameters such as respiratory rate (RR), heart rate (HR), oxygen saturation (SpO2), and rectal body temperature (RT) were monitored. Respiratory rate was determined by visual observation of chest movements and counted in breaths/minute. Heart rate was recorded in beats/minute with a 3M™ Littmann® Classic III™ Monitoring Stethoscope. Temperature was clinically taken transrectally, with a digital veterinary thermometer (Kerbl). Peripheral oxygen hemoglobin saturation (SpO2) and heart rate (HR) were measured using a reflectance pulse oximeter probe (Nonin) attached to the tongue. All monitoring parameters were assessed continuously by the same person and recorded every 10 minutes from lateral recumbency until standing position, throughout the immobilization period.

Atipamezole 0.15 mg/kg (Antisedan® 5 mg/ml, Orion Corporation Animal Health, Turku, Finland) was used for antagonization, via the intravenous route.

The quality of induction was evaluated with an equine recovery chart where behavior during lateral recumbency, transition to sternal recumbency, description of sternal recumbency, transition to standing position, balance and coordination while standing, remarks, an overall impression were assessed and led to a final score (Table 1). The time between each transition was documented, with notes on balance and coordination in rapport with the level of ataxia. The final score consisted of the number of

attempts to standing position, level of ataxia, and excitation.

Table 1. Recovery final scores, from 1 to 6

Final score 1	One attempt, little to no ataxia
Final score 2	Two or more attempts, ataxia
Final score 3	More attempts, quiet recovery
Final score 4	More attempts, moderate recovery
Final score 5	More attempts, excitation
Final score 6	Very bad recovery, high risk of injury

RESULTS AND DISCUSSIONS

The dental evaluation resulted in an age estimation of 11 years. The weight was estimated at 400 kg. BCS was assigned a 6/9 score (moderately fleshy) with a thicker neck and ribs not discernable (Bray R. E. & Edwards M. S., 1999). The first syringe dart (RDD) was administered remotely and intramuscularly in the rump on the left side, from 30 meters distance. The suspicion that it was not fully discharged is based on the author's experience with remote chemical immobilization, the rapid detachment of the RDD from the rump on impact, and the delayed onset of action.

The stallion was clinically assessed from a distance. The first signs of anesthesia occurred 6 minutes after darting. The first signs of anesthesia (Figure 1) were recorded when clinical signs of ataxia and stilted gait occurred (Costea R., 2021).

Fig. 1. Stallion in standing position, after the second dart, showing the first signs of anesthesia and waiting for induction

The waiting time after the first dart was 25 minutes, signifying 19 minutes after the first signs of anesthesia. The second RDD was darted in the right gluteal muscles from the closest approachable distance of 15 meters.

The time from drug administration (after the second dart) to recumbency was referred to as the induction time and lasted for 8 minutes.

The stallion was approached and the head was covered, then manually helped to achieve lateral recumbency. A bilateral locoregional intratesticular block was performed after induction with a total dose of 2 mg/kg Lidocaine and a wait time of 10 minutes was allocated before surgery. The surgery lasted 8 minutes and the scrotal closed castration was elected as a surgical technique.

Physiological parameters were recorded every 10 minutes after induction until antagonization with the following mean ($\bar{X}$) and standard deviation (SD): HR ($\bar{X}$ = 41 bpm; 3.46), RR ($\bar{X}$ = 35.83 bpm; 5.67), Sat. O2 ($\bar{X}$ = 93.16%; 2.31), RT ($\bar{X}$ = 37.55 Celsius; 0.15) and CRT ($\bar{X}$ = 1 seconds; 0) (Table 2).

Table 2. Physiological parameters recorded during the maintenance phase (heart rate in beats/minute, respiratory rate in respirations/minute, oxygen saturation in %, rectal temperature in Celsius, and capillary refill time in seconds)

HR	48	40	40	39	40	39
RR	34	30	30	36	42	43
Sat. O_2	97	94	91	92	91	94
RT	37.7	37.7	37.6	37,5	37.5	37.3
CRT	1	1	1	1	1	1

The patient was classified with a final recovery score of 1/6 (see Table 1) and assisted into a standing position, manually helped during reversal to a sternal position with their front limbs extended for a smooth recovery.

A total immobilization time was defined as the interval between the induction and antagonization or the time the stallion remained recumbent (54 minutes in total). Atipamezole 0.15 mg/kg was effective in 1 minute after intravenous administration. The period from the administration of an antagonist to the standing position was well-monitored, as equine recovery complications can occur in this phase.

The zebra presented stable coordination and reduced ataxia in standing position.

The gelding was visually monitored for a week after the surgery and did not show any signs of pain or discomfort.

CONCLUSIONS

The KBMM method proved to be suitable for the castration of a male Plains zebra, with lateral recumbency and in-field conditions, achieving optimal anesthesia and recovery.
The stallion was darted twice to achieve induction suggesting that further research should be done on a group of zebras. The authors recommend a higher concentration of Butorphanol (similar to the KBM method) in the dart.
The maintenance phase lasted 54 minutes and optimal anesthesia and analgesia proved to be just necessary for the procedure.
Hypoxia occurred but it was mild. Oxygen therapy remains a recommendation for zebra anesthesia.
The gelding did not show any signs of capture myopathy after recovery.
No perioperative complications were recorded.

ACKNOWLEDGEMENTS

This research work was carried out in Bethlehem, South Africa with the support of ARCA- Animal Care and Rescue Association.

REFERENCES

Balko, J. A., Fogle, C., Stuska, S. J., Fogle, J. E., & Posner, L. P. (2022). Retrospective and prospective assessment of butorphanol, azaperone, and medetomidine (BAM™) for immobilization of feral horses (Equus ferus caballus). *Equine Veterinary Journal,* 54(3), 549-555

Bohner, J., Painer, J., Bakker, D., Haw, A. J., Rauch, H., Greunz, E. M., ... & Goeritz, F. (2022). Immobilization of Captive Kulans (Equus hemionus kulan) Without Using Ultrapotent Opioids. *Frontiers in Veterinary Science*, 9, 885317.

Bray, R. E., & Edwards, M. S. (1999). Body condition scoring of captive (zoo) equids. In *Proceedings of the Third Conference on Zoo and Wildlife Nutrition*.

Breed, D., Meyer, L. C., Steyl, J. C., Goddard, A., Burroughs, R., & Kohn, T. A. (2019). Conserving wildlife in a changing world: Understanding capture myopathy - A malignant outcome of stress during capture and translocation. *Conservation Physiology*, *7*(1), coz027.

Brubaker, A. S., & Coss, R. G. (2015). Evolutionary constraints on equid domestication: Comparison of flight initiation distances of wild horses (Equus caballus ferus) and plains zebras (Equus quagga). *Journal of Comparative Psychology,* 129(4), 366.

Costea, R., Roşu, O., & Ene, I. (2021). Evaluation of an anaesthesia protocol following translocation of feral horses outside the Letea forest. *Scientific Works. Series C, Veterinary Medicine*, *67*(1).

King, S. R., Schoenecker, K. A., & Cole, M. J. (2022). Effect of adult male sterilization on the behavior and social associations of a feral polygynous ungulate: The horse. *Applied Animal Behaviour Science,* 249, 105598.

Landman, M., & Kerley, G. I. H. (2001). Dietary shifts: do grazers become browsers in the Thicket Biome? Koedoe, 44(1), 31-36.

Nacarino-Meneses, C. (2023). Evolution of Equid Body Size. In *The Equids: A Suite of Splendid Species* (pp. 113-141). Cham: Springer International Publishing.

Paterson, J. (2014). Capture myopathy. Zoo animal and wildlife immobilization and anesthesia, 171-179.

Rosu, O., Udrescu, L. A., Birtoiu, D., & Manu, E. (2014). Chemical immobilization of letea feral horses (Equus caballus) using ketamine and medetomidine. In *Proceedings of the International Conference on Diseases of Zoo and Wild Animals, Warsaw, Poland, 28-31 May 2014* (pp. 190-195). Leibniz Institute for Zoo and Wildlife Research.

Smuts, G. L. (1974). Age determination in Burchell's zebra (Equus burchelli antiquorum) from the Kruger National Park. *South African Journal of Wildlife Research-24-month delayed open access*, *4*(2), 103-115.

Stemmet, G. P. (2018). Cardiopulmonary effects of ketamine-butorphanol-medetomidine and etorphine-azaperone drug combinations used to immobilize zebra (Equus zebra). University of Pretoria (South Africa).

Stemmet, G. P., Meyer, L. C., Bruns, A., Buss, P., Zimmerman, D., Koeppel, K., & Zeiler, G. E. (2019). Compared to etorphine–azaperone, the ketamine–butorphanol–medetomidine combination is also effective at immobilizing zebra (Equus zebra). *Veterinary anaesthesia and analgesia,* 46(4), 466-475.

Taylor, L. A., Müller, D. W., Schwitzer, C., Kaiser, T. M., Castell, J. C., Clauss, M., & Schulz-Kornas, E. (2016). Comparative analyses of tooth wear in free-ranging and captive wild equids. *Equine Veterinary Journal*, *48*(2), 240-245.

Winkler, D. E., & Kaiser, T. M. (2015). Uneven distribution of enamel in the tooth crown of a Plains Zebra (Equus quagga). *PeerJ, 3*, e1002.

Zabek, M. A., Wright, J., Berman, D. M., Hampton, J. O., & Collins, C. W. (2015). Assessing the efficacy of medetomidine and tiletamine–zolazepam for remote immobilization of feral horses (Equus caballus). *Wildlife Research*, *41*(7), 615-622. Taylor, L. A., Müller, D. W., Schwitzer, C., Kaiser, T. M., Castell, J. C., Clauss, M., & Schulz-Kornas, E. (2016). Comparative analyses of tooth wear in free-ranging and captive wild equids. *Equine Veterinary Journal*, *48*(2), 240-245.

ANIMAL PRODUCTION, PUBLIC HEALTH AND FOOD QUALITY CONTROL

Scientific Works. Series C. Veterinary Medicine. Vol. LXX (2), 2024
ISSN 2065-1295; ISSN 2343-9394 (CD-ROM); ISSN 2067-3663 (Online); ISSN-L 2065-1295

ASSESSMENT OF THE SPOILAGE MICROFLORA IN POULTRY AND CARCASSES CONDEMNATION

Mădălina BELOUS

University "Spiru Haret", Faculty of Veterinary Medicine, 256 Basarabia Blvd, District 3, Bucharest, Romania

Corresponding author email: madalina.belous@spiruharet.ro

Abstract

The microbial load play an important role in hygiene abattoirs performance and risk categorisation, as an important part of a risk-based meat safety assurance system. The aim of our study was to investigate if risk categorisation of abattoirs based on microbiological indicators have a similar results like codecs used for condemnation (partial or total) of the carcasses on ante mortem or post mortem inspection. The research material was represented by poultry samples collected in compliance with the current legislation (RU2073/2005) and (RU627/2019) it is used for poultry condemnation. The results showed that differences regarding Campylobacter and Salmonella may be consider as variation in risk abattoir categorisation. A lower risk may be considered regarding Campylobacter level lower than Salmonella. Microbial load from the surface of carcasses is significantly influencing the risk abattoir categorization and the final condemnation.

Key words*: microbial residues, consumer safety, sustainable environment.*

INTRODUCTION

According to (FAO, 2023; Mottet & Tempio, 2017; USDA, 2023) the meat of the poultries is the most consumed globally and consumption is increasing and in this case food safety for happy and satisfied clients is a very important issue.

Food safety is one direction of European legislation and European Union (EU) designed to prevent risks and hazards on the hole food chain starting with the primary producers (from the farm to the abattoir) ante-mortem inspection (AMI) and post mortem inspection (PMI) of the poultry and broilers carcasses (EU, 2019b).

According to Vågsholm et al. (2023) the purpose of meat inspection is the same in starting past century with the maim focus on protecting health of consumers, (maintain the reputation of the meats in home and export markets and detect communicable diseases of animals before they have spread beyond easy control. Present days added more direction as to protection of animal welfare and consumer health with focus on chemical and biological hazards and food frauds.

The original meat inspection procedures were based on visual inspection of surfaces, and palpation and incision of tissues, particularly lymph nodes, to detect abnormalities (Huey, 2012). The top finding lesions are abscesses, tuberculous lesions, parasitic cysts and tissues with unusual colors, consistencies and odors affecting the carcass and/or the organs. Today meat inspection added other issues like fraud, adulteration, counterfeiting and other fraudulent practices are the new challenges in meat inspection adding Salmon's paper (1889), the American pioneer of Food Safety new practices.

In our days EU legislation establish national surveillance programs available in each European country in live chickens and broiler meat for testing *Salmonella, Campylobacter* in live chicken and broiler meat establish in control programmes based on standardised mycological reference analyse systems on (EC, 2003; EC, 2020; EFSA, 2012b).

Also, as mentioned before apart food safety, animal health and welfare may determine indicators for meat inspection, especially ante mortem inspection completing the food chain from farm to abattoir.

The antemortem inspection includes the control of the Food Chain Information inspecting information regarding animal welfare, treatment before slaughtering with the withdrawal period respected, documents and an inspection of the flock before slaughter. The aim of AMI is to verify if any incidents, related to health and welfare, which could have occurred on the farm (illegal treatments, signs of antibiotic

treatments) of during transport processes. Some Eu countries deciding for respecting young animals not to slaughter them and with the sop of avoiding transportation and the stress that may occur. In PMI, the detection of lesions/abnormalities as well as visible contaminations on the surface of the carcasses are recorded on the official documents with the result total or partial condemnation of the carcasses (EU, 2019b; Huneau-Salaün et al., 2015).

The EU legislation applicable is represented by article 45 of the Commission Implementing Regulation (EU) 2019/627 with the quotes of 18 reasons for declaring poultry meat unfit for human consumption (EU, 2019b). Most of abattoirs are using national codes based on EU legislation. These codes are covering different fields regarding AMI or PMI. Each EU country is applying some of the codes but not totally, general common use of the codes is differing from country to country or even in the same like in the case of Italy or Germany where each region has a different legislation.

PMI lesions observed in broilers based on anatomopathological inspection are skin lesions, ascites, discoloration, arthritis, polyserositis, and the presence of fibrin in various organs indicating systemic infection, cachexia or mortality before slaughter, contamination of the carcass with crop or intestinal/cloacal contents, or other slaughter process-related defects as mentioned in European codes (Alfifi et al., 2020; Koutsianos et al., 2021).

The aim of this paper was to analyse the codes used in Romania for broiler PMI findings and their implications for food safety, meat quality, broiler health or welfare and if exists a corelation with hygiene criteria.

The study was part from an original paper with the aim of analysing and comparing existing national PMI codes used in Europe and propose a new harmonized risk - based code set for Europe, but in the end the data was not used in the original study.

MATERIALS AND METHODS

Two poultry abattoirs one large sale (A) a one small scale (B) was choose representatively for the subject of the study. The average daily slaughter for the large abattoir is > 20000 birds and for the small one < 5000 birds.

The data was collected using the official annual abattoirs reports for National Sanitary Veterinary Authority. Three main units was subject of the study. Secondary data were collected using interviews with Official Veterinars (OV) regarding condemnation criteria used in PMI regarding the code system specified by European legislation and associated condemnation criteria in place applicable for Romanian case. We used data reported end of 2023.

The data analysed in Romania must targets the number of codes available and reported by official vets to national authority based on of PMI findings; if the condemnation was total or partial and the proportion or the number of carcasses declared inacceptable for human consumption.

RESULTS AND DISCUSSIONS

Romania is expected to increase poultry production, encouraged by strong consumer demand and the price competitiveness of chicken meat compared to pork how originally represented national meat. In Romania are licence 37 slaughterhouses authorised for chicken and broilers (ANSVSA). All European countries had implemented the code set based on article 45 of the Commission Implementing Regulation (EU) 2019/627 included Romania.

Most commune codes set found in Romania are chronic hepatitis, trauma before slaughter, dead before slaughter, footpath lesions as listed in article 45of RU 627/2019.

Analysing codes in different countries in Europe according Majewski et al. (2024), “acute arthritis”, “chronic arthritis”, and “footpad lesions” codes did not appear in the most-used codes list that was prepared and that covers 80% of condemnations. However, these three codes reflect broiler health and broiler welfare.

In the end we try to find a corelation between hygiene classification and number of condemnation (partial or total) after PMI.

Abattoirs were also grouped into two class categories (satisfactory or unsatisfactory) according to the current EU legislation.

The National Sanitary Veterinary Authority is auditing each facility annually and based on this evaluation a class of rick is establish for each abattoir with the fervency of the official controls based on RU2073/2005. Analysed indicator are *Salmonella* and *Campylobacter*.

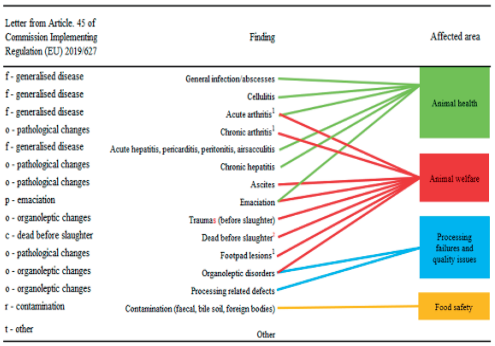

Figure 1. Reasons for declaring broiler meat as unfit for human consumption in European countries, considering the potential impact on food safety, meat quality, broiler health, and broiler welfare, based on the data from eight European countries and covering 80% of all condemned carcasses. The alphanumeric character corresponds to the reasons listed in Article 45 of Commission Implementing Regulation (EU) 2019/627 (EU, 2019b), cited in Majewski et al. (2024)

According to RU2073/2005, *Salmonella* (n = 50, c = 5; m = not detected in 25 g of a pooled sample of neck skin), abattoirs were considered satisfactory if *Salmonella* was detected in a maximum of c/n samples, and unsatisfactory if detected in more than c/n samples. For *Campylobacter* (n = 50, c = 15; m = 3 log 10 CFU/g), abattoirs were considered satisfactory if a maximum of c/n values were >m, and unsatisfactory, if more than c/n values were >m. Risk categorisations of abattoirs were performed based on EU legislation analysing and based on compliance with criteria set by European legislation. For indicators and pathogens, satisfactory compliance was given a numerical score of 1, acceptable by score 2 and unsatisfactory compliance a score of 3, according Cegar et al. (2022). In both abattoirs (small and large scale), all carcasses were *Campylobacter* positive on first sampling day while the small one was positive fortwo thirds on the second day. Carcasses in small abattoir B were all *Campylobacter* positive on one day, while on the second day, two thirds were positive in small abattoir. Small abattoir B had the best results for *Salmonella*, with a total of 4% of carcasses being positive and all carcasses being free of this pathogen during one of the sampling days.

The large abattoir A had with on-carcass *Salmonella* prevalences of 32%. *Salmonella* prevalences differed considerably between the two sampling days (i.e., 7-fold - 56% versus 8%)

Table 1. Microbiological status of chilled broiler based RU2073/2005

Abattoir	Sampling day (no. of samples)	*Campylobacter* mean log 10 CFU/g ± SD/prevalence	*Salmonella* prevalence
Large A	Day 1 (25) Day 2 (25) Both days (50)	2.95 ± 0.58[g]/100% 4.01 ± 0.28[h]/100% 3.48e ± 0.70/100%	56% 8% 32%
Small B	Day 1 (25) Day 2 (25) Both days (50)	3.03 ± 0.73[h]/100% 0.08 ± 0.70[g]/68% 1.55[d] ± 1.65/84%	8% 0% 4%

In this study we try to find a connection between the classification of abattoirs and the number of carcass condemnation in analysed facilities.

The Table 2 is presenting the abattoirs in decreasing order of the hygiene criteria with the most commune codes used in Romania expressed in percentage.

Table 2. Correlation in between hygiene criteria and carcasses condemnation

Abattoir (according to hygiene criteria)	Chronic hepatitis %	Traumas (before slaughter) %	Dead before slaughter, %	Footpad lesions, %
Small B	1.04	0.28	0.32	0.01
Large A	1.21	0.25	0.37	0.01
Abattoir	Chronic hepatitis t	Total SNCU, t	Dead before slaughter, t	Footpad lesions, no
Small B	175	234123	46	1246
Large A	250	338802	96	1697

CONCLUSIONS

The correlation between different codes with the main surveillance objectives in poultry inspection (food safety, meat quality, broiler health, and broiler welfare) is a new approach for the sanitary veterinary inspection objective. The food safety surveillance objective (detection of fecal and intestinal material on carcasses) might be corelated with the hygiene

objective and microbiological indicator (*Campylobacter* and *Sallmonela*) with the impact on the meat quality. These two objectives will be corelated with PMI criteria of Article 45 of the Commission Implementing Regulation (EU) 2019/ 627. The other two objectives: broiler health and broiler welfare will be linked with improvement in live broiler health and welfare will relate to AMI codes.

ACKNOWLEDGEMENTS

The author would like to thank colleagues from Rimbins project - COST Action 18105 (Risk based Meat Inspection and Integrated Meat Safety Assurance; www.ribmins.com) for the contribution on this research. The project was supported by COST (European Cooperation in Science and Technology; www.cost.eu). The authors would like to thank Michał Majewski for the original article (Development of a harmonized and risk-based code system for post-mortem inspection of broilers) for initiating this study even in the end data from Romania was not used.

REFERENCES

Alfifi, A., Dalsgaard, A., Christensen, J. P., Halberg Larsen, M., & Sandberg, M. (2020). The association between meat inspection codes, footpad lesions and thinning of broiler flocks in the Danish broiler production. Preventive Veterinary Medicine, 185. https://doi.org/10.1016/j.prevetmed.2020.105205. Article 105205.

Anon. (2005). Commission Regulation (EC) No 2073/2005 of 15 November 2005 on microbiological criteria for foodstuffs. Available at: https://eur-lex.europa.eu/legal-content/EN/TXT/PDF/?uri= CELEX:32005R2073&from=EN Accessed 8/7/21.

ANSVSA (2024). https://www.ansvsa.ro (Accessed 10 September 2024)

consolidated version 08.12.2022. Retrieved from http://data.europa.eu/eli/reg_del/ 2019/624/oj. (Accessed 10 September 2024).

EC (2005). Commission Regulation (EC) No 2073/2005 of 15 November 2005 on microbiological criteria for foodstuffs.

EC. (2003). Directive 2003/99/EC of the European parliament and of the council of 17 november 2003 on the monitoring of zoonoses and zoonotic agents, amending council decision 90/424/EEC and repealing council directive 92/117/EEC. Current consolidated version: 01/07/2013. Retrieved from http://data.europa.eu/eli/dir/2003/99/oj (Accessed 1 December 2023).

EC. (2019a). Commission Delegated Regulation (EU) 2019/624 of 8 February 2019 concerning specific rules for the performance of official controls on the production of meat and for production and relaying areas of live bivalve molluscs in accordance with Regulation (EU) 2017/625 of the European Parliament and of the Council. Current

EC. (2019b). Commission Implementing Regulation (EU) 2019/627 laying down uniform practical arrangements for the performance of official controls on products of animal origin intended for human consumption. Current consolidated version: 09.01.2023 http://data.europa.eu/eli/reg_impl/2019/627/oj. (Accessed 10 September 2024).

EC. (2020). Commission Implementing Decision (EU) 2020/1729 of 17 November 2020 on the monitoring and reporting of antimicrobial resistance in zoonotic and commensal bacteria and repealing Implementing Decision 2013/652/EU. . (Accessed 1 December 2023).

EFSA. (2012a). Technical specifications on harmonized epidemiological indicators for biological hazards to be covered by meat inspection of poultry. EFSA Journal, 10(6), 2764. https://doi.org/10.2903/j.efsa.2012.2764

EFSA. (2012b). Scientific opinion on the public health hazards to be covered by inspection of meat (poultry). EFSA panel on biological hazards (BIOHAZ), EFSA panel on contaminants in the food chain (CONTAM) and EFSA panel on animal health and welfare (AHAW), European food safety authority (EFSA), parma, Italy. EFSA Journal, 10(6), 2741. https://doi.org/10.2903/j.efsa.2012.2741

FAO. (2023). Meat market review: Emerging trends and outlook 2023. Rome.

Huey, R. (2012). Thoroughly modern meat inspection. The Veterinary Record, 170, 68–70. https://doi.org/10.1136/vr.e81 Kahneman, D. (2011). Thinking fast and slow. London, UK: Penguin Books. Kahneman, D., & Tversky, A. (1979). Prospect theory: An analysis of decision under risk.

Huneau-Salaün, A., St¨ark, K., Mateus, A., Lupo, C., Lindberg, A., & Le Bouquin-Leneveu, S. (2015). Contribution of Meat Inspection to the surveillance of poultry health and welfare in the European Union. Epidemiology and Infection, 143(11), 2459–2472. https://doi.org/10.1017/S0950268814003379

Ivar Vågsholm, Simone Belluco, Silvia Bonardi, Fredrik Hansen, Terje Elias, Mati Roasto, Eduarda Gomes Neves, Boris Antunovic, Arja Helena Kautto, Lis Alban, Bojan Blagojevic (2023). Health based animal and meat safety cooperative communities, Food Control, Volume 154,2023,110016, ISSN 0956-7135, https://doi.org/10.1016/j.foodcont.2023.110016.

Koutsianos, D., Athanasiou, L., Mossialos, D., & Koutoulis, K. C. (2021). Colibacillosis in poultry: A disease overview and the new perspectives for its control and prevention. Journal of the Hellenic Veterinary Medical Society, 71(4), 2425–2436. https://doi.org/ 10.12681/jhvms.25915

Michał Majewski, Lis Alban, Désirée S. Jansson, Thomai Lazou, Nina Langkabel, Dragan Antic, Eija Kaukonen, Helena Wall, Madalena Vieira Pinto, Laila Østergaard, Ole Gyvelgaard Nielsen, Sergio Ghidini,

Marianne Sandberg (2024). Development of a harmonized and risk-based code system for post-mortem inspection of broilers, Food Control, Volume 165, 2024, 110665, ISSN 0956-7135, https://doi.org/10.1016/j.foodcont.2024.110665.

Mottet, A., & Tempio, G. (2017). Global poultry production: Current state and future outlook and challenges. World's Poultry Science Journal, 73(2), 245 - 256. https://doi.org/10.1017/S0043933917000071.

RIBMINS (2024). Report on the scope of meat safety assurance systems (MSAS) and competences and roles of risk manager. CA18105 - risk-based meat inspection and integrated meat safety assurance, 86 pp. Available at: https://ribmins.com/wp-content/uploads/2023/02/RIBMINS-WG1-Deliverable.pdf. (Accessed 23 September 2024).

Simo Cegar, Ljiljana Kuruca, Bojana Vidovic, Dragan Antic, Sigrun J. Hauge, Ole Alvseike, Bojan Blagojevic (2022). Risk categorisation of poultry abattoirs on the basis of the current process hygiene criteria and indicator microorganisms, Food Control, Volume 132, 2022, 108530, ISSN 0956-7135, https://doi.org/10.1016/j.foodcont.2021.108530.

USDA (United States Department of Agriculture). (2023). Livestock and poultry: World markets and trade. Retrieved from https://usda.library.cornell.edu/concern/public actions/73666448x. (Accessed 10 October 2023).

EXPERIMENTAL MEDICINE

Scientific Works. Series C. Veterinary Medicine. Vol. LXX (2), 2024
ISSN 2065-1295; ISSN 2343-9394 (CD-ROM); ISSN 2067-3663 (Online); ISSN-L 2065-1295

ANTIBACTERIAL EFFECT OF ESSENTIAL OILS AGAINST BACTERIAL STRAINS ISOLATED FROM COWS WITH MASTITIS

Cristina CĂȘARU[1], Anca BULGARU[1], Elena NEGRU[1], Mihai DANEȘ[2], Doina DANEȘ[1]

[1]University of Agronomic Sciences and Veterinary Medicine of Bucharest, Faculty of Veterinary Medicine, 105 Splaiul Independenței Street, 050097, District 5, Bucharest, Romania
[2]Spiru Haret University, Faculty of Veterinary Medicine, 256 Basarabia Blvd, District 3, Bucharest, Romania

Corresponding author email: casarucristina@yahoo.com

Abstract

Antibiotic resistance has become a global concern, with major implications in both human and veterinary medicine. In recent years, new therapies have been sought as alternatives to antibiotics. In this regard, essential oils extracted from medicinal plants have been shown to be effective in many cases. The purpose of our study was to test the efficacy of the essential oils of thyme, clove, peppermint, and cinnamon against ten bacterial strains isolated from cows with clinical mastitis. Sixty percent of the bacterial strains examined in the study were found to be resistant to five or more antibiotics. The effectiveness of essential oils was tested using the aromatogram method. The results varied depending on the bacterial strain and concentration of the tested essential oils. Cinnamon, thyme, and the mixture of the four oils were the most effective products. The highly resistant S. aureus isolate (7 from 12 antibiotic molecules), proved to be extremely sensitive to the essential oils of thyme and cinnamon and highly sensitive to the mixture of oils.

Key words*: cow, mastitis, essential oils, antibacterial.*

INTRODUCTION

Since 1928, the year when penicillin was discovered, a new era of medicine has begun, saving millions of lives. In recent years, it has been found that infections considered common place have become a threat again, due to the development of antibiotic resistance. Alarm signals have been raised by most of the competent international institutions regarding the judicious use of antimicrobials and the rapid discovery of alternatives for them, since the research for the discovery of new molecules does not prove profitable for the pharmaceutical industry (Allen et al., 2014; Ventola, 2015). Tomanic et al. (2023) estimated that in veterinary medicine, the amount of antibiotics used is 73-100% higher than that used in human medicine. There is a worldwide concern about food safety and the effect of antibiotic use in animal husbandry, and a series of general recommendations have been issued for their administration, such as the selection of specific antimicrobials based on laboratory analysis, the use of appropriate therapeutic doses, optimal dosage, minimising the potential for transfer of genetic antimicrobial resistance, or administration of antimicrobials in order to reduce adverse effects for humans and animals (Guardabassi et al., 2008). Antibiotic resistance is estimated to cause 10 million deaths and $100 trillion in economic losses annually by 2050 (Tomanic et al., 2023).

Alternatives to which modern medicine is beginning to turn its face in recent years are phytotherapy, homeotherapy, apitherapy, acupuncture, phagitherapy, probiotics, immunotherapy, and vaccines. Compounds derived from plants could enter the current use in therapy due to their direct, antibacterial, but also indirect action, due to bioactive compounds that modify resistance to antibiotics and increase their effectiveness (Stephanovic, 2018).

The antibacterial activity of plants is mainly due to essential oils (Gîrd, 2014). The composition of all essential oils has a very high level of variability in terms of quality and quantity, which depends on intrinsic and extrinsic factors such as the area where the plant is grown (latitude and altitude), the amount of precipitation and the amount of UV radiation, the time of cultivation, the type of

soil and its fertilisation, plant age, extraction conditions, drying and storage conditions. All these factors influence and interconnect, making them difficult to treat separately (Hassiotis et al., 2014; Dhifi et al., 2016; Kulyas & Batiyash, 2018; Haro-González et al., 2021).

MATERIALS AND METHODS

Milk samples were collected from 10 cows showing clinical signs of mastitis. Collected milk samples were plated on solid culture media: defibrinated sheep blood agar, MacConkey agar, and Sabouraud agar. The seeded plates were incubated for 24 hours at 37°C and 72 hours at 25°C for Sabouraud. The resulting cultures were examined macroscopically and microscopically. Based on cultural, morphological, and biochemical characteristics using Api 20 NE, Api 20 E, Api 20 Strep and ID 32 Staph galleries, the bacterial isolates from the milk samples were identified and preserved.

To determine antibiotic sensitivity, the disc diffusion method was used, which is based on the property of antimicrobials to diffuse in a solid culture medium (defibrinated sheep blood agar) on which the bacterial culture to be tested is seeded.

The essential oils used were purchased from a processing company in France, 100% pure oils, containing no other similar essential oils, 100% natural, from certified organic crops, not denatured by synthetic molecules, 100% integral, obtained by complete distillation with steam. Testing the antibacterial effect of the essential oils of *Thymus serpillum*, *Syzygium aromaticum*, *Mentha piperita* Franco-Mitcham, and *Cinnamomum zeylanicum* on the isolated bacterial strains was carried out by the aromatogram method.

Bacterial suspensions were prepared from cultures on solid medium in sterile saline solution, at a known concentration of 0.5 McFarland, a concentration equivalent to 1-2 x 10^8 CFU/ml. Blood agar plates were seeded with 100 µl of the previously prepared inocula, then left ajar for 10 min in the laminar flow hood. Of the test oils, dilutions of 1/2, 1/4, and 1/10 were made in a mixture of distilled water with 10% DMSO and 0.5% Tween 80. An equal-parts mixture was also made of the four essential oils to be tested, undiluted. In the same experiment, the antibacterial effect of coconut oil and grape seed oil was also tested. Discs were placed on the previously inoculated plate using sterile forceps at a minimum of 15 mm from the edge and not less than 24 mm apart, and a micro disc of norfloxacin was used as a positive control. The plates were incubated aerobically at 37°C for 24 hours. Each sample was run in duplicate.

After 24 hours of incubation, the diameter of the zones of inhibition around each disc was measured using a ruler.

The correlation between the diameters of the inhibition zones and the sensitivity of the bacteria was established according to the specialised literature using the Duraffourd scale (Vasquez & Guardia, 2021). The sensitivity of the bacteria was assessed, depending on the diameter of the zone of inhibition that appeared around the disc impregnated with volatile oil, and the sensitivity of the bacteria to each essential oil used was noted as follows: < 8 mm = resistant; between 8 and 14 mm = sensitive; between 14 and 20 mm = very sensitive; > 20 mm = extremely sensitive.

RESULTS AND DISCUSSIONS

The following bacterial strains were isolated and identified from breast milk: *Escherichia coli* (two strains), *Lactococcus lactis* ssp. *cremosis*, *Listeria* spp., *Pateurella multocida*, *Staphylococcus xylosus*, *Staphylococcus* spp., *Staphylococcus intermedius*, *Staphylococcus epidermidis,* and *Staphylococcus aureus*. Of the tested strains, 90% showed multiple resistance to the tested antibiotics, 60% proved to be resistant to at least 5 antibiotics, and 30% to 7 or more antibiotics, results that reflect the upward trend of the antibiotic resistance phenomenon (Table 1). Similar results were also obtained in the western part of Romania, where 39 bacterial strains, belonging to different species, isolated from cows with mastitis, were tested. All strains showed resistance to at least 3 antibiotics from those tested, but were resistant to 9 or more antibiotics, the most frequently recorded resistance to erythromycin, ampicillin, gentamicin, amoxicillin, and clavulanic acid (Pascu et al., 2022).

Table 1. Bacterial sensitivity to antibiotics

Strain / Atb.	1*	2	3	4	5	6	7	8	9	10
AK	S**	S	R	R	R	-	-	S	-	-
AML	S	-	-	-	-	S	R	S	R	R
AMP	-	R	R	I	S	S	R	-	-	R
C	-	-	-	-	-	S	-	-	-	R
CFM	R	S	S	R	S	S	-	R	R	R
CS	R	-	-	-	-	-	R	R	-	-
CD	I	R	I	R	R	S	-	I	R	I
DXT	S	S	S	R	S	S	R	S	-	S
E	-	-	-	-	-	-	R	-	-	-
ENR	-	S	I	I	S	-	R	-	R	S
GM	S	S	I	R	R	S	-	S	R	S
K	-	-	-	-	-	-	-	-	R	R
KF	S	R	S	R	S	-	-	S	R	R
N	-	-	-	-	-	-	-	-	R	R
NOR	S	S	S	S	S	S	S	S	R	S
OX	-	-	-	-	-	-	R	-	-	-
P	R	R	S	I	S	S	-	R	-	R
RA	S	R	S	S	S	S	-	S	-	-
S	S	I	R	R	R	S	S	I	-	R
SPE	I	-	-	-	-	S	R	I	-	-
SXT	S	S	I	I	S	S	R	S	-	-
VA	R	-	-	-	-	R	-	R	-	-
TE	-	I	S	I	I	-	-	-	R	R

*1,2 - *Escherichia coli,* 3 - *Lactococcus lactis* ssp. *cremoris,* 4 - *Listeria* spp., 5 - *Pasteurella multocida,* 6 - *Staphylococcus xylosus,* 7 - *Staphylococcus* spp., 8 -*Staphylococcus intermedius,* 9 - *Staphylococcus epidermitis,* 10 - *Staphylococcus aureus*
** S-sensitive, I-intermediar, R-resistant

The effectiveness of the essential oils varied depending on the strain and concentration tested, but cinnamon and thyme oils were the most effective, as was the mixture of the four oils (Figure 1).

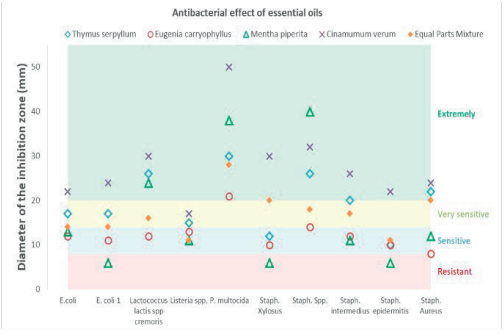

Figure 1. Antibacterial effect of essential oils

The strain of *S. aureus*, resistant to most of the antibiotics tested, was highly sensitive to the essential oils of thyme and cinnamon and very sensitive to the mixture of oils. Cinnamon oil had the strongest effect, with all bacteria being at least sensitive to the action of this oil. The smallest inhibition zone was 17 mm for *Listeria* spp., and the maximum inhibition zone was in the presence of the *Pasteurella multocida* strain, above 50 mm, a value that was preserved at all tested dilutions. Similar results were obtained by Casalina et al. (2023). For 117 strains of *E. coli* from birds, cinnamon oil proved effective against all strains tested. The same was reported by El Atki et al. (2019) for strains of *E. coli*, *S. aureus,* and *Pseudomonas aeruginosa* that were inhibited in the presence of cinnamon oil.
The sensitivity of the bacterial strains to the action of the essential oils, for the tested concentrations is shown in Table 2.

Table 2. Susceptibility of bacterial strains to essential oils

**	1*	2	3	4	5	6	7	8	9	10
Thymus serpillum										
A	17	17	26	15	30	2	26	22	10	20
B	15	12	24	12	28	10	24	18	8	18
C	10	10	14	10	26	7	10	12	6	12
D	6	6	8	6	6	6	7	6	6	6
Cinnamomum zeylanicum										
A	22	24	30	17	>50	30	32	24	22	26
B	22	22	28	16	>50	28	31	22	18	22
C	20	20	26	15	>50	26	30	20	17	20
D	14	16	22	12	>50	24	22	16	10	14
Syzygium aromaticum										
A	12	11	12	13	21	10	14	12	10	13
B	9	8	10	10	20	9	11	10	8	10
C	8	6	9	6	12	9	10	8	6	6
D	6	6	6	6	10	6	7	6	6	6
Mentha piperita										
A	13	6	22	11	38	6	40	11	6	12
B	8	6	16	8	30	6	24	9	6	10
C	6	6	12	6	12	6	16	6	6	6
D	6	6	16	6	6	6	6	6	6	6
Mixture E.O. 1:1:1:1										
	14	14	16	28	20	18	17	11	20	11

*1, 2 - *Escherichia coli,* 3 - *Lactococcus lactis* ssp. *cremoris,* 4 - *Listeria* spp., 5-*Pasteurella multocida,* 6 - *Staphylococcus xylosus,* 7 - *Staphylococcus* spp., 8 -*Staphylococcus intermedius,* 9 - *Staphylococcus epidermitis,* 10 - *Staphylococcus aureus.*
**A-integral E.O., B-1/2 dilution, C-1/4 dilution, and D-1/10 dilution

All tested bacterial strains were at least sensitive to the action of *Thymus serpyllum* essential oil. This is an oil rich in thymol and carvacrol, substances that induce changes in the integrity and permeability of the membrane where ATP and potassium ions are released, with changes in pH and the balance of organic ions; undergo oxidation at the level of the double bonds in the nucleus, releasing carbonyl, carboxyl, and hydrogen peroxide derivatives with an antiseptic effect at the cellular level. Both have phenolic structure; they are structural isomers; on the phenolic ring, only the position of the hydroxyl group differs. The activity of thymol and carvacrol is potentiated by p-cymene, without antimicrobial action but with hydrophobic action. Among the

many uses of thyme oil, its anti-inflammatory and antimicrobial properties stand out (Gîrd, 2014; Mahboubi & Kazempour, 2011; Kovacevic et al., 2022).

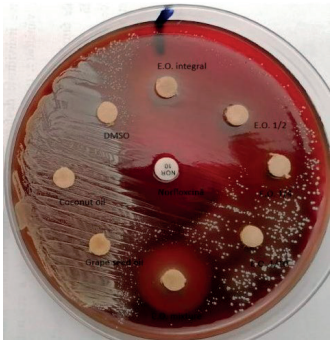

Figure 2. Efficacy of essential oils of thyme on the *Staphylococcus aureus* strain

Tested on bacteria isolated from cows with mastitis, the effect of *Thymus spp*. oil had remarkable results at concentrations of 2% and 3%, completely inhibiting the *in vitro* growth of bacteria *E. coli*, *S. aureus*, and *Str. agalactiae* (Mason et al., 2015). *Thymus* spp. oil used at a dose of 50 µl/ml against a strain of *S. aureus* and *Klebsiella pneumoniae* produced a zone of inhibition of 35 mm and 40 mm, respectively, and when the oil was combined with tetracycline, the zone of inhibition increased to 38 mm and, respectively, 41 mm (Pancu et al., 2022). The results are also confirmed by Sahin et al. (2003) concerning the extract of *Thymmus* spp., which he tested against 178 strains of microorganisms (55 species of bacteria, 4 species of fungi, and one fungus) *in vitro* using the disc diffusion method.

Thymus spp. extract inhibited the activity of 23 bacterial strains from 11 different species, as well as 6 strains of *Candida albicans*. Clove oil was most effective against the *Pasteurella multocida* strain (21 mm), retaining its effectiveness up to 1/10 dilution (10 mm). The same oil also proved effective against all other strains except *S. aureus*. The main component of *Syzygium aromaticum* oil is eugenol, at a percentage of 80.30%. All strains tested by Oyedemi et al. (2009) were the least sensitive to the action of clove oil. Eugenol caused a 7.9 log reduction when contacted with *E. coli* after 20 hours of incubation, followed by *Proteus vulgaris* with a 3-log reduction.

Yadav et al. (2015) tested the bactericidal effect of eugenol against some MRSA and MSSA strains. They were treated with serial dilutions of eugenol, carvacrol, or a combination thereof for 6 hours and incubated at 37ºC, after which the number of CFU was determined. The results suggested that eugenol had strong bactericidal activity during the first 3-6 hours of incubation.

Mint, known for its antispasmodic, antimicrobial, anti-inflammatory, carminative, antioxidant, analgesic, and more effects, showed a strong antibacterial effect against the 40 mm strain of *Staphylococcus* spp. The lowest activity of only 11 mm was observed for *S. epidermidis* and *Listeria* spp., against which only cinnamon oil showed high activity of 18 mm and 16 mm, respectively.

Peppermint essential oil was the only oil to which resistance was recorded from three bacterial strains (*Escherichia coli*, *Staphylococcus xylosus*, and *Staphylococcus epidermidis*). The results obtained by Muntean et al. (2019) on the efficacy of peppermint essential oil on multidrug-resistant Gram-positive and Gram-negative bacterial strains were superior to the present study, being effective against all strains tested, including *Staphylococcus aureus*, *Escherichia coli*, *Proteus mirabilis*, *Klebsiella pneumoniae*, *Pseudomonas aeruginosa*, and *Acinetobacter baumannii*.

The mixture in equal parts of the four integral essential oils showed an antibacterial effect on all 10 bacterial strains tested; the largest zone of inhibition was observed in the presence of the *Pasteurella multocida* strain (28 mm), with variations for the other strains between 11 and 20 mm, but did not show stronger activity than all the oils tested separately. In contrast, Kovacevic et al. (2022) for *Thymus vulgaris*, *Thymus serpyllum*, *Satureja montana*, and *Origanum vulgare* oils tested together had better results than when they were tested individually.

Grape seed oil and coconut oil did not inhibit the growth of any of the bacterial strains tested. A study conducted in 2019 to determine the effectiveness of coconut oil against strains of *S. aureus* isolated from goats with mastitis determined their inhibition, in vitro (Widianingrum et al., 2019).

Encouraging results were also obtained when coconut oil was used in concentrations of 25%, 50%, and 75% for the inhibition of *Streptococcus mutans* ATCC 25175, obtaining zones of inhibition of 17 mm, 21.75 mm, and 22 mm, respectively (Vásquez & Guardia, 2021). Coconut oil has been shown to be effective against some strains of *S. aureus*, *Str. pneumoniae*, and *E. coli*, but ineffective against the strain of *P. aeruginosa* tested. At the same time, two fungal strains were studied, thus, in contact with *Candida albicans*, coconut oil produced an inhibition zone of 18.5 mm, and in contact with *Aspergillus fumigatus* of 15.1 mm (Effiong et al., 2019).

The antibacterial activity of grape seed oil is primarily due to polyphenols, linolenic acid, but also to its higher acidity, compared to other carrier oils. Resveratrol also degrades the bacterial membrane without harming the host cells. Any change to the cell matrix will disrupt the normal functioning of the cell. The results in the scientific literature are varied, with greater efficacy against Gram-positive bacteria compared to Gram-negative ones. There are studies in which strains of *S. aureus* showed sensitivity to concentrations between 20 mg/mL and 1.25 mg/mL, with zones of inhibition ranging from 12.5 mm to 7 mm, but there are also studies in which strains of *S. aureus* were not sensitive to grape seed extract even at 20 mg/mL. Positive results have also been recorded against strains of *S. enteritidis*, *Bacillus subtilis*, *E. coli*, *L. monocytogenes*, and *Streptococcus pneumoniae*, but there are also strains of *E. coli*, *K. pneumoniae*, *C. parapsilosis*, *Listeria monocytogenes* and *Salmonella enteric*a that were not sensitive to any concentration tested (Belilli et al., 2018; Garaglavia et al., 2016; Memar et al., 2019; Bajpai et al., 2021).

CONCLUSIONS

According to the antibiogram, 90% of the strains showed multiple resistance to the tested antibiotics, 60% proved to be resistant to at least 5 antibiotics, and 30% to 7 or more antibiotics. All 10 bacterial isolates tested were found to be sensitive to cinnamon essential oil up to the 1/10 dilution, which had the strongest antibacterial effect among the oils tested. The mixture of equal parts of the four whole essential oils showed an antibacterial effect on all 10 bacterial strains tested. Both coconut oil and grape seed oil, through testing, demonstrated a lack of antibacterial activity against the strains studied.

REFERENCES

Allen, H. A., Trachsel, J., Looft, T., Casey, T. (2014). Finding alternatives to antibiotics. *Annals of the New York academy of science*, *1323*(1), 91–100.

Bajpai, S., Prabhakar, R., Chelakkot, R., Inamdar, M. (2021). Role of cell polarity dynamics and motility in pattern formation due to contact-dependent signalling. *Journal of the Royal Society Interface*, *18*, 20200825.

Bellili, S., Jazi, S., Nasr, S., Wissal, D., Neves, M.A., Miguel, M.G.C., Wissem. M. (2018). Grape seed oil: Chemical composition, biological properties and health benefits chapter 4, Seed oil, Production, uses and benefits. *Nova Science Publishers, University of Science and Technology, Hanoi,Vietnam,* 145-174.

Casalino, G., Dinardo, F.R., D'Amico, F., Bozzo, G., Bove, A., Camarda, A., Lombardi, R., Dimuccio, M.M., Circella, E. (2023). Antimicrobial Efficacy of Cinnamon Essential Oil against Avian Pathogenic Escherichia coli from Poultry. *Animals, 13*(16), 2639.

Dhifi, W., Bellili, S., Jazi, S., Bahloul, N., Mnif, W. (2016). Essential oils' chemical Characterization and Investigation of Some Biological Activities: A Critical Review. *Medicines (Basel), 3*(4), 25.

Effiong, E.B, Gwana, D.M., Okaro, C., (2018). Antimicrobial susceptibility pattern of coconut oil extract on selected bacterial and fungi. *World Journal of Advanced Research and Reviews, 1*(3), 1-13.

El Atki, Y., Aouam, I., El Kamari, F., Taroq, A., Nayme, K., Timinouni, M., Lyoussi, B., Abdellaoui, A. (2019). Antibacterial activity of cinnamon essential oils and their synergistic potential with antibiotics, *Journal of Advanced Pharmaceutical Technology & Research*, *10*(2), 63-67.

Garavaglia, J., Markoski, M.M., Oliveira, A., Marcadenti, A. (2016). Grape seed oil compounds: biological and chemical actions for health. *Nutrition and Metabolic Insights, 9*, 59-64.

Gîrd, C.E. (2014). Course in Pharmacognosy, Phytochemistry, Phytotherapy [in Romanian], vol. II, 2nd edition. Bucharest, RO: Printech Publishing House.

Guardabassi, L., Jensen, L.B., Kruse, H. (2008). *Guide to antimicrobial use in animals*, Oxford, UK: *Blackwel,* 143-161.

Haro-González, J.N, Castillo-Herrera, G.A., Martínez-Velázquez, M., Espinosa-Andrews, H. (2021). Clove Essential Oil (*Syzygium aromaticum* L. Myrtaceae): extraction, chemical composition, food applications, and essential bioactivity for human health. *Molecules, 26*(21), 6387.

Hassiotis, C.N., Ntana, F., Lazari, D.M., Poulios, S., Vlachonasios, K.E., (2014). Environmental and developmental factors affect essential oil production and quality of *Lavandula angustifolia* during flowering period. *Industrial Crops and Products, 62*, 359-366.

Kulyas, T., Batiyash, S., (2018). Chemical composition of the essential oil and flavonoids of *Thymus serpyllum* L., growing on territory of the East Kazakhstan. *Acta Poloniae Pharmaceutica ñ Drug Research*, *75*(6), 1329-1337.

Mahboubi, M., Kazempour, N., (2011). Chemical composition and antimicrobial activity of *Satureja hortensis* and *Trachyspermum copticum* essential oil, *Iranian Journal of Medical Microbiology*, *3*(4), 194–200.

Mason, S., Byrd, E., West, C., Thomas, M., Mullen, K., Lee, A., Lyman, R., Washburn, S., Anderson, K., (2015). antibacterial activity of an herbal product *in vitro* on mastitis pathogens, *Campbell University, Buies Creek, North Carolina, USA, 2015.*

Memar, M.Y., Adibkia, K., Farajnia, S., Kafil, H.S., Yekani, M., Alizadeh, N., Ghotaslou, R. (2019). The grape seed extract: a natural antimicrobial agent against different pathogens. *Reviews in Medical Microbiology, 30*(3), 173-182.

Muntean, D., Licker, M., Alexa, E., Popescu, I., Jianu, C., Buda, V., Dehelean, C.A., Ghiulai, R., Horhat, F., Horhat, D., Danciu, C. (2019). Evaluation of essential oil obtained from *Mentha×piperita* L. against multidrug-resistant strains *Infection and Drug Resistance.,12*, 2905-2914.

Oyedemi, S.O., Okoh, A.I., Mabinya, L.V., Pirochenva, G., Afolayan, A.J., (2009). The proposed mechanism of bactericidal action of eugenol, α-terpineol and γ-terpinene against *Listeria monocytogenes*, *Streptococcus pyogenes*, *Proteus vulgaris* and *Escherichia coli*, *African Journal of Biotechnology*, *8*(7), 1280-1286.

Pascu, C., Herman, V., Iancu, I., Costinar, L. (2022). Etiology of mastitis and antimicrobial resistance in dairy cattle farms in the Western part of Romania. *Antibiotics (Basel), 11*(1), 57.

Sahin, F., Karaman, I., Güllüce, M., Oğütçü, H., Sengül, M., Adigüzel, A., Oztürk, S., Kotan, R. (2003). Evaluation of antimicrobial activities of *Satureja hortensis* L., *Journal of Ethnopharmacology* , *87*(1).

Tomanic D., Kladar N., Radinović M., Stančić I., Erdeljan M., Stanojević J., Galić I., Bijelić K., Kovačević Z. (2023). Intramammary ethno-veterinary formulation in bovine mastitis treatment for optimization of antibiotic use. *Pathogens, 12*(2), 259.

Stefanović, O.D. (2018). Synergistic activity of antibiotics and bioactive plant extracts: a study against Gram-positive and Gram-negative bacteria. *Bacterial Pathogenesis and Antibacterial Control*, *23:*23–48.

Vasquez-Vereau, G., Guardia-Mendez, G. (2021). Antibacterial effect of coconut oil (*Cocus nucifera*) von *Streptococcus mutans* ATCC 25175: An *In vitro* Study**.** *International Journal of Odontostomatology*, *15*(4), 922-927.

Ventola, C. L. (2015). The Antibiotic Resistance Crisis, *Pharmacy and Therapeutics*, *40*(4), 277–283.

Yadav, M.K., Chae, S-W., Im, G.J., Chung, J.W., Song, J.J. (2015). Eugenol: A Phyto-Compound Effective against Methicillin-Resistant and Methicillin Sensitive *Staphylococcus aureus* clinical strain biofilms. *PLoS ONE, 10*(3), e0119564.

Widianingrum D.C., Noviandi C.T., Salasia S.I.O. (2019). Antibacterial and immunomodulator activities of virgin coconut oil (VCO) against *Staphylococcus aureus*, *Heliyon*, *5*(10).

Scientific Works. Series C. Veterinary Medicine. Vol. LXX (2), 2024
ISSN 2065-1295; ISSN 2343-9394 (CD-ROM); ISSN 2067-3663 (Online); ISSN-L 2065-1295

MICE MODELS IN METABOLIC SYNDROME RESEARCH - A REVIEW

Fabiola IONIȚĂ[1, 2], Cristin COMAN[1], Mario CODREANU[2]

[1]Cantacuzino National Military Medical Institute for Research and Development, 103 Splaiul Independentei Street, District 5, Bucharest, Romania
[2]University of Agronomic Sciences and Veterinary Medicine of Bucharest, Faculty of Veterinary Medicine, 105 Splaiul Independentei Street, 050097, District 5, Bucharest, Romania

Corresponding author email: ionitafabiola02@gmail.com

Abstract

Metabolic syndrome (MetS) consists in a cluster of metabolic complications, characterized by the simultaneous prevalence of at least three of the following medical conditions: central obesity, hyperglycemia, dyslipidemia and hypertension. MetS is a disorder with a complex etiology and an alarming prevalence rate, so the establishment of appropriate animal models mimicking MetS in humans is essential for understanding the pathophysiological mechanisms involved and for developing new therapeutic strategies. Although numerous animal models of MetS have been currently developed, the choice of a particular model requires a careful analysis in relation to the usefulness and suitability, in order to improve the applicability of the preclinical research to the clinical on.
The aim of this review is to summarize the main mice models, this species being the most frequently used in the study of MetS and obesity. Several approaches have been used in order to induce MetS in animal models including specific diet administration, genetic techniques, and chemically-induction. Apart from pathophysiological similarities with the human MetS, a suitable animal model should also have an increased accessibility and reliability, as well as being easy to reproduce in future research.

Key words*: metabolic syndrome, obesity, diet, animal models.*

INTRODUCTION

Obesity and metabolic syndrome are among the leading causes of worldwide morbidity and mortality, as their prevalence is rapidly increasing, reaching epidemic proportions especially in developing countries. In 2022, almost 2.5 billion adults were overweight, and over 890 million of these were obese (WHO, 2022). MetS includes a number of metabolic obesity-associated disorders such as hypertension, dyslipidemia, insulin resistance, nonalcoholic fatty liver and kidney dysfunction (Panchal & Brown, 2011). Human patients with MetS usually show a specific profile that includes systemic inflammation, oxidative stress and a pro-thrombotic state, linked to an increased risk of cardiovascular pathologies, type 2 diabetes, osteoporosis, cancer development and premature mortality (Della Vedova et al., 2016; Kulkarni et al., 2014; Mostafa et al., 2023).
MetS has a complex etiology due to the interaction of both environmental and genetic factors, being the consequence of a metabolic imbalance between the caloric intake, the basal metabolism, and the total energy expenditure, which leads to excessive or abnormal deposits of adipose tissue (Lang et al., 2019; Kaur, 2014).
The choice of appropriate animal models mimicking MetS in humans is highly important for the biomedical research, in order to understand not only the pathophysiological mechanisms of obesity but also the metabolic associated disorders (Wong et al., 2016). Animal models allow researchers to create a controlled environment and provide the opportunity to examine correlations among different metabolic pathways, in particular the cellular and molecular mechanisms involved in the early stages of their development, in order to refine diagnostic criteria and be able to establish therapeutic alternatives (Chalvon-Demersay et al., 2017; Wayhart & Lawson, 2017). The major challenge for researchers is to develop an animal model showing more than two of the key features of human MetS and to understand why metabolic comorbidities sometimes occur and

sometimes don`t (Della Vedova et al., 2016; Wayhart & Lawson, 2017).

Preclinical models of MetS comprise various species of animals such as: primates (Li et al., 2015; Bremer et al., 2011; Nugent et al., 2021), pigs (Zhang & Lerman, 2016; Cluzel et al., 2022), rabbits (Lozano et al., 2019; Arias-Mutis et al., 2018), dogs (Gregory et al., 2023) and even zebra fish (Benchoula et al., 2019).

However, murine models are widely used in MetS research, being relatively easy to breed maintain, and manipulate, while having standardized phenotyping protocols, essential in mouse strains characterization. Furthermore, the available genome database provides information about genome sequences in most commonly studied inbred murine lines (Wayhart & Lawson, 2017).

The extensive use of mice in human studies, is also due to the genetic homology between the two species and to the availability of manipulating the mouse genome and developing numerous methods of obtaining transgenic, knock-out, and knock-in lines (Perlman, 2016).

This paper will focus on the primary mouse models used in MetS research, though no murine model can exactly reproduce all aspects of human MetS. Therefore, the main criteria represents whether a certain model comes closest to fulfilling the key features of human MetS, especially obesity, type 2 diabetes, hypertension, and liver dysfunction, and to establish their suitability to evaluate potential treatments (Panchal & Brown, 2011). Herein we present the most important genetic models, dietary manipulated and chemically-induced murine models, often used in the study of MetS. This review has some limitations, as it does not refer to the surgical-induced models of metabolic syndrome in mice.

Genetic models of obesity and insulin resistance

Leptin-deficient mice (Lep$^{ob/ob}$ mice)

The ob/ob mouse is a monogenic model, most used in the study of the metabolic syndrome, mainly type 2 diabetes. The Lep$^{ob/ob}$ mouse has the origin in a spontaneous mutation at the Jackson Laboratory and has been known since the 1950s, but it wasn't used until 1994, when the mutated gene was well characterized. This mutation of the leptin gene results in the total lack of leptin production (Fuchs et al., 2018; Lutz & Woods, 2012).

Leptin is blood circulating hormone derived from the adipose tissue and encoded by the obese (*ob*) mouse gene. Its primary role is to regulate long-term energy balance, being involved in food intake, appetite control, and body mass. Leptin also has reproductive and neuroendocrine functions and mediates fetal growth, proinflammatory immune responses, angiogenesis and lipolysis (Obradovic et al., 2021; Dornbush & Aeddula, 2023).

In Lep$^{ob/ob}$ mice, hyperphagia and obesity occur due to the increased activity of neuropeptide Y neurons, which normally bind to leptin and regulate metabolic homeostasis and satiety (Wayhart & Lawson, 2017).

Currently, Lep$^{ob/ob}$ mice develop hyperphagia, hyperinsulinemia, hyperglycemia, reduced energy consumption and increased body mass, associated to elevated plasma cholesterol levels, mainly affecting high-density lipoprotein cholesterol, which doesn`t promote atherosclerosis (Panchal & Brown, 2011; Kennedy et al., 2010; Bracke et al., 2019; Plummer & Hasty, 2008).

In Lep$^{ob/ob}$ mice, obesity develops by 4 weeks of age, but the weight growth curve is still ascending at the age of 12 months. Lep$^{ob/ob}$ mice can exceed 100 grams when fed with a standard chow diet, which is four times greater than a wild-type mouse (Kennedy et al., 2010; Bracke et al., 2019). The blood glucose level usually reaches a peak after 12 weeks of age and eventually decreases and normalizes (Platt et al., 2016).

This mouse model shows hepatic steatosis and liver inflammation from an early age (Fang et al., 2022), and later the cardiac function is altered, developing left ventricular hypertrophy associated with fibrosis (Ren & Ma, 2008; Dobrzyn et al., 2010). However, unlike humans with metabolic syndrome, Lep$^{ob/ob}$ mice, did not show increased heart rate or abnormal blood pressure (Osório, 2014).

Due to leptin-deficiency, the hypothalamic-pituitary-adrenal (HPA) axis activity is increased in Lep$^{ob/ob}$ mice, leading to adrenal hyperplasia with elevated cortisol levels (Malendowicz et al., 2007; Sainsbury et al., 2002).

Physical appearance of a $Lep^{ob/ob}$ mouse compared to a wild-type mouse (Bracke et al., 2019).

Leptin receptor-deficient mice ($LepR^{db/db}$ mice)

The $LepR^{db/db}$ mouse model is frequently used to study type 2 diabetes and insulin resistance. $LepR^{db/db}$ mice have a mutation in the leptin receptor gene present on chromosome 4, leading to hyperglycemia, hyperinsulinemia and dyslipidemia (Chen et al., 1996, Kennedy et al., 2010).

Compared to $Lep^{ob/ob}$ mice, which develop extreme obesity, $LepR^{db/db}$ mice are more diabetic, showing an impaired glucose tolerance following oral glucose intake. (Suriano et al.,2021, Giesbertz et al., 2015).

In $LepR^{db/db}$ mice, the adipose tissue distribution is mainly subcutaneous, while $Lep^{ob/ob}$ mice develop epididymal fat and hepatic steatosis (Suriano et al., 2021). $LepR^{db/db}$ mice showed vascular endothelial dysfunction at an early age, although blood pressure was normal (Panchal & Brown, 2011). The main difference between the two monogenic models is that $LepR^{db/db}$ mice have increased circulating leptin levels, proportional to the adiposity degree, while $Lep^{ob/ob}$ lack in circulating leptin (Kennedy et al., 2010).

Melanocortin receptor deficient mice (MC4R/MC3R-KO mice)

The mechanisms by which changes in central nervous system signaling affects weight balance and homeostatic networks is related to the central melanocortin system, melanocortin receptors 3 and 4 being the most studied (Nogueiras et al., 2007; Song et al., 2008; Cone, 2005).

Melanocortin 4 receptor (MC4R) is a G protein coupled receptor, highly expressed in the hypothalamic nuclei, that plays an important role in food intake and energy expenditure. As a result, MC4R mutation leads to severe obesity, associated with hyperphagia, hyperglycemia, dyslipidemia, hyperinsulinemia and, cardiovascular disfunction (Nogueiras et al., 2007; Martinelli et al., 2011; Kennedy et al., 2010).

MC4R-KO mice fed with a high-fat diet exhibit accelerated body weight gain, dyslipidemia and hepatic steatosis, similar to human non-alcoholic steatohepatitis (Adan et al., 2006; Itoh et al., 2011; Collet et al., 2017). Despite the excessive lipid accumulation, MC4R deficient mice are rather hypotensive than hypertensive (Greenfield et al., 2009; Tallam et al., 2005).

Unlike MC4R-KO animals, Melanocortin 3 receptor deficient mice (MC3R-KO) develop visceral adiposity, but remain resistant to many of the negative features of obesity, such as insulin resistance, hyperglycemia and hepatic steatosis, even when fed a high-fat diet (Kennedy et al., 2010; Ellacott et al., 2008). The explication seems to be that expression of MC3R is mostly restricted to certain hypothalamic nuclei, where this receptor is mainly involved in central energy homeostasis, and less in food intake, compared to MC4R (Begriche et al., 2013).

Genetic models of hyperlipidemia

Low-density lipoprotein receptor- deficient mice ($LDLR^{-/-}$ mice)

$LDLR^{-/-}$ mice serve as models for studying familial hypercholesterolemia. These mice have a mutation in the low-density lipoprotein receptor gene, therefore they exhibit a moderate-increased blood cholesterol level, ~250 mg/dl on a normal chow diet (Kennedy et al., 2010).

When fed with a high-fat diet, the risk of developing atherosclerotic lesions is increased and mice show hepatic inflammation and steatosis, due to increased sensitivity for Ox-LDL uptake (Bentzon et al., 2010; Sanan et al., 1998; Bieghs et al., 2012).

Apolipoprotein E- deficient mice ($ApoE^{-/-}$ mice)

$ApoE^{-/-}$ mice are widely used as metabolic syndrome models, particularly for cardiovascular pathologies, because of the severe hypercholesterolemia and spontaneous atherosclerotic lesions.

Apolipoprotein E (ApoE) is a glycoprotein synthesized mainly in the liver, intestine, and artery wall and plays a central role in lipoprotein metabolism, being the principal ligand for low-density lipoprotein (LDL) receptor. It is involved in regulating the clearance of lipoproteins and maintaining normal plasma lipid levels (Getz & Reardo, 2009; Khalil et al., 2021).

ApoE deficiency results in severe hyperlipidemia, with an increased VLDL level, low HDL level and atherosclerotic lesions on an

early age (Meir, 2004; Kennedy et al., 2010; Nakashima et al., 1994). In ApoE$^{-/-}$ mice, atherosclerosis develops due to an impaired triglyceride uptake in the liver and the adipose tissue with the accumulation of VLDL and chylomicron residue in the plasma and foam cell accumulation in the artery wall (Pendse et al., 2008).

Compared to Lep$^{ob/ob}$ and LepR$^{db/db}$ mice, ApoE $^{-/-}$ mice are not obese and do not develop insulin resistance and hyperglycemia, even on a high-fat diet (Lo Sasso et al., 2016; Hofmann et al., 2008; Zhang et al., 2023). It seems that ApoE deficiency prevents the obesity and weight gain in mice by restraining adipose tissue expansion and improves glucose tolerance and insulin sensitivity (Zhang et al., 2023).

ApoE$^{-/-}$ mice exhibit hypertension, tachycardia and endothelial dysfunction mainly due to the atherosclerotic lesions (Vasquez et al., 2012).

Genetic models of obesity with hyperlipidemia

In order to develop a mouse model that more accurately reflects the features of human MetS, researchers crossed the Lep$^{ob/ob}$ and LepR$^{db/db}$ mice, with LDLR$^{-/-}$ and ApoE$^{-/-}$ backgrounds, resulting double knockout animals.

Lep$^{ob/ob}$/LDLR$^{-/-}$ and LepR$^{db/db}$ /LDLR$^{-/-}$ mice develop extreme obesity, with hypercholesterolemia characterized by increased VLDL and LDL. Atherosclerotic lesions develop spontaneously therefore this model is extremely useful for the study of cardiovascular pathologies (Kennedy et al., 2010, Lloyd et al., 2008). Double knockout mice showed important atherosclerotic lesions throughout the aorta by the age of 6 months (Hasty et al., 2001).

Meanwhile, Lep$^{ob/ob}$/ApoE$^{-/-}$ and LepR$^{db/db/}$ApoE$^{-/-}$ mice show features more specific to type 2 diabetes associated to a hyperlipidemic profile (Wu et al., 2005).

Triple knockout mice

These model from results from crossing and Lep$^{ob/ob}$/ApoE$^{-/-}$ and Lep$^{ob/ob}$/LDLR$^{-/-}$ mice with Apolipoprotein B100 background. Apolipoprotein B (ApoB) is the main component of LDL and plays a major role in regulating lipid metabolism by carrying lipoprotein molecules into the circulation: chylomicrons, LDL, VLDL, intermediate-density lipoprotein (IDL), and lipoprotein (a) (Devaraj et al., 2023). Triple knockout mice are severely obese with insulin resistance, hyperlipidemia, and hypertension, allowing researchers to study multiple pathologies that occur together in MetS (Kennedy et al., 2010; Lloyd et al., 2008).

Genetic models of metabolic syndrome without obesity

Adiponectin-deficient mice (Adipo$^{-/-}$ mice)

Adiponectin is an adipokine hormone secreted by the adipose tissue, with a key role in regulating glucose and lipid metabolism. Adiponectin is known to have anti-inflammatory, insulin-sensitizing, anti-obesity, anti-atherogenic, and antioxidant effects (Zhao & Liu, 2014; Khoramipour et al., 2021). Adiponectin also protects the liver through its anti-fibrosis and anti-inflammatory role (Gamberi et al., 2018).

As a result of the adiponectin deficiency, Adipo$^{-/-}$ mice develop obesity, hyperlipidemia, insulin-resistance, glucose tolerance and increased serum levels of hepatic markers (Asano et al., 2009; Nawrocki et al., 2006). When fed with a high fat diet, Adipo$^{-/-}$ mice show an increased systolic blood pressure with endothelial dysfunction (Ouchi et al., 2003).

Transgenic aP2 SREBP- 1c mice

This transgenic mouse model overexpresses nSREBP-1c gene (sterol regulatory element-binding protein-1c), which leads to features of congenital generalized lipodystrophy, a human autosomal recessive disorder (Shimomura et al., 1998). Although obesity and lipodystrophy differ in the way of the adipose tissue distribution, glucose and lipid metabolism resemble in both pathologies (Nakayama et al., 2007). These mice exhibit severe insulin resistance with hyperinsulinemia and hyperglycemia, and important liver steatosis. Animals have a reduced body weight, elevated plasma triglyceride and total cholesterol, and minimal serum levels of leptin and adiponectin (Shimomura et al., 1998). An important feature of transgenic aP2 SREBP- 1c mouse model is that no special diet is required for studying MetS mechanisms.

Diet-Induced Metabolic Syndrome

Diet plays an important role in the development of MetS in humans, therefore diet-induced animal models of obesity and MetS show a great interest. Researchers often use purified diets to study metabolic disorders, being more similar to the mechanisms found in human MetS, compared to genetic animal models (De Moura et al., 2023). Purified diets consist in purified ingredients, which essentially contains one main nutrient and minimal non-nutrient substances. In addition, purified diets have very little variability from batch to batch, compared to chow diets, and so help to minimize data variability and allow researcher to select and use individual nutrients to their purpose (Pellizzon & Ricci, 2020).

High-fat Diet

The most used diets for inducing mouse MetS models are high-fat diet (HFD), high-carbohydrate diet (HCD) and the respective combinations of the last two, collectively termed "Western diets" (Preguiça et al., 2020).

The high-fat diet-induced obesity in mice is essential for understanding the connections between the hyperlipidemic diet in humans and the development of MetS (Wang & Liao, 2012). A normal rodent diet contains about 10% fat, while in a HFD lipids range from 41 to 60%, due to the addition of purified lard, butter or pure cholesterol as ingredients. Due to the high caloric intake, the satietogenic potential of the diet is increased which will reduce food intake but still induce obesity (De Moura et al., 2021).

Although there are several mouse strains susceptible to develop diet-induced obesity, the C57BL/6J inbred mouse strain mouse is the most commonly used due to the similarities with human MetS (Martins et al., 2022; Kennedy et al., 2010).

Long-term high-fat diet intake in mice causes peripheral insulin resistance with moderate hyperglycemia followed by insufficient β-cell compensation, resulting in hyperinsulinemia, together with increased expression of oxidative stress and inflammation markers (Mosser et al., 2015). Blood tests show moderate-increased levels of total cholesterol, LDL and triglycerides, and reduced serum levels of HDL. Animals are susceptible to non-alcoholic fatty liver disease and endothelium damage, while hypertension is usually reported (Yang et al., 2014; Wang & Liao, 2012; Preguiça et al., 2020).

High-Carbohydrate Diet

Even though a high-fat/high-carbohydrate diet is the main cause for the development of obesity and metabolic syndrome in both humans and animals, evidence show that a high-carbohydrate/low-fat diet also represents an important risk factor in MetS (Zhang et al., 2023). An increased intake of intense refined carbohydrates, such as starch, disaccharide sucrose (consisting in α-glucose and β-fructose) and high fructose corn syrup) is associated to weight gain, insulin resistance, hyperglycemia, and hyperlipidemia (Chung & Lim, 2019). Increased plasma levels of triglycerides and cholesterol are the consequence of the fructose accumulation in the liver that supports lipogenesis. However, compared to the high-fat diet intake, in this case the weight gain is a slower process and might be better counterbalanced by corresponding energy expenditure (Basciano et al., 2005).

Costa et al. (2023) showed that an eight weeks high-carbohydrate diet in BALB/c mice led to mild obesity characterized by important visceral adiposity in the mesenteric, epididymal, and retroperitoneal, tissues, with increased serum levels of triglycerides, total cholesterol, leptin, and glucose. Zhang et al. (2023) concluded that high-carbohydrate diet led to a more severe cholesterol accumulation in the liver compared to a high-fat diet in C57BL/6 male mice. Also, results showed elevated fasting glucose levels (>300 mg/dl), increased lipid blood profile and mildly increased liver transaminase levels in mice fed with a hypercaloric diet, enriched with fructose, for a 60 days period (Ioniță et al., 2022).

High-fat/ High-Carbohydrate Diet

Diets containing high saturated fats and high carbohydrates most resemble the western diet that affects humans nowadays, leading to a high risk of obesity and MetS. Several studies have shown that the interaction between high-fat and high-sugar diets in rodent represents an important triggering factor in obesity (Morales et al., 2022; Rasool et al., 2018; Liu et al., 2018; Lang et al., 2019). Mice fed with a high-fat/high-

fructose diet for a 12 weeks period showed important weight gain, with visceral fat deposition, dyslipidemia, hyperinsulinemia, impaired glucose tolerance, hypertension, and hyperuricemia (Zhuhua et al., 2015).

A high-fat/high-carbohydrate diet given for 8 to 16 weeks in C57BL/6J mice led to an important weight gain with visceral adipose tissue, increased plasma levels of triglyceride and free fatty acids, associated with liver steatosis, fibrosis, and insulin resistance (Liu et al., 2018). Jarukamjorn et al. (2016) reported that a HF/HC diet induced the progression of nonalcoholic fatty liver disease in mice. A similar diet in mice (45% kcal fat, 15% kcal fructose) led to an inflammatory response, antioxidant imbalance, and oxidative stress with liver (Bayliak et al., 2022).

This model is extremely useful in MetS research due to the similarities with the human diet (referred as "cafeteria diet"), strongly responsible for inducing several obesity comorbidities.

Chemically Induced Models of diabetes and obesity

Streptozotocin (STZ) is an alkylating agent, initially known for its antineoplastic properties, which is selectively toxic to the beta cells of the pancreatic islets in mammals. Experimentally, STZ is widely used in research to induce type 1 and 2 diabetes mellitus (Furman, 2021). STZ damages pancreatic β cells, resulting in hypoinsulinemia and hyperglycemia. STZ can induce hyperglycemia and hypoinsulinemia by two mechanisms, depending on the dosage. In a single high dose, STZ damages pancreatic β cells because of the alkylating cytotoxic nitrosourea compounds.

When given in multiple, low doses, STZ induces the release of GAD (Glutamic acid decarboxylase), an autoantigen involved in in the development of autoimmune diabetes, in both human and mice. The result is a decrease in the β-cells number and Langerhans islets, pancreatic inflammation with lymphocytic infiltration, and insulitis, leading to impaired insulin production and hyperglycemia (Graham et al., 2011; Lenzen, 2008; Dufrane et al., 2006; Paik et al., 1980).

Graham et al., 2008, showed that a single STZ high dose injected intraperitoneally in mice induced diabetes in 96.5% of the cases by experimental day 5. Furman (2021) used a diabetes-inducing protocol by administering multiple, low STZ doses in CD1 and C57BL/6 mice on 5 consecutive days.

STZ side effects should also be carefully evaluated, because hepatotoxicity and kidney damage were reported, especially in high-dosage protocols (Kohl et al., 2013; Noshahr et al., 2020). However, multiple, low STZ dose animal models resemble more accurate human type 2 diabetes, being widely used for testing the effectiveness of potential antidiabetic agents.

Alloxan is an organic, pyrimidine derivative compound, widely used as a diabetogenic agent tool by causing pancreatic beta-cell destruction. Alloxan is a toxic glucose analogue which is transported into the beta pancreatic cells by GLUT2 glucose transporter (Lenzen, 2008).

Alloxan induces pancreatic islets damage by two different mechanisms: the inhibition of glucokinase with reduced insulin secretion and the induction of reactive oxygen species (ROS) formation which leads to beta cells necrosis, both pathways resulting in hyperglycemia and hypo-insulinemia (Queiroz et al., 2021).

The frequency, dosage and routes of Alloxan administration for type 2 diabetes induction in mice may vary, intraperitoneally single injection being the most accepted, with ranges between 100 to 200 mg/kg body weight (Njogu et al., 2018; Ighodaro et al., 2017; Queiroz et al., 2021).

Lower doses of Alloxan were associated with a reversibility and the auto-reversion of the blood glucose level, fact that should be carefully monitored and taken in consideration when inducing type 2 diabetes (Lenzen, 2008; Ighodaro et al., 2017). Another limitation in Alloxan use consists in a large variability regarding the mortality rate in mice, that can result from a hypoglycemic initial shock or severe kidney damage (Jain & Arya, 2011; Szkudelski, 2001).

STZ seems to be a more convenient diabetogenic agent due to a more constant level and longer duration of hyperglycemia together with a higher stability in solution before and after injection. In the same time, STZ is more selective to beta-pancreatic cells, feature that lowers the cellular toxicity and animal mortality (Manik et al., 2017; Lenzen, 2008; Ighodaro et al., 2017).

Monosodium glutamate (MSG) is a neurotoxin derived from L-glutamic acid, widely used as a flavor enhancer in a variety of food products. MSG is widely used for the experimental development of obesity and metabolic abnormalities in rodents (Zanfirescu et al., 2019).

In mice, MSG can be administered for several times, subcutaneously or intraperitoneal (2-4 mg/g of body weight) usually during the neonatal period in order to induce obesity (Martins et al., 2022). MSG toxic activity is selective for the arcuate nucleus of the hypothalamus, resulting in obesity, insulin resistance, and infertility. MSG administered in mice led to severe obesity, hyperlipidemia, hyperglycemia, and increased transaminase enzyme levels, associated to liver steatosis and fibrosis. In addition, serum cytokines levels (TNF-α and IL-6) in MSG treated animals were increased (Sasaki et al., 2011; Hernández Bautista et al., 2019). MSG administration in neonate mice allow researchers to study the connection between hypothalamus and MetS complications (Cameron et al., 1978).

CONCLUSIONS

The mouse models used to study obesity and metabolic syndrome are an extremely important tool in research, allowing the understanding of the molecular and cellular mechanisms underlying the development of MetS and metabolic obesity-associated abnormalities, but also the evaluation of new therapeutic strategies. Translating the preclinical research into humans can be a challenge, therefore, the choice of a proper animal model for the study of MetS, is compulsory. Mice models allow researchers to better monitor functional, biochemical, and histopathological changes and to have a more accurate view over this metabolic disorder.

Although numerous animal models of MetS are currently available, further research is still needed in order to better evaluate their advantages and limitations for testing potential therapies in human MetS.

ACKNOWLEDGEMENTS

This study was funded by the Ministry of Research and Innovation through Core program acronym - Bio -Epiterapii, 2019-2022, GRAND CODE - PN 19 14 01 06.

REFERENCES

Adan, R. A., Tiesjema, B., Hillebrand, J. J., la Fleur, S. E., Kas, M. J., & de Krom, M. (2006). The MC4 receptor and control of appetite. *British journal of pharmacology*, 149(7), 815–827.

Arias-Mutis, Ó. J., Genovés, P., Calvo, C. J., Díaz, A., Parra, G., Such-Miquel, L., Such, L., Alberola, A., Chorro, F. J., & Zarzoso, M. (2018). An Experimental Model of Diet-Induced Metabolic Syndrome in Rabbit: Methodological Considerations, Development, and Assessment. *Journal of visualized experiments*: JoVE, (134), 57117.

Asano, T., Watanabe, K., Kubota, N., Gunji, T., Omata, M., Kadowaki, T., & Ohnishi, S. (2009). *Adiponectin knockout mice on high fat diet develop fibrosing steatohepatitis. Journal of Gastroenterology and Hepatology, 24(10), 1669–1676.*

Basciano, H., Federico, L., & Adeli, K. (2005). Fructose, insulin resistance, and metabolic dyslipidemia. *Nutrition & metabolism*, 2(1), 5.

Bayliak, M. M., Vatashchuk, M. V., Gospodaryov, D. V., Hurza, V. V., Demianchuk, O. I., Ivanochko, M. V., Burdyliuk, N. I., Storey, K. B., Lushchak, O., & Lushchak, V. I. (2022). High fat high fructose diet induces mild oxidative stress and reorganizes intermediary metabolism in male mouse liver: Alpha-ketoglutarate effects. *Biochimica et biophysica acta. General subjects*, *1866*(12), 130226.

Begriche, K., Girardet, C., McDonald, P., & Butler, A. A. (2013). Melanocortin-3 receptors and metabolic homeostasis. *Progress in molecular biology and translational science*, 114, 109–146.

Benchoula, K., Khatib, A., Jaffar, A., Ahmed, Q. U., Sulaiman, W. M. A. W., Wahab, R. A., & El-Seedi, H. R. (2019). The promise of zebrafish as a model of metabolic syndrome. *Experimental animals*, 68(4), 407–416.

Bentzon, J. F., & Falk, E. (2010). Atherosclerotic lesions in mouse and man: is it the same disease? *Current Opinion in Lipidology, 21(5), 434–440.*

Bieghs, V., Van Gorp, P. J., Wouters, K., Hendrikx, T., Gijbels, M. J., van Bilsen, M., Shiri-Sverdlov, R. (2012). LDL Receptor Knock-Out Mice Are a Physiological Model Particularly Vulnerable to Study the Onset of Inflammation in Non-Alcoholic Fatty Liver Disease. *PLoS ONE*, 7(1), e30668.

Bracke, A., Domanska, G., Bracke, K., Harzsch, S., van den Brandt, J., Bröker, B., & von Bohlen und Halbach, O. (2019). Obesity Impairs Mobility and Adult Hippocampal Neurogenesis. *Journal of Experimental Neuroscience, 13, 117906951988358.*

Bremer, A. A., Stanhope, K. L., Graham, J. L., Cummings, B. P., Wang, W., Saville, B. R., & Havel, P. J. (2011). Fructose-Fed Rhesus Monkeys: A Nonhuman Primate Model of Insulin Resistance, Metabolic Syndrome, and Type 2 Diabetes. *Clinical and Translational Science*, 4(4), 243–252.

Cameron, D. P., Cutbush, L., & Opat, F. (1978). Effects of monosodium glutamate-induced obesity in mice on carbohydrate metabolism in insulin secretion. *Clinical and experimental pharmacology & physiology*, *5*(1), 41–51.

Chalvon-Demersay, T., Blachier, F., Tomé, D., & Blais, A. (2017). Animal Models for the Study of the Relationships between Diet and Obesity: A Focus on Dietary Protein and Estrogen Deficiency. *Frontiers in Nutrition*,vol 4.

Chen, H., Charlat, O., Tartaglia, L. A., Woolf, E. A., Weng, X., Ellis, S. J., … Morgenstern, J. P. (1996). Evidence That the Diabetes Gene Encodes the Leptin Receptor: Identification of a Mutation in the Leptin Receptor Gene in db/db Mice. *Cell, 84(3), 491–495.*

Chiang Morales, M. D., Chang, C. Y., Le, V. L., Huang, I. T., Tsai, I. L., Shih, H. J., & Huang, C. J. (2022). High-Fructose/High-Fat Diet Downregulates the Hepatic Mitochondrial Oxidative Phosphorylation Pathway in Mice Compared with High-Fat Diet Alone. *Cells*, *11*(21), 3425.

Chung, N., & Lim, K. (2019). Influence of high fat and different types of carbohydrate diet on energy metabolism in growing mice. *Journal of exercise nutrition & biochemistry*, 23(3), 1–12.

Cluzel, Gaston & Ryan, Paul & Herisson, Florence (2022). High-Fidelity Porcine Models of Metabolic Syndrome: A Contemporary Synthesis. *American Journal of Physiology-Endocrinology and Metabolism*. 322.

Collet, T.-H., Dubern, B., Mokrosinski, J., Connors, H., Keogh, J. M., Mendes de Oliveira, E., Van der Ploeg, L. H. T. (2017). Evaluation of a melanocortin-4 receptor (MC4R) agonist (Setmelanotide) in MC4R deficiency. *Molecular Metabolism,* 6(10), 1321–1329.

Cone, Roger. (2005). Anatomy and regulation of the central melanocortin system. *Nature* neuroscience. 8. 571-8. 10.1038/nn1455.

Costa, K. A., Oliveira, M. C., Cordeiro, L. M. S., Val, C. H., Machado, F. S., Fernandes, S. O. A., Cardoso, V. N., Teixeira, M. M., Silveira, A. L. M., & Ferreira, A. V. M. (2023). Effect of high-refined carbohydrate diet on intestinal integrity. *Nutrition (Burbank, Los Angeles County, Calif.)*, *113*, 112084.

De Moura E Dias, M., Dos Reis, S. A., da Conceição, L. L., Sediyama, C. M. N. O., Pereira, S. S., de Oliveira, L. L., Gouveia Peluzio, M. D. C., Martinez, J. A., & Milagro, F. I. (2021). Diet-induced obesity in animal models: points to consider and influence on metabolic markers. *Diabetology & metabolic syndrome*, *13*(1), 32.

Della Vedova, M. C., Muñoz, M. D., Santillan, L. D., Plateo-Pignatari, M. G., Germanó, M. J., Rinaldi Tosi, M. E., Garcia, S., Gomez, N. N., Fornes, M. W., Gomez Mejiba, S. E., & Ramirez, D. C. (2016). A Mouse Model of Diet-Induced Obesity Resembling Most Features of Human Metabolic Syndrome. *Nutrition and metabolic insights*, 9, 93–102.

Devaraj, S., Semaan, J. R., & Jialal, I. (2023). Biochemistry, Apolipoprotein B. In StatPearls. StatPearls Publishing.

Dobrzyn, P., Dobrzyn, A., Miyazaki, M., & Ntambi, J. M. (2010). Loss of stearoyl-CoA desaturase 1 rescues cardiac function in obese leptin-deficient mice. *Journal of lipid research*, 51(8), 2202–2210.

Dornbush, S., & Aeddula, N. R. (2023). Physiology, Leptin. In StatPearls. StatPearls Publishing, available from: https://www.ncbi.nlm.nih.gov/books/NBK537038/

Dufrane, D., van Steenberghe, M., Guiot, Y., Goebbels, R. M., Saliez, A., & Gianello, P. (2006). Streptozotocin-induced diabetes in large animals (pigs/primates): role of GLUT2 transporter and beta-cell plasticity. *Transplantation*, *81*(1), 36–45.

Ellacott, Kate & Murphy, Jonathan & Marks, Daniel & Cone, Roger. (2008). Obesity-Induced Inflammation in White Adipose Tissue Is Attenuated by Loss of Melanocortin-3 Receptor Signaling. *Endocrinology*. 148. 6186-94. 10.1210/en.2007-0699.

Fang, T., Wang, H., Pan, X., Little, P. J., Xu, S., & Weng, J. (2022). Mouse models of nonalcoholic fatty liver disease (NAFLD): pathomechanisms and pharmacotherapies. *International journal of biological sciences,* 18(15), 5681–5697.

Fuchs, T., Loureiro, M. de P., Macedo, L. E., Nocca, D., Nedelcu, M., & Costa-Casagrande, T. A. (2018). *Modelos animais na síndrome metabólica. Revista Do Colégio Brasileiro de Cirurgiões, 45(5).*

Furman B. L. (2021). Streptozotocin-Induced Diabetic Models in Mice and Rats. *Current protocols*, *1*(4), e78.

Gamberi, T., Magherini, F., Modesti, A., & Fiaschi, T. (2018). Adiponectin Signaling Pathways in Liver Diseases. *Biomedicines*, *6*(2), 52.

Ge, F., Zhou, S., Hu, C., Lobdell, H., 4th, & Berk, P. D. (2010). Insulin- and leptin-regulated fatty acid uptake plays a key causal role in hepatic steatosis in mice with intact leptin signaling but not in ob/ob or db/db mice. *American journal of physiology. Gastrointestinal and liver physiology,* 299(4), G855–G866.

Getz, G. S., & Reardon, C. A. (2009). Apoprotein E as a lipid transport and signaling protein in the blood, liver, and artery wall. *Journal of lipid research*, *50 Suppl* (Suppl), S156–S161.

Giesbertz, P., Padberg, I., Rein, D., Ecker, J., Höfle, A. S., Spanier, B., & Daniel, H. (2015). Metabolite profiling in plasma and tissues of ob/ob and db/db mice identifies novel markers of obesity and type 2 diabetes. *Diabetologia, 58(9), 2133–2143.*

Graham, M. L., Janecek, J. L., Kittredge, J. A., Hering, B. J., & Schuurman, H. J. (2011). The streptozotocin-induced diabetic nude mouse model: differences between animals from different sources. *Comparative medicine*, *61*(4), 356–360.

Greenfield, J. R., Miller, J. W., Keogh, J. M., Henning, E., Satterwhite, J. H., Cameron, G. S., Astruc, B., Mayer, J. P., Brage, S., See, T. C., Lomas, D. J., O'Rahilly, S., & Farooqi, I. S. (2009). Modulation of blood pressure by central melanocortinergic pathways. *The New England journal of medicine*, 360(1), 44–52.

Gregory JM, Kraft G, Dalla Man C, Slaughter JC, Scott MF, Hastings JR, et al. (2023) A high-fat and fructose diet in dogs mirrors insulin resistance and β-cell

dysfunction characteristic of impaired glucose tolerance in humans. *PLoS ONE* 18(12): e0296400.

Hasty, A. H., Shimano, H., Osuga, J., Namatame, I., Takahashi, A., Yahagi, N., Perrey, S., Iizuka, Y., Tamura, Y., Amemiya-Kudo, M., Yoshikawa, T., Okazaki, H., Ohashi, K., Harada, K., Matsuzaka, T., Sone, H., Gotoda, T., Nagai, R., Ishibashi, S., & Yamada, N. (2001). Severe hypercholesterolemia, hypertriglyceridemia, and atherosclerosis in mice lacking both leptin and the low-density lipoprotein receptor. *The Journal of biological chemistry*, *276*(40), 37402–37408.

Hernández Bautista, R. J., Mahmoud, A. M., Königsberg, M., & López Díaz Guerrero, N. E. (2019). Obesity: Pathophysiology, monosodium glutamate-induced model and anti-obesity medicinal plants. *Biomedicine & pharmacotherapy = Biomedecine & pharmacotherapie*, *111*, 503–516.

Hofmann, S. M., Perez-Tilve, D., Greer, T. M., Coburn, B. A., Grant, E., Basford, J. E., Tschöp, M. H., & Hui, D. Y. (2008). Defective lipid delivery modulates glucose tolerance and metabolic response to diet in apolipoprotein E-deficient mice. *Diabetes*, *57*(1), 5–12.

Ighodaro, O. M., Adeosun, A. M., & Akinloye, O. A. (2017). Alloxan-induced diabetes, a common model for evaluating the glycemic-control potential of therapeutic compounds and plants extracts in experimental studies. *Medicina (Kaunas, Lithuania)*, *53*(6), 365–374.

Ioniță, F., Ancuța, D., Coman, C., Codreanu, M.D. (2021). Evaluation of induced Metabolic Syndrome of obesity by administering a purified diet in mice. *Scientific Works. Series C. Veterinary Medicine.* Vol. LXVII (1), 2021 ISSN 2065-1295; ISSN 2343-9394 (CD-ROM); ISSN 2067-3663 (Online); ISSN-L 2065-1295

Ioniță, F., Ancuța, D., Coman, C., Codreanu, M.D. (2022). Development and evaluation of a diet-induced murine model of type II diabetes mellitus. *Rev Rom Med Vet*, 32 | 4: 5-11, ISSN: 1220-3173; E-ISSN: 2457-7618

Itoh, M., Suganami, T., Nakagawa, N., Tanaka, M., Yamamoto, Y., Kamei, Y., Ogawa, Y. (2011). Melanocortin 4 Receptor–Deficient Mice as a Novel Mouse Model of Nonalcoholic Steatohepatitis. *The American Journal of Pathology*, 179(5), 2454–2463.

Jain, D. K., & Arya, R. K. (2011). Anomalies in alloxan-induced diabetic model: It is better to standardize it first. *Indian journal of pharmacology*, *43*(1), 91.

Jarukamjorn, K., Jearapong, N., Pimson, C., & Chatuphonprasert, W. (2016). A High-Fat, High-Fructose Diet Induces Antioxidant Imbalance and Increases the Risk and Progression of Nonalcoholic Fatty Liver Disease in Mice. *Scientifica*, *2016*, 5029414.

Kaur, J. (2014). A Comprehensive Review on Metabolic Syndrome. *Cardiology Research and Practice*, 2014, 1–21.

Kennedy, A. J., Ellacott, K. L. J., King, V. L., & Hasty, A. H. (2010). Mouse models of the metabolic syndrome. Disease Models & Mechanisms, 3(3-4), 156–166.

Khalil, Y. A., Rabès, J.-P., Boileau, C., & Varret, M. (2021). APOE gene variants in primary dyslipidemia. *Atherosclerosis*, 328, 11–22.

Khoramipour, K., Chamari, K., Hekmatikar, A. A., Ziyaiyan, A., Taherkhani, S., Elguindy, N. M., & Bragazzi, N. L. (2021). Adiponectin: Structure, Physiological Functions, Role in Diseases, and Effects of Nutrition. *Nutrients*, 13(4), 1180.

Kleinert, M., Clemmensen, C., Hofmann, S. M., Moore, M. C., Renner, S., Woods, S. C., Tschöp, M. H. (2018). *Animal models of obesity and diabetes mellitus. Nature Reviews Endocrinology, 14(3), 140–162.*

Kohl, T., Gehrke, N., Schad, A., Nagel, M., Wörns, M. A., Sprinzl, M. F., Zimmermann, T., He, Y. W., Galle, P. R., Schuchmann, M., & Schattenberg, J. M. (2013). Diabetic liver injury from streptozotocin is regulated through the caspase-8 homolog cFLIP involving activation of JNK2 and intrahepatic immunocompetent cells. *Cell death & disease*, *4*(7), e712.

Kulkarni, N. M., Jaji, M. S., Shetty, P., Kurhe, Y. V., Chaudhary, S., Vijaykant, G., Narayanan, S. (2014). A novel animal model of metabolic syndrome with non-alcoholic fatty liver disease and skin inflammation. *Pharmaceutical Biology*, 53(8), 1110–1117. doi:10.3109/13880209.2014.960944.

Lang, P., Hasselwander, S., Li, H., & Xia, N. (2019). Effects of different diets used in diet-induced obesity models on insulin resistance and vascular dysfunction in C57BL/6 mice. *Scientific reports*, 9(1), 19556.

Lang, P., Hasselwander, S., Li, H., & Xia, N. (2019). Effects of different diets used in diet-induced obesity models on insulin resistance and vascular dysfunction in C57BL/6 mice. *Scientific reports*, *9*(1), 19556.

Lenzen S. (2008). The mechanisms of alloxan- and streptozotocin-induced diabetes. *Diabetologia*, *51*(2), 216–226.

Li, L., Liao, G., Yang, G., Lu, Y., Du, X., Liu, J., … Chen, Y. (2015). High-fat diet combined with low-dose streptozotocin injections induces metabolic syndrome in Macaca mulatta. *Endocrine,* 49(3), 659–668.

Lin, S., Thomas, T. C., Storlien, L. H., & Huang, X. F. (2000). Development of high fat diet-induced obesity and leptin resistance in C57Bl/6J mice. *International journal of obesity and related metabolic disorders: journal of the International Association for the Study of Obesity*, 24(5), 639–646.

Liu, X. J., Duan, N. N., Liu, C., Niu, C., Liu, X. P., & Wu, J. (2018). Characterization of a murine nonalcoholic steatohepatitis model induced by high fat high calorie diet plus fructose and glucose in drinking water. *Laboratory investigation; a journal of technical methods and pathology*, 98(9), 1184–1199.

Lloyd, D.J., McCormick, J., Helmering, J., Kim, K.W., Wang, M., Fordstrom, P., Kaufman, S.A., Lindberg, R.A., & Véniant, M.M. (2008). Generation and characterization of two novel mouse models exhibiting the phenotypes of the metabolic syndrome: Apob48-/-Lepob/ob mice devoid of ApoE or Ldlr. *American journal of physiology. Endocrinology and metabolism, 294 3*, E496-505.

Lo Sasso, G., Schlage, W. K., Boué, S., Veljkovic, E., Peitsch, M. C., & Hoeng, J. (2016). The Apoe(-/-) mouse model: a suitable model to study cardiovascular and respiratory diseases in the context of cigarette smoke exposure and harm reduction. *Journal of translational medicine*, *14*(1), 146.

Lozano, W. M., Arias-Mutis, O. J., Calvo, C. J., Chorro, F. J., & Zarzoso, M. (2019). Diet-Induced Rabbit Models for the Study of Metabolic Syndrome. *Animals: an open access journal from MDPI*, 9(7), 463.

Lutz, T. A., & Woods, S. C. (2012). Overview of animal models of obesity. *Current protocols in pharmacology*, *Chapter 5*, Unit5.61.

Malendowicz, L. K., Rucinski, M., Belloni, A. S., Ziolkowska, A., & Nussdorfer, G. G. (2007). Leptin and the regulation of the hypothalamic-pituitary-adrenal axis. *International review of cytology*, 263, 63–102.

Manik Islam, M. Rupeshkumar, K. Reddy (2017). Streptozotocin is more convenient than Alloxan for the induction of Type 2 diabetes. *International Journal of Pharmacological Research*, vol 7, (6-11). https://api.semanticscholar.org/CorpusID:55468799

Martinelli, C. E., Keogh, J. M., Greenfield, J. R., Henning, E., van der Klaauw, A. A., Blackwood, A., … Farooqi, I. S. (2011). Obesity due to Melanocortin 4 Receptor (MC4R) Deficiency Is Associated with Increased Linear Growth and Final Height, Fasting Hyperinsulinemia, and Incompletely Suppressed Growth Hormone Secretion. *The Journal of Clinical Endocrinology & Metabolism, 96(1), E181–E188.*

Martins, Tânia, Catarina Castro-Ribeiro, Sílvia Lemos, Tiago Ferreira, Elisabete Nascimento-Gonçalves, Eduardo Rosa, Paula Alexandra Oliveira, and Luís Miguel Antunes. (2022). "Murine Models of Obesity" *Obesities* 2, no. 2: 127-147.

Meir, K. S. (2004). Atherosclerosis in the Apolipoprotein E-Deficient Mouse: A Decade of Progress. *Arteriosclerosis, Thrombosis, and Vascular Biology, 24(6), 1006–1014.*

Mosser, R. E., Maulis, M. F., Moullé, V. S., Dunn, J. C., Carboneau, B. A., Arasi, K., Pappan, K., Poitout, V., & Gannon, M. (2015). High-fat diet-induced β-cell proliferation occurs prior to insulin resistance in C57Bl/6J male mice. *American journal of physiology. Endocrinology and metabolism*, 308(7), E573–E582.

Mostafa, Salma & Shalaby, Mostafa & El-Shiekh, Riham & Elbanna, Hossny & Emam, Shimaa & Bakr, Alaa. (2023). Metabolic syndrome: risk factors, diagnosis, pathogenesis, and management with natural approaches. *Food Chemistry Advances*. 3. 100335.

Moyce Gruber, B. L., Cole, L. K., Xiang, B., Fonseca, M. A., Klein, J., Hatch, G. M., Doucette, C. A., & Dolinsky, V. W. (2022). Adiponectin deficiency induces hepatic steatosis during pregnancy and gestational diabetes in mice. *Diabetologia*, 65(4), 733–747.

Nakashima, Y., Plump, A. S., Raines, E. W., Breslow, J. L., & Ross, R. (1994). ApoE-deficient mice develop lesions of all phases of atherosclerosis throughout the arterial tree. *Arteriosclerosis, Thrombosis, and Vascular Biology, 14(1), 133–140.*

Nakayama, H., Otabe, S., Ueno, T., Hirota, N., Yuan, X., Fukutani, T., Hashinaga, T., Wada, N., & Yamada, K. (2007). Transgenic mice expressing nuclear sterol regulatory element-binding protein 1c in adipose tissue exhibit liver histology similar to nonalcoholic steatohepatitis. *Metabolism: clinical and experimental*, *56*(4), 470–475.

Nawrocki, A. R., Rajala, M. W., Tomas, E., Pajvani, U. B., Saha, A. K., Trumbauer, M. E., Pang, Z., Chen, A. S., Ruderman, N. B., Chen, H., Rossetti, L., & Scherer, P. E. (2006). Mice lacking adiponectin show decreased hepatic insulin sensitivity and reduced responsiveness to peroxisome proliferator-activated receptor gamma agonists. The *Journal of biological chemistry,* 281(5), 2654–2660.

Njogu, S. M., Arika, W. M., Machocho, A. K., Ngeranwa, J. J. N., & Njagi, E. N. M. (2018). In Vivo Hypoglycemic Effect of Kigelia africana (Lam): Studies With Alloxan-Induced Diabetic Mice. *Journal of evidence-based integrative medicine*, *23*, 2515690X18768727.

Nogueiras, R., Wiedmer, P., Perez-Tilve, D., Veyrat-Durebex, C., Keogh, J. M., Sutton, G. M., Pfluger, P. T., Castaneda, T. R., Neschen, S., Hofmann, S. M. et al. (2007). The central melanocortin system directly controls peripheral lipid metabolism. *J. Clin. Invest*. 117, 3475-3488.

Noshahr, Z. S., Salmani, H., Khajavi Rad, A., & Sahebkar, A. (2020). Animal Models of Diabetes-Associated Renal Injury. *Journal of diabetes research*, *2020*, 9416419.

Nugent, J. L., Singh, A., Wirth, K. M., Oppler, S. H., Hocum Stone, L., Janecek, J. L., Sheka, A. C., Kizy, S., Moore, M. E. G., Staley, C., Hering, B. J., Ramachandran, S., Ikramuddin, S., & Graham, M. L. (2021). A nonhuman primate model of vertical sleeve gastrectomy facilitates mechanistic and translational research in human obesity. *iScience*, 24(12), 103421.

Obradovic, M., Sudar-Milovanovic, E., Soskic, S., Essack, M., Arya, S., Stewart, A. J., Gojobori, T., & Isenovic, E. R. (2021). Leptin and Obesity: Role and Clinical Implication. *Frontiers in endocrinology*, *12*, 585887.

Osório, J. (2014). The many faces of leptin—a novel role for leptin signalling in obesity-induced hypertension. *Nature Reviews Endocrinology, 11(3), 129–129.*

Ouchi, N., Ohishi, M., Kihara, S., Funahashi, T., Nakamura, T., Nagaretani, H., Kumada, M., Ohashi, K., Okamoto, Y., Nishizawa, H., Kishida, K., Maeda, N., Nagasawa, A., Kobayashi, H., Hiraoka, H., Komai, N., Kaibe, M., Rakugi, H., Ogihara, T., & Matsuzawa, Y. (2003). Association of hypoadiponectinemia with impaired vasoreactivity. *Hypertension (Dallas, Tex.: 1979)*, *42*(3), 231–234.

Paik, S. G., Fleischer, N., & Shin, S. I. (1980). Insulin-dependent diabetes mellitus induced by subdiabetogenic doses of streptozotocin: obligatory role of cell-mediated autoimmune processes. *Proceedings of the National Academy of Sciences of the United States of America*, *77*(10), 6129–6133.

Panchal, S. K., & Brown, L. (2011). Rodent models for metabolic syndrome research. *Journal of biomedicine & biotechnology*, *2011*, 351982.

Pellizzon, M. A., & Ricci, M. R. (2020). Choice of Laboratory Rodent Diet May Confound Data Interpretation and Reproducibility. *Current developments in nutrition*, 4(4), nzaa031.

Pendse, A. A., Arbones-Mainar, J. M., Johnson, L. A., Altenburg, M. K., & Maeda, N. (2008). Apolipoprotein E knock-out and knock-in mice: atherosclerosis, metabolic syndrome, and beyond: *Fig. 1. Journal of Lipid Research, 50(Supplement), S178–S182.*

Perlman R. L. (2016). Mouse models of human disease: An evolutionary perspective. *Evolution, medicine, and public health*, *2016*(1), 170–176.

Platt, T. L., Beckett, T. L., Kohler, K., Niedowicz, D. M., & Murphy, M. P. (2016). Obesity, diabetes, and leptin resistance promote tau pathology in a mouse model of disease. *Neuroscience, 315,162–174.*

Plummer, M. R., & Hasty, A. H. (2008). Atherosclerotic lesion formation and triglyceride storage in obese apolipoprotein AI-deficient mice. *The Journal of nutritional biochemistry*, 19(10), 664–673.

Preguiça, I., Alves, A., Nunes, S., Fernandes, R., Gomes, P., Viana, S. D., & Reis, F. (2020). Diet-induced rodent models of obesity-related metabolic disorders-A guide to a translational perspective. *Obesity reviews: an official journal of the International Association for the Study of Obesity*, 21(12), e13081.

Queiroz, L. A. D., Assis, J. B., Guimarães, J. P. T., Sousa, E. S. A., Milhomem, A. C., Sunahara, K. K. S., Sá-Nunes, A., & Martins, J. O. (2021). Endangered Lymphocytes: The Effects of Alloxan and Streptozotocin on Immune Cells in Type 1 Induced Diabetes. *Mediators of inflammation*, *2021*, 9940009.

Queiroz, L. A. D., Assis, J. B., Guimarães, J. P. T., Sousa, E. S. A., Milhomem, A. C., Sunahara, K. K. S., Sá-Nunes, A., & Martins, J. O. (2021). Endangered Lymphocytes: The Effects of Alloxan and Streptozotocin on Immune Cells in Type 1 Induced Diabetes. *Mediators of inflammation*, *2021*, 9940009.

Rasool, S., Geetha, T., Broderick, T. L., & Babu, J. R. (2018). High-Fat with High Sucrose Diet Leads to Obesity and Induces Myodegeneration. *Frontiers in physiology*, *9*, 1054.

Ren, J., & Ma, H. (2008). Impaired cardiac function in leptin-deficient mice. *Current hypertension reports*, 10(6), 448–453.

Saadane, A., Lessieur, E. M., Du, Y., Liu,H., & Kern, T. S. (2020). Successful induction of diabetes in mice demonstrates no gender difference in development of early diabetic retinopathy. *PLOS ONE*, 15(9), e0238727.

Sainsbury, A., Schwarzer, C., Couzens, M., & Herzog, H. (2002). Y2 Receptor Deletion Attenuates the Type 2 Diabetic Syndrome of ob/ob Mice. *Diabetes*, 51(12), 3420–3427.

Sanan, D. A., Newland, D. L., Tao, R., Marcovina, S., Wang, J., Mooser, V., Hammer, R. E., & Hobbs, H. H. (1998). Low density lipoprotein receptor-negative mice expressing human apolipoprotein B-100 develop complex atherosclerotic lesions on a chow diet: no accentuation by apolipoprotein(a). *Proceedings of the National Academy of Sciences of the United States of America*, *95*(8), 4544–4549.

Sasaki, Y., Shimada, T., Iizuka, S., Suzuki, W., Makihara, H., Teraoka, R., Tsuneyama, K., Hokao, R., & Aburada, M. (2011). Effects of bezafibrate in nonalcoholic steatohepatitis model mice with monosodium glutamate-induced metabolic syndrome. *European journal of pharmacology*, *662*(1-3), 1–8.

Shimomura, I., Hammer, R. E., Richardson, J. A., Ikemoto, S., Bashmakov, Y., Goldstein, J. L., & Brown, M. S. (1998). Insulin resistance and diabetes mellitus in transgenic mice expressing nuclear SREBP-1c in adipose tissue: model for congenital generalized lipodystrophy. *Genes & development*, *12*(20), 3182–3194.

Song, C. K., Vaughan, C. H., Keen-Rhinehart, E., Harris, R. B., Richard, D., & Bartness, T. J. (2008). Melanocortin-4 receptor mRNA expressed in sympathetic outflow neurons to brown adipose tissue: neuroanatomical and functional evidence. *American journal of physiology. Regulatory, integrative and comparative physiology*, *295*(2), R417–R428.

Suriano, F., Vieira-Silva, S., Falony, G. *et al.* (2021). Novel insights into the genetically obese (ob/ob) and diabetic (db/db) mice: two sides of the same coin. *Microbiome* 9, 147 (2021).

Szkudelski T. (2001). The mechanism of alloxan and streptozotocin action in B cells of the rat pancreas. *Physiological research*, *50*(6), 537–546.

Tallam, L. S., Stec, D. E., Willis, M. A., da Silva, A. A., & Hall, J. E. (2005). Melanocortin-4 receptor-deficient mice are not hypertensive or salt-sensitive despite obesity, hyperinsulinemia, and hyperleptinemia. *Hypertension* (Dallas, Tex.: 1979), 46(2), 326–332.

Vasquez, E. C., Peotta, V. A., Gava, A. L., Pereira, T. M., & Meyrelles, S. S. (2012). Cardiac and vascular phenotypes in the apolipoprotein E-deficient mouse. *Journal of biomedical science*, 19(1), 22.

Wang, C. Y., & Liao, J. K. (2012). A mouse model of diet-induced obesity and insulin resistance. *Methods in molecular biology (Clifton, N.J.)*, *821*, 421–433.

Wayhart, J. P., & Lawson, H. A. (2017). Animal Models of Metabolic Syndrome. *Animal Models for the Study of Human Disease*, 221–243.

Wong, S. K., Chin, K.-Y., Suhaimi, F. H., Fairus, A., & Ima-Nirwana, S. (2016). Animal models of metabolic syndrome: a review. *Nutrition & Metabolism*, 13(1).

Wu, K. K., Wu, T. J., Chin, J., Mitnaul, L. J., Hernandez, M., Cai, T. Q., Ren, N., Waters, M. G., Wright, S. D., & Cheng, K. (2005). Increased hypercholesterolemia and atherosclerosis in mice lacking both ApoE and leptin receptor. *Atherosclerosis*, *181*(2), 251–259.

Yang, Y., Smith, D. L., Jr, Keating, K. D., Allison, D. B., & Nagy, T. R. (2014). Variations in body weight, food intake and body composition after long-term high-fat diet feeding in C57BL/6J mice. *Obesity (Silver Spring, Md.)*, *22*(10), 2147–2155.

Zanfirescu, A., Ungurianu, A., Tsatsakis, A. M., Nițulescu, G. M., Kouretas, D., Veskoukis, A., Tsoukalas, D., Engin, A. B., Aschner, M., & Margină, D. (2019). A review of the alleged health hazards of monosodium glutamate. *Comprehensive reviews in food science and food safety*, *18*(4), 1111–1134.

Zhang, L., Li, X., Liu, X., Wu, X., Xu, Q., Qu, J., Li, X., Zhu, Y., Wen, L., & Wang, J. (2023). High-Carbohydrate Diet Consumption Poses a More Severe Liver Cholesterol Deposition than a High-Fat and High-Calorie Diet in Mice. *International journal of molecular sciences*, 24(19), 14700.

Zhang, X., & Lerman, L. O. (2016). Investigating the Metabolic Syndrome: Contributions of Swine Models. *Toxicologic pathology*, 44(3), 358–366.

Zhang, Y., Cheng, Z., Hong, L., Liu, J., Ma, X., Wang, W., Pan, R., Lu, W., Luo, Q., Gao, S., & Kong, Q. (2023). Apolipoprotein E (ApoE) orchestrates adipose tissue inflammation and metabolic disorders through NLRP3 inflammasome. *Molecular biomedicine*, *4*(1), 47.

Zhang, Y., Proenca, R., Maffei, M., Barone, M., Leopold, L., & Friedman, J. M. (1994). Positional cloning of the mouse obese gene and its human homologue. *Nature*, *372*(6505), 425–432.

Zhao, L., Fu, Z., & Liu, Z. (2014). Adiponectin and insulin cross talk: The microvascular connection. *Trends in Cardiovascular Medicine*, 24(8), 319–324.

Zhuhua, Z., Zhiquan, W., Zhen, Y., Yixin, N., Weiwei, Z., Xiaoyong, L., Yueming, L., Hongmei, Z., Li, Q., & Qing, S. (2015). A novel mice model of metabolic syndrome: the high-fat-high-fructose diet-fed ICR mice. *Experimental animals*, 64(4), 435–442.

***https://www.who.int/news-room/fact-sheets/detail/obesity-and-overweight, 2022

Scientific Works. Series C. Veterinary Medicine. Vol. LXX (2), 2024
ISSN 2065-1295; ISSN 2343-9394 (CD-ROM); ISSN 2067-3663 (Online); ISSN-L 2065-1295

RESEARCH ON INFLAMMATORY ANEMIA INDUCED BY CORTICOSTEROIDS

Adrian RĂDUȚĂ, Oana Diana MIHAI, Simona NICOLAE, Ioana Nicole REU

University of Agronomic Sciences and Veterinary Medicine of Bucharest, Faculty of Veterinary Medicine, 105 Splaiul Independentei Street, 050097, District 5, Bucharest, Romania

Corresponding author email: oprea_diana2008@yahoo.com

Abstract

Research was conducted on 10 CD1 laboratory mice, non-consanguineous strains, divided into two groups of 5 individuals per group. The body weight of individuals ranged from 20 to 30 grams. Both groups were given the same favourable climate, humidity and light conditions. The forage diet consisted of pelleted rodent feed, with feed and water administered at libitum. The control group was injected at the beginning of the experimental period with 1 ml NaCl subcutaneously and the experimental group with 1 ml dexamethasone i.e. 4 mg subcutaneously. The duration of the experiment was 14 days. At the end of the experiment, decreases in erythrocyte count, haemoglobin, haematocrit and increases in derived erythrocyte constants were observed. The results of the leukocyte formula showed an increase in the number of polymorphonuclear cells and a decrease in the other categories of leukocytes in the experimental group.

Key words*: dexamethasone, glucocorticosteroid, anti-inflammatory, mouse.*

INTRODUCTION

Dexamethasone is a synthetic glucocorticosteroid that is widely used to treat various types of conditions, but the same glucocorticosteroids are associated with many side effects (Alexandru et al, 2020). Therapeutic indications for glucocorticosteroids are mainly inflammatory conditions, autoimmune conditions, and hypersensitivity conditions, but the same glucocorticosteroids are also used as an anesthetic.

Although the practical applications of these types of substances are obvious, in practice it is also necessary to take into account the adverse effects that their administration may have.

Glucocorticosteroids can suppress the immune system 20-30 times greater than the ability of hydrocortisone. They have an anti-inflammatory role by suppressing the action of cytokines as well as nitric oxide.

The anti-inflammatory mechanism of these substances may be due to their anti-inflammatory effects, such as inhibiting leukocyte diapedesis and thus stopping the inflammatory reaction, and thus the algic component of inflammation (Cotor et al, 2021).

Glucocorticoids are synthesis and release moderators for prostaglandins, leukotrienes, PAF, various cytokines as well as for several enzymes such as collagenase

Among the negative effects of the administration of glucocorticoids in animals of economic interest, the decrease in milk production can be mentioned. This decrease in milk production is reported by several researchers and can be manifested by a decrease in the amount of fat, total protein, casein, but also of different minerals in milk (Oprea et al., 2019; Oprea et al., 2020; Petcu et al., 2020).

MATERIALS AND METHODS

The experiment was carried out in the biobase of the Faculty of Veterinary Medicine in Bucharest, on two groups of laboratory mice, a control group and an experimental group.

The mice were CD1 non-consanguineous strains and were divided into 5 individuals per group.

The experimental animals had body weights between 20 and 30 grams and were kept under favourable climate, humidity, and lighting conditions at all times.

Feed was administered ad libitum and consisted of combined granulated rodent feed, also water was administered at discretion.

Mice in the control group were injected subcutaneously with 1 ml NaCl 0.9% at the beginning of the experiment and mice in the experimental group were injected with 1 ml dexamethasone, i.e. 4 mg. Injection of the mice in the experimental group was performed twice, the first time at the start of the experiment and the second time at 7 days.

The duration of the experiment was 14 days. On the last day of the experiment blood was taken on anticoagulant. Erythrocyte count, leukocyte count, hemoglobin, hematocrit and derived erythrocyte constants were determined for each individual in both groups. Investigations were performed using a 5 DIFF LaserCyte haematology analyser from Idexx Laboratory.

The leukocyte formula was performed by the classical method under the light microscope and smear staining was performed by the May Grunwald Giemsa method. Interpretation of the results was performed using the T (Student) test.

RESULTS AND DISCUSSIONS

Decreases in erythrocyte count, haemoglobin and haematocrit were observed in the experimental group. Slight increases in MCV MCH and MCHC were recorded.

The leukocyte count decreased significantly in the dexamethasone-injected group (Table 1).

Erythrocyte count determination showed a slight decrease in the experimental group, the mean value being 2.36% lower than the control group.

Haemoglobin in the group that was inoculated with dexamethasone was 0.29% lower than in the control group.

Haematocrit also showed a slight downward trend, being 0.69% lower.

The secondary erythrocyte constants, MCV, MCH, and MCHC had slightly increased values compared to the control group: 1.72%, 2.15%, and 0.44%, respectively.

A marked decrease could be observed in the dexamethasone-injected mice group, the mean leukocyte count was 36.21% lower than the mean in the control group (Figure 1 and Figure 2).

As far as primary erythrocyte constants are concerned, a slight downward trend can be observed but without major significance. In contrast, the secondary erythrocyte constants showed an increasing trend (Ganz T., 2019; Jamela J., 2016).

Table 1. Mean values of haematological investigations

Parameter	Control group	Experimental group	Percentage (%)
E x 10^6 / µl	8.48	8.28	↓2.36
Hb g/dl	13.78	13.74	↓0.29
HTC %	43.28	42.98	↓0.69
MCV μ^3	51.1	51.98	↑1.72
MCH pg Hb/E	16.26	16.61	↑2.15
MCHC g Hb/dl E	31.83	31.97	↑0.44
Leucocyte x 10^3/µl	11.02	7.03	↓36.21

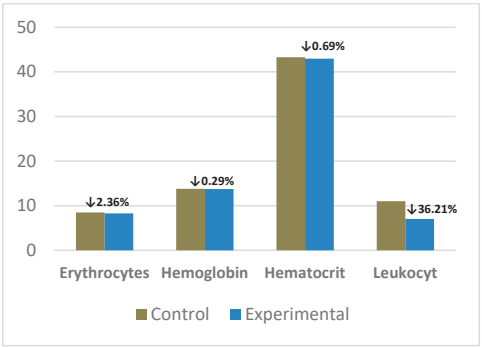

Figure 1. Mean values of haematological investigations (primary erythrocyte constants) and leucocytes

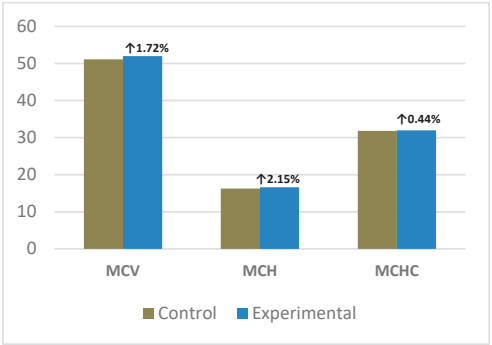

Figure 2. Mean values of haematological investigations (secondary erythrocyte constants)

Glucocorticosteroids may have a positive effect on circulating haemoglobin by delaying the phenomenon of erythrophagocytosis (Cringanu D. et al., 2021). The marked decrease in circulating leukocytes is a consequence of

dexamethasone administration in the experimental group.

White circulating cellular elements are affected by corticosteroids. An increase in polymorphonuclear cells is known following treatment with glucocorticoids, due to the increase in their release from the hematoforming marrow and also due to the decrease in the percentage of their removal from the circulatory sector (Ghiță M. et al., 2015).

In contrast, lymphocytes, eosinophils, monocytes, and basophils decrease in number after glucocorticoid administration.

Glucocorticoids prevent or suppress the entire inflammatory response to infectious, physical or immunological agents by inhibiting early inflammatory events such as oedema, cellular exudation, fibrin deposition, capillary dilation, leukocyte migration, and phagocytic activity. Later events such as capillary and fibroblast proliferation, collagen deposition, and scarring are also inhibited. The anti-inflammatory mechanism of glucocorticoids, although not fully understood, is of great therapeutic relevance and is the subject of intense scientific investigation (Forbes N. et al., 2015). Following the administration of dexamethasone to the mice in the experimental group, the following results were observed in the leukocyte count: the percentage of neutrophils was 4.84% higher and the other white cell populations showed decreases: eosinophils 50%, lymphocytes 8.76%, monocytes 50% (Table 2).

Similar results, but in postpartum dairy cows were also found by Jitkamol in 2004. In that paper it is mentioned that the animals received a single dose of dexamethasone. Dexamethasone being used in the respective experiment because it is used very often in practice to treat fatty liver syndrome and ketosis in ruminants (Shamay et al., 2000).

Following the administration of dexamethasone to lactating cows, the authors were able to observe the onset of a slight leukopenia. After performing the leukocyte formula, they observed the percentage increase of neutrophils.

No circulating basophils were recorded in the smears examined (Figure 3 and Figure 4).

Table 2. Mean leucocyte formula values

Category	Control group	Experimental group	Percent
Neutrophil %	25.64	26.88	↑4.84
Eosinophil %	0.4	0.2	↓50
Bazophile %	0.2	0	↓100
Lymphocytes %	50.2	45.8	↓8.76
Monocytes %	0.4	0.2	↓50

The increase in the percentage of neutrophils is attributed to the action of dexamethasone, a hormone glucocorticosteroid.

It stops the diapedesis of polymorphonuclears and they remain confined to the blood circulation (Ionita F., 2021; Alexandru D., 2020).

Glucocorticoids attenuate the ability of neutrophils to adhere to capillary endothelial cells by a dual mechanism.

They block the normal increase in expression of endothelial adhesion molecules (i.e., ELAM-1) and intercellular adhesion molecules (i.e., ICAM-1) and induce lipocortin, a protein inhibitor of phospholipase A2 (PLA2) (Marx J. et al., 2015).

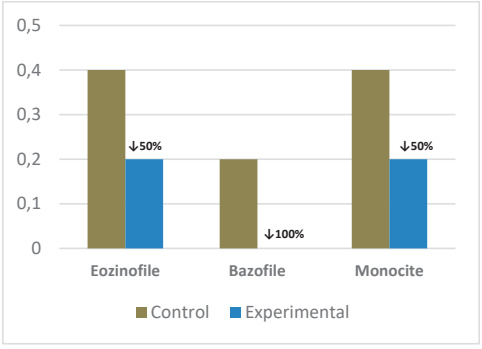

Figure 3. Average leukocyte counts (eosinophils, basophils, monocytes)

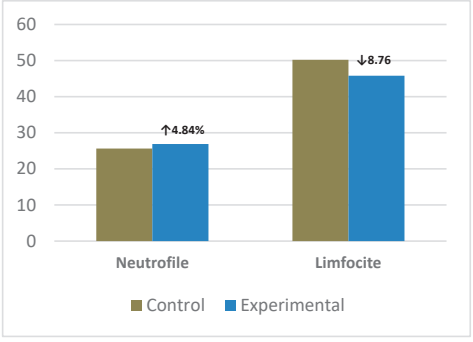

Figure 4. Mean values of leukocyte counts (neutrophils and lymphocytes)

The plasminogen activator and the inhibitory factor for cell movement are inhibited by glucocorticoids, which leads to a low release of hydrolytic enzymes and histamine. The specialty literature also mentions the decrease in chemokines, which attract white cells (Mittelstad et al., 2018; Salehzadeh M. et al., 2022).

Other researchers have demonstrated that the increased number of neutrophils in the blood circulation, after stress or after glucocorticoid treatments, is caused by several factors: first of all, an increased supply of neutrophils from the hematoforming bone marrow reserve, then a reduced diapedesis of neutrophils. The decrease in margination and diapedesis of neutrophils could be caused by the known ability of corticosteroids to reduce the adhesion of neutrophils to the vascular endothelium.

In the macrophages and monocytes from the inflamed tissue sectors, the production of free oxygen radicals and phagocytosis are inhibited. As the inflammation progresses, fibroblasts are inhibited, resulting in poor scarring. This inappropriate scarring affects the healing of the animals and thus implicitly the food safety (Petcu et al., 2007; Petcu, 2013; Petcu, 2015).

This impairment of neutrophil kinetics and margination may increase susceptibility to infectious diseases such as bovine mastitis.

Glucocorticoids slow normal wound healing by blocking inflammatory. collagen breakdown and disorganisation reaction (Leica I. et al, 2020; Curca D., 2008).

So basically there is an apparent increase in circulating neutrophils, they are just prevented from leaving the circulatory system (Cotor G. et al., 2017).

Mononuclear cells decrease numerically after the administration of the experimental substance. A single dose can lead to a decrease of up to 70% of lymphocytes and up to 90% of monocytes (Supeanu et al., 2020).

The redistribution of mononuclear cell populations leads to their numerical decrease in the blood. It should also be mentioned that glucocorticoids can lead to the death of some lymphocytes, an aspect shown by several researchers.

The most sensitive to apoptosis induced by these anti-inflammatories are T-lymphocytes. B-lymphocytes are a little more resistant. Different subpopulations of T-lymphocytes differ among themselves in their sensitivity to glucocorticoids. The decrease of basophils occurs through an incompletely elucidated mechanism (Vagnerová K. et al., 2023).

Corticosteroids in lactating cows can lead to lower milk production. This is the glucose sparing phenomenon. Following a marked hyperglycemia, the body's response is to secrete a larger amount of insulin. But glucocorticoids lead to the inhibition of the neoglucogenesis phenomenon by insulin and facilitate the installation of resistance to it in the peripheral areas, further ensuring hyperglycemia. Also from the category of negative effects of corticosteroids, it should be remembered that they exert some effects on the water and electrolyte balance, increasing potassium excretion and sodium retention. This aspect is explained by the activity of corticosteroids at the renal level.

Fluorinated corticosteroids do not have mineral and corticoid activity. They have an effect of polyuria and polydipsia due to the antidiuretic hormone that is inhibited as a result of a low renal sensitivity to this type of hormone.

In the specialized literature it is mentioned that they lead to the drastic decrease of calcium reserves through a low absorption of it and by increasing the renal threshold Depletion of systemic calcium reserves has negative effects on milk production but also on young bovine infants.

Also related to calcium metabolism, glucocorticoids inhibit osteoclasts and increase parathyroid secretion, which could structurally affect the bone but also bone healing. Affections at the skeletal level are not compatible with an industrial animal breeding system, the economic yield being strongly affected.

CONCLUSIONS

Haematological investigations in both groups of mice show that dexamethasone injection leads to a slight decrease in erythrocyte count (2.36%), haemoglobinemia (0.29%) and haematocrit (0.69).

Derived erythrocyte constants (MCV MCH and MCHC) showed increasing trends in

individuals of the experimental group (1.72%, 2.15% and 0.44%).

Results of leukocyte formula showed a higher percentage of circulating polymorphonuclear cells in the experimental group (4.48%).

Lymphocytes, eosinophils, basophils and monocytes had lower values than in the control group following dexamethasone administration. The percentage of lymphocytes was 8.76% lower, eosinophils 50% lower and monocytes 50% lower. No circulating basophils were found in blood smears from mice in the experimental group at the end of the research.

REFERENCES

Alexandru D. M., Dobre I.R., Crivineanu M. (2020). Diagnosis and treatment of canine appendicular osteosarcoma. A case report. *Scientific Works. Series C. Veterinary Medicine*. Vol. LXVI(1), ISSN 2065-1295; ISSN 2343-9394 (CD-ROM); ISSN 2067-3663 (Online); ISSN-L 2065-1295.

Cotor G., Zagrai G., Gâjâilă G., Ghiță M., Ionescu A.M., Damian A., Zagrai (Măierean) A.M., Dragosloveanu S, Cotor D.C. (2021). The evolution of some blood parameters in hypovolemia conditions in rabbits. *Polish Journal of Veterinary Sciences*, 24(4), 589–594, ISSN:1505-1773,doi 0.24425/pjvs.2021.139984.

Cotor, G., Bălăceanu, R., Ghiță, M. (2017). *Laboratory exercises in animal pathophysiology, a clinical and experimental approach*. Ed. Printech, București, ISBN: 978-606-23-0793-6

Curcă Dumitru C. (2008). *Tratat de Fiziopatologie*. Ed. Printech, București.

Cringanu D., Negreanu R., Garjoaba I, Cringanu I., (2021). Therapeutic approach in veterinarian oncological emergencies. *Scientific Works. Series C. Veterinary Medicine.* Vol. LXVII(2), ISSN 2065-1295; ISSN 2343-9394 (CD-ROM); ISSN 2067-3663 (Online); ISSN-L 2065-1295.

Forbes et al. (2015). P39. Comparative Performance of Two Bench-Top Hematology Instruments for Macaques and Mice. *JAALAS*, 54(5): 568-668. PROCYTE + HEMAVET.

Ganz T. (2019). Anemia of inflammation, *The New England Journal of Medicine,* London, 3; 133(1): 40-50. doi: 10.1182/blood-2018-06-856500.

Ghiță, M., Cotor, G., Vițălaru, A., Brăslașu, D. (2015), Comparative study on the effect of prednisone and dexamethasone on leucocytes, in rabbit. *Journal of Biotechnology*, Volume 208, Supplement, Page S92, ISSN 0168-1656.

Ionita F., Ancuta D., Coman C. (2021). Evaluation of induced metabolic syndrome of obesity by administering a purified diet in mice. *Scientific Works. Series C. Veterinary Medicine*. Vol. LXVII (1), ISSN 2065-1295; ISSN 2343-9394 (CD-ROM); ISSN 2067-3663 (Online); ISSN-L 2065-1295.

Jamela Jouda (2016) The effect of long-term oral dexamethasone on blood cells counts and brain regions of young mice. *AENSI Publication,* pages 63-71 ISSN: 1995-0772 EISSN: 1998-1090.

Leica L., Mitrea I.L., Mariana I. (2020). Coagulopathy as a complication of babesiosis in a dog with hemothorax: clinical case report. *Scientific Works. Series C. Veterinary Medicine*. Vol. LXVI(1), ISSN 2065-1295; ISSN 2343-9394 (CD-ROM); ISSN 2067-3663 (Online); ISSN-L 2065-1295.

Marx, J. O., et al. (2015). The Effects of Acute Blood Loss for Diagnostic Bloodwork and Fluid Replacement in Clinically Ill Mice. *Comp Med*, 65(3): 202-216. C57BL/6J.

Oprea, O.D., Petcu, C.D., & Ciobotaru-Pîrvu, E. (2019). A study concerning quality assessment and processing particularities in certain dairy products. *Scientific Works. Series C. Veterinary Medicine,* LXV(1), 121-126.

Oprea, O.D., Răduță, A., Călin (Nicolae), S., Andrei, C. (2020). Research on percentage variation concerning cow's milk protein, lactose and fat, depending on the season. *Scientific Papers. Series D. Animal Science,* LXIII(1), 182-186.

Petcu, C.D., Savu, C., Mitrănescu, E., & Chirilă, S. (2007). The implementation of the integrated quality and food safety management system in the food industry units. *Lucrări Ştiinţifice Medicină Veterinară, XL*, 545-51.

Petcu, C.D., Ciobotaru-Pîrvu, E., Oprea, O.D., & Ghimpețeanu, O.M. (2020). Ecological dairy products: healthy or just a trend? *Scientific Works. Series C. Veterinary Medicine*, LXVI(1), 87-95.

Petcu, C.D. (2013). Researches concerning some meat products control in a specialized unit. *Scientific Papers. Series D. Animal Science*, LVI, 323-325.

Petcu, C.D. (2015). *Meat quality and technology. Bucharest*, RO: Granada Publsihing House.

Salehzadeh, M. et al. (2022). Glucocorticoid production in lymphoid organs: Acute effects of lipopolysaccharide in neonatal and adult mice. *Endocrinology,* 163, bqab244.

Shamay A., Shapiro F., Barash H. (2000), Israel Bruckental, Nissim Silanikove. Effect of dexamethasone on milk yield and composition in dairy cows. *Annales de zootechnie*, 49(4), pp.343-352. 10.1051/animres: 2000125.hal-00889900.

Supeanu T.D., Supeanu A., Lucica S., Roman V., Cobzariu D., Baraitareanu S., Menchetti L., Danes D. (2020). A comparative clinical and paraclinical evaluation of the effects of polyspecific avian immunoglobulin y in Fiv+/- cats. *Scientific Works. Series C. Veterinary Medicine*. Vol. LXVI (1), ISSN 2065-1295; ISSN 2343-9394 (CD-ROM); ISSN 2067-3663 (Online); ISSN-L 2065-1295.

Vagnerová K., Jágr M., Mekadim C. Ergang P. , Sechovcová H., Vodička M., Fliegerová K., V. Dvořáček , Mrázek J., Pácha J. (2023). Profiling of adrenal corticosteroids in blood and local tissues of mice during chronic stress. *Scientific Reports*, 13: 7278, https://doi.org/10.1038/s41598-023-34395-2

ISSN 2065 – 1295
ISSN-L 2065 – 1295